frontiers | Research Topics

Imaging of adipose tissue in bone and muscle: Implications for osteoporosis, sarcopenia and frailty

Edited by
Ling Wang, Xiaoguang Cheng, Klaus Engelke and Annegreet Vlug

Published in
Frontiers in Endocrinology

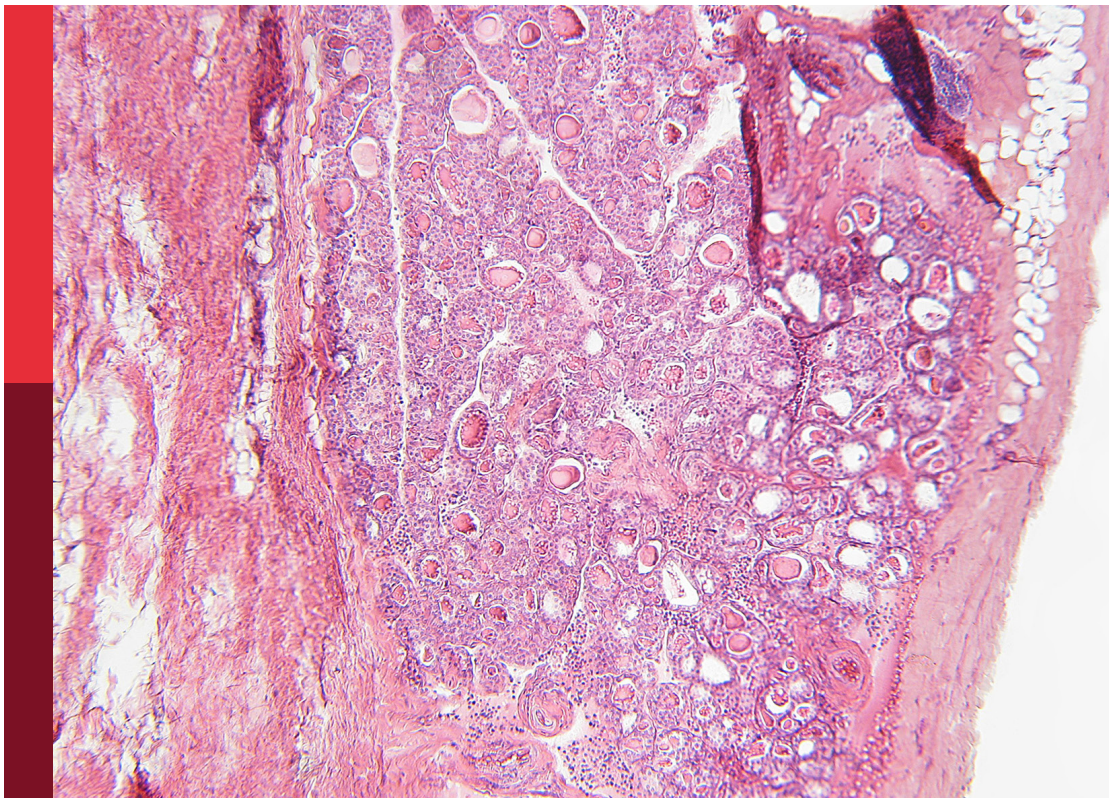

ISSN 1664-8714
ISBN 978-2-8325-3242-3
DOI 10.3389/978-2-8325-3242-3

About Frontiers

Frontiers is more than just an open access publisher of scholarly articles: it is a pioneering approach to the world of academia, radically improving the way scholarly research is managed. The grand vision of Frontiers is a world where all people have an equal opportunity to seek, share and generate knowledge. Frontiers provides immediate and permanent online open access to all its publications, but this alone is not enough to realize our grand goals.

Frontiers journal series

The Frontiers journal series is a multi-tier and interdisciplinary set of open-access, online journals, promising a paradigm shift from the current review, selection and dissemination processes in academic publishing. All Frontiers journals are driven by researchers for researchers; therefore, they constitute a service to the scholarly community. At the same time, the *Frontiers journal series* operates on a revolutionary invention, the tiered publishing system, initially addressing specific communities of scholars, and gradually climbing up to broader public understanding, thus serving the interests of the lay society, too.

Dedication to quality

Each Frontiers article is a landmark of the highest quality, thanks to genuinely collaborative interactions between authors and review editors, who include some of the world's best academicians. Research must be certified by peers before entering a stream of knowledge that may eventually reach the public - and shape society; therefore, Frontiers only applies the most rigorous and unbiased reviews. Frontiers revolutionizes research publishing by freely delivering the most outstanding research, evaluated with no bias from both the academic and social point of view. By applying the most advanced information technologies, Frontiers is catapulting scholarly publishing into a new generation.

What are Frontiers Research Topics?

Frontiers Research Topics are very popular trademarks of the *Frontiers journals series*: they are collections of at least ten articles, all centered on a particular subject. With their unique mix of varied contributions from Original Research to Review Articles, Frontiers Research Topics unify the most influential researchers, the latest key findings and historical advances in a hot research area.

Find out more on how to host your own Frontiers Research Topic or contribute to one as an author by contacting the Frontiers editorial office: frontiersin.org/about/contact

Imaging of adipose tissue in bone and muscle: Implications for osteoporosis, sarcopenia and frailty

Topic editors

Ling Wang — Beijing Jishuitan Hospital, China

Xiaoguang Cheng — Beijing Jishuitan Hospital, China

Klaus Engelke — University of Erlangen Nuremberg, Germany

Annegreet Vlug — Leiden University Medical Center (LUMC), Netherlands

Citation

Wang, L., Cheng, X., Engelke, K., Vlug, A., eds. (2023). *Imaging of adipose tissue in bone and muscle: Implications for osteoporosis, sarcopenia and frailty*. Lausanne: Frontiers Media SA. doi: 10.3389/978-2-8325-3242-3

Table of contents

frontiers in Endocrinology

ORIGINAL RESEARCH
published: 24 December 2021
doi: 10.3389/fendo.2021.811770

Comparison of Muscle Density in Middle-Aged and Older Chinese Adults Between a High-Altitude Area (Kunming) and a Low-Altitude Area (Beijing)

Xingli Liu[1,2,3,4†], Ling Wang[5†], Meng Gao[3,4†], Gang Wang[3,4], Kai Tang[2], Jin Yang[2], Wei Song[1,2,3,4], Jingsong Yang[3,4], Liang Lyu[1,2,3,4] and Xiaoguang Cheng[5*]*

[1] Faculty of Life Science and Technology, Kunming University of Science and Technology, Kunming, China, [2] Medical School, Kunming University of Science and Technology, Kunming, China, [3] Department of Radiology, The First People's Hospital of Yunnan Province, Kunming, China, [4] Department of Radiology, The Affiliated Hospital of Kunming University of Science and Technology, Kunming, China, [5] Department of Radiology, Beijing Jishuitan Hospital, Beijing, China

OPEN ACCESS

Edited by:
Han Lv,
Capital Medical University, China

Reviewed by:
Yijie Fang,
The Fifth Affiliated Hospital of Sun Yat-sen University, China
Kailiang Xu,
Fudan University, China

***Correspondence:**
Liang Lyu
lyuliang0720@hotmail.com
Xiaoguang Cheng
xiao65@263.net

†These authors have contributed equally to this work and share first authorship

Specialty section:
This article was submitted to Bone Research, a section of the journal Frontiers in Endocrinology

Received: 09 November 2021
Accepted: 06 December 2021
Published: 24 December 2021

Citation:
Liu X, Wang L, Gao M, Wang G, Tang K, Yang J, Song W, Yang J, Lyu L and Cheng X (2021) Comparison of Muscle Density in Middle-Aged and Older Chinese Adults Between a High-Altitude Area (Kunming) and a Low-Altitude Area (Beijing). Front. Endocrinol. 12:811770. doi: 10.3389/fendo.2021.811770

Background and Purpose: A high-altitude environment was known to have a negative effect on bone and lead to a higher incidence of hip fracture. However, the dependence of muscle composition on altitude is unclear. Thus, we aimed to compare muscle density and area in plateau and low altitude area and to determine the effect of the altitude on these outcomes.

Methods: Community dwelling adults over 60 years old living in Beijing (elevation 50 m; 300 subjects,107 men and 193 women) or Kunming (elevation 2000 m; 218 subjects,83 men and 135 women) for more than 10 years were enrolled. Quantitative CT was performed in all subjects and cross-sectional area and attenuation measured in Hounsfield units (HU) were determined for the trunk, gluteus, and mid-thigh muscles.

Results: Compared to Beijing, Kunming adults were slimmer (Beijing men *vs* Kunming men: 25.08 ± 2.62 *vs* 23.94 ± 3.10kg/m^2, P=0.013; Beijing women *vs* Kunming women: 25.31 ± 3.1 *vs* 23.98 ± 3.54 kg/m^2, P= 0.001) and had higher muscle density in the L2-trunk and gluteus maximus muscles after adjustment for age and BMI (L2-trunk muscles: Beijing men 29.99 ± 4.17 HU *vs* Kunming men 37.35 ± 4.25 HU, P< 0.0001; Beijing women 27.37 ± 3.76 HU *vs* Kunming women 31.51 ± 5.12 HU, P< 0.0001; Gluteus maximus muscle: Beijing men 35.11 ± 6.54 HU *vs* Kunming men 39.36 ± 4.39 HU, P= 0.0009; Beijing women 31.47 ± 6.26 HU *vs* Kunming women 34.20 ± 5.87 HU P=0.0375). Age was similar in both cohorts and no differences were observed in the gluteus medius and minimus muscle or the mid-thigh muscle, either in the area or density.

Conclusions: Compared with Beijing, the adults in Kunming had higher muscle density of the gluteus maximus and L2 trunk muscles, showing that living at a higher altitude might be beneficial to muscle quality.

Keywords: altitude, muscle density, muscle area, older adults, computed tomography

INTRODUCTION

Hip fractures are the most severe type of osteoporotic fracture and in an aging society have become a heavy public health burden. Recent studies based on large sample sizes have found that the incidence rate of hip fracture is associated with altitude, with higher altitude areas having higher hip fracture rates than lower altitude (1). The underlining mechanisms are still unknown, but hypoxia may play an important role. Hypoxic environments have been shown to influence body composition (eg. reductions in body weight, fat-free mass, fat mass, muscle mass, and/or body water) (2–4). Weight loss has been widely reported in hypoxic chamber experiments and after sojourns at high altitudes (5–7). Some studies have found that skeletal muscle mass decreased with increasing altitude as the hypoxic environment accelerated the decomposition of skeletal muscle and inhibited protein synthesis (8, 9). Muscle weakness is a key factor in the increased risk of falls and might also play a significant role in the increased risk of hip fracture (10, 11). Muscle density, which has been proved to be an important indicator for the evaluation of muscle function, correlates well with muscle strength and physical performance (12). However, few studies have explored the effects on skeletal muscle of hypoxic conditions at high altitude, and the existing findings are mostly based on bioimpedance analysis (BIA) or dual-energy X-ray absorptiometry (DXA) acquisition (8, 13). More precise techniques and data were needed for further validation.

Thus, this study aims to compare the muscle characteristics of people living in Beijing (elevation: 50 meters above sea level) and in Kunming (elevation: 2000 meters above sea level) by quantitative CT to explore the effect of altitude on muscle in middle-aged and older adults. We hypothesized that people in Kunming (high altitude) have poor muscle quality compared to the Beijing population (low altitude).

MATERIALS AND METHODS

Study Participants

Independently living community-dwelling adults residing within the region of Beijing Jishuitan Hospital and the First People's Hospital of Yunnan Province were recruited using convenience sampling, respectively. 300 subjects in Beijing (107 men and 193 women) were enrolled between March 2017 and July 2017, and 218 subjects in Kunming (83 men and 135 women) were enrolled between March 2021 and July 2021. All participants were aged 60 years or older and had been living in either Beijing or Kunming for at least 10 years. Exclusion criteria were as follows: 1. Inability to move independently; 2. Non-osteoporotic pathologic fractures; 3. Deformity of the lumbar spine and hip joint; 4. Tumors treated with radiotherapy or chemotherapy; 5. Patients with metallic implants *in vivo*; 6. Other serious or life-threatening diseases. The study was approved by the local ethics committees in Beijing and Kunming respectively [approval number: 201512-02 (Beijing) and KHLL2021-KY056 (Kunming)]. Informed consent was obtained from each participant.

CT Acquisition

Lumber, hip, and midthigh CT imaging together with a Mindways calibrated CT/QCT acquisition phantom (Mindways Software Inc, Austin, TX, USA) was performed for all study participants. CT scanner information was as follows: Kunming cohort: a third generation dual-source CT scanner (Siemens Force CT, Siemens Healthcare, Germany); Beijing cohort: Toshiba Aquilion CT scanner (Toshiba Medical Systems Division, Tokyo, Japan). All scans were acquired in the supine position. Scan parameters for all CT scans were 120 kVp, 150 mAs, slice thickness: 1.5mm, Pitch 1.5mm, 512 x 512matrix.

Muscle Assessments

The density and axial area of trunk muscle at the L2 level, left side of gluteus maximus muscle, gluteus minimus & medius muscle and mid-thigh muscle were each measured on a single slice. The criteria of measurement section position were as follows: 1. trunk muscle: at the level of the second lumbar vertebra transverse process; 2. left gluteus maximus muscle: at the level of greater trochanter of the femur gluteus; 3. left gluteus minimus & medius muscles: at the 3rd sacral (S3) level; 4. left mid-thigh muscles: at the level of 3cm below the lesser trochanter (**Figure 1**).

OsiriX software (Lite version 10.0.2; Pixmeo, Geneva, Switzerland) was used for muscle analysis. Firstly, The Dicom images of the participant were imported into Orisix software. Secondly, muscle segmentation was performed manually using the 'pencil' tool to outline muscle contours. Thirdly the 'GrowRegion (2D/3D Segmentation)' tool was used to semiautomatically select skeletal muscle regions within our preset HU intensity thresholds (-30 to150HU) (14). Within the resulting muscle region of interest (ROIs), a threshold of -29 HU was applied to distinguish muscle tissue from fat (15). Then the muscle CSA and density of the selected ROI were displayed on the screen. To minimize the resulting error caused by layer selection, all the muscle measurements were performed by the same investigator who had received professional training in CT muscle imaging before the analysis.

The HU values of water equivalent materials of the European spine phantom (ESP-128) were measured and used for the cross-calibration of muscle attenuations of the two CT scanners.

Statistical Analyses

All statistical analyses were conducted using SPSS (Version 22, IBM) and MedCalc (Version 18, MedCalc). Continuous variables were presented as mean ± standard deviation. Spearman correlation testing was used to analyze the correlation of muscle density with age and BMI. Independent t-test was selected for normal distribution data while the nonparametric test (Mann-Whitney U) was applicable to non-normal distribution data to compare muscle size and density between Beijing and Kunming participants. Comparisons among groups were performed using variance analysis and linear regression models. All models were adjusted for BMI and age. The area of the gluteus minimus & medius muscle was not included in the

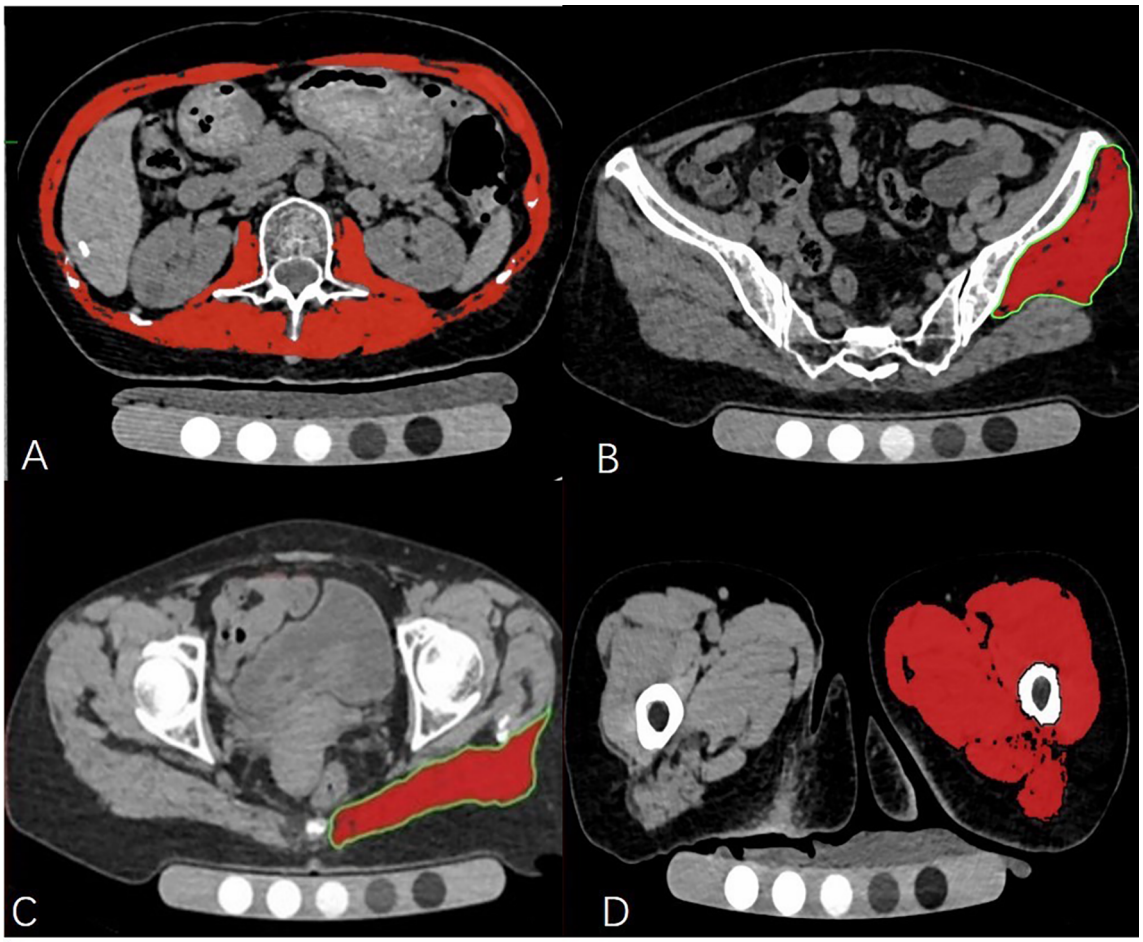

FIGURE 1 | The cross-sectional level of muscle measurement **(A–D)**. Measurement of the trunk muscle at mid—L2 level **(A)**; Measurement of the left gluteus medius and minimus muscle at the 3rd sacral (S3) level **(B)**; Measurement of the left gluteus maximus at the level of the greater trochanter of the femur **(C)**; Measurement of the left mid-thigh muscle group **(D)**.

analysis, as the inconsistent measurement slices in the Beijing population introduced a 10% bias, which was described in a previous study (12). A *P* value of less than 0.05 indicated statistical significance.

RESULTS

Basic Information and Muscle Difference Between Beijing and Kunming Group

Men and women in the Kunming and Beijing cohorts were well matched for age (**Table 1**). However, compared to the Kunming cohort, both men and women in the Beijing cohort had a statistically significantly higher BMI. Men in the Beijing cohort, but not the women, had a statistically larger waist circumference compared with the Kunming cohort. Unexpectedly, a higher muscle density in the gluteus maximus and L2-trunk muscles was observed in the Kunming group (gluteus maximus muscle: Beijing *vs* Kunming P_{men}<0.0001, P_{women}=0.0002; L2-trunk muscles: Beijing *vs* Kunming P_{men}<0.0001, P_{women}<0.0001) (**Table 1**).

Effects of Age and BMI on Muscles

Muscle density and area were associated with age or/and BMI (**Table 2**). Except for the gluteus maximus muscle of the male Beijing group, muscle density was correlated with age. However, the gluteus minimus and mid-thigh muscle densities were not significantly associated with BMI. The density differences of L2 trunk muscle and gluteus maximus muscle between subgroups were significant, no matter whether the data were adjusted for age or BMI. A density difference of gluteus medius and minimus muscles between women was found after adjusting for both age and BMI (*P*=0.0116). In addition, we noticed that only the area of the gluteus maximus and mid-thigh muscle was significant after BMI adjustment between the muscle area comparison ($P_{Gmax\text{-}men}$ = 0.0453; $P_{midthigh\text{-}women}$ = 0.0407). The specific adjustment results are shown in **Table 3**.

TABLE 1 | Difference of variables between Beijing and Kunming group.

	Men			Women		
	BeiJing (n = 107)	**KunMing (n = 83)**	***P* value**	**BeiJing (n = 193)**	**KunMing (n = 135)**	***P* value**
Age (years)	69.6 ± 6.63	67.9 ± 5.75	0.11	67.68 ± 5.77	66.9 ± 5.79	0.15
BMI (kg/m^2)	25.08 ± 2.62	23.94 ± 3.10	**0.013**	25.31 ± 3.08	23.98 ± 3.54	**0.001**
G.MaxM density (HU)	35.11 ± 6.54	39.36 ± 4.39	**< 0.0001**	31.47 ± 6.26	34.20 ± 5.87	**0.0002**
G.MaxM area (cm^2)	43.11 ± 7.9	44.67 ± 7.4	0.2802	37.27 ± 6.28	36.85 ± 6.15	0.5789
G.Med/MinM density (HU)	42.73 ± 4.0	43.48 ± 3.84	0.1355	41.11 ± 4.32	40.25 ± 4.48	0.2017
Midthigh muscle density (HU)	46.04 ± 3.64	46.57 ± 2.58	0.2419	43.49 ± 3.85	44.09 ± 3.17	0.2698
Midthigh muscle area (cm^2)	123.55 ± 22.23	120.14 ± 18.85	0.1344	93.15 ± 14.51	93.13 ± 13.33	0.9769
L2 trunk muscle density (HU)	29.99 ± 4.17	37.35 ± 4.25	**< 0.0001**	27.37 ± 3.76	31.51 ± 5.12	**< 0.0001**
L2 trunk muscle area (cm^2)	125.90 ± 18.01	125.60 ± 20.14	0.9327	90.35 ± 13.40	88.76 ± 11.96	0.5232
Waistline (cm)	89.93 ± 8.04	85.57 ± 8.40	**0.0005**	84.78 ± 8.44	85.84 ± 9.11	0.1885

Data presented as (mean ± SD). The values of P < 0.05 were marked in bold.

TABLE 2 | Correlation of variables with BMI and age.

	BeiJing Men		KunMing Men		BeiJing Women		KunMing Women	
	Age	**BMI**	**Age**	**BMI**	**Age**	**BMI**	**Age**	**BMI**
G.MaxM density (HU)	-0.12 (0.22);	**-0.35 (**)**	**-0.32 (*); -0.238 (*)**		**-0.28 (**); -0.27 (**)**		**-0.28 (*); -0.29 (**)**	
G.MaxM area (cm^2)	**-0.21 (*); 0.39 (**)**		-0.20 (0.07);	-0.10 (0.36)	-0.15 (0.04)**; 0.51 (**)**		-0.08 (0.38);	**0.51 (**)**
Midthigh muscle density (HU)	**-0.30 (*)**;	-0.13 (0.17)	**-0.22 (*)**;	-0.02 (0.86)	**-0.36 (**);**	-0.10 (0.18)	**-0.25 (*)**;	-0.16 (0.06)
Midthigh muscle area (cm^2)	**-0.31 (*); 0.44 (**)**		-0.21 (0.06)**;**	0.006 (0.96)	**-0.34 (**); 0.55 (**)**		**-0.23 (*); 0.45 (**)**	
G.Med/MinM density (HU)	**-0.34 (**)**;	-0.13 (0.17)	**-0.31 (*);**	-0.17 (0.12)	**-0.36 (**)**;	-0.08 (0.26)	**-0.48 (**);**	-0.12 (0.16)
L2 trunk muscle density (HU)	**-0.32 (**)**;	-0.17 (0.09)	**-0.34 (*); -0.17 (0.13)**		**-0.3 (**); -0.23 (*)**		**-0.34 (**); -0.38 (**)**	
L2 trunk muscle area (cm^2)	**-0.28 (*); 0.57 (**)**		**-0.31 (*);** 0.008 (0.94)		**-0.2 (*)**; **0.54 (**)**		**-0.18 (*)**; **0.42 (**)**	

*Data presented as correlation coefficient R and (P value)*P <.05 **P <.001. The values of P < 0.05 were marked in bold.*

TABLE 3 | Difference of variables between Beijing and Kunming after adjusted factors.

	G.MaxM density (HU)	**G.MaxM area (cm^2)**	**Midthigh density (HU)**	**Midthigh area (cm^2)**	**G.Med/MinM density (HU)**	**L2 trunk muscle density (HU)**	**L2 trunk muscle area (cm^2)**
Adjusted age factor							
BJM-KMM	**P<0.0001**	P=0.3431	P=1	P=0.1108	P=1	**P<0.0001**	P=0.5117
BJW-KMW	**P=0.0006**	P=0.4202	P=1	P=0.7357	P=0.0769	**P<0.0001**	P=0.1526
Adjusted BMI factor							
BJM-KMM	**P=0.0001**	**P=0.0453**	P=1	P=0.5913	P=1	**P<0.0001**	P=0.4415
BJW-KMW	**P=0.0134**	P=0.1722	P=1	**P=0.0407**	P=0.1613	**P<0.0001**	P=0.5956
Adjusted age and BMI factors							
BJM-KMM	**P=0.0009**	P=0.1239	P=1	P=0.3019	P=1	**P<0.0001**	P=0.8350
BJW-KMW	**P=0.0375**	P=0.2590	P=1	P=0.1020	P=**0.0116**	**P<0.0001**	P=0.8197

Data presented as (mean ± SD) BJM, Beijing Men; BJW, Beijing Women; KMM, Kunming Men; KMW, Kunming Women. The values of P < 0.05 were marked in bold.

Age Stratified and Influence Factors Adjusted Results

To further explore age-related muscle degeneration, we stratified the analyses by age with a cut point of 70 years (**Table 4**). In the younger group, there was no difference in age between the Beijing and Kunming groups (P>0.05), but the BMI difference was statistically significant (P_{men}=0.0148, P_{women}<0.0001). After age and BMI adjustment, the L2-trunk muscle density of the male and female Kunming groups was significantly higher than those of the Beijing population both in the younger and older groups ($P_{adjusted}$< 0.0001). However, after adjustment for age and BMI the density difference in the gluteus maximus muscle disappeared in the younger women as well as the older men (younger women group: $P_{adjusted}$ = 0.0689; older men group: $P_{adjusted}$ =0.0667).

TABLE 4 | Difference of variables between Beijing and Kunming after age-stratified and variables adjusted.

Younger group[60~70]	Beijing men	Kunming men	P/P_a value	Beijing Women	Kunming Women	P/P_a value
	N=73	N=58		N=142	N=103	
Age (years)	65.67 ± 3.01	64.84 ± 3.17	**P=0.12**	64.77 ± 3.01	64.27 ± 3.18	P=0.20
BMI (kg/m^2)	25.40 ± 2.65	24.03 ± 3.27	**P=0.0148**	25.53 ± 3.20	23.08 ± 3.68	**P<0.0001**
G.MaxM density (HU)	35.52 ± 6.71	40.17 ± 4.37	**P< 0.0001**	32.52 ± 6.16	35.00 ± 5.44	**P=0.0043**
			P_a = 0.0005			P_a = 0.0689
G.MaxM area (cm^2)	44.29 ± 8.01	45.87 ± 7.17	P=0.3638	37.89 ± 6.05	37.17 ± 6.29	P=0.3502
			P_a =0.1068			P_a =0.2115
G.Med/MinM density (HU)	43.46 ± 4.06	44.21 ± 3.53	P=0.2686	41.99 ± 4.04	41.22 ± 3.92	P=0.246
			P_a = 0.7337			**P_a =0.0141**
Midthigh muscle density (HU)	46.67 ± 3.48	47.05 ± 2.07	P=0.7384	44.17 ± 3.76	44.55 ± 2.96	P=0.7011
			P_a = 0.8827			P_a = 0.8330
Midthigh muscle area (cm^2)	127.37 ± 22.93	122.76 ± 18.44	P=0.073	95.96 ± 14.50	94.94 ± 12.82	P=0.5687
			P_a =0.4905			P_a 0.0900
L2 trunk muscle density (HU)	30.90 ± 4.09	38.13 ± 4.08	**P< 0.0001**	28.13 ± 3.55	32.37 ± 4.58	**P< 0.0001**
			P_a=<0.0001			**P_a <0.0001**
L2 trunk muscle area (cm^2)	129.43 ± 17.25	129.60 ± 20.98	P =0.8784	92.61 ± 13.41	89.47 ± 11.98	P =0.0921
			P_a =0.4249			P_a =0.9195
The older group(>70years)	**N=34**	**N=25**		**N=51**	**N=32**	
Age (years)	78.0 ± 3.84	74.96 ± 3.85	**P=0.0028**	75.80 ± 3.21	75.34 ± 3.87	P=0.33
BMI (kg/m^2)	24.37 ± 2.44	23.74 ± 2.72	P=0.39	24.69 ± 2.64	24.55 ± 3.95	P=0.97
G.MaxM density (HU)	34.24 ± 6.18	37.48 ± 3.88	**P=0.0272**	28.55 ± 5.64	31.622 ± 6.52	**P=0.0432**
			P_a=0.0667			**P_a = 0.0297**
G.MaxM area (cm^2)	40.57 ± 7.11	41.88 ± 7.32	P=0.3989	35.53 ± 6.65	35.79 ± 5.64	P=0.6233
			P_a =0.8109			P_a =0.8999
G.Med/MinM density (HU)	41.15 ± 3.42	41.80 ± 4.08	P=0.4075	38.69 ± 4.21	37.14 ± 4.81	P=0.2066
			P_a =0.7323			P_a = 0.0898
Midthigh muscle density (HU)	44.68 ± 3.65	45.46 ± 3.27	P=0.2025	41.59 ± 3.45	42.62 ± 3.42	P=0.2693
			P_a =0.5807			P_a =0.2378
Midthigh muscle area (cm^2)	115.34 ± 18.43	113.62 ± 18.29	P=0.7706	85.57 ± 11.58	87.62 ± 13.54	P=0.6601
			P_a =0.4735			P_a =0.4871
L2 trunk muscle density (HU)	28.03 ± 3.68	35.53 ± 4.13	**P<0.0001**	25.27 ± 3.54	28.72 ± 5.79	**P=0.0032**
			P_a <0.0001			**P_a= 0.0006**
L2 trunk muscle area (cm^2)	118.32 ± 17.50	116.32 ± 14.58	P=0.83	84.08 ± 11.36	86.10 ± 11.46	P=0.1633
			P_a =0.2749			P_a =0.4279

Data presented as (mean ± SD) P-value: unadjusted P-value; P_a value: age and BMI adjusted P-value. The values of P < 0.05 were marked in bold.

DISCUSSION

To our knowledge, this is the first study to compare the muscle characteristics (density and area) between people living in high- and low-altitude areas using quantitative CT scans. After adjustment for age and BMI, the density of L2-trunk muscle and gluteus maximus muscle in people living at high altitude (Kunming) were significantly higher. We also found that BMI decreased with the increased altitude. All the results above indicate that people living with higher attitude are slimmer and have better muscle quality. This critical finding may be valuable for the update of the international consensus statements of sarcopenia such as those from the Asian Working Group for Sarcopenia (AWGS) in 2019 and from the European Working Group on Sarcopenia in Older People (EWGSOP) in 2018 (16, 17). The role of CT or MRI to measure muscle size as a diagnostic criterion of sarcopenia has not been well specified. The associations of muscle mass and size with muscle function are weak. In this study we found the altitude affected the muscle density (muscle quality) but not the size, which high value the use of muscle quality by CT or MRI better characterizes muscle function and may assign a more domain role to CT and MR in the diagnosis of sarcopenia in treatment planning and monitoring response to treatment. The findings in our study provide evidence that muscle density assessed by CT imaging may be a sensitive screening tool for sarcopenia at different altitudes.

Recent data indicated that the incidence of hip fractures is associated with increased altitude (1). Muscle function is important in preventing falls and related osteoporotic fractures (10). To date, the relationship between muscle density or muscle size with attitude is still unclear. In our study, both for men and women, the muscle density of L2 trunk muscle and gluteus maximus muscle in the Kunming population was higher than that in Beijing, and those results were independent of BMI and age. However, no significant difference was observed in the muscle area. This density difference is believed to be associated with fatty infiltration of skeletal muscle., Muscle density in this study was measured by CT threshold segmentation. After removing the influence of fat infiltration in muscle space, factors such as fat infiltration in muscle cells and myoglobin concentration may be the main influencing factors affecting muscle density. A study by Chia et al. found that total body fat mass measured by DXA was significantly decreased and lean mass increased in ten young male swimmers after 3-weeks of

training at an altitude of 2,300 m, while there was no change in body composition in eight male control subjects who resided at sea level for the same period (13). In addition, the total hemoglobin was simultaneously increased significantly in the skeletal muscle. Similar results were obtained in previous animal experiments (18). Based on the findings of previous studies, the decrease of fat content under hypoxia may be related to the following factors: 1) sympathetic power is significantly elevated under hypoxia, which might influence the regulation of body composition by altering blood distribution among adipose and muscle tissues. This change is followed by energy fuel redistribution and increased insulin delivery toward skeletal muscle (19); 2) hypoxic regulation of human skeletal muscle mitochondria. A study reported that mitochondrial volume density increased after twenty-eight days of acclimatization at 3,454 m (20). However, the current interpretation of the effect of hypoxia on skeletal muscle mitochondria is inconsistent or even contradictory and needs to be further clarified; 3) Effect of endocrine metabolism, particularly glucose homeostasis and lipid metabolism. Interestingly, studies found that individuals living at higher altitudes have lower fasting glycemia and better glucose tolerance compared with those who live near sea level (21). In short, contrary to our initial hypothesis, muscle density increases with altitude. Meanwhile, with an increase in altitude, bone mass decreases and fragility increases (1). The high incidence of hip fracture in the plateau area might be the consequence of muscle and bone interaction, but the specific regulatory mechanism is not clear. We hypothesize that the difference between the muscle measurements in Kunming and Beijing might be a self-protection compensation mechanism for the body to resist bone loss under the hypoxic environment. Further researches, however, are needed. Trunk muscle density was the most sensitive variable in our research. Compared to gluteus and mid-thigh muscles, the density of trunk muscle was a more sensitive parameter indicating that people living with higher attitude have better muscle quality, independent of BMI and age. This also indicated that the trunk muscle may be somewhat different from the other muscles in its response to hypoxia or underlying obesity, but the mechanism is unclear. A previous study showed similar results that hepatic steatosis predicted psoas muscle fat content independent of BMI (22). In addition, low trunk muscle density has proved to be associated with poor balance, lower and faster declines in functional capacity in older adults (23, 24). These results suggest that trunk muscle density may have potential value in future fat deposition assessment and sarcopenia diagnosis for the plateau area residents.

In this study, we observed the interesting finding of decreased BMI but no changes in muscle size with increased attitude, which indicated that people living in Beijing at low attitude have more fat depots in the body, and the male Beijing group showed a larger waist circumference as expected. De Carvalho et al. found that abdominal obesity was associated with accelerated muscle strength decline in men (25). His study may provide a strong reference for the interpretation of our findings. Tissue-specific lipid partitioning changes could lead to altering the distribution of fat in the body (26). The location of triglyceride (TG) storage has important metabolic consequences. Visceral fat was also found to be strongly associated with elevated triglycerides levels and fatty infiltration of muscle tissue (27, 28). Our findings show that high attitude impacts fat deposition, namely by decreasing the fat in the abdomen and intramyocellular lipids.

Bodyweight reduction is an inevitable consequence of chronic hypoxic exposure (5). In our study, people living at higher altitude were found to have lower BMI, consistent with the study of Ye et al. (8). Previous studies on the relationship between muscle and altitude mainly focused on the mass assessed by DXA or BIA but the results are inconsistent. Some reports showed that skeletal muscle mass decreases with increased altitude, while in others it was unchanged or increased (8, 13, 20). The variations of BMI may be the main reason for this discrepancy. The decrease of muscle mass with increased altitude in some studies may be caused the decrease in BMI. Meanwhile, due to the obvious influence of BMI, the muscle mass of different studies may not be directly compared. Furthermore, body mass by DXA or BIA may not fully reflect the underlying pathophysiology of muscle strength and related functional outcomes. These findings suggest that muscle mass may not be a appropriate index to evaluate the effect of hypoxia on muscles. Muscle strength and physical performance have come to be recognized as deserving more attention in the musculoskeletal field study (17, 29). Muscle density may be a better quantitative index in this case (12). Nevertheless, there remains a lack of research on muscle density and the corresponding reference density value in the hypoxia environment. This study was undertaken to provide a reference for further clinical research and mechanism exploration in this field.

This study has several limitations. A major limitation is a cross-sectional design and a limited sample size. Another limitation is the lack of evaluation of physical activity (PA) and local eating habits for both cohorts. However, the respective dietary habit surveys from Beijing and Kunming suggested the diet type and energy intake in the old population were not considered to be significant (30, 31). Moreover, previous studies showed that the PA differences were mainly concentrated between urban and rural areas and all subjects included in this study were elder urban residents (32, 33), so the differences in PA between the two groups of our study were hypothesized to be relatively small. Further, a large epidemiologic study in China found that the total average physical activity level was obviously lower for the 60 to79 years old population compared to young age groups (33), and the main types of PA were occupational PA (62%), followed by domestic PA (26%) and leisure-time PA (4%). The subjects in this study were over 60 years old and most of them were retired, the domestic and leisure time PA becoming the main part. A study showed 85.4% of the elderly (over 60 years) in China did not engage in leisure-time exercise (34). These results indicate that the PA difference between the two groups in this study might be small and may have little influence on interpreting the results in this study. What's more, physical activity or exercise increases muscle size (35) which did not differ between Beijing and Kunming subjects. Thus, in our cohort,

there was probably no significant difference in PA behaviors and eating habits between the two groups.

CONCLUSION

In conclusion, people living in the Yunnan plateau region have a higher density of L2-trunk muscle and gluteus maximus muscle compared with those living in a low altitude area such as Beijing. In addition, our study provides reference data for muscle density of the plateau population for the first time.

DATA AVAILABILITY STATEMENT

The original contributions presented in the study are included in the article/supplementary material. Further inquiries can be directed to the corresponding authors.

ETHICS STATEMENT

The studies involving human participants were reviewed and approved by Beijing Jishuitan Hospital (No:201512-02) and The first people's hospital of Yunnan province (No.KHLL2021-KY056). The patients/participants provided their written informed consent to participate in this study. Written informed consent was obtained from the individual(s) for the publication of any potentially identifiable images or data included in this article.

AUTHOR CONTRIBUTIONS

LL and XC designed the study, developed the theoretical framework, and supervised the project. XL, LW, MG, and GW analysed the results and drafted the manuscript. KT, JinY, WS, and JingsongY completed the data collection, such as questionnaire information collection, scanning and data input. All authors contributed to the article and approved the submitted version.

FUNDING

This work was supported by the National Natural Science Foundation of China [grant number: 81901718, 81771831], The Beijing Hospitals Authority Clinical Medicine Development of Special Funding Support [grant number: ZYLX202107] and Yunnan "Ten thousand people plan"-famous doctor special project [grant number: YNWR-MY-2019-011]. The funders had no role in study design, data collection, and analysis, or preparation of the manuscript.

ACKNOWLEDGMENTS

The authors would like to thank Prof. Glen Blake (King's College London, UK) for his most helpful comments on drafts of this paper. And we are grateful to all participants, interviewers, postgraduates, radiologists who took part in this study.

REFERENCES

1. Gong XF, Li XP, Zhang LX, Center JR, Bliuc D, Shi Y, et al. Current Status and Distribution of Hip Fractures Among Older Adults in China. *J Osteoporos Int* (2021) 32(9):1785–93. doi: 10.1007/s00198-021-05849-y
2. Wen X, An P, Chen WC, Lv Y, Fu Q. Comparisons of Sarcopenia Prevalence Based on Different Diagnostic Criteria in Chinese Older Adults. *J Nutr Heal Aging* (2015) 19(3):342–7. doi: 10.1007/s12603-014-0561-x
3. Chen LK, Liu LK, Woo J, Assantachai P, Auyeung TW, Bahyah KS, et al. Sarcopenia in Asia: Consensus Report of the Asian Working Group for Sarcopenia. *J Am Med Dir Assoc* (2014) 15(2):95–101. doi: 10.1016/j.jamda.2013.11.025
4. Buckinx F, Landi F, Cesari M, Fielding RA, Visser M, Engelke K, et al. Pitfalls in the Measurement of Muscle Mass: A Need for a Reference Standard. *J Cachexia Sarcopenia Muscle* (2018) 9(2):269–78. doi: 10.1002/jcsm.12268
5. Hamad N, Travis SP. Weight Loss at High Altitude: Pathophysiology and Practical Implications. *Eur J Gastroenterol Hepatol* (2006) 18(1):5–10. doi: 10.1097/00042737-200601000-00002
6. Macdonald JH, Oliver SJ, Hillyer K, Sanders S, Smith Z, Williams C, et al. Body Composition at High Altitude: A Randomized Placebo-Controlled Trial of Dietary Carbohydrate Supplementation. *Am J Clin Nutr* (2009) 90 (5):1193–202. doi: 10.3945/ajcn.2009.28075
7. Wing-Gaia SL. Nutritional Strategies for the Preservation of Fat Free Mass at High Altitude. *Nutrients* (2014) 6(2):665–81. doi: 10.3390/nu6020665
8. Ye L, Wen Y, Chen Y, Yao J, Li X, Liu Y, et al. Diagnostic Reference Values for Sarcopenia in Tibetans in China. *Sci Rep* (2020) 10(1):3067–76. doi: 10.1038/s41598-020-60027-0
9. Wandrag L, Siervo M, Riley HL, Khosravi M, Fernandez BO, Leckstrom CA, et al. Does Hypoxia Play a Role in the Development of Sarcopenia in Humans? Mechanistic Insights From the Caudwell Xtreme Everest Expedition. *Redox Biol* (2017) 13(2):60–8. doi: 10.1016/j.redox.2017.05.004
10. Szulc P. Impact of Bone Fracture on Muscle Strength and Physical Performance-Narrative Review. *Curr Osteoporos Rep* (2020) 18(6):633–45. doi: 10.1007/s11914-020-00623-1
11. Wang L, Yin L, Zhao Y, Su Y, Sun W, Liu Y, et al. Muscle Density Discriminates Hip Fracture Better Than Computed Tomography X-Ray Absorptiometry Hip Areal Bone Mineral Density. *J Cachexia Sarcopenia Muscle* (2020) 11(6):1799–812. doi: 10.1002/jcsm.12616
12. Wang L, Yin L, Zhao Y, Su Y, Sun W, Chen S, et al. Muscle Density, But Not Size, Correlates Well With Muscle Strength and Physical Performance. *J Am Med Dir Assoc* (2021) 22(4):751–759.e2. doi: 10.1016/j.jamda.2020.06.052
13. Chia M, Liao CA, Huang CY, Lee WC, Hou CW, Yu SH, et al. Reducing Body Fat With Altitude Hypoxia Training in Swimmers: Role of Blood Perfusion to Skeletal Muscles. *Chin J Physiol* (2013) 56(1):18–25. doi: 10.4077/CJP.2013.BAA07
14. Yin L, Xu Z, Wang L, Li W, Zhao Y, Su Y, et al. Associations of Muscle Size and Density With Proximal Femur Bone in a Community Dwelling Older Population. *Front Endocrinol* (2020) 11:503. doi: 10.3389/fendo.2020.00503
15. Engelke K, Museyko O, Wang L, Laredo JD. Quantitative Analysis of Skeletal Muscle by Computed Tomography Imaging-State of the Art. *J Orthop Translat* (2018) 15:91–103. doi: 10.1016/j.jot.2018.10.004
16. Chen LK, Woo J, Assantachai P, Auyeung TW, Chou MY, Iijima K, et al. Asian Working Group for Sarcopenia: 2019 Consensus Update on Sarcopenia Diagnosis and Treatment. *J Am Med Dir Assoc* (2020) 21(3):300–307.e2. doi: 10.1016/j.jamda.2019.12.012
17. Cruz-Jentoft AJ, Bahat G, Bauer J, Boirie Y, Bruyère O, Cederholm T, et al. Sarcopenia: Revised European Consensus on Definition and Diagnosis. *Age Ageing* (2019) 48(1):16–31. doi: 10.1093/ageing/afy169

18. Chen CY, Tsai YL, Kao CL, Lee SD, Wu MC, Mallikarjuna K, et al. Effect of Mild Intermittent Hypoxia on Glucose Tolerance, Muscle Morphology and AMPK-PGC-1alpha Signaling. *Chin J Physiol* (2010) 53(1):62–71. doi: 10.4077/CJP.2010.AMK078
19. Heinonen IH, Kemppainen J, Kaskinoro K, Peltonen JE, Borra R, Lindroos M, et al. Regulation of Human Skeletal Muscle Perfusion and Its Heterogeneity During Exercise in Moderate Hypoxia. *AJP Regul Integr Comp Physiol* (2010) 299(1):R72–79. doi: 10.1152/ajpregu.00056.2010
20. Jacobs RA, Lundby AK, Fenk S, Gehrig S, Siebenmann C, Flück D, et al. Twenty-Eight Days of Exposure to 3454 M Increases Mitochondrial Volume Density in Human Skeletal Muscle. *J Physiol* (2016) 594(5):1151–66. doi: 10.1113/jp271118
21. Woolcott OO, Ader M, Bergman RN. Glucose Homeostasis During Short-Term and Prolonged Exposure to High Altitudes. *Endocr Rev* (2015) 36 (2):149–73. doi: 10.1210/er.2014-1063
22. Sebro R. Obesity, Hepatic Steatosis, and Their Impact on Fat Infiltration of the Trunk Musculature Using Unenhanced Computed Tomography. *J Comput Assist Tomogr* (2017) 41(2):298–301. doi: 10.1097/RCT.0000000000000507
23. Anderson DE, Quinn E, Parker E, Allaire BT, Muir JW, Rubin CT, et al. Associations of Computed Tomography-Based Trunk Muscle Size and Density With Balance and Falls in Older Adults. *J Gerontol A Biol Sci Med Sci* (2016) 71(6):811–6. doi: 10.1093/gerona/glv185
24. Hicks GE, Simonsick EM, Harris TB, Newman AB, Weiner DK, Nevitt MA, et al. Trunk Muscle Composition as a Predictor of Reduced Functional Capacity in the Health, Aging, and Body Composition Study: The Moderating Role of Back Pain. *J Gerontol A Biol Sci Med Sci* (2005) 60:1420–4. doi: 10.1093/gerona/60.11.1420
25. de Carvalho DHT, Scholes S, Santos JLF, de Oliveira C, Alexandre TDS. Does Abdominal Obesity Accelerate Muscle Strength Decline in Older Adults? Evidence From the English Longitudinal Study of Ageing. *J Gerontol A Biol Sci Med Sci* (2019) 74(7):1105–11. doi: 10.1093/gerona/gly178
26. Lv H, Li M, Liu Y, Zhao L, Sun J, Cao D, et al. The Clinical Value and Appropriateness Criteria of Upper Abdominal Magnetic Resonance Examinations in Patients Before and After Bariatric Surgery: A Study of 837 Images. *Obes Surg* (2020) 30(10):3784–91. doi: 10.1007/s11695-020-04688-w
27. Tseng YY, Yang TC, Tu PH, Lo YL, Yang ST. Repeated and Multiple New Vertebral Compression Fractures After Percutaneous Transpedicular Vertebroplasty. *Spine* (2009) 34(18):1917–22. doi: 10.1097/BRS.0b013e3181ac8f07
28. Docampo E, Ciria M, Serra-Burges J, Blanch J, Pérez Edo L, Carbonel J. Risk Factors of New Fractures After Vertebroplasty. *Med Clin* (2009) 133(1):17–9. doi: 10.1016/j.medcli.2008.07.027
29. Barbat—Artigas S, Rolland Y, Vellas B, Aubertin-Leheudre M. Muscle Quantity Is Not Synonymous With Muscle Quality. *J Am Med Dir Assoc* (2013) 14(11):852.e1–7. doi: 10.1016/j.jamda.2013.06.003
30. Yan F, Xu WL, Zhang MR, Yang Z. Survey on Diet Habit and Diet Structure Among the Elderly, Kunming City, 2014. *Prev Med Tribune* (2017) 23(2):93–96,99. doi: 10.16406/j.pmt.issn.1672-9153.2017.02.004. (in Chinese).
31. Dong Z, Huang L, Sha YM, Zhao Y, Xu J, Zhang Z, et al. Investigation of Dietary Structure and Nutritional Status of People Aged 50 and Over in Beijing. *Chin J Public Health* (2005) 21(6):727–8. doi: 10.3321/j.issn:1001-0580.2005.06.043. (in Chinese).
32. Zhu W, Chi A, Sun Y. Physical Activity Among Older Chinese Adults Living in Urban and Rural Areas: A Review. *J Sport Health Sci* (2016) 5(3):281–6. doi: 10.1016/j.jshs.2016.07.004
33. Du H, Bennett D, Li L, Guo Y, Collins R, Chen JS, et al. Physical Activity and Sedentary Leisure Time and Their Associations With BMI, Waist Circumference, and Percentage Body Fat in 0.5 Million Adults: The China Kadoorie Biobank Study. *Am J Clin Nutr* (2013) 97(3):487–96. doi: 10.3945/ajcn.112.046854
34. Zhang M, Chen X, Wang Z, Wang L, Jiang Y. Leisure-Time Physical Exercise and Sedentary Behavior Among Chinese Elderly, in 2010. *Zhonghua Liu Xing Bing Xue Za Zhi* (2014) 35:242–5. doi: 10.3760/cma.j.issn.0254-6450.2014.03.005. (in Chinese).
35. Stewart VH, Saunders DH, Greig CA. Responsiveness of Muscle Size and Strength to Physical Training in Very Elderly People: A Systematic Review. *Scand J Med Sci Sports* (2014) 24(1):e1–10. doi: 10.1111/sms.12123

Conflict of Interest: The authors declare that the research was conducted in the absence of any commercial or financial relationships that could be construed as a potential conflict of interest.

frontiers in Endocrinology

ORIGINAL RESEARCH
published: 21 February 2022
doi: 10.3389/fendo.2022.817418

The Role of Sex Hormones on Bone Mineral Density, Marrow Adiposity, and Muscle Adiposity in Middle-Aged and Older Men

Li Xu[1†], Qian Zhao[2†], Kai Li[1], Yong Zhang[1], Chao Wang[3], Karen Hind[4], Ling Wang[1], Yandong Liu[1] and Xiaoguang Cheng[1]*

[1] Department of Radiology, Beijing Jishuitan Hospital, Beijing, China, [2] International Medical Center, West China Hospital, Sichuan University, Chengdu, China, [3] Department of Epidemiology and Biostatistics, Beijing Research Institute of Traumatology and Orthopedics, Beijing Jishuitan Hospital, Beijing, China, [4] Department of Sport and Exercise Sciences, Durham University, Durham, United Kingdom

OPEN ACCESS

Edited by:
Abdul Malik Tyagi,
Emory University, United States

Reviewed by:
Bing Han,
Shanghai Jiao Tong University, China
Vikram Khedgikar,
Brigham and Women's Hospital and Harvard Medical School, United States

****Correspondence:***
Xiaoguang Cheng
xiao65@263.net

[†]These authors have contributed equally to this work and share first authorship

Specialty section:
This article was submitted to Bone Research, a section of the journal Frontiers in Endocrinology

Received: *18 November 2021*
Accepted: *31 January 2022*
Published: *21 February 2022*

Citation:
Xu L, Zhao Q, Li K, Zhang Y, Wang C, Hind K, Wang L, Liu Y and Cheng X (2022) The Role of Sex Hormones on Bone Mineral Density, Marrow Adiposity, and Muscle Adiposity in Middle-Aged and Older Men. Front. Endocrinol. 13:817418. doi: 10.3389/fendo.2022.817418

Purpose: The etiology of age-related bone loss is less clear in men. This study is aimed to observe the variations of endogenous sex hormone concentrations with increasing of age in men, and investigate their relations to bone mass, marrow adiposity, and muscle adiposity.

Methods: A total of 199 community-dwelling Chinese men (aged 41 to 82 years) were included and measured of serum total estradiol, total testosterone, and follicle-stimulating hormone (FSH) concentrations by enzyme-linked immunosorbent assay (ELISA). Vertebral trabecular volumetric bone mineral density (vBMD) was measured by quantitative computed tomography for all participants, and vertebral marrow fat content and erector muscle fat content were quantified by Chemistry-shift-encoding magnetic resonance imaging in 62 participants.

Results: In this population, FSH concentration increased ($p < 0.001$) gradually with aging. Lower vBMD was independently associated with higher FSH concentration ($\beta = -0.216$, $p < 0.001$), but not with total estradiol or total testosterone. For each standard deviation increase in FSH there was a 50% higher risk of an individual having osteopenia or osteoporosis (vBMD < 120 mg/cm^3). Marrow fat content and erector muscle fat content were greater in osteopenic and osteoporotic men, but there were no associations with sex hormones concentrations.

Conclusion: In summary, FSH but not total estradiol or total testosterone is related to vertebral trabecular vBMD in middle-aged and older Chinese men. Neither marrow adiposity nor muscle adiposity is associated with sex hormones.

Keywords: bone mineral density, marrow adiposity, muscle adiposity, follicle-stimulating hormone, men

INTRODUCTION

Although men do not experience a phase of accelerated bone loss similar to the menopause in women, their bone health status declines gradually with age (1). According to the World Health Organization (WHO) diagnostic standard using bone mineral density (BMD) measured by dual-energy X-ray absorptiometry (DXA), approximately 3-6% of men have osteoporosis and 28-47% have osteopenia, and the prevalence of osteoporosis rises to 19% in men who are aged 50 and older (2, 3). While it is established that the primary cause of menopausal-bone loss in women is driven by ovarian failure, in men, the etiology of age-related bone loss is less clear.

In men, sex steroids have an important role in the maintenance of bone strength, as demonstrated by the rapid reductions in bone density following androgen deprivation therapy (4). There is evidence of a small and progressive age-related decline in free testosterone, estradiol and to a lesser extent, progesterone (5, 6) and increases in luteinizing hormone, follicle-stimulating hormone (FSH) and sex hormone-binding globulin (SHBG) (7). However, research into the role of age-related sex hormone changes in the development of male osteoporosis has primarily focused on testosterone and estradiol. Endogenous testosterone levels have been related to bone turnover markers, BMD, and hip structural geometry in normal aging men (8–11). The actions of testosterone on the male skeleton are partly mediated by the aromatization of testosterone to estradiol, with estrogen deficiency also contributing to age-related bone loss in men, and there is cross-sectional and longitudinal evidence to suggest that bioavailable estradiol is more strongly associated with male BMD and fracture (10, 12, 13). Testosterone has been suggested to also play an indirect role in male skeletal health with aging by allowing for relative maintenance of balance and muscle strength in men compared to women (14). SHBG levels in men increase with age and influence the amount of hormone that is available to enter cells, and are predictive of vertebral fracture (15, 16) and/or lower bone density (17).

Relatively less attention has been directed toward the role of other sex steroids in male bone health, particularly of FSH. In women, a sharp rise in serum FSH during late perimenopause coincides with the most rapid rate of bone loss (18) and epidemiological data suggest that bone turnover markers and BMD in perimenopausal and early postmenopausal women are independent of serum estrogen, but negatively associated with FSH (19–21). However, the relationship between FSH and bone mass in men has not yet been fully explored.

Musculoskeletal fragility associated with sarcopenia (loss of muscle mass) and osteopenia (loss of bone mass) can result in fall and fracture. People are diagnosed with osteoporosis often combining with muscles weakness, and increased spine kyphosis leading vertebral fractures (22). Partial androgen deficiency may contribute to the age-related decrease in muscle mass and strength and to the higher risk of fall and fractures in elderly men (23, 24).

In the present cross-sectional study, we observed the variations of endogenous sex hormone concentrations with increasing of age, and investigated their relations to bone mass. Considering the potential roles of marrow adiposity and paravertebral muscle fragility in bone loss and vertebral fractures in old men which may be correlated with sex hormones, we furthermore explored the relationships between endogenous sex hormones concentrations and vertebral marrow fat content as well as paravertebral muscle fat content.

METHODOLOGY

Study Subjects

A total of 199 men aged from 41 and 82 years were recruited from a population study to investigate the degeneration of spine and knee (China Action on Spine and Hip study). All subjects were healthy adults who have lived in Beijing for more than 5 years, and the subjects with the following conditions were excluded: (1) spine or knee disorders due to congenital, tumor or tuberculosis; (2) a history of spine or knee injury or surgery; (3) suffering from other major diseases (such as infection, tumor, rheumatic immune disease, renal failure, coronary heart disease, stroke, and mental diseases) and taking bone metabolism regulating drugs; (4) heart pacemaker, coronary stent, orthopedic implants, and implant teeth; and (5) familial hereditary disease (25). The regional ethics committee approved the study and all participants provided signed, informed consent. The study was carried out in accordance with The Code of Ethics of the World Medical Association (Declaration of Helsinki).

All participants received blood serum tests for the measurement of total estradiol, total testosterone and FSH, and a quantitative computed tomography (QCT) scan for the measurement of vertebral trabecular volumetric BMD (vBMD). Sixty-two participants received Chemistry-shift-encoding magnetic resonance imaging (CSE-MRI) (mDixon-MRI) scans for vertebral marrow fat content and erector muscle fat content.

QCT Scan and Measurements

We performed quantitative CT scan using a Toshiba CT scanner (Aquilion Prime ESX-302A; Toshiba Medical Systems Corporation, Otawara, Japan) with a five-rod calibration phantom (Model 3 phantom; Mindways Inc., Austin, TX, USA) placed beneath the subject and scanned simultaneously. The scanning parameters were as follows: 120kV, 187mAs, table height 120cm, 1 mm slice thickness, field of view (FOV) 500 mm. The scan range included 2 cm above L1 vertebra to 2 cm below L5 vertebra. Reconstruction parameters were standard algorithm, 1 mm section thickness and interval, and 400 mm display FOV.

The CT data were transferred to QCT workstation and analyzed using Mindways QCT PRO three-dimensional (3D) spine module software version 4.2. On the 3D reconstructed images, an elliptical cylinder region of interest (ROI) was individually placed in the central part of L2, L3, and L4 vertebral bodies. The ROIs contained the largest areas of the trabecular bone, but not included the cortical bone or basivertebral plexus. The values of vBMD of L2, L3, and L4 were automatically output. vBMD of lumbar spine was calculated as the mean value of vBMD of L2 to L4.

CSE-MRI Scan and Measurements

On the same day as the QCT examination, the participants underwent a multiecho 3D spoiled gradient-echo sequence, referred to as an mDixon-Quant study, by using a 3.0-T MRI system with a 32-channel torso body coil (Ingenia, Philips Healthcare, Best, the Netherlands). The mDixon-Quant sequence is a 3D-FFE sequence, and uses multiple acquired echoes to generate water, fat, T2*, R2*, and in-phase and oppose-phase images synthesized from the water-fat images. The scan parameters of the single breath-hold mDixon-Quant were as follows: repetition time, 9.1 ms; echo time 1, 1.33 ms; six echoes with echo time shift, 1.3 ms; FOV, 360 × 330 × 120 mm^3; flip angle, 3°; voxel size, 2.5 × 2.5 × 3.0 mm^3; sensitivity encoding, 2; number of signal average, 2; and scan time, 12.5 s.

The CSE-MRI dataset were processed with ISP version 7 software (Philips Healthcare, Best, the Netherlands). ROIs for marrow fat content measurement were drawn manually encompassing the largest region of the cancellous bone of vertebral bodies on central L2, L3, and L4 axial image eliminating the vertebral cortex, schmorl's nodules or hemangiomas. Marrow fat content was calculated as the mean value of L2, L3, and L4 marrow fat contents. The fat content of erector muscle was measured on the same central L3 image. Clear cavities of fat at the periphery of the erector muscle visually identify the edge of the muscle.

Sex Hormone Analyses

For the assessment of endogenous hormone concentrations, a fasted, morning blood sample was taken from each participant on the same day as the imaging examinations. Blood was centrifuged, separated and refrigerated at -80°C until assay. Serum was sent to the laboratory at the Dopbio Biotechnology Co., Ltd for determination of testosterone, estradiol, and FSH concentrations.

Hormone assays were conducted by enzyme-linked immunosorbent assay (ELISA) using the MULTISKAN MK3 automated analyzer (Thermo Scientific, USA). Serum total estradiol concentrations were measured with a solid phase ELISA (DRG Estradiol ELISA, EIA-2693) based to the principle of competitive binding. Inter- and intra-assay coefficients of variation (CV) averaged 9.0% and 10.9%, respectively over the assay range. Serum FSH concentrations were measured with a two-step capture enzyme immunoassay test using constant amounts of two monoclonal antibodies (ALPCO FSH ELISA, 11-FSHHU-E01). One monoclonal antibody specific for FSH is immobilized onto the microplate and another monoclonal antibody specific for a different region of FSH is conjugated to horseradish peroxidase. Inter- and intra-assay CV averaged 4.2% and 5.2%, respectively. Total testosterone concentrations were determined with a competitive enzyme immunoassay (R&D Testosterone Parameter Assay Kit, KGE010). A monoclonal antibody specific for testosterone bounded to the goat anti-mouse antibody coated onto the microplate and then testosterone in a serum sample competed with a fixed amount of horseradish peroxidase-labeled testosterone for sites on the monoclonal antibody. Inter- and intra-assay CV averaged 3.3% and 6.2%, respectively.

Statistical Analysis

Data management and analyses were completed using SPSS version 22.0 (SPSS Inc., Chicago, IL, USA). Distributions of the variables were examined for departure from normality by the Shapiro-Wilk test. Data with normal distribution are presented as the mean ± standard deviation (SD), while data with skewed distribution are presented as the median (interquartile, IQR). For the inter-group comparisons, *t* test was used for normally distributed variables and Mann-Whitney *U* test was used for skewed variables. Multivariate linear regression analysis was performed to estimate the contributions of each sex hormone to vBMD, marrow fat content, and erector muscle fat content, with and without adjustments for age, BMI, and other sex hormones. According to the criteria suggested by the International Society for Clinical Densitometry in 2007 (26) and by the American College of Radiology in 2008 (27) for QCT, the thresholds of vBMD were < 120 mg/cm3 for osteopenia and < 80 mg/cm3 for osteoporosis. The odds ratios (ORs) and 95% confidence intervals (95% CI) of osteopenia/osteoporosis (defined as vBMD < 120 mg/cm^3), higher marrow fat content (marrow fat content ≥ 45%), and higher muscle fat content (erector muscle fat content ≥ 10%) were calculated by logistic regression models with and without adjustments for age, BMI, and other sex hormones, in which sex hormone levels were fitted as continuous variables with results expressed in terms of per SD increase in hormone concentration.

RESULTS

The general characteristics of the study participants are shown in **Table 1**. Participants were stratified into four sub-groups according to age, and the characteristics of each group and inter-group comparisons are also presented in **Table 1**. FSH concentrations were higher with increasing age ($p < 0.001$), but there were no age related differences in total estradiol concentration ($p = 0.90$). With aging, lumbar spine vertebral vBMD decreased ($p < 0.001$) and erector muscle fat content increased ($p = 0.034$) gradually. There were no significant age-related differences in marrow fat content ($p = 0.574$).

Further sub-group analysis was completed according to presence of osteopenia and osteoporosis (normal bone mass: vBMD ≥ 120 mg/mm^3 and osteopenia/osteoporosis: vBMD < 120 mg/mm^3) and of obesity (non-obesity: BMI < 25 kg/m^2 and obesity: BMI ≥ 25 kg/m^2), respectively, and inter-group comparisons are shown in **Table 2**. Participants who were osteopenic or osteoporotic had significantly higher FSH concentrations ($p = 0.005$), marrow fat content ($p = 0.002$), and erector muscle fat content ($p = 0.003$). Obese participants had significantly higher total testosterone concentrations ($p = 0.004$), but there were no differences in vBMD or fat content measurements.

Associations between sex hormone concentrations, vBMD, and fat content measurements are shown in **Table 3**. Lower vBMD was associated with higher FSH concentration ($\beta = -0.216$, $p < 0.001$), but not with total estradiol or total testosterone concentration (**Table 3**), after adjustment for age,

TABLE 1 | Demographic and biologic characteristics of 199 men overall, and of the men at different levels of age.

	Mean Value (± SD)/Median (IQR)[b]					
	All (n = 199)	**age ≤ 50 yrs (n = 35)**	**50 < age ≤ 60 yrs (n = 51)**	**60 < age ≤ 70 yrs (n = 75)**	**age > 70 yrs (n = 38)**	***P* value[c]**
Age (years)	61 (52, 68)	46 (44, 47)	56 (52, 58)	64 (61, 67)	72 (71, 75)	<0.001
BMI (kg/m^2)	24.8 (22.4, 28.9)	23.1 (21.7, 25.3)	25.4 (22.8, 29.8)	25.6 (22.6, 34.4)	24.85 ± 4.14	0.062
Follicle-stimulating hormone (IU/L)	10.87 (7.52, 16.55)	9.02 ± 3.60	10.70 (6.42, 16.48)	11.09 (7.67, 16.39)	13.42 (9.03, 26.39)	<0.001
Estradiol (pg/mL)	32.66 (19.62, 51.24)	30.24 (15.97, 52.37)	34.94 (19.84, 53.14)	30.05 (20.58, 50.44)	39.10 (19.31, 46.83)	0.90
Testosterone (ng/mL)	7.90 (4.98, 11.18)	5.50 (3.50, 8.33)	8.55 ± 4.16	9.54 ± 4.69	7.20 (4.82, 9.68)	0.017
Volumetric bone mineral density (mg/mm^3)	115.07 ± 32.51	139.07 ± 24.11	122.69 ± 23.49	111.64 ± 32.31	89.52 ± 31.15	<0.001
Marrow Fat Content (%)[a]	44.67 ± 8.23	39.84 ± 6.97	44.90 ± 7.28	45.09 ± 9.28	46.91 (45.16, 47.06)	0.574
Erector Muscle Fat Content (%)[a]	8.44 ± 4.63	5.57 (3.04, 5.57)	7.74 ± 3.62	8.46 ± 4.25	12.67 ± 6.97	0.034

[a]*For marrow fat content and erector muscle fat content measurements, number of the whole study sample group and of each group stratified by age with an interval of 10 years was as follow: 62 for all, 5 for the group aged no more than 50 years, 15 for the group aged between 50 to 60 years, 35 for the group aged between 60 to 70 years, and 7 for the group aged over 70 years, respectively;*

[b]*Continuous variables were tested by the Shapiro-Wilk test: normally distributed variables are presented as mean± SD, while skewed variables are presented as the median (first-fourth quartiles);*

[c]*For the comparisons among the groups stratified by age, t test was used for normally distributed variables and Mann-Whitney U test was used for skewed variables.*

TABLE 2 | Comparisons of demographic and biologic characteristics between the participants with normal bone mineral content and with decreased bone mineral content (osteopenia or osteoporosis), and between non-obese and obese participants.

	Mean Value (± SD)/Median (IQR)[b]							
	Normal bone mass (vBMD ≥ 120 mg/mm^3) (n = 92)	**Osteopenia/ Osteoporosis (vBMD < 120 mg/mm^3) (n = 107)**	***P* value[c]**	***power***	**BMI < 25 kg/m^2 (n = 105)**	**BMI ≥ 25 kg/m^2 (n = 94)**	***P* value[c]**	***power***
Age (years)	58 (47, 61)	65 (58, 70)	<0.001	1	60 (50, 69)	61 (57, 67)	0.227	0.301
BMI (kg/m^2)	24.4 (22.4, 27.5)	25.1 (22.3, 30.0)	0.410	0.220	22.2 (20.8, 23.7)	29.2 (26.3, 36.8)	<0.001	1
Follicle-stimulating hormone (IU/L)	9.35 (6.94, 13.7)	11.45 (7.97, 19.4)	0.005	0.933	10.95 (7.67, 17.15)	10.80 (7.10, 16.23)	0.565	0.088
Estradiol (pg/mL)	31.8 (19.43, 52.95)	34.19 (19.62, 49.72)	0.615	0.131	34.70 (18.06, 52.38)	29.99 (20.50, 48.53)	0.619	0.064
Testosterone (ng/mL)	7.81 (4.98, 10.85)	7.97 (4.85, 11.38)	0.933	0.052	6.61 (4.73, 9.68)	9.17 (5.33, 12.38)	0.004	0.720
Volumetric bone mineral density (mg/mm^3)	138.42 (128.38, 155.42)	94.17 (77.86, 107.89)	< 0.001	1	117.73 ± 34.40	112.11 ± 30.17	0.341	0.024
Marrow Fat Content (%)[a]	40.74 ± 7.83	47.16 ± 7.56	0.002	0.838	42.08 (39.78, 52.10)	44.49 ± 8.27	0.938	0.062
Erector Muscle Fat Content (%)[a]	6.31 ± 4.11	9.79 ± 4.47	0.003	0.843	8.79 ± 5.46	8.35 ± 4.44	0.685	0.299

[a]*For marrow fat content and erector muscle fat content measurements, number of those with normal bone mineral content, those with decreased bone mineral content (osteopenia/ osteoporosis), those of non-obesity (BMI < 25), and those of obesity (BMI ≥ 25) was 24, 38, 13, and 49, respectively;*

[b]*Continuous variables were tested by the Shapiro-Wilk test: normally distributed variables are presented as mean± SD, while skewed variables are presented as the median (first-fourth quartiles);*

[c]*For the comparison between normal bone mineral content and osteopenia/osteoporosis and the comparison between non-obesity (BMI < 25) and obesity (BMI ≥ 25), t test was used for normally distributed variables and Mann-Whitney U test was used for skewed variables.*

BMI, and other sex hormones. Neither bone marrow fat content nor erector muscle fat content was associated with sex hormone concentrations after adjustment for age, BMI, and other sex hormones.

Adjusted and non-adjusted logistic regression analysis found that for each SD increase in FSH there was a 50% higher risk of an individual having osteopenia or osteoporosis (**Table 4**). All the three sex hormones showed no significant contributions to

TABLE 3 | Multivariate linear regression analysis showing the factors determining vBMD and fat measurements.

	Follicle-stimulating hormone		Estradiol		Testosterone	
	Unadjusted β	MV adjusted[a] β	Unadjusted β	MV Adjusted[a] β	Unadjusted β	MV Adjusted[a] β
Volumetric bone mineral density	-0.349**	-0.216**	0.017	0.014	-0.027	-0.018
Marrow Fat Content	0.181	0.164	-0.087	-0.099	-0.011	0.052
Erector Muscle Fat Content	0.114	-0.006	-0.140	-0.119	-0.248*	-0.145

[a]*Adjusted for age, BMI and mutual adjustment for other sex hormones;*
**Indicates 0.01 ≤ p < 0.05, and **indicates p < 0.01.*

the risk of higher marrow fat content or higher erector fat content after multivariate adjustment.

DISCUSSION

This study is the first to explore associations between sex hormones, bone density, marrow adiposity and muscle adiposity in community-dwelling middle and older aged men. In doing so, we found that high concentration of FSH, but not total testosterone or estradiol, was a risk factor for lower vBMD, osteopenia and osteoporosis. While marrow fat content and erector muscle fat content were greater in osteopenic and osteoporotic men, there were no associations with sex hormones concentrations.

Our primary finding was of significant associations between high FSH and low vertebral trabecular vBMD in men. There is accumulating evidence that FSH acts on bone through both direct and indirect mechanisms. First, FSH acts directly through the FSHR on osteoclast precursors to increase osteoclastogenesis by sensitizing MAP kinase, NF-κB, and Akt pathways, and blocking FSHRs or the β-subunit of FSH, can prevent bone loss in mice independent of estrogen (28). Second, FSH increases expression of the receptor activator of NF-κB (29) and indirectly stimulates osteoclastogenesis by releasing cytokines, namely IL-1β, TNF-α, and IL-6 in proportion to the surface expression of FSHR (21, 30). Elsewhere, *in-vivo* evidence regarding the relationship between FSH and bone mass in men is limited. Hsu B, et al. reported that lower levels of serum FSH were protective against bone loss and were negatively associated with incident fractures in a cohort of elderly men (31). In addition, Jing, et al. have demonstrated associations between FSH, lumbar spine BMD and osteoporosis in men with type 2 diabetes mellitus (32).

In this study, we found no associations between total estradiol, total testosterone and vertebral trabecular vBMD. Elsewhere, studies have supported estradiol as the crucial sex steroid for bone health in men, and others, provide evidence for testosterone and SHBG (8–11, 32–37). In elderly men, bioavailable estradiol has been found to be positively associated with BMD at multiple sites (8, 10, 11, 33–35), and higher bioavailable estradiol is suggested to be a protective factor for osteopenia (9). Total estradiol has also been reported to be a significant determinant of bone mass in elderly men (10, 24, 34, 36). In a study involving a diverse sample of men (Black, Hispanic, and White, aged 30 to 79 years), total and free estradiol showed larger positive correlations with BMD outcomes and correlations between estradiol levels and hip BMD were robust after multivariate-adjustment, whereas no correlation between total or free estradiol and lumbar spine BMD after multivariate-adjustment (8). In aging Chinese men, both bioavailable and total estradiol have been demonstrated with a positive association with both total hip and lumbar spine BMD after multivariate- or age-adjustment (32, 37). The bioavailable sex steroids comprise the fractions that are free or associated with albumin in the circulation (38), and it is these fractions that have rapid access to target tissues (39). The free fraction constitutes only 1-3% of the total circulating sex steroids (38). In contrast, the fraction bound to SHBG does not have free access to target tissue. As SHBG levels increase with age in men, measurement of total testosterone or estradiol levels does not accurately reflect the actual levels of these steroids available to tissue.

TABLE 4 | OR of osteopenia/osteoporosis, higher marrow fat, and higher muscle fat (erector muscle fat content ≥ 10%) per SD increase in FSH, estradiol, and testosterone concentrations in men.

	Follicle-stimulating hormone		Estradiol		Testosterone	
	Unadjusted OR (95% CI)	MV adjusted[a] OR (95% CI)	Unadjusted OR (95% CI)	MV adjusted[a] OR (95% CI)	Unadjusted OR (95% CI)	MV adjusted[a] OR (95% CI)
Osteopenia/Osteoporosis	1.895** (1.299-2.762)	1.509* (1.015-2.242)	0.886 (0.669-1.172)	0.853 (0.618-1.179)	0.983 (0.743-1.299)	0.881 (0.629-1.234)
higher marrow fat content (≥ 45%)	1.374 (0.859-2.199)	1.186 (0.695-2.024)	0.867 (0.485-1.550)	0.801 (0.407-1.575)	0.580 (0.289-1.166)	0.702 (0.332-1.484)
higher erector muscle fat content (≥ 10%)	1.124 (0.717-1.761)	0.994 (0.561-1.760)	0.803 (0.421-1.529)	0.715 (0.332-1.538)	0.475 (0.215-1.051)	0.524 (0.220-1.247)

[a]*Adjusted for age, BMI and mutual adjustment for other sex hormones.*
**Indicates 0.01 ≤ p < 0.05, and **indicates p < 0.01.*

The evidence around the role of testosterone for bone health in elderly men is more conflicting, than the evidence for estradiol (9–11, 24, 34, 36). A study on American men aged 20–90 years found that men with free testosterone level at the lowest quartile were more likely to be osteopenic (9). A study by Van Den Beld et al. also found a positive and significant association between testosterone levels (total, free, and bioavailable fraction and androgen index) and proximal femoral BMD in older men (10). The Swedish Osteoporotic Fractures in Men (MrOS) Study discovered that free testosterone was an independent positive predictor of BMD in total body, total hip, femur trochanter, and arm but not in the lumbar spine (11). The Hong Kong MrOS study also found a positive and significant relationship between femoral and vertebral BMD and free testosterone in Chinese men aged 65 years and above (37). However, discrepancies exist among different studies, and some have reported no associations between bone health status in men and total testosterone (8, 9, 34), and studies have found that the relationship between testosterone and BMD is not consistent at different testing sites (35). The effects of testosterone can be exerted either directly through the androgen receptor or indirectly through aromatization to estrogens and further through estrogen receptor-α and/or –β (40). These sex steroid receptors are expressed in bone, and experimental animal studies, using sex steroid receptor-inactivated transgenic mouse model, have indicated that each of these three receptors mediate the site-specific skeletal effects of sex steroids (41, 42).

To date, most studies have been conducted using DXA measured BMD, which cannot separate trabecular from cortical bone. Trabecular bone is known to have a more rapid rate of age-related loss than cortical bone. This may diminish the sensitivity of DXA for assessing osteoporosis. QCT is a truly three dimensional technique for quantifying volumetric trabecular bone density that is not affected by spine degeneration and abdominal aortic calcification (43). Khosla et al, measured vBMD using QCT and showed that vertebral trabecular vBMD was significantly associated with bioavailable estradiol and bioavailable testosterone in the entire group of men (22 to 91 years) (33). After adjusting for age, bioavailable testosterone was more strongly associated with vertebral trabecular vBMD than bioavailable estradiol in the middle-aged men (40-59 years), while bioavailable estradiol was the best predictor of vBMD at most sites in the elderly men (≥ 60 years) (33).

In the current study, there were no associations between sex hormone concentrations and marrow fat content, despite evidence that marrow fat increases with age (44, 45). Mistry et al, have reported that marrow adiposity is negatively associated with both total estradiol and total testosterone in aging men (74 to 95 years of age) after adjusting for age and total percent fat (46). The possible reasons for the discrepancies with Mistry's results may be firstly, the number size of this study (n = 62) was small and secondly, the participants in this study are much younger than those in Mistry's study (61 years vs. 82.4 years). FSH receptor cDNA and protein have been identified on osteoclasts and mesenchymal stem cells (28). An animal study showed that both sham-operated and ovariectomized mice presented a decrease in marrow adipose volume after FSH antibody treatments (47). Our study did not find a significant association between marrow fat content and FSH concentration in this middle-aged to older male population, and furthermore, the increase of FSH was not a risk factor for higher marrow fat content.

In the context of muscle aging, it is important to remember that it is not just a decline in muscle mass which contributes to the deterioration of muscle function. Factors underpinning muscle quality come into play, including muscle composition, aerobic capacity and metabolism, fatty infiltration, insulin resistance, fibrosis and neural activation (48). Observational studies have shown that lean mass and strength are reduced in men with low testosterone levels (10, 23), and testosterone replacement increases lean mass in men with hypogonadism (49). In the present cross-sectional study, total testosterone concentration was detected with a weakly negative correlation with erector muscle fat content by unadjusted linear regression analysis, however, the correlation was insignificant after adjusting for age, BMI, total estradiol concentration, and FSH concentration. The increase of total testosterone for 1 SD was not a significant protective factor for higher erector muscle fat content (≥ 10%). Considering lean mass, muscle area, and muscle strength were preserved until gonadal steroid deficiency was more mark according to Finkelstein et al. (a testosterone level ≤ 200 ng per deciliter) (50), our results are not unexpected.

The main limitation of this study was the relative small sample size (n = 199), especially only 62 participants had MR measurements of marrow fat content and muscle fat content, and as a result, the relationships between sex hormones and MR-quantified marrow fat and muscle fat content may not be fully revealed. In addition, luteinizing hormone and SHBG were not measured, and therefore, free estradiol and free testosterone could not be calculated and investigated in this study. The smoking and drinking history were not obtained in this study, and therefore, neither multivariate linear regression analyses for the contributions of sex hormones to vBMD nor ORs of osteopenia/osteoporosis were adjusted for smoking and drinking.

CONCLUSION

FSH but not total estradiol or total testosterone is related to vertebral trabecular vBMD in middle-aged and older Chinese men. Neither marrow adiposity nor muscle adiposity is associated with total estradiol, total testosterone, or FSH.

DATA AVAILABILITY STATEMENT

The original contributions presented in the study are included in the article/supplementary files. Further inquiries can be directed to the corresponding author.

ETHICS STATEMENT

The studies involving human participants were reviewed and approved by Beijing Jishuitan Hospital Ethics Committee. The patients/participants provided their written informed consent to participate in this study.

AUTHOR CONTRIBUTIONS

The first authorship of LX and QZ is of an equal rank. LX and QZ designed the study and prepared the first draft of the paper. KL, YZ, and YL contributed the experimental work and data collection. KH and LW edited the draft. CW was responsible of the statistical analysis of the data. XC supervised the study and paper organization. All authors revised the paper critically for intellectual content and approved the final version. All authors agree to be accountable for the work and to ensure that any questions relating to the accuracy and integrity of the paper are investigated and properly resolved.

FUNDING

This work was funded by the grants from the National Key Research and Development Program of China [No. 2020YFC2004902], the Beijing Hospitals Authority Clinical Medicine Development of Special Funding Support [No. ZYLX202107], the National Natural Science Foundation of China [No. 81771831, 2018], and the High Level Talents "Discipline backbone" Project of Beijing Jishuitan Hospital [No. XKGG2021123].

ACKNOWLEDGMENTS

We thank our study participants for contributing their time and efforts. We wish to thank Dopbio Biotechnology for their technical supports in blood testing. We also thank National Natural Science Foundation of China for the fund support to this study.

REFERENCES

1. Melton LJ 3rd, Khosla S, Achenbach SJ, O'Connor MK, O'Fallon WM, Riggs BL. Effects of Body Size and Skeletal Site on the Estimated Prevalence of Osteoporosis in Women and Men. *Osteoporos Int* (2000) 11(11):977–83. doi: 10.1007/s001980070037
2. Looker AC, Orwoll ES, Johnston CC Jr, Lindsay RL, Wahner HW, Dunn WL, et al. Prevalence of Low Femoral Bone Density in Older U.S. Adults From NHANES III. *J Bone Miner Res* (1997) 12(11):1761–8. doi: 10.1359/jbmr.1997.12.11.1761
3. Melton LJ 3rd, Atkinson EJ, O'Connor MK, O'Fallon WM, Riggs BL. Bone Density and Fracture Risk in Men. *J Bone Miner Res* (1998) 13(12):1915–23. doi: 10.1359/jbmr.1998.13.12.1915
4. Daniell HW, Dunn SR, Ferguson DW, Lomas G, Niazi Z, Stratte PT. Progressive Osteoporosis During Androgen Deprivation Therapy for Prostate Cancer. *J Urol* (2000) 163(1):181–6. doi: 10.1097/00005392-200001000-00043
5. Wu IC, Lin XZ, Liu PF, Tsai WL, Shiesh SC. Low Serum Testosterone and Frailty in Older Men and Women. *Maturitas* (2010) 67(4):348–52. doi: 10.1016/j.maturitas.2010.07.010
6. Walther A, Philipp M, Lozza N, Ehlert U. The Rate of Change in Declining Steroid Hormones: A New Parameter of Healthy Aging in Men? *Oncotarget* (2016) 7(38):60844–57. doi: 10.18632/oncotarget.11752
7. Feldman HA, Longcope C, Derby CA, Johannes CB, Araujo AB, Coviello AD, et al. Age Trends in the Level of Serum Testosterone and Other Hormones in Middle-Aged Men: Longitudinal Results From the Massachusetts Male Aging Study. *J Clin Endocrinol Metab* (2002) 87(2):589–98. doi: 10.1210/jcem.87.2.8201
8. Araujo AB, Travison TG, Leder BZ, McKinlay JB. Correlations Between Serum Testosterone, Estradiol, and Sex Hormone-Binding Globulin and Bone Mineral Density in a Diverse Sample of Men. *J Clin Endocrinol Metab* (2008) 93(6):2135–41. doi: 10.1210/jc.2007-1469
9. Paller CJ, Shiels MS, Rohrmann S, Basaria S, Rifai N, Nelson W, et al. Relationship of Sex Steroid Hormones With Bone Mineral Density (BMD) in a Nationally Representative Sample of Men. *Clin Endocrinol (Oxf)* (2009) 70(1):26–34. doi: 10.1111/j.1365-2265.2008.03300.x
10. van den Beld AW, de Jong FH, Grobbee DE, Pols HA, Lamberts SW. Measures of Bioavailable Serum Testosterone and Estradiol and Their Relationships With Muscle Strength, Bone Density, and Body Composition in Elderly Men. *J Clin Endocrinol Metab* (2000) 85(9):3276–82. doi: 10.1210/jcem.85.9.6825
11. Mellström D, Johnell O, Ljunggren O, Eriksson AL, Lorentzon M, Mallmin H, et al. Free Testosterone Is an Independent Predictor of BMD and Prevalent Fractures in Elderly Men: MrOS Sweden. *J Bone Miner Res* (2006) 21(4):529–35. doi: 10.1359/jbmr.060110
12. Khosla S, Melton LJ 3rd, Atkinson EJ, O'Fallon WM. Relationship of Serum Sex Steroid Levels to Longitudinal Changes in Bone Density in Young Versus Elderly Men. *J Clin Endocrinol Metab* (2001) 86(8):3555–61. doi: 10.1210/jcem.86.8.7736
13. Mellström D, Vandenput L, Mallmin H, Holmberg AH, Lorentzon M, Odén A, et al. Older Men With Low Serum Estradiol and High Serum SHBG Have an Increased Risk of Fractures. *J Bone Miner Res* (2008) 23(10):1552–60. doi: 10.1359/jbmr.080518
14. Khosla S, Melton LJ 3rd, Riggs BL. The Unitary Model for Estrogen Deficiency and the Pathogenesis of Osteoporosis: Is a Revision Needed? *J Bone Miner Res* (2011) 26(3):441–51. doi: 10.1002/jbmr.262
15. Cawthon PM, Schousboe JT, Harrison SL, Ensrud KE, Black D, Cauley JA, et al. Sex Hormones, Sex Hormone Binding Globulin, and Vertebral Fractures in Older Men. *Bone* (2016) 84:271–8. doi: 10.1016/j.bone.2016.01.009
16. Vandenput L, Mellström D, Kindmark A, Johansson H, Lorentzon M, Leung J, et al. High Serum SHBG Predicts Incident Vertebral Fractures in Elderly Men. *J Bone Miner Res* (2016) 31(3):683–9. doi: 10.1002/jbmr.2718
17. Hsu B, Seibel MJ, Cumming RG, Blyth FM, Naganathan V, Bleicher K, et al. Progressive Temporal Change in Serum SHBG, But Not in Serum Testosterone or Estradiol, Is Associated With Bone Loss and Incident Fractures in Older Men: The Concord Health and Ageing in Men Project. *J Bone Miner Res* (2016) 31(12):2115–22. doi: 10.1002/jbmr.2904
18. Zaidi M, Lizneva D, Kim SM, Sun L, Iqbal J, New MI, et al. FSH, Bone Mass, Body Fat, and Biological Aging. *Endocrinology* (2018) 159(10):3503–14. doi: 10.1210/en.2018-00601
19. Sowers MR, Greendale GA, Bondarenko I, Finkelstein JS, Cauley JA, Neer RM, et al. Endogenous Hormones and Bone Turnover Markers in Pre- and Perimenopausal Women: SWAN. *Osteoporos Int* (2003) 14(3):191–7. doi: 10.1007/s00198-002-1329-4
20. Gallagher CM, Moonga BS, Kovach JS. Cadmium, Follicle-Stimulating Hormone, and Effects on Bone in Women Age 42–60 Years, NHANES III. *Environ Res* (2010) 110(1):105–11. doi: 10.1016/j.envres.2009.09.012
21. Cannon JG, Cortez-Cooper M, Meaders E, Stallings J, Haddow S, Kraj B, et al. Follicle-Stimulating Hormone, Interleukin-1, and Bone Density in Adult Women. *Am J Physiol Regul Integr Comp Physiol* (2010) 298(3):R790–8. doi: 10.1152/ajpregu.00728.2009
22. Hsu WL, Chen CY, Tsauo JY, Yang RS. Balance Control in Elderly People With Osteoporosis. *J Formos Med Assoc* (2014) 113(6):334–9. doi: 10.1016/j.jfma.2014.02.006
23. Baumgartner RN, Waters DL, Gallagher D, Morley JE, Garry PJ. Predictors of Skeletal Muscle Mass in Elderly Men and Women. *Mech Aging Dev* (1999) 107(2):123–36. doi: 10.1016/s0047-6374(98)00130-4

24. Szulc P, Claustrat B, Marchand F, Delmas PD. Increased Risk of Falls and Increased Bone Resorption in Elderly Men With Partial Androgen Deficiency: The MINOS Study. *J Clin Endocrinol Metab* (2003) 88(11):5240–7. doi: 10.1210/jc.2003-030200
25. Zhang Y, Zhou Z, Wu C, Zhao D, Wang C, Cheng X, et al. Population-Stratified Analysis of Bone Mineral Density Distribution in Cervical and Lumbar Vertebrae of Chinese From Quantitative Computed Tomography. *Korean J Radiol* (2016) 17(5):581–9. doi: 10.3348/kjr.2016.17.5.581
26. Engelke K, Adams JE, Armbrecht G, Augat P, Bogado CE, Bouxsein ML, et al. Clinical Use of Quantitative Computed Tomography and Peripheral Quantitative Computed Tomography in the Management of Osteoporosis in Adults: The 2007 ISCD Official Positions. *J Clin Densitom* (2008) 11 (1):123–62. doi: 10.1016/j.jocd.2007.12.010
27. American College of Radiology. *Reston, "ACR Practice Guide Line for the Performance of Quantitative Computed Tomogramphy (QCT) Bone Densitometry (Resolution33)* (2008). Available at: http://www.acr.org/w/media/ACR/Documents/PGTS/guidelines/QCT.pdf.
28. Sun L, Peng Y, Sharrow AC, Iqbal J, Zhang Z, Papachristou DJ, et al. FSH Directly Regulates Bone Mass. *Cell* (2006) 125(2):247–60. doi: 10.1016/j.cell.2006.01.051
29. Cannon JG, Kraj B, Sloan G. Follicle-Stimulating Hormone Promotes RANK Expression on Human Monocytes. *Cytokine* (2011) 53(2):141–4. doi: 10.1016/j.cyto.2010.11.011
30. Iqbal J, Sun L, Kumar TR, Blair HC, Zaidi M. Follicle-Stimulating Hormone Stimulates TNF Production From Immune Cells to Enhance Osteoblast and Osteoclast Formation. *Proc Natl Acad Sci USA* (2006) 103(40):14925–30. doi: 10.1073/pnas.0606805103
31. Hsu B, Cumming RG, Seibel MJ, Naganathan V, Blyth FM, Bleicher K, et al. Reproductive Hormones and Longitudinal Change in Bone Mineral Density and Incident Fracture Risk in Older Men: The Concord Health and Aging in Men Project. *J Bone Miner Res* (2015) 30(9):1701–8. doi: 10.1002/jbmr.2493
32. Jing Y, Wang X, Yu J, Wang X, Zhou Y, Tao B, et al. Follicle-Stimulating Hormone and Estradiol are Associated With Bone Mineral Density and Risk of Fracture in Men With Type 2 Diabetes Mellitus. *J Diabetes* (2020) 12 (6):426–37. doi: 10.1111/1753-0407.13011
33. Khosla S, Melton LJ 3rd, Robb RA, Camp JJ, Atkinson EJ, Oberg AL, et al. Relationship of Volumetric BMD and Structural Parameters at Different Skeletal Sites to Sex Steroid Levels in Men. *J Bone Miner Res* (2005) 20 (5):730–40. doi: 10.1359/JBMR.041228
34. Khosla S, Melton LJ 3rd, Atkinson EJ, O'Fallon WM, Klee GG, Riggs BL. Relationship of Serum Sex Steroid Levels and Bone Turnover Markers With Bone Mineral Density in Men and Women: A Key Role for Bioavailable Estrogen. *J Clin Endocrinol Metab* (1998) 83(7):2266–74. doi: 10.1210/jcem.83.7.4924
35. Venkat K, Desai M, Arora MM, Singh P, Khatkhatay MI. Age-Related Changes in Sex Steroid Levels Influence Bone Mineral Density in Healthy Indian Men. *Osteoporos Int* (2009) 20(6):955–62. doi: 10.1007/s00198-008-0765-1
36. Amin S, Zhang Y, Sawin CT, Evans SR, Hannan MT, Kiel DP, et al. Association of Hypogonadism and Estradiol Levels With Bone Mineral Density in Elderly Men From the Framingham Study. *Ann Intern Med* (2000) 133(12):951–63. doi: 10.7326/0003-4819-133-12-200012190-00010
37. Woo J, Kwok T, Leung JC, Ohlsson C, Vandenput L, Leung PC. Sex Steroids and Bone Health in Older Chinese Men. *Osteoporos Int* (2012) 23(5):1553–62. doi: 10.1007/s00198-011-1552-y
38. Södergård R, Bäckström T, Shanbhag V, Carstensen H. Calculation of Free and Bound Fractions of Testosterone and Estradiol-17 Beta to Human Plasma Proteins at Body Temperature. *J Steroid Biochem* (1982) 16(6):801–10. doi: 10.1016/0022-4731(82)90038-3
39. Manni A, Pardridge WM, Cefalu W, Nisula BC, Bardin CW, Santner SJ, et al. Bioavailability of Albumin-Bound Testosterone. *J Clin Endocrinol Metab* (1985) 61(4):705–10. doi: 10.1210/jcem-61-4-705
40. Riggs BL, Khosla S, Melton LJ 3rd. Sex Steroids and the Construction and Conservation of the Adult Skeleton. *Endocr Rev* (2002) 23(3):279–302. doi: 10.1210/edrv.23.3.0465
41. Sims NA, Clément-Lacroix P, Minet D, Fraslon-Vanhulle C, Gaillard-Kelly M, Resche-Rigon M, et al. A Functional Androgen Receptor Is Not Sufficient to Allow Estradiol to Protect Bone After Gonadectomy in Estradiol Receptor-Deficient Mice. *J Clin Invest* (2003) 111(9):1319–27. doi: 10.1172/JCI17246
42. Vidal O, Lindberg MK, Hollberg K, Baylink DJ, Andersson G, Lubahn DB, et al. Estrogen Receptor Specificity in the Regulation of Skeletal Growth and Maturation in Male Mice. *Proc Natl Acad Sci U S A* (2000) 97(10):5474–9. doi: 10.1073/pnas.97.10.5474
43. Xu XM, Li N, Li K, Li XY, Zhang P, Xuan YJ, et al. Discordance in Diagnosis of Osteoporosis by Quantitative Computed Tomography and Dual-Energy X-Ray Absorptiometry in Chinese Elderly Men. *J Orthop Translat* (2018) 18:59–64. doi: 10.1016/j.jot.2018.11.003
44. Kugel H, Jung C, Schulte O, Heindel W. Age- and Sex-Specific Differences in the 1H-Spectrum of Vertebral Bone Marrow. *J Magn Reson Imaging* (2001) 13 (2):263–8. doi: 10.1002/1522-2586(200102)13:2<263::aid-jmri1038>3.0.co;2-m
45. Griffith JF, Yeung DK, Ma HT, Leung JC, Kwok TC, Leung PC. Bone Marrow Fat Content in the Elderly: A Reversal of Sex Difference Seen in Younger Subjects. *J Magn Reson Imaging* (2012) 36(1):225–30. doi: 10.1002/jmri.23619
46. Mistry SD, Woods GN, Sigurdsson S, Ewing SK, Hue TF, Eiriksdottir G, et al. Sex Hormones are Negatively Associated With Vertebral Bone Marrow Fat. *Bone* (2018) 108:20–4. doi: 10.1016/j.bone.2017.12.009
47. Liu P, Ji Y, Yuen T, Rendina-Ruedy E, DeMambro VE, Dhawan S, et al. Blocking FSH Induces Thermogenic Adipose Tissue and Reduces Body Fat. *Nature* (2017) 546(7656):107–12. doi: 10.1038/nature22342
48. Curtis E, Litwic A, Cooper C, Denison E. Determinants of Muscle and Bone Aging. *J Cell Physiol* (2015) 230(11):2618–25. doi: 10.1002/jcp.25001
49. Page ST, Amory JK, Bowman FD, Anawalt BD, Matsumoto AM, Bremner WJ, et al. Exogenous Testosterone (T) Alone or With Finasteride Increases Physical Performance, Grip Strength, and Lean Body Mass in Older Men With Low Serum T. *J Clin Endocrinol Metab* (2005) 90(3):1502–10. doi: 10.1210/jc.2004-1933
50. Finkelstein JS, Lee H, Burnett-Bowie SA, Pallais JC, Yu EW, Borges LF, et al. Gonadal Steroids and Body Composition, Strength, and Sexual Function in Men. *N Engl J Med* (2013) 369(11):1011–22. doi: 10.1056/NEJMoa1206168

Conflict of Interest: The authors declare that the research was conducted in the absence of any commercial or financial relationships that could be construed as a potential conflict of interest.

frontiers | Frontiers in Endocrinology

ORIGINAL RESEARCH
published: 26 May 2022
doi: 10.3389/fendo.2022.792819

Association of Paraspinal Muscle CSA and PDFF Measurements With Lumbar Intervertebral Disk Degeneration in Patients With Chronic Low Back Pain

Yilong Huang[1†], Ling Wang[2†], Xiaomin Zeng[1,3], Jiaxin Chen[1], Zhenguang Zhang[1], Yuanming Jiang[1], Lisha Nie[4], Xiaoguang Cheng[2] and Bo He[1*]*

[1] Department of Medical Imaging, the First Affiliated Hospital of Kunming Medical University, Kunming, China, [2] Department of Radiology, Beijing Jishuitan Hospital, Beijing, China, [3] GE Healthcare, Magnetic Resonance Field Application Team, Chengdu, China, [4] GE Healthcare, Magnetic Resonance Research China, Beijing, China

OPEN ACCESS

Edited by:
Giuseppe Guglielmi,
University of Foggia, Italy

Reviewed by:
Maria Pilar Aparisi Gomez,
Auckland District Health Board,
New Zealand
Wenmin Guan,
Capital Medical University, China

***Correspondence:**
Bo He
hebo_ydyy@qq.com
Xiaoguang Cheng
xiao65@263.net

†These authors have contributed equally to this work

Specialty section:
This article was submitted to Bone Research, a section of the journal Frontiers in Endocrinology

Received: 11 October 2021
Accepted: 21 April 2022
Published: 26 May 2022

Citation:
Huang Y, Wang L, Zeng X, Chen J, Zhang Z, Jiang Y, Nie L, Cheng X and He B (2022) Association of Paraspinal Muscle CSA and PDFF Measurements With Lumbar Intervertebral Disk Degeneration in Patients With Chronic Low Back Pain. Front. Endocrinol. 13:792819. doi: 10.3389/fendo.2022.792819

There is an interaction between the lumbar spine and paraspinal muscles, which may play a role in the development of intervertebral disc (IVD) degeneration and may affect CLBP. The study aims to assess the relationship between IVD degeneration and paraspinal muscle fat infiltration in CLBP patients by quantitative MR imaging, and to evaluate the influence of sex and age on CLBP muscle fat infiltration. Sixty CLBP patients (46.3 years ±17.0) and thirty-two healthy subjects (44.9 years ±17.6) were recruited for this study. 3.0 T MRI was used to perform the sagittal and axial T1, T2 of the lumbar spine, and axial paraspinal muscle IDEAL imaging at the L4/5 and L5/S1 levels. Proton density fat fraction (PDFF) of the multifidus and erector spinae at two IVD levels were measured. The Pfirrmann grades of IVD degeneration, Oswestry Disability Index (ODI), and Visual Analog Scale (VAS) were also evaluated. Compare the cross-sectional area (CSA) and PDFF of the paraspinal muscles between CLBP patients and healthy subjects, and analyze the relationship between the muscle PDFF and Pfirrmann grades, gender, and age of CLBP patients. Compared with healthy subjects, the CSA of the multifidus muscle in CLBP patients decreased (1320.2±188.1mm^2 *vs.* 1228.7±191.0 mm^2, $p<0.05$) at the L4/5 level, the average PDFF increased, (7.7±2.6% *vs.* 14.79±5.3%, 8.8±4.2% *vs.* 16.03±5.3%, all $p<0.05$) at both L4/5 and L5/S1 levels. The PDFF of paraspinal muscles were correlated with adjacent IVD degeneration, ODI and VSA in CLBP patients (all $p<0.05$). After using age and body mass index (BMI) as control variables, significance was retained (all $p<0.05$). Multiple regression analysis revealed sex and age also were significantly associated with multifidus PDFF (all $p < 0.05$). This study confirmed that the CSA decreased and the PDFF increased of the paraspinal muscles in CLBP patients. It reveals a significant correlation between the PDFF of CLBP paraspinal muscles and the grade of IVD degeneration. Sex and age are also important factors influencing CLBP paraspinal muscle infiltration.

Keywords: chronic low back pain, quantitative MRI, paraspinal muscles, fatty infiltration, lumbar intervertebral disk degeneration

INTRODUCTION

Low back pain (LBP) has become a global challenge with tremendous economic burden for society and public health systems (1, 2). The lifetime prevalence of LBP is reported to be as high as 84%, with chronic low back pain (CLBP) accounting for approximately 23% of LBP (3). Furthermore, more than 10% of patients with LBP develop severe disabilities (4). The diversity and complexity of etiology limit the prevention and treatment strategies of LBP. Intervertebral disc (IVD) degeneration refers to the physiological and pathological process of natural degeneration and aging of the IVD, in which structural damage causes the degeneration of the disc and the surrounding area (5). IVD degeneration is the basis of various clinical spinal diseases, for example, annulus tears, instability of the spine, degeneration in the facet joints, disc herniation, spinal stenosis and CLBP (5, 6). And IVD degeneration is usually considered as the leading cause of CLBP, especially at the L4-S1 level, but the treatments are mainly limited to partial symptomatic relief (7, 8).

The paraspinal muscles (multifidus, erector spinae, and psoas) are essential determinants of the structural stability and functions of the lumbar spine (9). Previous animal and human studies suggested that increased myoelectric activity and structural remodeling of muscles (e.g. muscle atrophy, fat infiltration, and fiber type changes) were associated with CLBP (10–14). Given the important role of paraspinal muscles on the lumbar spine, muscle lesions may worsen CLBP. It is crucial to study the interactions between paraspinal muscle changes and CLBP, but they are often underestimated. In addition, it is unclear whether the degeneration of the lumbar IVD is related to increased fatty infiltration within the paraspinal muscles in CLBP patients.

Previous studies had reported the muscle cross-sectional area (CSA) and fat content of the paraspinal muscles in CLBP patients (15–18). Based on anatomical imaging, the CSA variable of muscles is routinely preferred (19), which can be used as a structural measure of muscle hypertrophy or atrophy. The assessments of fat infiltration were mainly based on the decrease of CT attenuation values (14–16, 20, 21) or the increase of the relative signal intensity on the conventional MRI T1 and T2 images (17, 22, 23). There is no published literature on CLBP related to the intramuscular adipose tissue in CLBP study. In recent years, an advanced chemical shift encoding-based water-fat MRI has been used for non-invasive quantitative assessment of fat and water signals in various parts of the human body (24–26), such as available Iterative Decomposition of water and fat with Echo Asymmetry and Least Square Estimation (IDEAL-IQ). Proton density fat fraction (PDFF) outcomes can be obtained with high resolution and high accuracy from IDEAL-IQ (25). This method is considered to be a reliable measurement method comparable to MR spectroscopy (the gold standard method *in vivo*) for quantifying fat infiltration in muscles (27–29). Sollmann et al. showed that the PDFF measurement after paraspinal muscle segmentation is a potential biomarker for muscle changes in the future (30). Furthermore, Zhao and Patzelt et al. found a negative correlation between the PDFF of paraspinal muscles and the bone mineral density of the lumbar spine, and the progress and severity of tumor cachexia can be monitored through the PDFF of the paraspinal muscles (31, 32). Therefore, PDFF help accurately quantify the fat content, especially intramuscular lipids in the paraspinal muscles of CLBP, and further explore the relationship between IVD degeneration and paraspinal muscle remodeling in CLBP patients. Furthermore, results of previous studies reveal that a decrease in the multifidus CSA, a decrease of muscle density, and a decrease in the size of Type I and Type II/MHC-2X fibers and interstitial fibrosis in patients with intervertebral herniation. And the fat infiltration may be associated with these muscle changes (14, 33, 34). We hypothesized that paraspinal muscle CSA and fat content are changed in CLBP patients compared to healthy subjects, significantly, and are associated with the degeneration of the adjacent IVD.

The purpose of our study was to compare the CSA and PDFF of paraspinal muscles in patients with CLBP and healthy subjects using novel quantitative MRI, investigate the relationship between IVD degeneration and paraspinal muscle fat infiltration. Furthermore, we compared the age-related and sex-related changes in CSA and PDFF of the paraspinal muscles in patients with CLBP.

MATERIALS AND METHODS

Participants

In this retrospective study, sixty patients with CLBP and thirty-two healthy subjects were selected in this study from January 2019 to December 2020 (46 males, 46 females; mean age: 45.82 years; age range: 24-72 years). Patients with CLBP and healthy subjects were matched for age and sex. Informed consent forms were signed by each participant, and ethical committee approval was obtained. The inclusion criteria were as follows: the untreated patient has symptoms of LBP for more than 3 months; Healthy subjects have no symptoms of LBP;BMI ranged from 18.5 to 23.9 kg/m^2. The exclusion criteria were visceral LBP (such as urinary tract stones); spinal trauma, fracture, tumor, infection, deformity, spondylolisthesis, surgery, and other musculoskeletal diseases; pregnancy; and contraindications for MRI. Except that the subjects in the control group had no low back pain, the other inclusion and exclusion criteria were the same as those in the low back pain group. The control group did not have any clinical symptoms, and the other inclusion and exclusion criteria were identical to those described previously. The selected subjects also completed the Oswestry Disability Index (ODI) (35) and Visual Analog Scale (VAS) (36) to assess the level of back pain and dysfunction. The ODI covers 10 items (pain, lifting, walking, social life, personal care, sitting, standing, sleeping, travelling and sex life), and each scored from 0 to 5. Total ODI score = score of each item × 2, the total ODI score ranges from 0 to 100. A higher total ODI score reflects higher disability. According to the median age of the included participants, participants under 45 years old are classified as the young group, and 45 years old or older are classified as the elderly group. **Table 1** shows the baseline clinical characteristics of the participants.

TABLE 1 | Comparison of clinical characteristics and CSA of paraspinal muscle between healthy subjects and CLBP patients.

Characteristics	Healthy subjects (n = 32)	CLBP (n = 60)	*p*
Male/Female	16/16	30/30	1.000
Age (year)	44.87 ± 17.59	46.32 ± 16.99	-0.412
Male	44.99 ± 16.51	45.80 ± 15.77	-0.350
Female	44.75 ± 18.27	47.21 ± 17.69	-0.650
Height (cm)	164.13 ± 3.01	162.65 ± 3.28	0.069
Weight (kg)	58.50 ± 3.01	57.76 ± 4.71	0.110
BMI (kg/m^2)	21.75 ± 1.23	21.71 ± 1.16	0.056
Male	22.20 ± 1.14	22.34 ± 1.22	0.077
Female	21.30 ± 1.25	21.08 ± 1.08	0.054
CSA of MF (mm^2)			
L4/5	1320.22 ± 188.10	1228.72 ± 190.99	0.041*
L5/S1	1271.01 ± 213.39	1127.48 ± 282.89	0.720
CSA of ES (mm^2)			
L4/5	2320.40 ± 303.77	2263.16 ± 485.71	0.398
L5/S1	1127.48 ± 282.89	999.04 ± 463.23	0.907
ODI scores	NA	28.45 ± 13.17	–
VAS scores	NA	5.99 ± 1.42	–

CLBP, chronic low back pain; CSA, cross-sectional area; MF, multifidus; ES, erector spinae. ODI, Oswestry Disability Index; VAS, Visual Analog Scale. All values were expressed as mean ± standard deviation. Significant p-values are marked with "". NA, Not Applicable.*

MR Data Acquisition

All MRI experiments were performed using a 3.0T MR system (Discovery 750w, GE Healthcare, USA). A 32-channel the phased array spine coil was used for CLBP patients and healthy subjects. To reduce motion artifacts, an abdominal bandage was used to compress the abdomen and a wedge-shaped foam pad was placed under the lower limbs of participants in a standard supine position. MRI scanning for participants included sagittal T1-weighted imaging (T1), T2-weighted imaging (T2) of the lumbar spine, and axial T2, IDEAL-IQ of paraspinal muscles. The MRI protocols of participants are summarized in **Table 2**.

Image Analyses

All raw MR images were processed on a commercially available workstation (Advantage Windows 4.6, GE Medical Systems, USA). The degeneration degree of IVD at L4/5 and L5/S1 was assessed by two blinded experienced radiologists according to Pfirrmann grading system (I-V) by MRI T2 (37). The Pfirrmann grading system was divided into five grades to evaluate the homogeneity of intervertebral disc structure, signal strength, discrimination between nucleus and anulus, and disc height. When there was a disagreement, both radiologists discussed to achieve a consensus. Muscle cross-sectional area (CSA) and PDFF values of the bilateral paraspinal muscles were obtained on a region of interest (ROI) basis at the central level of L4/5 and L5/S1. The CSA and PDFF of the paraspinal muscles were measured at two-disc levels for each participant. The two radiologists manually delineated the shape of the bilateral multifidus and erector spinae (**Figure 1**). The muscle CSA was measured by manually delineating the ROI on the axial T2 images, then the same ROI was automatically copied by the workstation to the fat fraction map to obtain the PDFF value. The average of the two measurements was calculated and used for later analysis.

Statistical Analysis

SPSS 22.0 was performed for the statistical analysis. Mean ± SD was used to express data. Comparisons between patients with CLBP and healthy subjects were determined using the independent-sample t-test. Pearsons correlations and Spearman's rank correlations were computed between paraspinal muscles CSA, PDFF and Pfirrmann grade, ODI, VSA. One-way analysis of variance (ANOVA) was employed for the comparisons among multiple groups, and Tukey's multiple comparisons test was utilized for the *post hoc* test after ANOVA. Analysis of covariance was used with age as a covariate to ensure that there was no effect of age on the differences of

TABLE 2 | MRI scan parameters.

Images	TE (ms)	TR (ms)	ST (mm)	SL (mm)	FOV (mm^2)	NEX	Spatial resolution (mm^2)	Acquisition time
Sagittal T1	8.3	361	4	4	320×180	2	1.0×1.4	1 min 28 s
Sagittal T2	142	2500	4	4	320×180	2	1.0×1.4	1 min 25 s
Axial T2	110.5	4024	3	4	200×200	3	0.7×0.9	1 min 15 s
IDEAL-IQ	1.2/3.2/5.2/ 7.2/9.2/11.2	7.8	4	0	240×240	2	1.0×1.5	5 min 35 s

TR, time of repetition; TE, echo time; ST, slice thickness; SL, slice increment; FOV, field of view; NEX, number of excitation.

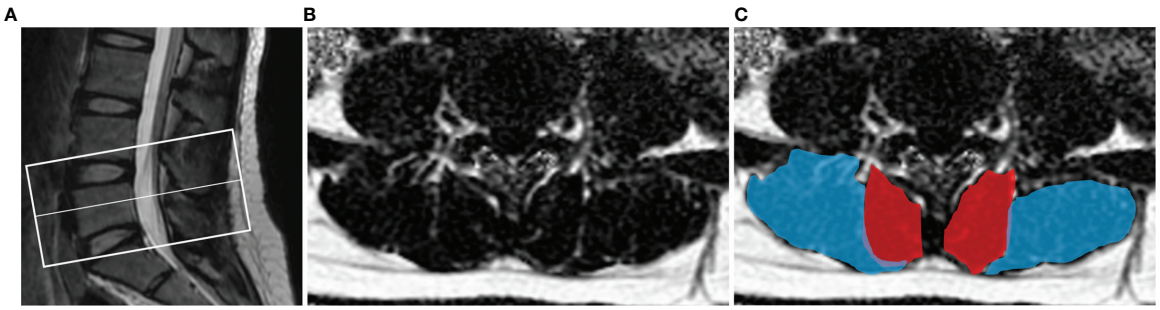

FIGURE 1 | Demonstration of paraspinal muscle segmentation. **(A)** The center level of the scan was at the midline of L5. **(B)** Processed PDFF maps of paraspinal muscles; **(C)** manual segmentation of paraspinal muscles, multifidus (red) and erector spinae (blue).

muscle PDFF. The Cochran-Armitage trend test was used between Pfirrmann grade and other variables. A p-value <0.05 was reported statistically significant.

RESULT

Comparison of CSA and PDFF in the Paraspinal Muscle Between Healthy Subjects and Patients With CLBP

There were no differences in gender, age, height, weight, and BMI between healthy subjects and CLBP patients (**Table 1**). The inter-observer agreement of measured CSA and PDFF between two radiologists was good (ICC=0.964, p<0.001). The CSAs of the multifidus and erector spinae of CLBP were smaller than those of healthy subjects, but the difference was statistically significant only in the multifidus at the L4/5 level (p<0.05, **Table 1**). The PDFF maps showed that the paraspinal muscle PDFFs were increased in patients with CLBP (**Figure 2**). At the level of L4/5 and L5/S1, the multifidus and erector spinae PDFF of CLBP patients were significantly increased than those of healthy subjects, and the differences were statistically significant (all p <0.05, **Figure 2**).

Correlation Between Paraspinal Muscles CSA, PDFF and Pfirrmann Grade of IVDs

The multifidus CSA was weakly correlated to Pfirrmann grade of IVD degeneration (r=-0.265, p =0.004), but there was no significant correlation between the CSA of erector spinae and the Pfirrmann grade (r=-0.305, p =0.708). With the increase of Pfirrmann grade of IVDD, the PDFF values of the multifidus and erector spinae in CLBP patients gradually increased, in the order of Grade V>Grade IV>Grade III>Grade II>Grade I (**Table 3**). In the multifidus muscle, the PDFFs of Grade V and Grade IV were higher than that of Grade III and Grade II, and the difference was statistically significant (p<0.05, **Table 3**). There were differences in the age of CLBP patients with different Pfirrmann grades, but there was no statistically significant difference in BMI among the groups. After adjusting for age, comparing the multifidus and erector spinae PDFF among different Pfirrmann grades, the results showed that the PDFF of the high-grade Pfirrmann grade were higher than that of the low-grade Pfirrmann grade (**Table 3**). **Figures 3** and **4** show the relationships between multifidus and erector spinae age-adjusted PDFF with Pfirrmann grade at the L4/5 and L5/S1 levels. There was a significant correlation (r = 0.717 and 0.744, all p < 0.05) between PDFF of MF and Pfirrmann grade at the IVD levels. In addition, the correlation between erector spinae PDFFs and Pfirrmann grade was lower than that of multifidus (r=0.651 and 0.658, all p <0.05). The Pfirrmann grade of IVD degeneration in the control group, 5, 44, 13, 2, 0 discs had Grade I-V, respectively.

Correlation Between Paraspinal Muscles CSA, PDFF and the ODI, VSA of Patients With CLBP

Table 4 shows the overall relationships between CSA, PDFF of paraspinal muscles and ODI, VSA of CLBP patients. There was a moderate correlation between PDFF, ODI and VSA, and higher than CSA.

Analysis of the Difference of CSA and PDFF Regarding Sex and Age

In healthy subjects and CLBP patients, male paraspinal muscle CSAs at the L4/5 and L5/S1 were larger than females, and the difference was statistically significant (**Figure 5**, all p <0.05). In addition, the CSAs of paraspinal muscles in female CLBP patients were lower than that of the healthy subjects, and the difference was statistically significant (**Figure 5**, all p <0.05). Regardless of male or female, the PDFFs of the paraspinal muscles showed a significant increase in the CLBP patients. And female CLBP patients were higher than males in the PDFFs at the level of L4/5 (**Figure 5**, all p<0.05). The paraspinal muscle CSAs of the old were slightly smaller than that of the young in the both healthy subjects and CLBP patients, but the difference was not statistically significant(**Figure 6**, all p>0.05). Whether the old group or young group, CLBP patients were significantly higher than healthy subjects in the PDFFs of the paraspinal muscles (**Figure 6**, all p<0.05). And the PDFFs of the paraspinal muscles of the elderly CLBP patients were higher than that of the young at the level of L4/5 (**Figure 6**, p<0.05).

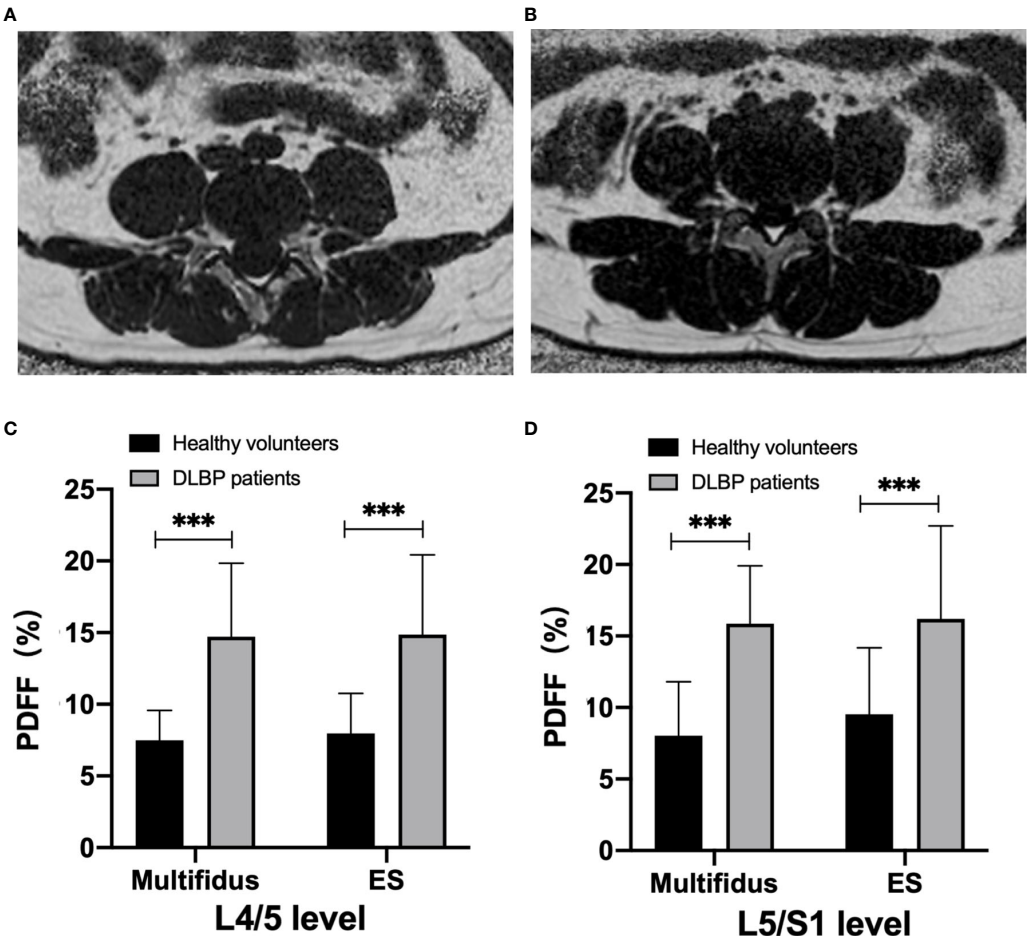

FIGURE 2 | MRI PDFF of lumbar paraspinal muscle in patients with CLBP. **(A)** Patient with CLBP, Male, 29 years old, CLBP for 9 years, $PDFF_{\text{left multifidus}}$ = 10.9%, $PDFF_{\text{right multifidus}}$ =11.9%, $PDFF_{\text{left erector spinae}}$ =10.8%, $PDFF_{\text{right erector spinae}}$ = 10.1%. **(B)** Healthy Volunteer, male, 30 years old, $PDFF_{\text{left multifidus}}$= 7.2%, $PDFF_{\text{right multifidus}}$ = 7.1%, $PDFF_{\text{left erector spinae}}$ = 5.1%, $PDFF_{\text{right erector spinae}}$ = 4.8%. **(C, D)** Bar chart of paraspinal muscle PDFF at L4/5 and L5/S1 levels. Data are reported as mean ± standard deviation of mean. ***$p < 0.001$.

Multiple Linear Regression Analysis

Table 5 shows the multiple linear regression analysis of paraspinal muscle PDFFs. Age, gender, and Pfirrmann grade of IVDs were independent factors of multifidus FF value (p <0.05), and Pfirrmann grade of IVDs was an independent factor of erector spinae PDFF value (p <0.05).

DISCUSSION

Using quantitative MR imaging, our study showed that the paraspinal muscles atrophy and fat content increase in patients with CLBP compared to healthy subjects. And a significant correlation was observed between the degeneration of the

TABLE 3 | Differences in PDFF and age-adjusted PDFF values of paraspinal muscles between different Pfirrmann grades of two intervertebral discs in CLBP patients ($\bar{x} \pm s$).

Pfirrmann grade	Age	BMI	Multifidus PDFF	Erector spinae PDFF	Multifidus PDFF (adjusted age)	Erector spinae PDFF (adjusted age)
Grade I	23.0 ± 2.8	22.1 ± 1.3	9.9 ± 0.0	9.1 ± 1.1	9.9 ± 0.0	9.1 ± 1.1
Grade II	31.6 ± 6.6	21.8 ± 1.5	11.3 ± 2.1	13.2 ± 4.52	11.2 ± 2.7	14.2 ± 5.5
Grade III	43.3 ± 10.7	22.8 ± 1.4	13.8 ± 3.7*	15.3 ± 4.9*	13.7 ± 3.9	15.3 ± 5.2
Grade IV	50.6 ± 13.7	22.4 ± 1.9	15.5 ± 4.8*	16.5 ± 6.6*	15.3 ± 5.0*	16.5 ± 7.0*
Grade V	53.6 ± 10.1	22.3 ± 1.7	18.4 ± 4.8*	19.6 ± 7.2*	17.5 ± 5.2*	19.0 ± 8.3*
p for trend	0.000	0.651	0.001	0.008	–	–

**Compared with Grade I, $p < 0.05$.*

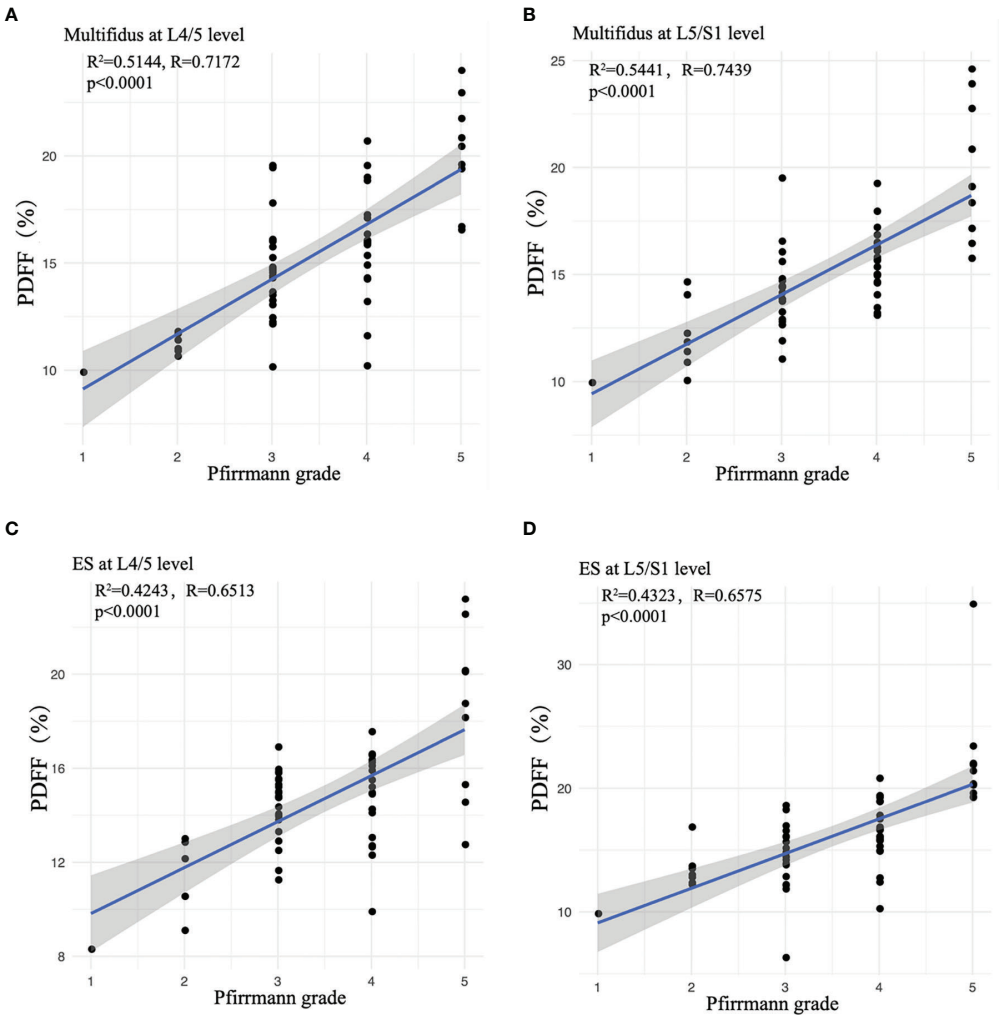

FIGURE 3 | Correlation between age-adjusted PDFF of paraspinal muscles and Pfirrmann grade. **(A)** Multifidus at L4/5 level; **(B)** Multifidus at L5/S1 level; **(C)** ES at L4/5 level; **(D)** ES at L5/S1 level. ES, erector spinae. Spearman's Rank-Order Correlation was used.

lumbar spine IVD and the PDFF of adjacent paraspinal muscle in patients with CLBP. Furthermore, sex and age were also independently associated with the paraspinal muscle fat.

Compared with healthy subjects, the CSA of the paraspinal muscles of CLBP patients were decreased only in the multifidus muscle at the L4/5 level. Although the muscle CSA is the most studied, paraspinal muscle atrophy in CLBP remains controversial (38–40). Barker et al. used conventional MRI to compare the multifidus CSA of patients with unilateral pain CLBP, and the results showed that the multifidus CSA of the painful side was lower than that of the asymptomatic side (41). The strength of the paraspinal muscles measured during maximal isometric trunk flexion and trunk extension contractions is decreased in patients with CLBP (42). Some studies have found that muscle CSA was reduced but not significant (38). This may be related to changes in the composition of muscles. When muscle tissue is atrophy, fat infiltration occurs in the paraspinal muscles (29, 43). To some extent, due to the filling and replacement of adipose tissue, the overall muscle CSA has not changed significantly. Our findings in this study further support this view.

In our study, compared with the control group, the PDFF of the paraspinal muscles of CLBP patients was significantly increased. Yanik et al. quantified the fat content of multifidus muscle in patients with CLBP and asymptomatic subjects by conventional MRI, and the results were consistent with this study (33, 44, 45). On the basis of the previous research, we manually delineated the edge of the muscle as the ROI, and further applied the multi-echo Dixon method, which corrected the main magnetic field inhomogeneity effect, T2* effect, T1 effect and other confounding factors, in order to make the quantification of paraspinal muscle fat content is more accurate, better repeatability and reliability (46–48). In order to minimize the possible impact of the slightly differences in spatial resolutions of

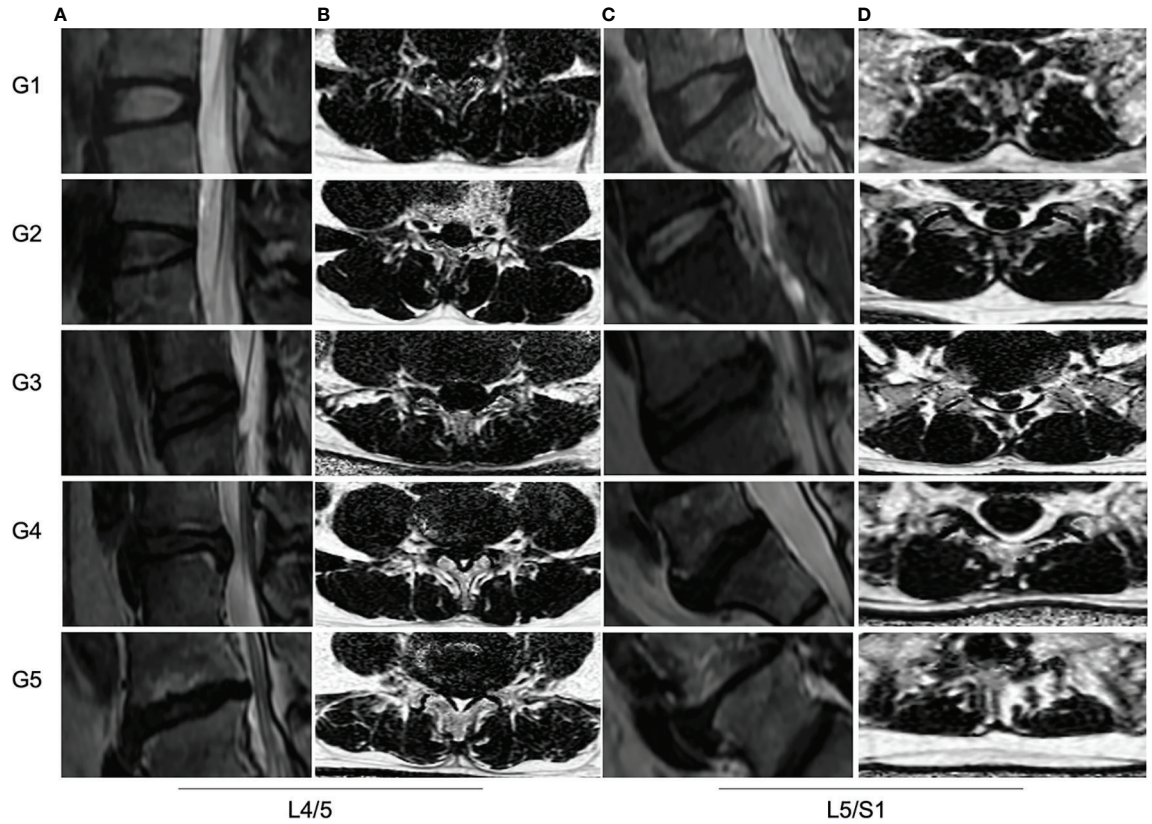

FIGURE 4 | MRI PDFF of lumbar paraspinal muscles at different Pfirrmann grade of IVDs degeneration. **(A, C)** Sagittal T2 images of IVDs at L4/5 and L5/S1 levels. The Pfirrmann grade of IVDs degeneration from left to right are for G1, G2 G3, G4 and G5, respectively. **(B, D)** The PDFF of paraspinal muscles at L4/5 and L5/S1 levels. The mean PDFF at the L4/5 from up to bottom are for 9.1%, 10.5%, 14.2%, 16.3% and 22.3%, respectively. The mean PDFF at L5/S1 from up to bottom are for 10.8%, 12.1%, 14.0%, 16.5% and 24.0%, respectively.

T2 and PDFF images, we selected the layers at the center of the L4/5 and L5/S1 intervertebral discs as much as possible to delineate the ROI of the paraspinal muscles. In addition, we artificially removed cases with obvious motion artifacts. In this study, we further found the correlation between PDFF and IVD degeneration is higher than correlations between CSA and IVD degeneration. It indicated that the paraspinal muscles of CLBP patients had muscle tissue atrophy and fat replacement.

Recently, much attention has focused on lumbar IVD degeneration in CLBP patients and it is related to the Oswestry Disability Index (41, 49). Paraspinal muscle may play an important role in elucidating and treating lumbar spine dysfunction and spinal imbalance (50, 51). Indeed, we found significant correlations between IVD degeneration of the lumbar spines and the PDFF of adjacent paraspinal muscles in our cohort. Sato et al. revealed that muscle CSA changes were more correlated with pressure pain sensitivity in CLBP patients (52). This difference may be related to the different pain measurement methods we use. Furthermore, the multifidus muscle is more significantly affected. The anatomical relationships between the multifidus muscle and lumbar spine

TABLE 4 | Correlation analysis between CSA, PDFF of paraspinal muscles and ODI, VSA of CLBP patients.

Measurement		ODI			VAS		
		r	*p*	95%CI	*r*	*p*	95%CI
CSA							
	MF	-0.257*	0.043	-0.480, 0.026	-0.225	0.102	-0.464, 0.045
	ES	-0.198	0.152	-0.442, 0.074	-0.180	0.214	-0.483, 0.042
PDFF							
	MF	0.437*	0.034	0.023, 0.52	0.368*	0.054	-0.004, 0.505
	ES	0.3134*	0.035	0.021, 0.52	0.379*	0.055	0.119, 0.591

*CSA, cross-sectional area; PDFF, proton density fat fraction; MF, multifidus; ES, erector spinae. ODI, oswestry disability index; VAS, visual analog scale. *p < 0.05.*

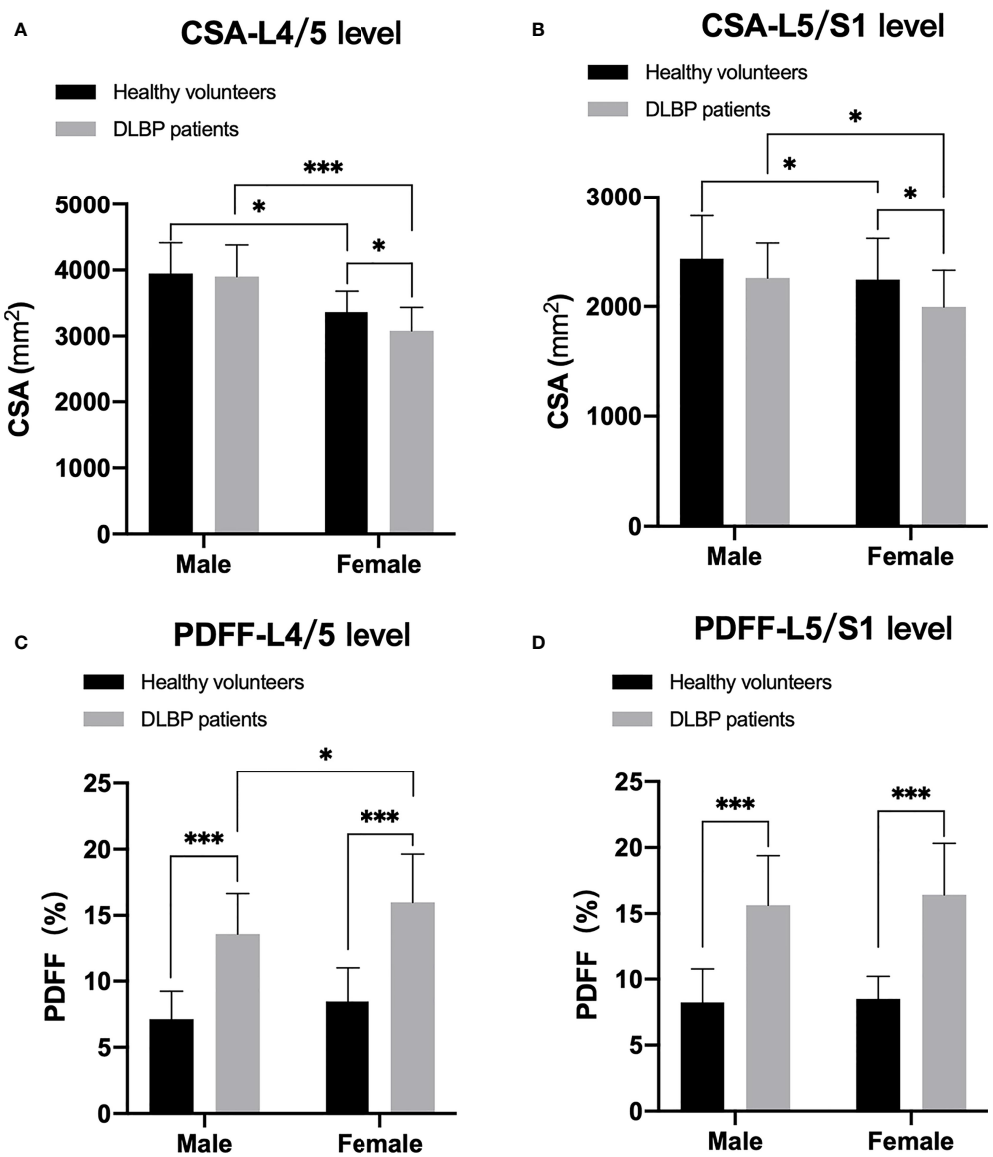

FIGURE 5 | Difference of CSA and PDFF regarding sex. **(A)** CSA at L4/5 level; **(B)** CSA at L5/S1 level; **(C)** PDFF at L4/5 level; **(D)** PDFF at L5/S1 level. *$p < 0.05$, ***$p < 0.001$.

would be relevant to this interpretation. In the lumbar spine, the multifidus muscle is the most developed and important. The multifidus contributes to side bending (tilting) and rotation (twisting) (53). Compared with the erector spinae, the multifidus muscle is more closely related to the lamina and spinous process (54). And the multifidus is a short muscle which makes it more local and prone to changes at the L4/5 and L5/S1levels. The stability of the spine is reduced after CLBP, and muscle changes may be used as a compensatory strategy to cause long-term paraspinal muscle fatigue. When the muscle is decompensated, it will promote the recurrence or exacerbation of CLBP (55). This underlines the importance of the muscles PDFF in the context of IVD degradation. The increased fat infiltration in the paraspinal muscles may be related to the inflammatory disorders found in the multifidus muscles of patients with degenerative spine (56). In animal experiments, James et al. found an increase in macrophages and TNF in the multifidus muscle of a sheep model of IVD degeneration (57). The increased inflammation is likely to be an important factor in promoting fat infiltration of skeletal muscle (58). At the same time, we found that the level of pain and dysfunction in CLBP patients were higher, but the direct relationship between IVD degeneration, paraspinal muscle remodeling, pain, and dysfunction still needs further exploration.

In this study, we account for the potential effects of sex, age, and BMI on muscle fat. In the normal population, males have a larger CSA of paraspinal muscles and lower fat content than

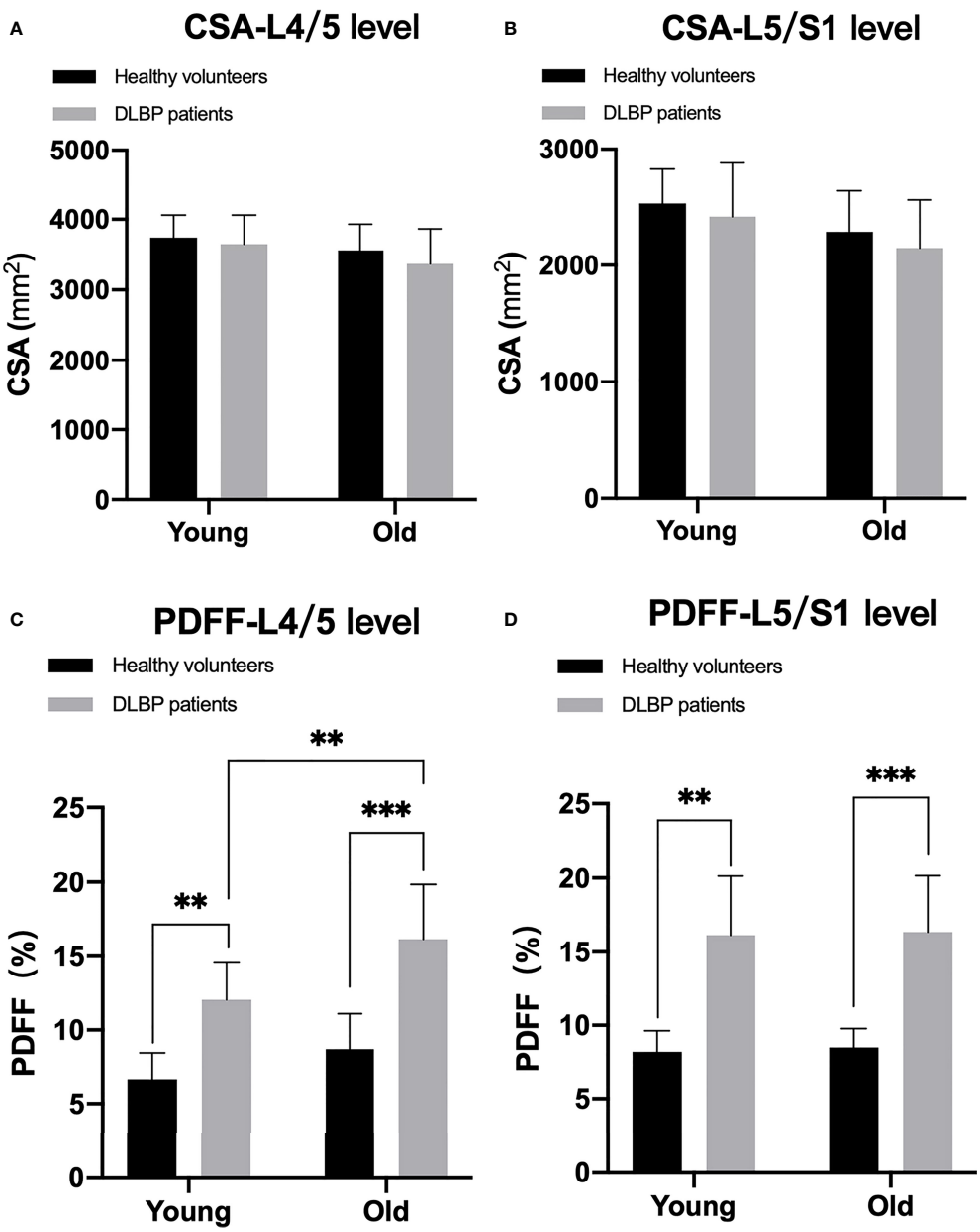

FIGURE 6 | Difference of CSA and PDFF regarding age. **(A)** CSA at L4/5 level; **(B)** CSA at L5/S1 level; **(C)** PDFF at L4/5 level; **(D)** PDFF at L5/S1 level. $^{**}p < 0.05$, $^{***}p < 0.001$.

TABLE 5 | Multiple linear regression analysis of PDFF of paraspinal muscles.

Factor	PDFF of multifidus			PDFF of erector spinae		
	Standardized β	95% CI	*p*	Standardized β	95% CI	*p*
Age	0.233	(0.054, 0.412)	0.011	0.192	(-0.004, 0.388)	0.055
Gender	0.193	(0.033, 0.354)	0.019	0.107	(-0.069, 0.283)	0.232
Pfirrmann grading	0.322	(0.141, 0.503)	0.001	0.215	(0.017, 0.413)	0.034

Standardized β is the standardized regression coefficient.

females. This is consistent with the results of previous studies (59). We found that both males and females with CLBP have muscle fat infiltration. And it seems to be more pronounced in females, the underlying mechanism is the decline in muscle performance caused by hormone deficiency after menopause in women (43, 60). Age is an important factor in the fat infiltration of paraspinal muscles. Our results show that paraspinal muscle fat increases with age (59, 61), indicating that paraspinal muscle are gradually deteriorating, even in healthy individuals. Therefore, it is necessary to consider the relationship between paraspinal muscles and spinal degeneration with age as a covariate. The PDFFs of the paraspinal muscles in both young and old CLBP patients were significantly increased, the increase was more significant in the elderly. This may be related to the poorer basic muscle strength and performance of the elderly. Fat infiltration of paravertebral muscles in CLBP patients can only be supported if age and sex effects are fully clear. In this study, through the ODI scale test, we observed that the activity level of CLBP patients was reduced. Hodges and Goubert et al. believes that pain leads to disuse muscle atrophy caused by reduced multifidus muscle activity (45, 62). But several previous researches conclude that as to the assumption that patients with CLBP suffer from disuse and physical deconditioning empirical evidence is still lacking (63, 64). In future studies, the activity level of CLBP patients deserves further consideration.

There are several limitations of this study. First, cross-sectional design with relatively small subjects is considered the main limitation. Subsequent longitudinal cohort studies are warranted to further investigate and confirm the relationship between IVD degeneration and paraspinal muscle fat infiltration. Furthermore, the current intervertebral degeneration grading system is qualitative and subjective, and a quantitative method is a better choice. Moreover, the L4/5 and L5/S1 IVDs are regarded as the level of interest because they are the most degradable levels. However, it is unclear whether the paraspinal muscles at the level of the L1-4 IVDs have changed. The post-processing software used in this study can obtain the PDFF of muscle, but not the PDFF of muscle tissue. So, the intermuscular and intramuscular fat cannot be completely distinguished in this study. At last, it will be interesting to further explore the distribution of fat in the paraspinal muscles and clearly quantify the levels of lipids within and outside muscle cells.

Using quantitative MRI to measure CSA and PDFF, this study confirmed the changes in CSA and PDFF of the paraspinal muscles in CLBP patients and found a significant correlation between lumbar IVD degeneration and the PDFF of paraspinal muscles. Sex and age are important factors also considered influencing factors for the paraspinal muscles in CLBP patients. Our findings clearly highlighted the assessment of fat content within paraspinal muscles in CLBP patients and might trigger a paradigm shift in the intervention strategy to CLBP. Paraspinal muscle fat infiltration should also be evaluated as treatment outcome, and its use as a treatment endpoint for therapies should be further investigated.

DATA AVAILABILITY STATEMENT

The original contributions presented in the study are included in the article/supplementary material. Further inquiries can be directed to the corresponding authors.

ETHICS STATEMENT

The studies involving human participants were reviewed and approved by Kunming Medical University. The patients/participants provided their written informed consent to participate in this study. Written informed consent was obtained from the individual(s) for the publication of any potentially identifiable images or data included in this article.

AUTHOR CONTRIBUTIONS

BH and XC: Designed the study and conceived the report. YH and LW: Wrote the draft of the manuscript and revised it critically. XZ, JC, ZZ and YJ: Data acquisition and processing. BH and YH: Analyzed and interpreted the results of MRI. LN: Technical support for MRI scanning. YH, LW and XZ: Statistical analysis, and created the figures and tables. All authors had read and approved the final manuscript.

FUNDING

This work is supported by the Applied Basic Research Project of Yunnan Province- Kunming Medical University Joint Fund (202001AY070001-038), Beijing Hospitals Authority Youth Programme (QMS20200402), and Yunnan Provincial Bone and Joint Disease Clinical Medicine Center Project (ZX2019-03-04).

REFERENCES

1. Buchbinder R, van Tulder M, Öberg B, Costa LM, Woolf A, Schoene M, et al. Low Back Pain: A Call for Action. *Lancet* (2018) 391(10137):2384–8. doi: 10.1016/s0140-6736(18)30488-4
2. Hartvigsen J, Hancock MJ, Kongsted A, Louw Q, Ferreira ML, Genevay S, et al. What Low Back Pain is and Why We Need to Pay Attention. *Lancet* (2018) 391(10137):2356–67. doi: 10.1016/s0140-6736(18)30480-x
3. Balagué F, Mannion AF, Pellisé F, Cedraschi C. Non-Specific Low Back Pain. *Lancet* (2012) 379(9814):482–91. doi: 10.1016/s0140-6736(11)60610-7
4. Côté P, Cassidy JD, Carroll L. The Saskatchewan Health and Back Pain Survey. The Prevalence of Neck Pain and Related Disability in Saskatchewan Adults. *Spine (Phila Pa 1976)* (1998) 23(15):1689–98. doi: 10.1097/00007632-199808010-00015
5. Wang F, Cai F, Shi R, Wang XH, Wu XT. Aging and Age Related Stresses: A Senescence Mechanism of Intervertebral Disc Degeneration. *Osteoarthr Cartil* (2016) 24(3):398–408. doi: 10.1016/j.joca.2015.09.019

6. Silagi ES, Shapiro IM, Risbud MV. Glycosaminoglycan Synthesis in the Nucleus Pulposus: Dysregulation and the Pathogenesis of Disc Degeneration. *Matrix Biol* (2018) 71-72:368–79. doi: 10.1016/j.matbio.2018.02.025
7. Berman BM, Langevin HM, Witt CM, Dubner R. Acupuncture for Chronic Low Back Pain. *N Engl J Med* (2010) 363(5):454–61. doi: 10.1056/NEJMct0806114
8. Cherkin D, Balderson B, Wellman R, Hsu C, Sherman KJ, Evers SC, et al. Effect of Low Back Pain Risk-Stratification Strategy on Patient Outcomes and Care Processes: The MATCH Randomized Trial in Primary Care. *J Gen Intern Med* (2018) 33(8):1324–36. doi: 10.1007/s11606-018-4468-9
9. Hodges PW, Danneels L. Changes in Structure and Function of the Back Muscles in Low Back Pain: Different Time Points, Observations, and Mechanisms. *J Orthop Sports Phys Ther* (2019) 49(6):464–76. doi: 10.2519/jospt.2019.8827
10. Geisser ME, Ranavaya M, Haig AJ, Roth RS, Zucker R, Ambroz C, et al. A Meta-Analytic Review of Surface Electromyography Among Persons With Low Back Pain and Normal, Healthy Controls. *J Pain* (2005) 6(11):711–26. doi: 10.1016/j.jpain.2005.06.008
11. Solomonow M, Hatipkarasulu S, Zhou BH, Baratta RV, Aghazadeh F. Biomechanics and Electromyography of a Common Idiopathic Low Back Disorder. *Spine (Phila Pa 1976)* (2003) 28(12):1235–48. doi: 10.1097/01.Brs.0000065568.47818.B9
12. Ranger TA, Cicuttini FM, Jensen TS, Heritier S, Urquhart DM. Paraspinal Muscle Cross-Sectional Area Predicts Low Back Disability But Not Pain Intensity. *Spine J* (2019) 19(5):862–8. doi: 10.1016/j.spinee.2018.12.004
13. Agten A, Stevens S, Verbrugghe J, Timmermans A, Vandenabeele F. Biopsy Samples From the Erector Spinae of Persons With Nonspecific Chronic Low Back Pain Display a Decrease in Glycolytic Muscle Fibers. *Spine J* (2020) 20(2):199–206. doi: 10.1016/j.spinee.2019.09.023
14. Kalichman L, Carmeli E, Been E. The Association Between Imaging Parameters of the Paraspinal Muscles, Spinal Degeneration, and Low Back Pain. *BioMed Res Int* (2017) 2017:2562957. doi: 10.1155/2017/2562957
15. Danneels LA, Vanderstraeten GG, Cambier DC, Witvrouw EE, De Cuyper HJ. CT Imaging of Trunk Muscles in Chronic Low Back Pain Patients and Healthy Control Subjects. *Eur Spine J* (2000) 9(4):266–72. doi: 10.1007/s005860000190
16. Kamaz M, Kireşi D, Oğuz H, Emlik D, Levendoğlu F. CT Measurement of Trunk Muscle Areas in Patients With Chronic Low Back Pain. *Diagn Interv Radiol* (2007) 13(3):144–8.
17. Wan Q, Lin C, Li X, Zeng W, Ma C. MRI Assessment of Paraspinal Muscles in Patients With Acute and Chronic Unilateral Low Back Pain. *Br J Radiol* (2015) 88(1053):20140546. doi: 10.1259/bjr.20140546
18. Lee CH. Quantitative T2-Mapping Using MRI for Detection of Prostate Malignancy: A Systematic Review of the Literature. *Acta Radiol* (2019) 60(9):1181–9. doi: 10.1177/0284185118820058
19. Peng X, Li X, Xu Z, Wang L, Cai W, Yang S, et al. Age-Related Fatty Infiltration of Lumbar Paraspinal Muscles: A Normative Reference Database Study in 516 Chinese Females. *Quant Imaging Med Surg* (2020) 10(8):1590–601. doi: 10.21037/qims-19-835
20. Wang L, Yin L, Zhao Y, Su Y, Sun W, Liu Y, et al. Muscle Density Discriminates Hip Fracture Better Than Computed Tomography X-Ray Absorptiometry Hip Areal Bone Mineral Density. *J Cachexia Sarcopenia Muscle* (2020) 11(6):1799–812. doi: 10.1002/jcsm.12616
21. Wang L, Yin L, Zhao Y, Su Y, Sun W, Chen S, et al. Muscle Density, But Not Size, Correlates Well With Muscle Strength and Physical Performance. *J Am Med Dir Assoc* (2021) 22(4):751–9. doi: 10.1016/j.jamda.2020.06.052
22. Baum T, Cordes C, Dieckmeyer M, Ruschke S, Franz D, Hauner H, et al. MR-Based Assessment of Body Fat Distribution and Characteristics. *Eur J Radiol* (2016) 85(8):1512–8. doi: 10.1016/j.ejrad.2016.02.013
23. Lee JH, Yoon YC, Kim HS, Kim JH, Choi BO. Texture Analysis Using T1-Weighted Images for Muscles in Charcot-Marie-Tooth Disease Patients and Volunteers. *Eur Radiol* (2021) 31(5):3508–17. doi: 10.1007/s00330-020-07435-y
24. Ma Q, Cheng X, Hou X, Yang Z, Ma D, Wang Z. Bone Marrow Fat Measured by a Chemical Shift-Encoded Sequence (Ideal-IQ) in Patients With and Without Metabolic Syndrome. *J Magn Reson Imaging* (2021) 54(1):146–53. doi: 10.1002/jmri.27548
25. Sollmann N, Dieckmeyer M, Schlaeger S, Rohrmeier A, Syvaeri J, Diefenbach MN, et al. Associations Between Lumbar Vertebral Bone Marrow and Paraspinal Muscle Fat Compositions-An Investigation by Chemical Shift Encoding-Based Water-Fat Mri. *Front Endocrinol (Lausanne)* (2018) 9:563. doi: 10.3389/fendo.2018.00563
26. Naarding KJ, van der Holst M, van Zwet EW, van de Velde NM, de Groot IJM, Verschuuren J, et al. Association of Elbow Flexor MRI Fat Fraction With Loss of Hand-To-Mouth Movement in Patients With Duchenne Muscular Dystrophy. *Neurology* (2021) 97(17):e1737–42. doi: 10.1212/wnl.0000000000012724
27. Agten CA, Rosskopf AB, Gerber C, Pfirrmann CW. Quantification of Early Fatty Infiltration of the Rotator Cuff Muscles: Comparison of Multi-Echo Dixon With Single-Voxel MR Spectroscopy. *Eur Radiol* (2016) 26(10):3719–27. doi: 10.1007/s00330-015-4144-y
28. Marty B, Reyngoudt H, Boisserie JM, Le Louër J, CAA E, Fromes Y, et al. Water-Fat Separation in MR Fingerprinting for Quantitative Monitoring of the Skeletal Muscle in Neuromuscular Disorders. *Radiology* (2021) 300(3):652–60. doi: 10.1148/radiol.2021204028
29. Mengiardi B, Schmid MR, Boos N, Pfirrmann CW, Brunner F, Elfering A, et al. Fat Content of Lumbar Paraspinal Muscles in Patients With Chronic Low Back Pain and in Asymptomatic Volunteers: Quantification With MR Spectroscopy. *Radiology* (2006) 240(3):786–92. doi: 10.1148/radiol.2403050820
30. Sollmann N, Zoffl A, Franz D, Syväri J, Dieckmeyer M, Burian E, et al. Regional Variation in Paraspinal Muscle Composition Using Chemical Shift Encoding-Based Water-Fat MRI. *Quant Imaging Med Surg* (2020) 10(2):496–507. doi: 10.21037/qims.2020.01.10
31. Zhao Y, Huang M, Serrano Sosa M, Cattell R, Fan W, Li M, et al. Fatty Infiltration of Paraspinal Muscles is Associated With Bone Mineral Density of the Lumbar Spine. *Arch Osteoporos* (2019) 14(1):99. doi: 10.1007/s11657-019-0639-5
32. Patzelt L, Junker D, Syväri J, Burian E, Wu M, Prokopchuk O, et al. Mri-Determined Psoas Muscle Fat Infiltration Correlates With Severity of Weight Loss During Cancer Cachexia. *Cancers (Basel)* (2021) 13(17):4433. doi: 10.3390/cancers13174433
33. Yanik B, Keyik B, Conkbayir I. Fatty Degeneration of Multifidus Muscle in Patients With Chronic Low Back Pain and in Asymptomatic Volunteers: Quantification With Chemical Shift Magnetic Resonance Imaging. *Skeletal Radiol* (2013) 42(6):771–8. doi: 10.1007/s00256-012-1545-8
34. Yoshihara K, Shirai Y, Nakayama Y, Uesaka S. Histochemical Changes in the Multifidus Muscle in Patients With Lumbar Intervertebral Disc Herniation. *Spine (Phila Pa 1976)* (2001) 26(6):622–6. doi: 10.1097/00007632-200103150-00012
35. Fairbank JC, Couper J, Davies JB, O'Brien JP. The Oswestry Low Back Pain Disability Questionnaire. *Physiotherapy* (1980) 66(8):271–3. doi: 10.1037/t04205-000
36. Chiarotto A, Maxwell LJ, Ostelo RW, Boers M, Tugwell P, Terwee CB. Measurement Properties of Visual Analogue Scale, Numeric Rating Scale, and Pain Severity Subscale of the Brief Pain Inventory in Patients With Low Back Pain: A Systematic Review. *J Pain* (2019) 20(3):245–63. doi: 10.1016/j.jpain.2018.07.009
37. Pfirrmann CW, Metzdorf A, Zanetti M, Hodler J, Boos N. Magnetic Resonance Classification of Lumbar Intervertebral Disc Degeneration. *Spine (Phila Pa 1976)* (2001) 26(17):1873–8. doi: 10.1097/00007632-200109010-00011
38. Ranger TA, Cicuttini FM, Jensen TS, Peiris WL, Hussain SM, Fairley J, et al. Are the Size and Composition of the Paraspinal Muscles Associated With Low Back Pain? A Systematic Review. *Spine J* (2017) 17(11):1729–48. doi: 10.1016/j.spinee.2017.07.002
39. Fortin M, Macedo LG. Multifidus and Paraspinal Muscle Group Cross-Sectional Areas of Patients With Low Back Pain and Control Patients: A Systematic Review With a Focus on Blinding. *Phys Ther* (2013) 93(7):873–88. doi: 10.2522/ptj.20120457
40. Fortin M, Gibbons LE, Videman T, Battie MC. Do Variations in Paraspinal Muscle Morphology and Composition Predict Low Back Pain in Men? *Scandinavian J Med Sci sports* (2015) 25(6):880–7. doi: 10.1111/sms.12301
41. Barker KL, Shamley DR, Jackson D. Changes in the Cross-Sectional Area of Multifidus and Psoas in Patients With Unilateral Back Pain: The Relationship

to Pain and Disability. *Spine (Phila Pa 1976)* (2004) 29(22):E515–9. doi: 10.1097/01.brs.0000144405.11661.eb
42. Moreno Catalá M, Schroll A, Laube G, Arampatzis A. Muscle Strength and Neuromuscular Control in Low-Back Pain: Elite Athletes Versus General Population. *Front Neurosci* (2018) 12:436. doi: 10.3389/fnins.2018.00436
43. Kjaer P, Bendix T, Sorensen JS, Korsholm L, Leboeuf-Yde C. Are MRI-Defined Fat Infiltrations in the Multifidus Muscles Associated With Low Back Pain? *BMC Med* (2007) 5:2. doi: 10.1186/1741-7015-5-2
44. Lee SK, Jung JY, Kang YR, Jung JH, Yang JJ. Fat Quantification of Multifidus Muscle Using T2-Weighted Dixon: Which Measurement Methods are Best Suited for Revealing the Relationship Between Fat Infiltration and Herniated Nucleus Pulposus. *Skeletal Radiol* (2020) 49(2):263–71. doi: 10.1007/s00256-019-03270-5
45. Goubert D, De Pauw R, Meeus M, Willems T, Cagnie B, Schouppe S, et al. Lumbar Muscle Structure and Function in Chronic Versus Recurrent Low Back Pain: A Cross-Sectional Study. *Spine J* (2017) 17(9):1285–96. doi: 10.1016/j.spinee.2017.04.025
46. Yoo YH, Kim HS, Lee YH, Yoon CS, Paek MY, Yoo H, et al. Comparison of Multi-Echo Dixon Methods With Volume Interpolated Breath-Hold Gradient Echo Magnetic Resonance Imaging in Fat-Signal Fraction Quantification of Paravertebral Muscle. *Korean J Radiol* (2015) 16(5):1086–95. doi: 10.3348/kjr.2015.16.5.1086
47. Han G, Jiang Y, Zhang B, Gong C, Li W. Imaging Evaluation of Fat Infiltration in Paraspinal Muscles on MRI: A Systematic Review With a Focus on Methodology. *Orthop Surg* (2021) 13(4):1141–8. doi: 10.1111/os.12962
48. Fischer MA, Nanz D, Shimakawa A, Schirmer T, Guggenberger R, Chhabra A, et al. Quantification of Muscle Fat in Patients With Low Back Pain: Comparison of Multi-Echo MR Imaging With Single-Voxel MR Spectroscopy. *Radiology* (2013) 266(2):555–63. doi: 10.1148/radiol.12120399
49. Liu ZZ, Wen HQ, Zhu YQ, Zhao BL, Kong QC, Chen JY, et al. Short-Term Effect of Lumbar Traction on Intervertebral Discs in Patients With Low Back Pain: Correlation Between the T2 Value and ODI/VAS Score. *Cartilage* (2021) 13(1_suppl):1947603521996793. doi: 10.1177/1947603521996793
50. Hori Y, Hoshino M, Inage K, Miyagi M, Takahashi S, Ohyama S, et al. Issls PRIZE in CLINICAL SCIENCE 2019: Clinical Importance of Trunk Muscle Mass for Low Back Pain, Spinal Balance, and Quality of Life-A Multicenter Cross-Sectional Study. *Eur Spine J* (2019) 28(5):914–21. doi: 10.1007/s00586-019-05904-7
51. Owen PJ, Miller CT, Mundell NL, Verswijveren S, Tagliaferri SD, Brisby H, et al. Which Specific Modes of Exercise Training are Most Effective for Treating Low Back Pain? Network Meta-Analysis. *Br J Sports Med* (2020) 54 (21):1279–87. doi: 10.1136/bjsports-2019-100886
52. Goubert D, Meeus M, Willems T, De Pauw R, Coppieters I, Crombez G, et al. The Association Between Back Muscle Characteristics and Pressure Pain Sensitivity in Low Back Pain Patients. *Scand J Pain* (2018) 18(2):281–93. doi: 10.1515/sjpain-2017-0142
53. Kalimo H, Rantanen J, Viljanen T, Einola S. Lumbar Muscles: Structure and Function. *Ann Med* (1989) 21(5):353–9. doi: 10.3109/07853898909149220
54. Macintosh JE, Valencia F, Bogduk N, Munro RR. The Morphology of the Human Lumbar Multifidus. *Clin Biomech (Bristol Avon)* (1986) 1(4):196–204. doi: 10.1016/0268-0033(86)90146-4
55. Bailey JF, Fields AJ, Ballatori A, Cohen D, Jain D, Coughlin D, et al. The Relationship Between Endplate Pathology and Patient-Reported Symptoms for Chronic Low Back Pain Depends on Lumbar Paraspinal Muscle Quality. *Spine (Phila Pa 1976)* (2019) 44(14):1010–7. doi: 10.1097/brs.0000000000003035
56. James G, Chen X, Diwan A, Hodges PW. Fat Infiltration in the Multifidus Muscle is Related to Inflammatory Cytokine Expression in the Muscle and Epidural Adipose Tissue in Individuals Undergoing Surgery for Intervertebral Disc Herniation. *Eur Spine J* (2021) 30(4):837–45. doi: 10.1007/s00586-020-06514-4
57. James G, Sluka KA, Blomster L, Hall L, Schmid AB, Shu CC, et al. Macrophage Polarization Contributes to Local Inflammation and Structural Change in the Multifidus Muscle After Intervertebral Disc Injury. *Eur Spine J* (2018) 27 (8):1744–56. doi: 10.1007/s00586-018-5652-7
58. Wu H, Ballantyne CM. Skeletal Muscle Inflammation and Insulin Resistance in Obesity. *J Clin Invest* (2017) 127(1):43–54. doi: 10.1172/jci88880
59. Crawford RJ, Filli L, Elliott JM, Nanz D, Fischer MA, Marcon M, et al. Age- and Level-Dependence of Fatty Infiltration in Lumbar Paravertebral Muscles of Healthy Volunteers. *AJNR Am J Neuroradiol* (2016) 37(4):742–8. doi: 10.3174/ajnr.A4596
60. Sions JM, Elliott JM, Pohlig RT, Hicks GE. Trunk Muscle Characteristics of the Multifidi, Erector Spinae, Psoas, and Quadratus Lumborum in Older Adults With and Without Chronic Low Back Pain. *J Orthop Sports Phys Ther* (2017) 47(3):173–9. doi: 10.2519/jospt.2017.7002
61. Lee SH, Park SW, Kim YB, Nam TK, Lee YS. The Fatty Degeneration of Lumbar Paraspinal Muscles on Computed Tomography Scan According to Age and Disc Level. *Spine J* (2017) 17(1):81–7. doi: 10.1016/j.spinee.2016.08.001
62. Hodges P, Holm AK, Hansson T, Holm S. Rapid Atrophy of the Lumbar Multifidus Follows Experimental Disc or Nerve Root Injury. *Spine (Phila Pa 1976)* (2006) 31(25):2926–33. doi: 10.1097/01.brs.0000248453.51165.0b
63. Bousema EJ, Verbunt JA, Seelen HAM, Vlaeyen JWS, Knottnerus AJ. Disuse and Physical Deconditioning in the First Year After the Onset of Back Pain. *Pain* (2007) 130(3):279–86. doi: 10.1016/j.pain.2007.03.024
64. Verbunt JA, Seelen HA, Vlaeyen JW, van de Heijden GJ, Heuts PH, Pons K, et al. Disuse and Deconditioning in Chronic Low Back Pain: Concepts and Hypotheses on Contributing Mechanisms. *Eur J Pain* (2003) 7(1):9–21. doi: 10.1016/s1090-3801(02)00071-x

Conflict of Interest: XZ and LN were employed by GE Healthcare.

The remaining authors declare that the research was conducted in the absence of any commercial or financial relationships that could be construed as a potential conflict of interest.

Publisher's Note: All claims expressed in this article are solely those of the authors and do not necessarily represent those of their affiliated organizations, or those of the publisher, the editors and the reviewers. Any product that may be evaluated in this article, or claim that may be made by its manufacturer, is not guaranteed or endorsed by the publisher.

frontiers | Frontiers in Endocrinology

TYPE Original Research
PUBLISHED 11 August 2022
DOI 10.3389/fendo.2022.884306

OPEN ACCESS

EDITED BY
Xiaoguang Cheng,
Beijing Jishuitan Hospital, China

REVIEWED BY
Songtao Ai,
Radiology/Shanghai Ninth Hospital, China
Patrizio Barca,
University of Pisa, Italy

*CORRESPONDENCE
Yan Wu
yanzi155@hotmail.com

†These authors have contributed equally and share first authorship

SPECIALTY SECTION
This article was submitted to Bone Research, a section of the journal Frontiers in Endocrinology

RECEIVED 26 February 2022
ACCEPTED 31 May 2022
PUBLISHED 11 August 2022

CITATION
Li Y, Jiang Y, Yu X, Ren B, Wang C, Chen S, Ma D, Su D, Liu H, Ren X, Yang X, Gao J and Wu Y (2022) Deep-learning image reconstruction for image quality evaluation and accurate bone mineral density measurement on quantitative CT: A phantom-patient study. *Front. Endocrinol.* 13:884306. doi: 10.3389/fendo.2022.884306

Deep-learning image reconstruction for image quality evaluation and accurate bone mineral density measurement on quantitative CT: A phantom-patient study

Yali Li†, Yaojun Jiang†, Xi Yu, Binbin Ren, Chunyu Wang, Sihui Chen, Duoshan Ma, Danyang Su, Huilong Liu, Xiangyang Ren, Xiaopeng Yang, Jianbo Gao and Yan Wu*

Department of Radiology, The First Affiliated Hospital of Zhengzhou University, Zhengzhou, China

Background and purpose: To investigate the image quality and accurate bone mineral density (BMD) on quantitative CT (QCT) for osteoporosis screening by deep-learning image reconstruction (DLIR) based on a multi-phantom and patient study.

Materials and methods: High-contrast spatial resolution, low-contrast detectability, modulation function test (MTF), noise power spectrum (NPS), and image noise were evaluated for physical image quality on Caphan 500 phantom. Three calcium hydroxyapatite (HA) inserts were used for accurate BMD measurement on European Spine Phantom (ESP). CT images were reconstructed with filtered back projection (FBP), adaptive statistical iterative reconstruction-veo 50% (ASiR-V50%), and three levels of DLIR(L/M/H). Subjective evaluation of the image high-contrast spatial resolution and low-contrast detectability were compared visually by qualified radiologists, whilst the statistical difference in the objective evaluation of the image high-contrast spatial resolution and low-contrast detectability, image noise, and relative measurement error were compared using one-way analysis of variance (ANOVA). Cohen's kappa coefficient (k) was performed to determine the interobserver agreement in qualitative evaluation between two radiologists.

Results: Overall, for three levels of DLIR, 50% MTF was about 4.50 (lp/cm), better than FBP (4.12 lp/cm) and ASiR-V50% (4.00 lp/cm); the 2 mm low-contrast object was clearly resolved at a 0.5% contrast level, while 3mm at FBP and ASiR-V50%. As the strength level decreased and radiation dose increased, DLIR at three levels showed a higher NPS peak frequency and lower noise level, leading to leftward and rightward shifts, respectively. Measured L1, L2, and L3 were slightly lower than that of nominal HA inserts (44.8, 95.9, 194.9 versus 50.2, 100.6, 199.2mg/cm^3) with a relative measurement error of 9.84%, 4.08%, and 2.60%. Coefficients of variance for the L1, L2, and L3 HA inserts were 1.51%,

1.41%, and 1.18%. DLIR-M and DLIR-H scored significantly better than ASiR-V50% in image noise (4.83 ± 0.34, 4.50 ± 0.50 versus 4.17 ± 0.37), image contrast (4.67 ± 0.73, 4.50 ± 0.70 versus 3.80 ± 0.99), small structure visibility (4.83 ± 0.70, 4.17 ± 0.73 versus 3.83 ± 1.05), image sharpness (3.83 ± 1.12, 3.53 ± 0.90 versus 3.27 ± 1.16), and artifacts (3.83 ± 0.90, 3.42 ± 0.37 versus 3.10 ± 0.83). The CT value, image noise, contrast noise ratio, and image artifacts in DLIR-M and DLIR-H outperformed ASiR-V50% and FBP (P<0.001), whilst it showed no statistically significant between DLIR-L and ASiR-V50% (P>0.05). The prevalence of osteoporosis was 74 (24.67%) in women and 49 (11.79%) in men, whilst the osteoporotic vertebral fracture rate was 26 (8.67%) in women and (5.29%) in men.

Conclusion: Image quality with DLIR was high-qualified without affecting the accuracy of BMD measurement. It has a potential clinical utility in osteoporosis screening.

KEYWORDS

bone mineral density, osteoporosis, deep learning iterative reconstruction, Catphan 500, European Spine Phantom

1 Introduction

The elderly men and postmenopausal women had a high incidence rate of osteoporosis and related vertebral fracture (1). Vertebral fracture, especially thoracolumbar osteoporotic compression fracture, often occurs in the mid-thoracic (T7-8) and thoracolumbar spine (T12-L1) (2, 3). Bone mineral density (BMD) obtained from quantitative computed tomography (QCT) is a volumetric measure of vertebral trabecular bone with high sensitivity and accuracy for predicting bone strength and fracture risk (4–6). QCT not only reduces the influence of overlying ribcage (2) but also prevents severe spinal degeneration and vascular calcification without requiring the oral contrast agent and body position (5) compared with dual-energy X-ray absorptiometry (DXA). QCT is superior to DXA in BMD measurement for early screening of osteoporosis. However, a high level of radiation exposure delivered to patients with QCT limits its further clinical application (6). Recently, the combination of low-dose CT (LDCT) and lumbar QCT has been initiated by the China Health Big Data (China Biobank) project for opportunistic screening of osteoporosis and lung cancer simultaneously in terms of reducing radiation dose, repeated scan, patient time, and additional costs. Wu et al. (5) described the study protocol of the combination of QCT with LDCT. Inherently, Cheng et al. (7) conducted a multicenter population-based cohort study with QCT to determine the prevalence of osteoporosis in China.

Unfortunately, image noise increased obviously after reducing radiation dose, while image quality decreased significantly, particularly in the spine (5), contributing to an inevitable decrease in diagnostic performance. An iterative reconstruction (IR) algorithm is introduced to reduce image noise and preserve image quality between radiation risk and diagnostic performance (8, 9). But many IR algorithms can change the magnitude of the image noise and texture details and may cause an adverse impact on the detection of low-contrast lesions, particularly at high strength levels (10–12).

Currently, a new-generation deep-learning image reconstruction (DLIR) (TrueFidelity, GE Healthcare) was proposed to improve the CT image quality. It utilizes deep neural networks that consist of layers of mathematical equations, with millions of connections and parameters to generate CT images, and is designed with a fast reconstruction speed for routine CT use, even in acute care settings. And it consists of three selectable reconstruction strength levels (low, medium, and high) to control the amount of noise reduction corresponding to clinical applications and radiologist preference (13).

To assess the image quality of LDCT, accurate BMD measurement, and the performance of DLIR for image quality at ultralow-dose level, Li et al. (14) systemically evaluated the physical image quality on Catphan 500 phantom. Results indicated that the CT number linearity was unbiasedly contributing to accurate BMD quantification. DLIR performed better than iterative model reconstruction (IMR, level 2) at 0.25 and 0.75 mGy, but they didn't evaluate the accuracy of BMD value on European Spine Phantom (ESP). Therefore, on the basis of Li et al.'s experiment, our study aimed to evaluate CT image quality and accurate BMD measurement on the Catphan 500 phantom and ESP and patient study using DLIR algorithm in comparison to 50% adaptive

statistical iterative reconstruction-veo (ASiR-V 50%) and filtered back projection (FBP) reconstruction algorithms.

2 Materials and methods

This prospective study was strictly adhered to HIPAA Privacy Rule and approved by the ethics committee of the First Affiliated Hospital of Zhengzhou University and Beijing Jishuitan Hospital. The China Biobank project is a multicenter cohort study and has been registered with the US clinical trials database (https://clinicaltrials.gov/ct2/show/NCT03699228; trial identifier: NCT03699228). Our hospital is one of the collaborating hospitals and provided the patient cohort for this study. The informed consent of the patients was all obtained.

Data acquisitions were obtained from Catphan 500 phantom (Phantom Laboratory, Salem, NY, USA) and ESP (No. 145, Germany ORM company), as well as patients on Revolution CT (GE Healthcare, WI, USA) from April 2020 to June 2021. The weekly air calibration and monthly QA were performed by qualified technologists before data acquisitions and BMD measurement throughout the whole study using the Model 3 synchronous QA phantom. To reduce the uncertainty of measurements, data acquisitions were scanned 10 consecutive times separately on Catphan 500 and ESP without repositioning.

2.1 Catphan 500 Phantom

The Catphan 500 phantom consists of 4 modules, including CTP401, CTP528, CTP515, and CTP486 modules. The module CTP528, CTP515, and CTP486 were selected to evaluate the high-contrast spatial resolution, low-contrast detectability, and image noise, respectively (15).

2.2 European Spine Phantom

ESP consisted of water-equivalent plastic made of epoxy resin and 3 cylindrical inserts of artificial vertebrae with nominal trabecular BMD values of L1 (50.5mg/cm^3), L2 (100.6mg/cm^3), and L3 (199.2mg/cm^3), which are equivalent to water and bone solid compartments that simulate lumbar spine of the human body (16).

2.3 Study participants

A total of 716 patients (300 women and 416 men, age, 62.4 ± 7.2 years, range, 55-78 years) who derived from the China Biobank Study were prospectively enrolled in our hospital during March and June 2021 (Table 1). The exclusion criteria included: patients aged below 50 years old; patients with the use of oral corticosteroids or anti-osteoporotic medication such as vitamin D supplementation; and patients with metal implants in the upper abdominal.

2.4 Scan protocol

Data acquisitions were obtained with a fixed tube voltage of 120 kV. And the tube current was set to yield a volume CT dose index ($CDTI_{vol}$) at 2 ultralow-dose levels of 0.25 and 0.75mGy. Images were reconstructed using FBP, ASiR-V50% and DLIR (level, low, medium, and high) with a standard kernel (Table 1).

TABLE 1 Summary of data acquisitions at two phantoms and clinical setting of patient.

CT parameters	Catphan 500	ESP	Participants
Acquisition mode	Axial/Helical	Axial/Helical	Helical
Reconstruction kernel	Standard	Standard	Standard
Tube voltage (kV)	120	120	120
Tube current-time product (mAs)	25/75	25/75	25/75
Thickness/increment (mm)	1.25/5	1.25/5	1.25/5
Pitch	0.992	0.992	0.992
Beam collimation (mm)	40	40	40
DFOV (mm)	500	500	500
Matrix size	512×512	512×512	512×512
X-ray tube rotation speed(s/r)	0.5	0.5	0.5
Reconstruction algorithm	FBP/ASiR-V50%/DLIR(L/M/H)	FBP/ASiR-V50%/DLIR(L/M/H)	FBP/ASiR-V50%/DLIR(L/M/H)
Detector configuration (mm)	256×0.625	256×0.625	256×0.625
Voxel size (mm)	0.61	0.61	0.61
$CTDI_{vol}$ (mGy)	0.25/0.75	0.25/0.75	0.25/0.75

CT, computed tomography; ESP, European Spine Phantom; FBP, filtered back projection; ASiR-V50%, adaptive statistical iterative reconstruction-veo 50%; DLIR(L/M/H), deep-learning image reconstruction, level low, medium, and high; $CTDI_{vol}$, volume CT dose index; mGy, milligray; DFOV, display field of view.

2.5 Data measurement and image evaluation

High-contrast spatial resolution, low-contrast detectability, and image noise are the standard image quality parameters of CT system.

2.5.1 High-contrast spatial resolution

High-contrast spatial resolution indicates the capability of a CT system to differentiate the small high-contrast objects (15). The module CTP528 is used to measure the high-contrast spatial resolution *via* subjective and objective evaluation. For subjective evaluation, two radiologists with 6 and 8 years of radiological experience visually assess the 21 lp/cm high-resolution gauges by adjusting the window width (WW) and window level (WL) until resolving the highest number of visible line pairs. For objective evaluation, the MTF curve that represents the imaging capability of CT system for different frequency components is used to distinguish the line pairs to decimal level, and analyze the curve trend in the low- and high-frequency ranges (15).

2.5.2 Low-contrast detectability

Low-contrast detectability determines the capability to distinguish different lesions with a minor density difference (17). The The module CTP515 consists of 3 groups supra-slice targets at the contrast levels of 1%, 0.5%, and 0.3% with the diameter of 15, 9, 8, 7, 6, 5, 4, 3, and 2 mm, respectively. The low-contrast detectability is estimated by the nominal contrast level of 1.0% (15). Two radiologists independently and blindly adjusted the WW and WL to identify the smallest supra-slice target diameter and performed a direct side-by-side comparison (18).

2.5.3 Image noise

Image noise represents the standard deviation of CT values within an ROI in the uniform phantom image (15). The noise power spectrum (NPS) is used to calculate the noise characterization, and the NPS curve reflects the variation of image intensity over high-contrast resolution frequency (19). The CTP489 module is an image uniformity module that is cast from uniform material with the CT number within 2% of water density (-25~25HU). Five circular regions of interest (ROIs) with radii of 5-6mm were cropped in the central and peripheral sites of the image (clock positions 12, 3, 6, and 9). The image uniformity was measured by the deviation of the minimum and maximum CT number values between central and peripheral sites and recommended within ±4HU (15, 20).

2.5.4 Bone mineral density measurement

CT images were transferred to a dedicated QCT PRO BMD workstation (Mindways QCT PRO workstation). All QCT analyses were performed by professionally trained radiologists using Mindways QCT PRO software (3D spine function version 6.10, Mindways software Inc., Austin, TX, USA) and conducted by a Mindways QCT-PRP operator's manual (21).

Firstly, start the QCT PRO software, click on the 3D Spine Analysis module button, and select the L1, L2, and L3 HA inserts to analyze. Then, click the rotation tab, drag the yellow crosshair to the center of L1, L2, and L3 on the sagittal image, rotate them until it resembles a vertical box, mark the middle of them on the coronal images, and correlate to the corresponding axial images. Finally, set 3 ROIs at L1, L2, and L3 with the circular area of about 2/3 in the entire axial image and slice thickness of 9 mm, click the report tab, and calculate the BMD of L1, L2, and L3. Unless obvious errors occurred in the measurement process, workstation software were processed for automatic analysis, including automatic functions, automatic detection of boundaries, and automatic generation of ROIs throughout the whole operation.

2.5.5 Accurate bone mineral density quantification

The accuracy of the BMD value on QCT is evaluated by calculating the measurement error for each HA insert. Measurement error is defined as a deviation between the measured HA and true HA concentration (units: mg/cm^3). Relative measurement error reflects the accuracy error in proportion to true HA concentration (16, 22). The precision error is used to interpret significant changes in BMD and expressed as the percentage coefficient of variation (%CV) (23).

$$\text{Measurement error}(mg/cm^3) = \text{Measured HA concentration} - \text{true HA concentration} \quad (1)$$

$$\text{Relative measurement error}(\%) = \frac{\text{Measurement error}(mg/cm^3)}{\text{True HA concentration}(mg/cm^3)} \times 100 \quad (2)$$

$$\%CV = \frac{SD}{Mean} \times 100 \quad (3)$$

2.5.6 Qualitative image analysis

Two radiologists independently and blindly assess the image quality of CT images using a point-based Likert scale (Table 2) (19). Patient information and examination details were anonymized, images were presented in a random order, and radiologists were allowed to freely scroll or zoom the images and adjust the WW/WL. Consensus reading was used when there was any disagreement between two radiologists.

2.5.7 Quantitative image analysis

The circular ROIs with radii of 7 mm were manually drawn on the lung, air, liver parenchyma, and right side of the paraspinal muscle in five image sets to measure the mean CT value and SD in Hounsfield units (HU).

Lung measurements were obtained from the lower lung lobes toward the periphery, liver measurements from the liver parenchyma avoiding large vessels and biliary tree, air measurements were defined

TABLE 2 Grading scale of the qualitative image analysis.

Grading score	Image noise	Image contrast	Small structure visibility	Image sharpness	Artifacts
1	Unacceptable	Unacceptable	Unacceptable	Severe	Severe
2	Above average	Suboptimal	Suboptimal	Moderate	Major
3	Average	Acceptable	Acceptable	Minimal	Minor
4	Less than average	Above average	Above average	No blurring	None
5	Minimal	Excellent	Excellent		

as the SD of air external and anterior to the patient at the sternomanubrial junction, and muscle measurements were measured at the right side of the paraspinal muscle of the posterior margin of the L2 vertebra. The SD of air and muscle were considered as image noise for chest and abdomen (8, 24).

$$Noise = SD_{background} \tag{4}$$

$$CNR = \frac{ROI_{organ} - ROI_{\text{background}}}{SD_{\text{background}}} \tag{5}$$

where ROI_{organ} and $ROI_{background}$ refer to the mean CT value of the lung, liver parenchyma, air, and paraspinal muscle, respectively; SD_{organ} and $SD_{background}$ are image noise determined as SD in the lung, liver parenchyma, air, and muscle, respectively.

2.6 Statistical analysis

All statistical analyses were performed using SPSS 20 software (IBM Corp., Armonk, NY, USA). The MTF and NPS curves were calculated with MATLAB R2018b (MathWorks, Natick, MA, USA). The continuous variables were expressed as mean ± SD. Subjective evaluation of the image high-contrast spatial resolution and low-contrast detectability were compared visually by qualified radiologists, whilst the statistical difference of objective evaluation of the image high-contrast spatial resolution, low-contrast detectability, image noise, and relative measurement error were compared using one-way analysis of variance (ANOVA) and Bonferroni correction. Friedman test was used to perform the qualitative evaluation. Cohen's kappa coefficient (k) was used to determine the interobserver agreement between two radiologists. A Kappa value of 0.21-0.40 was defined as poor, 0.41-0.60 as moderate, 0.61-0.80 as substantial, and 0.81-1.00 as excellent. A $P<0.05$ was considered as statistically significant.

3 Results

3.1 High-contrast spatial resolution

3.1.1 Subjective evaluation

In general, the high-resolution bars were clearly separable at 6 lp/cm, but started blurring at 7 or 8 lp/cm, the resolving power was all high-qualified (Figures 1, 2). The bars of the three levels of DLIR at 0.25mGy were comparable to those of ASiR-V50% at 0.75mGy. There were no statistically significant differences in slice thickness and scan type ($P>0.05$).

3.1.2 Objective evaluation

The MTF values of FBP and ASiR-V50% at 50%MTF were ≤ 4.00lp/cm or less, while that of DLIR at three levels was at 4.50lp/cm. The resolving power at 10%MTF (6.78 ± 0.40 lp/cm) was generally similar to the subjective evaluation results, which showed no significant difference from that at 5%MTF. Thus, it could be used to evaluate the high-contrast spatial resolution of the CT system (Figures 3, 4). The differences were not significant in slice thickness and scan type ($P>0.05$). The MTF value of DLIR (three levels) at 0.25mGy was comparative to that of FBP but slightly better than that of ASiR-V50% at 0.75mGy.

3.2 Low-contrast detectability

All CT images were visualized at a fixed window setting (WW/WL, 70/100 HU) (Figures 5, 6). In general, the 3 mm low-contrast object at a 0.5% contrast level was clearly resolved, the 2 mm low-contrast object could be resolved for DLIR at three levels, and the diameters were all less than 5mm, which confirmed that the images were qualified (25). In respect of low-contrast detectability, DLIR-M and DLIR-H were superior to ASiR-V50%, DLIR-L was comparable to ASiR-V50% and better than FBP, and DLIR (three levels) at 0.25mGy was comparable to ASiR-V50% at 0.75mGy. Although DLIR were clearer as the strength level, slice thickness, and radiation dose increased, there was a slightly significant difference in scan type ($P>0.05$).

3.3 Image noise

In general, as the strength level decreased and the radiation dose increased, the noise level decreased while the peak frequency of the NPS curve increased (Figures 7, 8). DLIR-M and DLIR-H achieved a lower noise level than FBP and ASiR-V50%, whilst DLIR-L was comparative to ASiR-V50%. The peak frequency of the NPS curve was higher at 0.75mGy than at

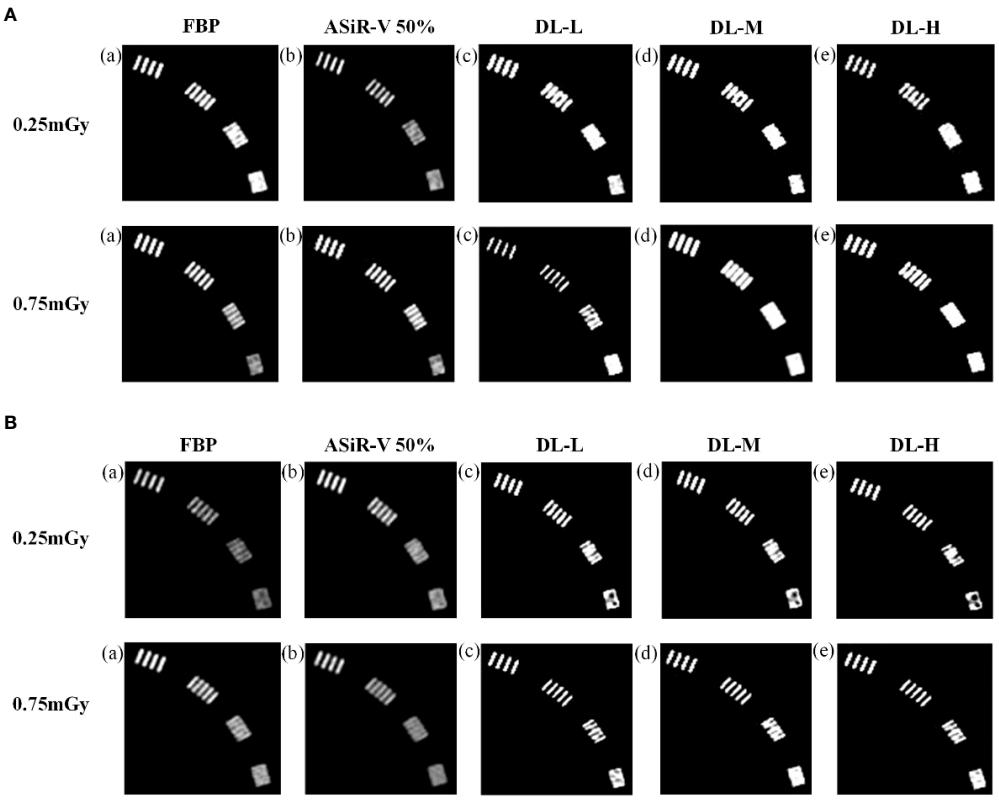

FIGURE 1
High-contrast images in helical mode reconstructed with FBP (a, f), ASiR-50% (b, g), and DLIR (L/M/H) (c, h; d, i; e, j) at 0.25mGy and 0.75mGy with a slice thickness of 1.25mm **(A)** and 5mm **(B)**, respectively. CT, computed tomography; FBP, filtered back projection; ASiR-50%, adaptive statistical iterative reconstruction-veo 50%; DLIR(L/M/H), deep-learning image reconstruction, level low, medium, and high; mGy, milligray.

0.25mGy, and those of DLIR (three levels) at 0.25mGy and ASiR-V50% at 0.75mGy were comparable. Increasing the radiation dose, the NNPS curve of FBP and ASiR-V50% indicated a rightward in the peak frequency. As the strength level increased and radiation dose decreased, the NNPS curve of DLIR at three levels presented a leftward shift in the peak frequency and showed a similar shape with only a slight frequency shift under all scan protocols (Figures 7, 8).

3.4 Accuracy of bone mineral density

Measured BMD of L1, L2, and L3 was slightly lower than that of nominal HA inserts (45.8, 95.9, 194.9 versus 50.2, 100.6, 199.2mg/cm^3, respectively). The measurement error for L1, L2, and L3 HA inserts was 4.9, 4.1, and 5.1mg/cm^3, with a relative measurement error of 9.84%, 4.08%, and 2.60%, respectively. Coefficients of variance for the L1, L2, and L3 HA inserts were 1.51%, 1.41%, and 1.18%. There were no statistically significant differences among L1, L2, and L3 under all scan protocols (P>0.05). The accuracy of BMD value varied greatly with FBP but little with DLIR in L1, L2, and L3, and BMD in L1 varied mostly compared with L2 and L3 (Figure 9).

3.5 Basic characteristics with participants

Of the 716 patients including 300 women and 416 men, with an age of 62.40 ± 7.20 (50-97) years, a body weight 63.07 ± 10.82 (45.00-76.50) kg, a height of 1.66 ± 0.69 (1.55-1.78) m, and BMI of 23.05 ± 3.58 (16.65-26.93) kg/m^2 were recruited. The prevalence of osteoporosis was found in 74 (24.67%) women and 49 (11.79%) men, while osteoporotic vertebral fracture rate was observed in 26 (8.67%) women and 22 (5.29%) men (Table 3).

3.6 Qualitative image analysis

DLIR-M and DLIR-H were scored significantly better than ASiR-V50% in image noise (4.83 ± 0.34, 4.50 ± 0.50 vs 4.17 ± 0.37), image contrast (4.67 ± 0.73, 4.50 ± 0.70 vs 3.80 ± 0.99),

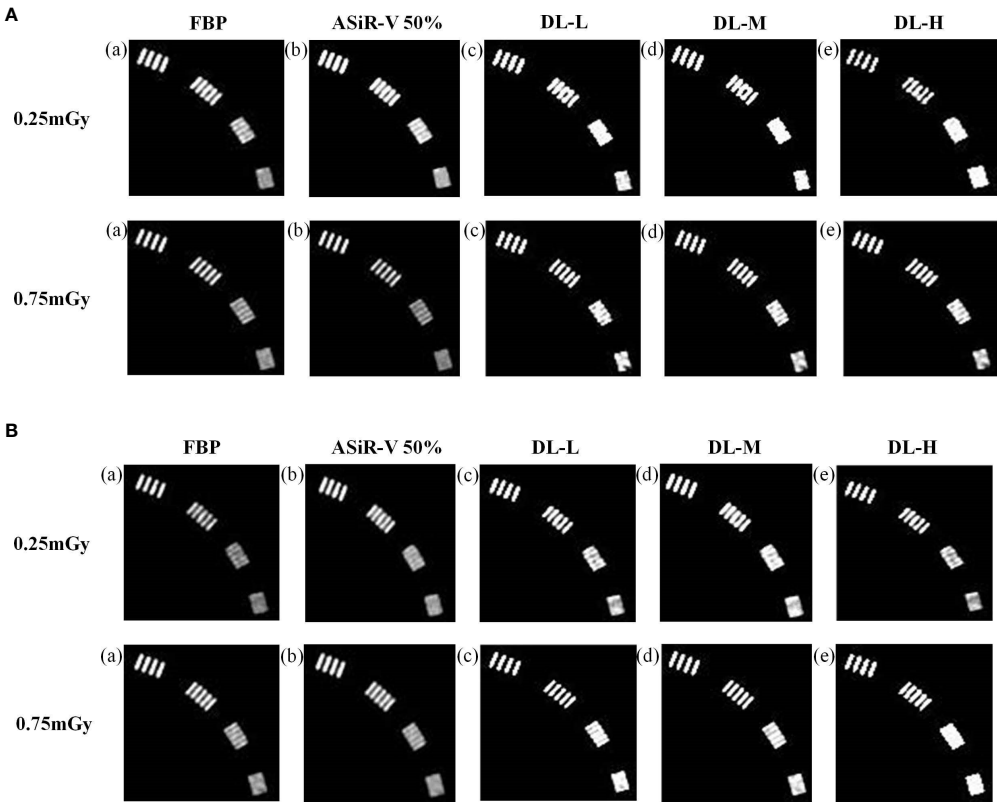

FIGURE 2
High-contrast images in axial mode reconstructed with FBP (a, f), ASiR-50% (b, g), and DLIR at three levels (L/M/H) (c, h; d, i; e, j) at 0.25mGy and 0.75mGy with a slice thickness of 1.25mm **(A)** and 5mm **(B)**, respectively. CT, computed tomography; DLIR(L/M/H), deep-learning image reconstruction, level low, medium, and high; mGy, milligray; ASiR-50%, adaptive statistical iterative reconstruction-veo 50%.

small structure visibility (4.83 ± 0.70, 4.17 ± 0.73 vs 3.83 ± 1.05), image sharpness (3.83 ± 1.12, 3.53 ± 0.90 vs 3.27 ± 1.16), and artifacts (3.83 ± 0.90, 3.42 ± 0.37 vs 3.10 ± 0.83). There were statistically significant differences among DLIR-L, DLIR-M, and DLIR-H in all image quality metrics (P<0.001) (Figure 10 and Table 4). The interobserver agreement between two radiologists showed an excellent agreement with a kappa value of 0.852.

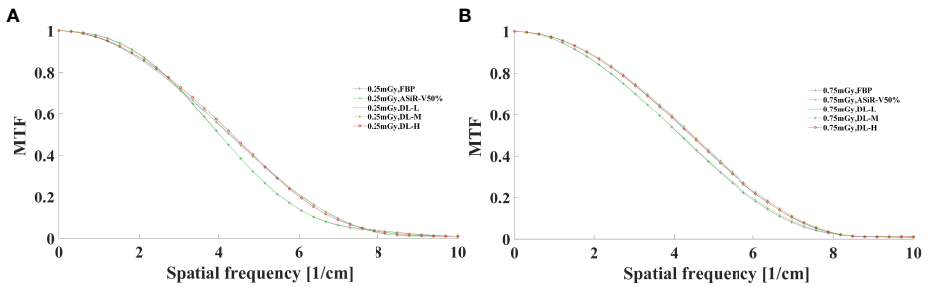

FIGURE 3
MTF curves in helical mode reconstructed with FBP, ASiR-V50%, and DLIR (L/M/H) at 0.25mGy **(A)** and 0.75mGy **(B)**. CT, computed tomography; FBP, filtered back projection; ASiR-50%, adaptive statistical iterative reconstruction-veo 50%; DLIR(L/M/H), deep-learning image reconstruction, level low, medium, and high; mGy, milligray.

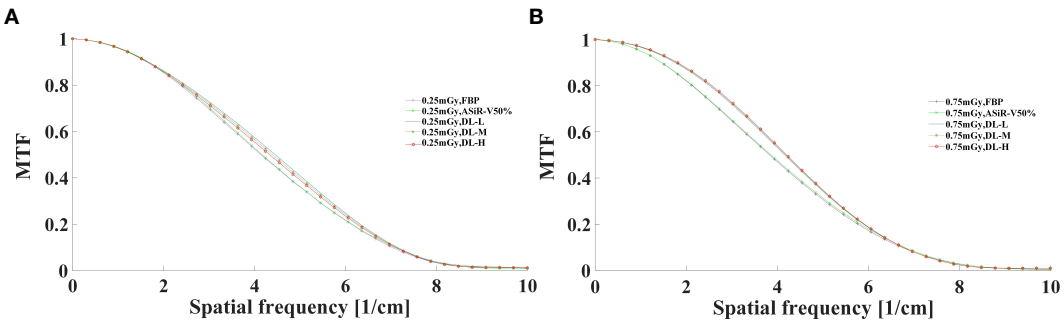

FIGURE 4
MTF curves in axial mode reconstructed with FBP, ASiR-50%, and DLIR (L/M/H) at 0.25mGy **(A)** and 0.75mGy **(B)**. CT, computed tomography; DLIR(L/M/H), deep-learning image reconstruction, level low, medium, and high; mGy, milligray; ASiR-50%, adaptive statistical iterative reconstruction-veo 50%.

3.7 Quantitative image analysis

The overall image quality, CT value, image noise, CNR, and image artifacts were outperformed for DLIR compared with ASiR-V50% and FBP (P<0.001), whilst it was not a statistically significant difference between DLIR-L and ASiR-V50% (P>0.05). As radiation dose and strength level increased, image noise significantly decreased, CNR obviously increased, whilst CT value showed no significant difference (Table 5).

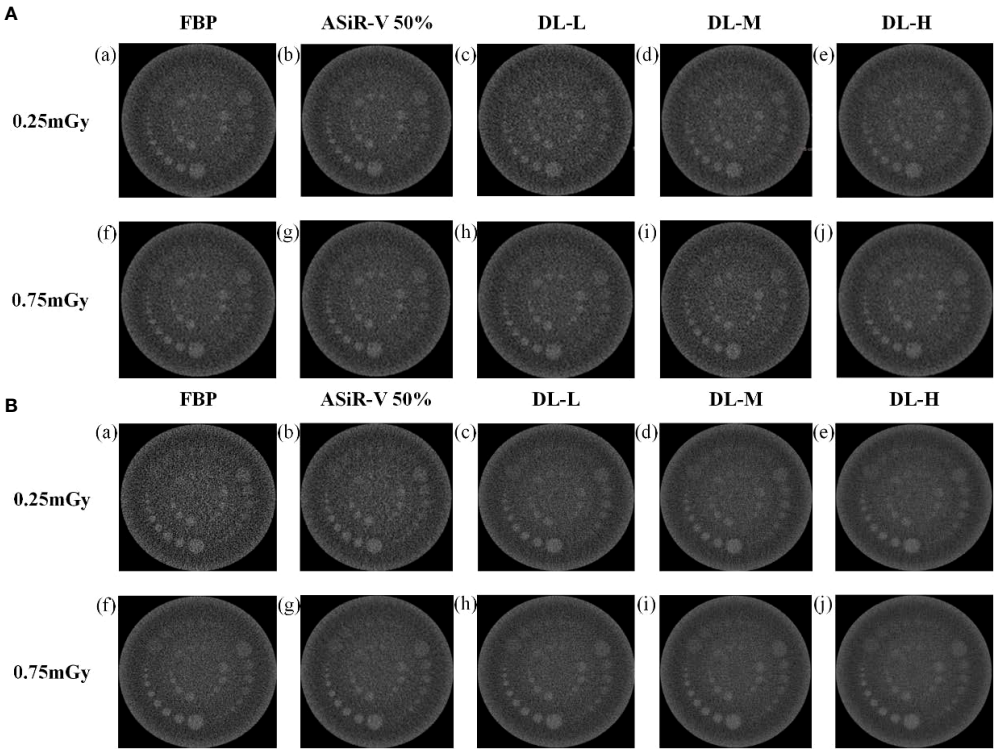

FIGURE 5
Low-contrast detectability images in helical mode reconstructed with FBP (a, f), ASiR-50% (b, g), and DLIR(L/M/H) (c, h; d, i; e, j) at 0.25mGy and 0.75mGy with a slice thickness of 1.25mm **(A)** and 5mm **(B)**, respectively. CT, computed tomography; FBP, filtered back projection; ASiR-50%, adaptive statistical iterative reconstruction-veo 50%; DLIR(L/M/H), deep-learning image reconstruction, level low, medium, and high; mGy, milligray.

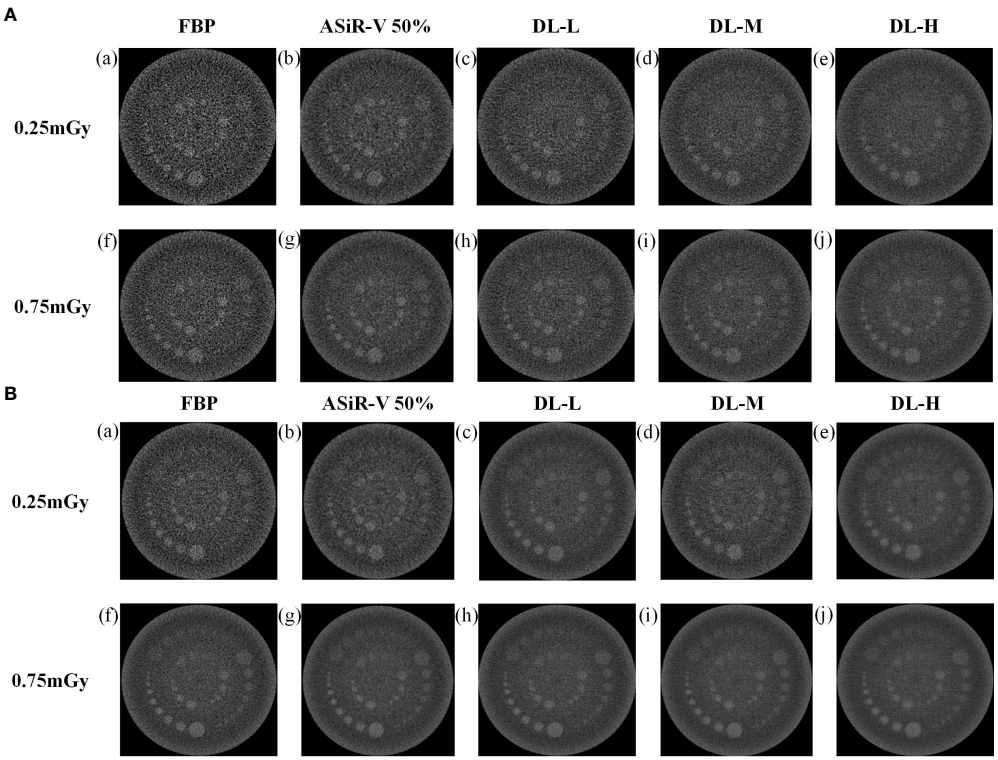

FIGURE 6
Low-contrast detectability images in axial mode reconstructed with FBP (a, f), ASiR-50% (b, g), and DLIR(L/M/H) (c, h; d, i; e, j) at 0.25mGy and 0.75mGy with a slice thickness of 1.25mm **(A)** and 5mm **(B)**, respectively. CT, computed tomography; DLIR(L/M/H), deep-learning image reconstruction, level low, medium, and high; mGy, milligray; ASiR-50%, adaptive statistical iterative reconstruction-veo 50%.

4 Discussion

In our study, we systematically evaluated the image quality, accurate BMD measurement, and clinical applicability of QCT with DLIR based on multi-phantom and patient studies. Results indicated great clinical importance without requiring any additional equipment and patient time, repeated CT scan, radiation dose, and additional costs. To our knowledge, it is the first systemic study to research the application of BMD measurements at an ultralow-dose level. QCT can be utilized for further opportunistic screening of osteoporosis, osteoporotic fracture, or other clinical applications (e.g., health check-ups) in China or worldwide countries accessing to CT easily than DXA (7).

Our results are consistent with Li et al. (15) findings on Catphan 500. For three levels of DLIR, MTF value at 50%MTF was about 4.50lp/cm, better than those for FBP (4.12 lp/cm) and ASiR-V50% (4.00 lp/cm). The 2 or 3 mm low-contrast object was clearly resolved at a 0.5% contrast level or at FBP and ASiR-V50%. Abdullah et al. (16) reported that the 50%MTF value and smallest size of objects were about 0.41 lp/cm and 3mm with ASiR-V (level: 40% and 60%), slightly lower than 4.50lp/cm and 2mm with DLIR. It showed an obviously lower NPS peak frequency and noise level, and a shift towards a lower spatial frequency in NNPS curve. As the strength level increased, the peak and spatial frequency of NPS curves with DLIR were decreased, which is consistent with a study reported by Greffier et al. (26). DLIR has been developed to reduce radiation dose and maintain image quality without changing the image texture or affecting the anatomical and pathological structures (13). And it can decrease the low-frequency noise component to improve low-contrast detectability for soft tissues ranging from 50 to 200 HU in abdominal CT (27), while maintaining the high-contrast spatial resolution of detailed structures, such as sharp edges and vessel boundaries at a low-dose level.

For image analysis in patients, DLIR-M and DLIR-H were scored better than ASiR-V50% in image noise, image contrast, small structure visibility, image sharpness, and artifacts. As radiation dose and strength level increased, image noise significantly decreased, CNR obviously increased, whilst CT value showed no significant difference (P>0.05). Results indicated that DLIR had better overall image quality than ASiR-V50%. Our finding was in accordance with Singh et al.

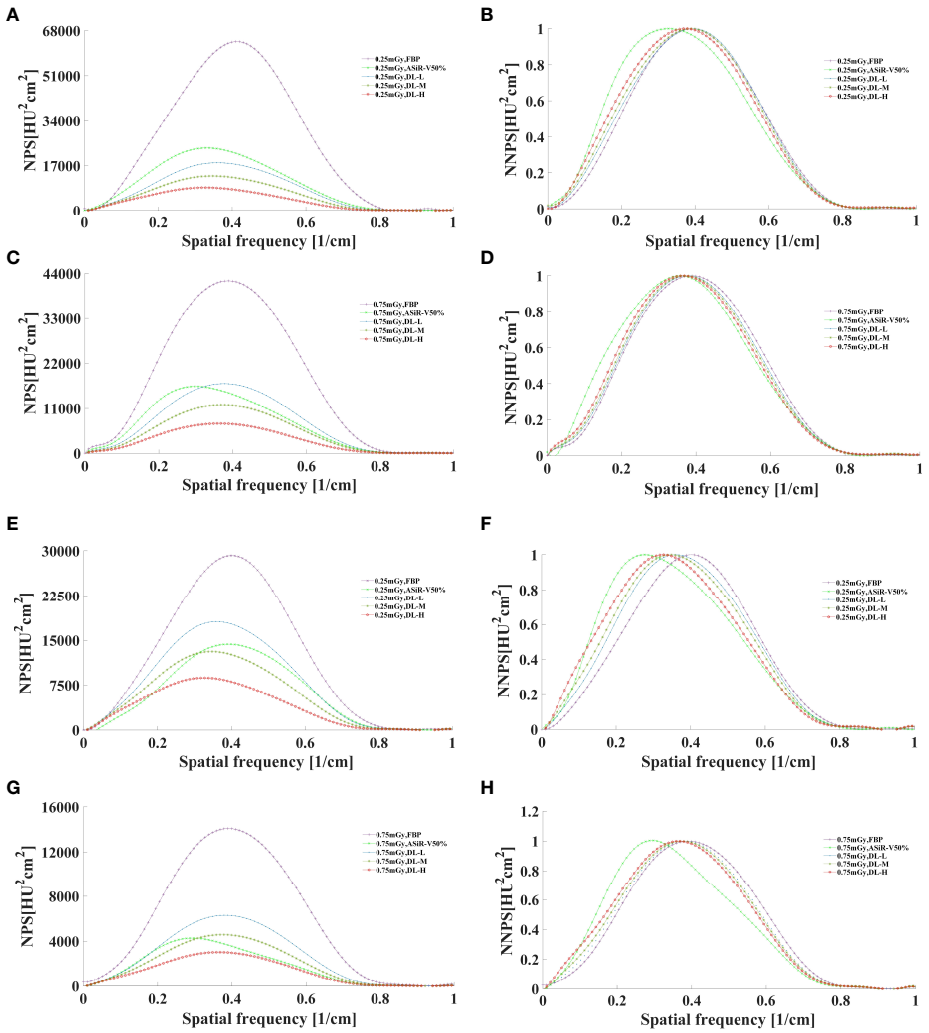

FIGURE 7
The curves of NPS and NNPS in helical mode reconstructed with FBP, ASiR-V50%, and DLIR (L/M/H) at 0.25mGy **(A, B, E, F)** and 0.75mGy **(C, D, G, H)** with a slice thickness of 1.25mm **(A–D)** and 5mm **(E–H)**. NPS, noise power spectrum; NNPS, normalized noise power spectrum; HU, Hounsfield units; FBP, filtered back projection; ASiR-50%, adaptive statistical iterative reconstruction-veo 50%; DLIR(L/M/H), deep-learning image reconstruction, level low, medium, and high; mGy, milligray.

(28) and Kim et al. (29)'s study that both obtained with relatively small sample sizes, but revealed a better significance due to the large patient cohort. Several studies suggested that DLIR was scored significantly better in overall image quality than different strengths of ASiR-V (level: 30%, 40%, and 50%) (24, 29) and comparable to ASiR-V (level: 70%, 100%) (30, 31).

Three HA inserts of 50.2-199.2 mg/cm^3 provided a range of trabecular BMD mimicking the physiological range of BMD seen in all age groups (32). The relative measurement error of L1, L2, and L3 was 9.84%, 4.08%, and 2.60%, respectively. Coefficients of variance for the L1, L2, and L3 HA inserts were 1.51%, 1.41%, and 1.18%. Those all falling within the range of 4-15% and meeting the clinical BMD measurement requirements (4, 32, 33). The largest and smallest deviations were found in L3 and L1, respectively. As the BMD value decreased, the relative measurement error increased significantly; especially with BMD less than 100.2 mg/cm^3, thus more attention should be paid to osteoporosis patients when evaluating the risk of osteoporotic fractures. Wu et al. (4) investigated the repeatability and accuracy of QCT measurement of BMD by low-mAs with iterative model reconstruction (IMR) algorithm based on phantom level and showed the maximum deviation of accuracy was 11% for L1, 4% for L2, and 6% for L3. In contrast, our study demonstrated that the accuracy of BMD at

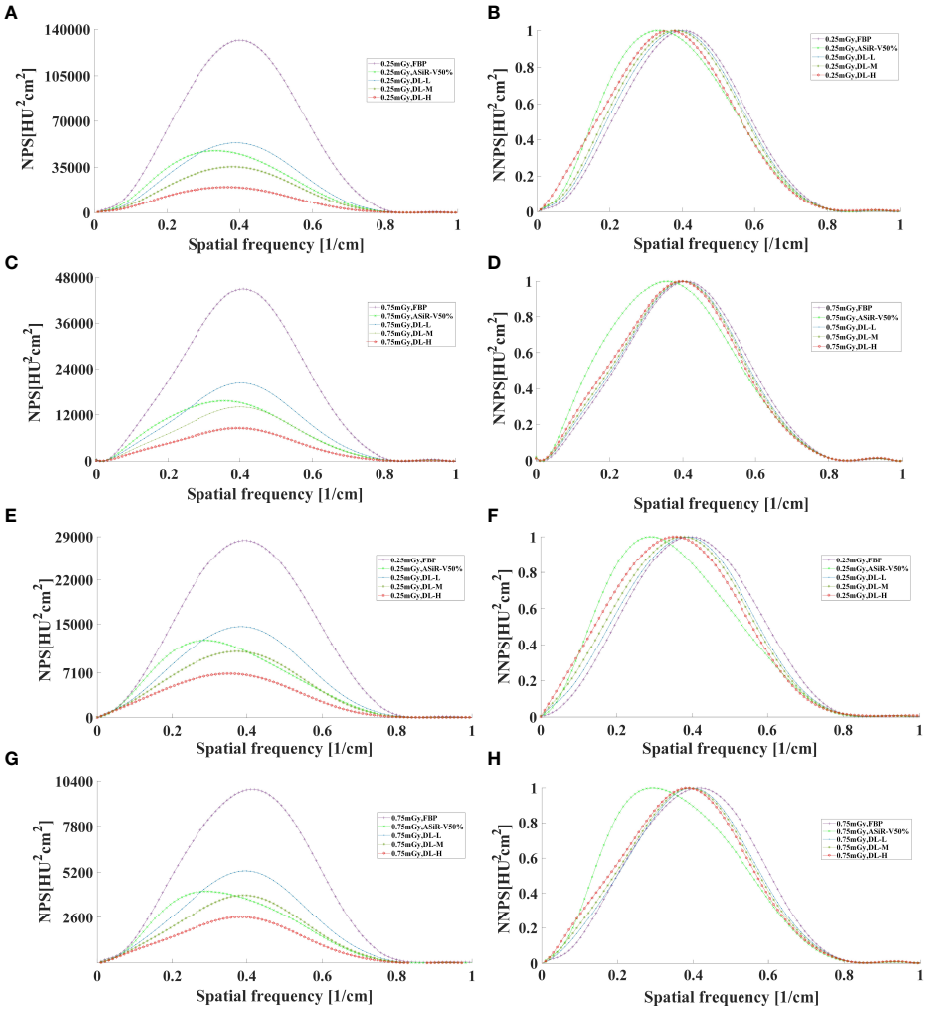

FIGURE 8
The curves of NPS and NNPS in axial mode reconstructed with FBP, ASiR-V50%, and DLIR (L/M/H) at 0.25mGy **(A, B, E, F)** and 0.75mGy **(C, D, G, H)** with a slice thickness of 1.25mm **(A–D)** and 5mm **(E–H)**. NPS, noise power spectrum; NNPS, normalized noise power spectrum; HU, Hounsfield units; FBP, filtered back projection; ASiR-50%, adaptive statistical iterative reconstruction-veo 50%; DLIR(L/M/H), deep-learning image reconstruction, level low, medium, and high; mGy, milligray.

TABLE 3 Demographic characteristics of patient study.

Basic characteristics	Female patients (n=300)	Male patients (n=416)	Total patients (n=716)
Age (years)	58.86 ± 6.90 (range, 50-97)	63.86 ± 8.03 (range, 52-89)	62.40 ± 7.20 (range, 50-97)
Weight (kg)	57.29 ± 9.57	67.29 ± 8.19	62.29 ± 10.22
Height (m)	1.61 ± 0.06	1.70 ± 0.05	1.68 ± 0.07
BMI (kg/m^2)	22.06 ± 3.43	23.39 ± 3.17	23.05 ± 3.58
BMD (mg/cm^3)	63.96 ± 28.75	82.51 ± 47.30	73.24 ± 40.22
Osteoporosis n [%]	74 (24.67%)	49 (11.79%)	123 (17.18%)
Vertebral fracture n [%]	26 (8.67%)	22 (5.29%)	48 (6.70%)

Continuous variables are expressed as mean± standard deviation unless otherwise indicated. BMI, body mass index; BMD, bone mineral density.

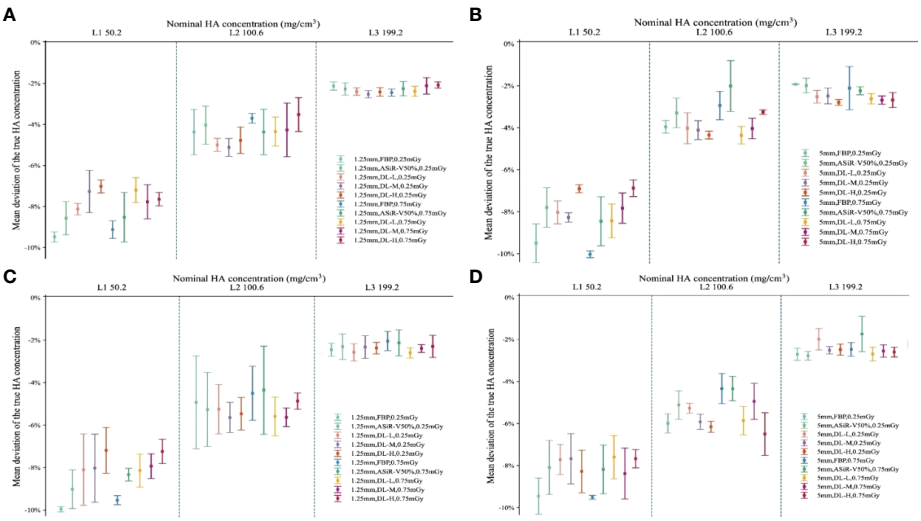

FIGURE 9
Accuracy deviation of bone mineral density in L1, L2, and L3 with ESP. Error bars standard deviation indicated the relative accuracy error (%) of 3 nominal HA concentrations (ESP, No.145; L1, 50.2; L2, 100.6; L3, 199.2 mg/cm^3 HA) for helical **(A, B)** and axial **(C, D)** scan type. The relative measurement errors and coefficient of variation of L1, L2, and L3 were fell within the range of 4-15%, indicating no statistically significant differences among L1, L2, and L3 at different scan protocols (P>0.05). ESP, European Spine Phantom; HA, calcium hydroxyapatite; FBP, filtered back projection; ASiR-V50%, adaptive statistical iterative reconstruction-veo 50%; DLIR(L/M/H), deep-learning image reconstruction, level low, medium, and high; mGy, milligray.

L1 and L3 was improved with DLIR in comparison to IMR (2), indicating that DLIR may potentially improve the low-contrast detectability and maintain the high-contrast spatial resolution. However, further studies should be implemented to verify whether DLIR can makes the images more homogeneous in terms of CT numbers. Consistent with our findings, Wang et al. (6) observed an excellent accuracy with 3 HA inserts ranging from 3.7% to 5.9%. Zhao et al. (16) found that the mean trabecular BMD measurement of 3 HA inserts were 2.4%, 2.1%, and 0.5% at L1, L2, and L3 for forty different systems on ESP, indicating a smaller measurement error than our study.

For patients aged over 50 years, the prevalence rate of osteoporosis was 24.67% in women and 11.79% in men, and it was comparable to 29.1% in women but more than twice in men

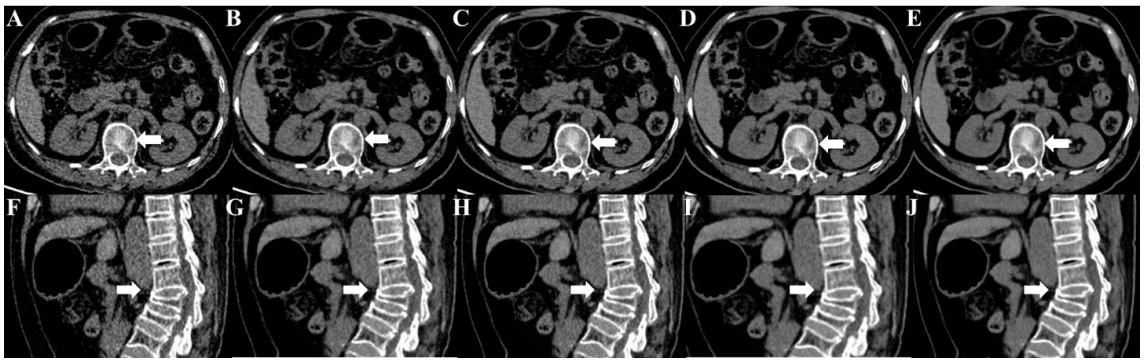

FIGURE 10
Unenhanced CT images of a 67-year-old female for osteoporotic vertebral fracture in the L3 vertebrae. CT images were reconstructed with FBP **(A, F)**, ASiR-V50% **(B, G)**, DLIR-L **(C, H)**, DLIR-M **(D, I)** and DLIR-H **(E, J)** with a slice thickness of 1.25mm at 0.75 mGy. The L3 vertebrae body was shown as a severe collapse in sagittal images (arrow), and the vertebral compression appearance was presented in axial images (arrow). The BMD values of FBP, ASiR-V50%, DLIR-L, DLIR-M and DLIR-H were 72.49, 72.74, 71.68, 70.11 and 69.24 mg/cm^3 for L1 vertebrae, 67.33, 69.11, 70.25, 65.38, 68.49 mg/cm^3 for L2 vertebrae, 62.08, 45.92, 49.57, 52.21, 50.93mg/cm^3 for L3 vertebrae, respectively. CT, computed tomography; FBP, filtered back projection; ASiR-V50%, adaptive statistical iterative reconstruction-veo 50%; DLIR(L/M/H), deep-learning image reconstruction, level low, medium, and high; mGy, milligray; BMD, bone mineral density.

TABLE 4 The qualitative image analysis.

Variables	FBP	ASiR-V50%	DLIR-L	DLIR-M	DLIR-H	*P*
Image noise	3.83 ± 0.37	4.17 ± 0.37	4.23 ± 0.31	4.50 ± 0.50	4.83 ± 0.34	<0.001
Image contrast	3.33 ± 1.25	3.80 ± 0.99	4.00 ± 0.35	4.50 ± 0.70	4.67 ± 0.73	<0.001
Small structure visibility	3.50 ± 1.31	3.83 ± 1.05	4.01 ± 0.53	4.17 ± 0.73	4.83 ± 0.70	<0.001
Image sharpness	2.17 ± 1.16	3.27 ± 1.16	3.22 ± 0.70	3.53 ± 0.90	3.83 ± 1.12	<0.001
Artifacts	2.81 ± 1.18	3.10 ± 0.83	3.17 ± 0.53	3.42 ± 0.37	3.83 ± 0.90	<0.001

FBP, filtered back projection; ASiR-V50%, adaptive statistical iterative reconstruction-veo 50%; DLIR(L/M/H), deep-learning image reconstruction, level low, medium, and high; There showed significant statistical differences across 3 levels of DLIR (P<0.001).

TABLE 5 Quantitative image analysis in patient study.

Variables	FBP	ASiR-V50%	DLIR-L	DLIR-M	DLIR-H	*P*
The mean CT value (HU)						
Lung	37.77 ± 2.82	40.57 ± 2.04	37.97 ± 3.32	38.10 ± 3.25	38.20 ± 3.40	0.875
Air	-872.87 ± 18.26	-872.53 ± 18.57	-873.67 ± 18.75	-872.77 ± 19.14	-871.63 ± 18.88	1.000
Liver	65.17 ± 3.07	65.77 ± 2.83	65.93 ± 4.00	66.00 ± 4.38	65.87 ± 4.77	0.999
Muscle	52.87 ± 2.50	53.90 ± 2.25	53.33 ± 2.75	52.90 ± 2.97	52.43 ± 3.21	0.986
Image noise (HU)						
Lung	15.60 ± 1.40	10.50 ± 1.90	9.60 ± 0.20	7.40 ± 0.10	5.35 ± 0.55	0.002*
Air	48.80 ± 0.00	43.25 ± 0.55	38.90 ± 0.70	34.30 ± 0.90	31.10 ± 1.00	<0.001*
Liver	19.35 ± 1.85	19.05 ± 2.65	13.30 ± 0.90	10.10 ± 0.90	7.40 ± 0.30	0.002*
Muscle	19.75 ± 1.15	15.10 ± 0.50	11.15 ± 0.75	8.45 ± 0.35	6.15 ± 0.05	<0.001*
CNR						
Lung	20.18 ± 0.28	21.55 ± 0.14	19.58 ± 0.01	21.50 ± 0.34	21.69 ± 0.22	<0.001*
Liver	0.67 ± 0.01	1.12 ± 0.08	1.16 ± 0.03	1.45 ± 0.05	2.23 ± 0.07	<0.001*

Data is expressed as mean ± standard deviation (SD); *P<0.05; mGy, milligray; HU, Hounsfield units; FBP, filtered back projection; ASiR-V50%, adaptive statistical iterative reconstruction-veo 50%; DLIR(L/M/H), deep-learning image reconstruction, level low, medium, and high; CNR, contrast-to-noise ratio.

by DXA, and similar to 29.0% in women and 13.5% in men by QCT reported by Cheng et al. (7). The prevalence rate of osteoporotic fracture was 8.67% in women and 5.29% in men, which was significantly lower than 17.3% in women and 17% in men for more than 14000 subjects in Shanghai conducted by Gao et al. (34). Conversely, a study in Norway enrolled 2887 participants demonstrated a higher prevalence rate of vertebral fracture 11.8% in women and 13.8% in men (35). The difference in osteoporotic fracture between DXA and QCT may be attributed to the patient cohort mostly obtained from the health check-up participants for osteoporosis screening, thus further studies should be performed to assess the fracture risk of QCT in multiple participants.

There are some limitations to be highlighted. Firstly, the results acquired with QCT should be further compared with DXA corresponding to the prevalence of osteoporosis. Secondly, a longitudinal study should be further performed to verify the clinical utility of DLIR algorithms in osteoporosis screening. Thirdly, we didn't evaluate the risk factors of osteoporosis, such as age, BMI, smoking, and fragility fracture history.

In conclusion, image quality with DLIR was high-qualified without affecting the accuracy of BMD measurement. It may provide a great clinical utility in osteoporosis screening.

Data availability statement

The raw data supporting the conclusions of this article will be made available by the authors, without undue reservation.

Ethics statement

The studies involving human participants were reviewed and approved by the Ethics Committees of First Affiliated Hospital of Zhengzhou University. The patients/participants provided their written informed consent to participate in this study. Written informed consent was obtained from the individual(s) for the publication of any potentially identifiable images or data included in this article.

Author contributions

YL, YJ, and YW designed the study. YL and YJ performed the data analysis. YL researched the related literatures. All authors contributed the data collection, measurements, and interpretation. YL wrote the manuscript and all authors reviewed the manuscript.

Funding

This study is supported by the National Natural Science Foundation of China (grant no. U1504821).

Conflict of interest

The authors declare that the research was conducted in the absence of any commercial or financial relationships that could be construed as a potential conflict of interest.

Publisher's note

All claims expressed in this article are solely those of the authors and do not necessarily represent those of their affiliated organizations, or those of the publisher, the editors and the reviewers. Any product that may be evaluated in this article, or claim that may be made by its manufacturer, is not guaranteed or endorsed by the publisher.

References

1. Liang C, Zhang G, Wang J, Tang X, Chen H, Yu R. An epidemiological investigation of patients with hip fracture over 50 years old in changning district. *Chin J Bone Joint Injury* (2013) 28:1122–4. doi: 10.7531/j.issn.1672-9935.2013.12.004

2. Nevitt MC, Ross PD, Palermo L, Musliner T, Genant HK, Thompson DE. Association of prevalent vertebral fractures, bone density, and alendronate treatment with incident vertebral fractures: Effect of number and spinal location of fractures. *Fract Intervent Trial Res Group Bone* (1999) 25(5):613–9. doi: 10.1016/s8756-3282(99)00202-1

3. Patil S, Rawall S, Singh D, Mohan K, Nagad P, Shial B, et al. Surgical patterns in osteoporotic vertebral compression fractures. *Eur Spine J* (2013) 22(4):883–91. doi: 10.1007/s00586-012-2508-4

4. Wu Y, Guo Z, Fu X, Wu J, Gao J, Zeng Q, et al. The study protocol for the China health big data (China biobank) project. *Quant Imaging Med Surg* (2019) 9 (6):1095–102. doi: 10.21037/qims.2019.06.16

5. Wu Y, Jiang Y, Han X, Wang M, Gao J. Application of low-tube current with iterative model reconstruction on philips brilliance iCT elite FHD in the accuracy of spinal QCT using a European spine phantom. *Quant Imaging Med Surg* (2018) 8 (1):32–8. doi: 10.21037/qims.2018.02.03

6. Wang L, Su Y, Wang Q, Duanmu Y, Yang M, Yi C, et al. Validation of asynchronous quantitative bone densitometry of the spine: Accuracy, short-term reproducibility, and a comparison with conventional quantitative computed tomography. *Sci Rep* (2017) 7(1):6284. doi: 10.1038/s41598-017-06608-y

7. Cheng X, Zhao K, Zha X, Du X, Li Y, Chen S, et al. China Health big data (China biobank) project investigators. opportunistic screening using low-dose CT and the prevalence of osteoporosis in China: A nationwide, multicenter study. *J Bone Miner Res* (2021) 36(3):427–35. doi: 10.1002/jbmr.4187

8. Cao L, Liu X, Li J, Qu T, Chen L, Cheng Y, et al. A study of using a deep learning image reconstruction to improve the image quality of extremely low-dose contrast-enhanced abdominal CT for patients with hepatic lesions. *Br J Radiol* (2021) 94(1118):20201086. doi: 10.1259/bjr.20201086

9. Han WK, Na JC, Park SY. Low-dose CT angiography using ASiR-V for potential living renal donors: a prospective analysis of image quality and diagnostic accuracy. *Eur Radiol* (2020) 30(2):798–805. doi: 10.1007/s00330-019-06423-1

10. Liu L. Model-based iterative reconstruction: A promising algorithm for today's computed tomography imaging. *J Med Imaging Radiat Sci* (2014) 45 (2):131–6. doi: 10.1016/j.jmir.2014.02.002

11. Verdun FR, Racine D, Ott JG, Tapiovaara MJ, Toroi P, Bochud FO, et al. Image quality in CT: From physical measurements to model observers. *Phys Med* (2015) 31(8):823–43. doi: 10.1016/j.ejmp.2015.08.007

12. Samei E, Richard S. Assessment of the dose reduction potential of a model-based iterative reconstruction algorithm using a task-based performance metrology. *Med Phys* (2015) 42(1):314–23. doi: 10.1118/1.4903899

13. JHsieh J, Liu E, Nett B, Tang J, Thibault JB, Sahney S. A new era of image reconstruction: TrueFidelity technical white paper on deep learning image reconstruction. *GE Healthcare* (2019).

14. Li Y, Jiang Y, Liu H, Yu X, Chen S, Ma D, et al. A phantom study comparing low-dose CT physical image quality from five different CT scanners. *Quant Imaging Med Surg* (2022) 12(1):766–80. doi: 10.21037/qims-21-245

15. Goodenough DJ. *Catphan 500 and 600 manual*. Greenwish, NY: The Phantom Laboratory, Inc (2006).

16. Zhao Y, Li K, Duanmu Y, Wang L, Xu X, Zhang Y, et al. Accuracy, linearity and precision of spine QCT vBMD phantom measurements for different brands of CT scanner: A multicentre study. *J Clin Densitom* (2022) 25(1):34–42. doi: 10.1016/j.jocd.2021.02.004

17. Abdullah KA, McEntee MF, Reed WM, Kench PL. Increasing iterative reconstruction strength at low tube voltage in coronary CT angiography protocols using 3D-printed and catphan 500 phantoms. *J Appl Clin Med Phys* (2020) 21 (9):209–14. doi: 10.1002/acm2.12977

18. Ehman EC, Yu L, Manduca A, Hara AK, Shiung MM, Jondal D, et al. Methods for clinical evaluation of noise reduction techniques in abdominopelvic CT. *Radiographics* (2014) 34(4):849–62. doi: 10.1148/rg.344135128

19. Bujila R, Kull L, Danielsson M, Andersson J. Applying three different methods of measuring CTDIfree air to the extended CTDI formalism for wide-beam scanners (IEC 60601-2-44): A comparative study. *J Appl Clin Med Phys* (2018) 19(4):281–9. doi: 10.1002/acm2.12363

20. Gulliksrud K, Stokke C, Martinsen AC. How to measure CT image quality: variations in CT-numbers, uniformity and low contrast resolution for a CT quality assurance phantom. *Phys Med* (2014) 30(4):521–6. doi: 10.1016/j.ejmp.2014.01.006

21. PROTM QCT. Bone mineral density software. *User's Guide Mindways Soft Inc* (2013).

22. van Hamersvelt RW, Schilham AMR, Engelke K, den Harder AM, de Keizer B, Verhaar HJ, et al. Accuracy of bone mineral density quantification using dual-layer spectral detector CT: A phantom study. *Eur Radiol* (2017) 27(10):4351–9. doi: 10.1007/s00330-017-4801-4

23. Wong JC, Griffiths MR. Precision of bone densitometry measurements: When is change true change and does it vary across bone density values? *Australas Radiol* (2003) 47(3):236–9. doi: 10.1046/j.1440-1673.2003.01169.x

24. Nam JG, Hong JH, Kim DS, Oh J, Goo JM. Deep learning reconstruction for contrast-enhanced CT of the upper abdomen: Similar image quality with lower radiation dose in direct comparison with iterative reconstruction. *Eur Radiol* (2021) 31(8):5533–43. doi: 10.1007/s00330-021-07712-4

25. Li G, Gao G, Xia H. Detection and influencing factors of CT spatial resolution and low-contrast resolution. *China Med Dev* (2010) 25:7–9. doi: 10.3969/j.issn.1674-1633.2010.01.003

26. Greffier J, Hamard A, Pereira F, Barrau C, Pasquier H, Beregi JP, et al. Image quality and dose reduction opportunity of deep learning image reconstruction algorithm for CT: a phantom study. *Eur Radiol* (2020) 30(7):3951–9. doi: 10.1007/s00330-020-06724-w

27. Higaki T, Nakamura Y, Zhou J, Yu Z, Nemoto T, Tatsugami F, et al. Deep learning reconstruction at CT: Phantom study of the image characteristics. *Acad Radiol* (2020) 27(1):82–7. doi: 10.1016/j.acra.2019.09.008

28. Singh R, Digumarthy SR, Muse VV, Kambadakone AR, Blake MA, Tabari A, et al. Image quality and lesion detection on deep learning reconstruction and iterative reconstruction of submillisievert chest and abdominal CT. *AJR Am J Roentgenol* (2020) 214(3):566–73. doi: 10.2214/AJR.19.21809

29. Kim JH, Yoon HJ, Lee E, Kim I, Cha YK, Bak SH. Validation of deep-learning image reconstruction for low-dose chest computed tomography scan: Emphasis on image quality and noise. *Kor J Radiol* (2021) 22(1):131–8. doi: 10.3348/kjr.2020.0116

30. Sun J, Li H, Li J, Yu T, Li M, Zhou Z, et al. Improving the image quality of pediatric chest CT angiography with low radiation dose and contrast volume using deep learning image reconstruction. *Quant Imaging Med Surg* (2021) 11(7):3051–8. doi: 10.21037/qims-20-1158

31. Benz DC, Benetos G, Rampidis G, von Felten E, Bakula A, Sustar A, et al. Validation of deep-learning image reconstruction for coronary computed tomography angiography: Impact on noise, image quality and diagnostic accuracy. *J Cardiovasc Comput Tomogr* (2020) 14(5):444–51. doi: 10.1016/j.jcct.2020.01.002

32. Kalender WA, Felsenberg D, Genant HK, Fischer M, Dequeker J, Reeve J. The European spine phantom–a tool for standardization and quality control in spinal bone mineral measurements by DXA and QCT. *Eur J Radiol* (1995) 20 (2):83–92. doi: 10.1016/0720-048x(95)00631-y

33. Glüer CC, Engelke K, Lang TF, Grampp S, Genant HK. Quantitative computed tomography (QCT) of the lumbar spine and appendicular skeleton. *Eur J Radiol* (1995) 20(3):173–8. doi: 10.1016/0720-048x(95)00651-6

34. Gao C, Xu Y, Li L, Gu W, Yi C, Zhu Q, et al. Prevalence of osteoporotic vertebral fracture among community-dwelling elderly in shanghai. *Chin Med J (Engl)* (2019) 132(14):1749–51. doi: 10.1097/CM9.0000000000000332

35. Waterloo S, Ahmed LA, Center JR, Eisman JA, Morseth B, Nguyen ND, et al. Prevalence of vertebral fractures in women and men in the population-based tromsø study. *BMC Musculoskelet Disord* (2012) 13:3. doi: 10.1186/1471-2474-13-3

frontiers | Frontiers in Endocrinology

TYPE Original Research
PUBLISHED 20 September 2022
DOI 10.3389/fendo.2022.980576

OPEN ACCESS

EDITED BY
Xiaoguang Cheng,
Beijing Jishuitan Hospital, China

REVIEWED BY
Shuang Chen,
Fudan University, China
Weiwu Yao,
Shanghai Jiao Tong University, China

*CORRESPONDENCE
Fan He
fhe@tjh.tjmu.edu.cn
Xiaoming Li
lilyboston2002@sina.com

†These authors have contributed equally to this work and share first authorship

SPECIALTY SECTION
This article was submitted to Bone Research, a section of the journal Frontiers in Endocrinology

RECEIVED 28 June 2022
ACCEPTED 29 August 2022
PUBLISHED 20 September 2022

CITATION
Xiong Y, He T, Liu WV, Zhang Y, Hu S, Wen D, Wang Y, Zhang P, He F and Li X (2022) Quantitative assessment of lumbar spine bone marrow in patients with different severity of CKD by IDEAL-IQ magnetic resonance sequence. *Front. Endocrinol.* 13:980576. doi: 10.3389/fendo.2022.980576

Quantitative assessment of lumbar spine bone marrow in patients with different severity of CKD by IDEAL-IQ magnetic resonance sequence

Yan Xiong[1†], Tongxiang He[1†], Weiyin Vivian Liu[2], Yao Zhang[1], Shuang Hu[1], Donglin Wen[1], Yanan Wang[3], Peisen Zhang[4], Fan He[3*] and Xiaoming Li[1*]

[1]Department of Radiology, Tongji Hospital, Tongji Medical College, Huazhong University of Science and Technology, Wuhan, China, [2]Magnetic Resonance (MR) Research, GE Healthcare, Beijing, China, [3]Department of Nephrology, Tongji Hospital, Tongji Medical College, Huazhong University of Science and Technology, Wuhan, China, [4]College of Life Science and Technology, Beijing University of Chemical Technology, Beijing, China

Background: Chronic kidney disease (CKD) has a significant negative impact on bone health. Bone marrow is an essential component of bone, mainly composed of trabecular bone and fat. The IDEAL-IQ sequence of MRI allows indirect quantification of trabecular bone mass by R2* and direct quantification of bone marrow fat content by FF map, respectively.

Objective: Our objective was to explore the association of CKD severity with bone marrow using IDEAL-IQ and whether mineral and bone metabolism markers alter this association.

Method: We recruited 68 CKD patients in this cross-sectional research (15 with CKD stages 3-4, 26 with stage 5, and 27 with stage 5d). All patients underwent lumbar spine IDEAL-IQ, BMD, and several bone metabolism markers (iPTH, 25-(OH)-VitD, calcium and phosphorus). Multiple linear regression analysis was used to examine the association of CKD severity with MRI measurements (R2* and FF).

Results: More severe CKD was associated with a higher R2* value [CKD 5d versus 3-4: 30.077 s^{-1} (95% CI: 12.937, 47.217), *P* for trend < 0.001], and this association was attenuated when iPTH was introduced [CKD 5d versus 3-4: 19.660 s^{-1} (95% CI: 0.205, 39.114), *P* for trend = 0.042]. Furthermore, iPTH had an association with R2* value [iPTH (pg/mL): 0.033 s^{-1} (95% CI: 0.001, 0.064), *P* = 0.041]. Besides, FF was mainly affected by age and BMI, but not CKD.

Conclusions: The bone marrow R2* value measured by IDEAL-IQ sequence is associated with CKD severity and iPTH. The R2* of IDEAL-IQ has the potential to reflect lumbar bone changes in patients with CKD.

10.3389/fendo.2022.980576

KEYWORDS
chronic kidney disease, bone marrow, IDEAL-IQ, PTH, R2*

Introduction

Chronic kidney disease (CKD) affects 8-16% of the world's population, with the global all-age prevalence growing by 29.3% from 1990 to 2017 (1, 2). CKD has a significant negative impact on bone health (3, 4). CKD-mineral and bone disorder (CKD-MBD) is the most common complication of CKD, a bone metabolic disease characterized by systemic bone, biochemical, and cardiovascular abnormalities that affect most patients from moderate to severe CKD (5, 6). Currently, clinicians can only roughly assess bone abnormalities in CKD patients based on clinical symptoms and commonly used clinical bone metabolism markers, including parathyroid hormone (PTH), vitamin D, phosphorus (P), and calcium (Ca) (7). This makes it important to find other clinically feasible methods to assess bone abnormalities in CKD.

Unlike primary osteoporosis (decrease in both trabecular and cortical bone), CKD patients always have secondary hyperparathyroidism, especially in end-stage patients (8). As PTH increases, trabecular and cortical bone behave differently (increases and decreases, respectively) (9, 10). In our previous study, we explored the changes of cortical porosity in patients with different stages of CKD (11). Trabecular bone (TB), which accounts for merely 20% of the total bone but two-thirds of the total bone surface area, shows greater metabolic activity than cortical bone (12). Moreover, TB is the main load-bearing bone of the vertebral body. Therefore, it is of great significance to study the changes of TB. Although it is challenging to obtain magnetic resonance imaging (MRI) signals of TB directly, it is possible to identify it indirectly. Studies have shown that bone marrow matrix in contact with TB exhibits an elevated transverse relaxation rate (R2*) because of local field inhomogeneities where mineralized matrix interfaced with it (13–15). The R2* value is approximately linearly related to TB density (16, 17), and increases as the interface area between TB and bone marrow matrix increases (13, 18). Therefore, R2* can indirectly quantify TB.

Besides TB, bone marrow fat (BMF) is an essential research topic of imaging studies on metabolic bone diseases since it is associated with the pathogenesis of bone loss (19). According to some research, BMF and TB density have a competitive relationship (20, 21). Only several studies have aimed at the association between CKD severity and BMF changes, but none of them included dialysis patients (22, 23). Dialysis is a key predictor of bone abnormalities in CKD patients (24), so it is essential to include them in the study.

MRI has been receiving widespread attention because of its non-invasive and non-radiation quantification of tissues. The iterative decomposition of water and fat with the echo asymmetry and least-squares estimation quantitation (IDEAL-IQ) sequence of MRI is a new water-fat separation algorithm developed from the IDEAL technology, which is a well-established clinical sequence with fast scanning time and no special post-processing. This sequence can generate fat fraction (FF) and R2* map in one scan (25, 26). Compared to traditional MRI techniques used to detect fat, this sequence further corrects common biases known in tissue fat measurement, including main magnetic field (B0) inhomogeneity, T1 effect, and T2* effect (27). It improves the water-fat separation from qualitative to quantitative. The FF map can directly measure the fat content in the tissue (i.e., liver and bone marrow) without further calculation (28, 29). The R2* map can also explain the inhomogeneity of the T2* effect/field, which is often used in liver iron assessment, such as liver iron overload and liver fibrosis (30, 31). Therefore, considering the imaging principle and the output results, this sequence shows excellent potential for investigating CKD bone marrow composition changes.

Besides, CKD patients are often combined with secondary hyperparathyroidism, vitamin D deficiency, and calcium and phosphorus metabolism disorders (5). And studies show that many bone metabolism markers, including PTH, are associated with abnormal cortical bone density, TB density, abnormal bone microstructure, and fracture (32).Therefore, we included several bone metabolism markers recommended by the KDIGO (Kidney Disease: Improving Global Outcomes) guidelines for the initial evaluation CKD-MBD (i.e., intact PTH (iPTH), 25-hydroxyvitamin D (25-(OH)-VitD), corrected calcium (cCa), phosphate (P)) and areal bone mineral density (aBMD) measured by dual-energy X-ray absorptiometry (DXA) (33, 34). Among them, PTH remains the best alternative biomarker for CKD-MBD (35). The aBMD is widely used in osteoporosis, but it is controversial in CKD, which deserves further study.

Our objective was to explore the association of CKD severity with bone marrow using IDEAL-IQ and whether mineral and bone biochemical parameters alter this association.

Materials and methods

Subjects

The cross-sectional study was approved by the Medical Ethics Committee of Tongji Hospital, TJ-IRB20210108. Before

the study, we obtained the written informed consent from all subjects. We registered the study on ClinicalTrials.gov as NCT04564924. Patients were recruited in the Department of Nephrology of Tongji Hospital from September 2020 to May 2021. All subjects were ambulatory and over 18 years old. The inclusion criteria were hospitalized patients diagnosed with CKD stages 3-5d. The exclusion criteria included taking drugs known to affect bone metabolism (e.g., steroid hormones, oral glucocorticoids, salmon calcitonin, and bisphosphonates); disease known to affect bone metabolism (e.g., hyperthyroidism, diabetes, rheumatic immunity disease, osteomalacia, rickets, scurvy, Paget's disease, acromegaly, treatment with radiotherapy or chemotherapy, history of malignant tumors, fractures within six months, lumbar trauma surgery, motor neuron disease, scoliosis, and anorexia nervosa); and general MRI contraindications (e.g., cochlear implant, claustrophobia, pacemaker, and IUD). 68 patients were included in the final study population. Among them, 15 subjects were in CKD stages 3-4, 26 were in stage 5, and 27 were on maintenance hemodialysis (5d) at least three months. The flow chart of patient inclusion and exclusion was shown in Figure 1.

MRI scanning

The study was carried out on a 3.0 T clinical scanner (Signa Pioneer, GE Healthcare, USA), the lumbar spine was scanned in a sagittal position using a spine coil while patients were placed in a supine position. Routine MRI sequences (T1 FSE, T2 FRFES, and T2 FLEX) were used to assess lumbar pathological findings, such as neoplastic lesions, compression fractures, lipomas, etc. Routine MRI parameters were provided in Supplementary Material 1. Besides routine sequences, the IDEAL-IQ sequence scan parameters were set as TE, minimum; TR, 8.4 ms; NEX, 2; Freq.FOV, 24 cm; flip angle, 4°; slice thickness, 3 mm; in-plane spatial resolution, 1.5 mm × 1.5 mm; bandwidth, 83.33 kHz; and scan time, 2 minutes 24 seconds. FF and R2* maps were automatically generated after scanning.

Vertebral bone marrow quantification

The IDEAL-IQ imaging data (FF and R2* map) were analyzed using ImageJ (National Institutes of Health). All assessments were performed independently by two musculoskeletal radiologists with 3 and 5 years of experience, respectively, who were blinded to the clinical and DXA results. Similar to the lumbar DXA measurement, only the L1-L4 vertebrae were manually segmented. The ROIs were drawn on the mid-sagittal plane and the two para-mid-sagittal planes on the FF map and then copied to the R2* map. And the averages of all ROIs of FF and R2* were calculated respectively. ROIs were needed to avoid focal fatty degenerations, motion artifacts, the cortical bone of the vertebrae, vertebral discs, and the venous plexus. The ROI size could be adjusted based on the area of the vertebral body. Figure 2 shows the example of ROIs.

Laboratory analysis

Early morning fasting blood samples were drawn to evaluate serum markers. Laboratory tests were collected within one week

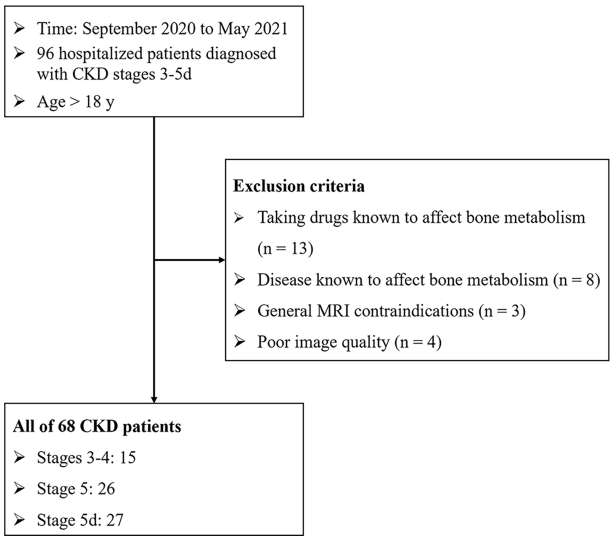

FIGURE 1
Flow chart of patient inclusion and exclusion.

before the MRI scan. Routine biochemical parameters including serum alkaline phosphatase (ALP), P, cCa, and creatinine (Cr) were determined using standard methods. Based on serum Cr, the estimated glomerular filtration rate (eGFR) was calculated through the CKD-EPI formula (36). The iPTH was measured on the Cobas e602 (Elecsys, Roche Diagnostics, Mannheim, Germany) using an electrochemiluminescence immunoassay (ECLIA). The 25-(OH)-VitD was analyzed by a chemiluminescence immunoassay on the Liaison XL (DiaSorin, Italy). The inter- and intra-assay coefficients of variation (CV) of iPTH and 25-(OH)-VitD were less than 4.31% and 7.87%, respectively. The minimum detection limit of iPTH and 25-(OH)-VitD were 1.20 pg/ml and 4 ng/ml, respectively. The normal ranges were as follows: iPTH, 15-65 pg/ml; 25-(OH)-VitD, lack < 12 ng/ml, insufficient 12-20 ng/ml, sufficient ≥ 20 ng/ml.

Dual-energy X-ray absorptiometry

One week after MRI examination, the aBMD of the lumbar spine (from L1 to L4) was evaluated by DXA (Prodigy Lunar scanner, GE Healthcare, Waukesha, WI, USA).

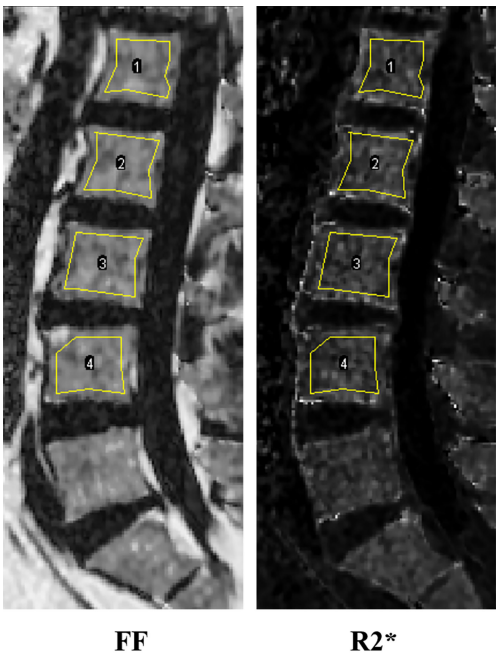

FIGURE 2
Representative IDEAL-IQ images and ROI of the lumbar spine (from L1 to L4).

Statistical analysis

Data were presented as frequency (%) for categorical variables and mean ± standard deviation (SD) for continuous variables. The linear trends of baseline characteristics among three CKD groups (CKD stages 3-4, 5, and 5d) were acquired using Chi-squared statistics and one-way analysis of variance appropriately. Pearson's and Spearman's correlation analysis was performed to calculate the correlation between MRI measurements (FF and R2*) with demographics and other indicators respectively, according to Shapiro-Wilk Normality Test. The criteria for the Pearson r or Spearman ρ: higher than 0.8, strong correlation; 0.3-0.8, moderate correlation; lower than 0.3, weak correlation.

The association of CKD groups with MRI measurements was examined by multiple linear regression analysis. Firstly, an unadjusted model was established. Secondly, the model was adjusted for age, sex, and BMI. Finally, we added the significant indicators based on the correlation analysis mentioned above to the adjusted model. P for trends were calculated by treating CKD groups as ordered categorical variable (CKD 3-4 = 0, CKD 5 = 1, CKD 5d = 2). CKD groups were treated as unordered categorical variable in other linear regression analysis. The above three models were used to evaluate the association between CKD groups and MRI measurements, and whether adding indicators with significant correlations to the model could affect this association.

Finally, interobserver agreement between the two observers on parameter measurements was analyzed by calculating the interclass correlation coefficients (ICCs).

The *R* software (version 4.1.2) was performed for all statistical analyses. A two-tailed P <0.05 meant statistically significant.

Results

Baseline characteristics

Comparisons of demographics, bone metabolism markers, aBMD, and MRI measurements among CKD groups were presented in Table 1. More severe CKD patients had significantly higher BMI, P, iPTH, and R2* values. There was no significant difference in sex, age, ALP, cCa, aBMD, 25-(OH)-VitD, or FF.

Correlation analysis

FF only showed positive correlation with age (Spearman ρ = 0.373, P = 0.002) and BMI (Pearson r = 0.400, P < 0.001), while no correlation with other indicators. R2* was positively correlated with iPTH (Spearman ρ = 0.351, P = 0.003). There was no significant correlation between R2* with age, BMI and other indicators (Table 2).

10.3389/fendo.2022.980576

TABLE 1 Baseline characteristics among three groups (CKD 3-4, 5, and 5d).

	Overall	CKD 3-4	CKD 5	CKD 5d	*P* for trend
Demographics					
Number	68	15 (22.1)	26 (38.2)	27 (39.7)	NA
Males	40 (58.8)	9 (60.0)	14 (53.8)	17 (63.0)	0.762
Age (years)	50 (13.2)	55.3 (11.4)	46.5 (13.9)	50.4 (12.8)	0.422
BMI (kg/m^2)	22.7 (3.0)	24.0 (3.5)	22.7 (3.1)	21.8 (2.5)	**0.029**
eGFR (mL/min/1.73m^2)	12.3 (11.7)	31.3 (10.9)	8.6 (3.4)	5.4 (2.3)	**<0.001**
ALP (U/L)	75 (29)	82 (33)	67 (24)	79 (29)	0.988
Bone metabolism markers					
P (mmol/L)	1.69 (0.70)	1.34 (0.37)	1.75 (0.73)	1.82 (0.76)	**0.047**
cCa (mmol/L)	2.23 (0.25)	2.29 (0.12)	2.19 (0.19)	2.24 (0.33)	0.666
iPTH (pg/mL)	269.4 (235.1)	108.3 (57.8)	199.6 (147.7)	426.0 (272.6)	**<0.001**
25-(OH)-VitD (ng/mL)	18.35 (9.39)	16.73 (9.53)	17.44 (9.27)	20.14 (9.48)	0.224
L1-L4 aBMD (g/cm^2)	1.13 (0.17)	1.07 (0.14)	1.13 (0.18)	1.17 (0.17)	0.06
MRI measurements					
FF (%)	51.6 (11.6)	51.9 (9.6)	50.5 (12.7)	52.4 (11.8)	0.822
R2* (s^{-1})	155.2 (27.8)	140.7 (20.2)	149.7 (25.2)	168.5 (28.7)	**<0.001**

Categorical variables are summarized as count (%); continuous variables as mean (SD). *P* for trend reflect the significance of the linear trend across the CKD groups, using Chi-square and one-way ANOVA appropriately. Bold *P*-values consider statistical significance.

Linear regression analysis

The association of CKD groups with FF presented no statistical significance both in unadjusted and adjusted models, whereas two covariates presented significant effect in the adjusted model [age (year): 0.269% (95% confidence interval [CI]: 0.060%, 0.477%), $P = 0.013$; BMI (kg/m^2): 1.371% (95% CI: 0.442%, 2.301%), $P = 0.004$] (Table 3).

In the multiple linear regression models of CKD with R2*, CKD groups was positively associated with R2*, with a significant gradient in the unadjusted model [CKD 5d versus 3-4: 27.875 s^{-1} (95% CI: 11.331, 44.419), *P* for trend < 0.001]. After adjusting for age, sex, and BMI, the association remained [CKD 5d versus 3-4: 30.077 s^{-1} (95% CI: 12.937, 47.217), *P* for trend < 0.001]. Furthermore, no covariate presented a significant effect in the adjusted model (Table 4).

After introducing iPTH into the adjusted model, all the variance inflation factor (VIF) values were less than 5 suggesting that no multicollinearity existed. Interaction effects of CKD groups and iPTH were not statistically significant. We found that the association of CKD groups with R2* was attenuated but still significant [CKD 5d versus 3-4: 19.660 s^{-1} (95% CI: 0.205, 39.114), *P* for trend = 0.042]. At the same time, the regression coefficient of iPTH was statistically significant [iPTH (pg/mL): 0.033 s^{-1} (95% CI: 0.001, 0.064), $P = 0.041$], suggesting that iPTH was still associated with R2* after adjusted age, sex, BMI, and CKD groups (Table 5).

Interobserver agreement

The ICCs for R2* and FF was 0.965 (95% CI: 0.944 -0.978) and 0.958 (95% CI: 0.933-0.974), respectively.

TABLE 2 Correlation analysis of MRI measurements (FF and R2*) with demographics and clinical characteristics.

	FF (%)	*P*-value	R2* (s^{-1})	*P*-value
Age (years)	**0.373**$^{\#}$	**0.002**	-0.163$^{\#}$	0.183
BMI (kg/m^2)	**0.400**	**<0.001**	0.035	0.776
ALP (U/L)	-0.021$^{\#}$	0.866	-0.169$^{\#}$	0.169
P (mmol/L)	-0.136$^{\#}$	0.269	0.228$^{\#}$	0.062
cCa (mmol/L)	0.051	0.677	-0.200	0.102
iPTH (pg/mL)	-0.025$^{\#}$	0.842	**0.351**$^{\#}$	**0.003**
25-(OH)-VitD (ng/mL)	-0.003$^{\#}$	0.978	0.166$^{\#}$	0.176
L1-L4 aBMD (g/cm^2)	0.073	0.552	0.100	0.416

Data are presented as Pearson's or Spearman's rank (#) correlation coefficients appropriately. Bold *P*-values consider statistical significance.

10.3389/fendo.2022.980576

TABLE 3 Association of CKD groups with FF (%) in unadjusted and adjusted models.

Independent variable	Unadjusted	Adjusted
CKD groups		
CKD 3-4	(ref.)	(ref.)
CKD 5	-1.366 (-8.977, 6.245)	2.433 (-4.401, 9.266)
CKD 5d	0.467 (-7.092, 8.026)	4.769 (-2.050, 11.588)
P for trend	0.822	0.158
Age (years)		**0.269 (0.060, 0.477)**[a]
BMI (kg/m^2)		**1.371 (0.442, 2.301)**[b]
Sex		
Male		(ref.)
Female		3.665 (-1.461, 8.791)

Data are presented as FF% (95% CI). The adjusted model was adjusted for age, sex, and BMI.
Bold *P*-values consider statistical significance. [a] $P < 0.05$; [b] $P < 0.01$.

Discussion

We investigated the association between CKD severity and lumbar bone marrow FF and R2* values. We found R2* was associated with CKD and iPTH, independent of age or BMI. In contrast, FF was mainly affected by age and BMI, but not CKD in our study. Despite the growing recognition of the importance of bone marrow composition in bone biomechanics, there are still few studies on bone marrow in CKD patients.

The underlying mechanism of the association between CKD severity and BMF content is not fully understood. We found that although FF was little affected by CKD severity, it was significantly affected by age and BMI, which was consistent with other studies. Veldhuis et al. (19) found a constant increase in BMF with age in healthy adults. Cohen et al. (37) found that obese individuals had a higher rate of bone marrow obesity

TABLE 4 Association of CKD groups with R2* (s^{-1}) in unadjusted and adjusted models.

Independent variable	Unadjusted	Adjusted
CKD groups		
CKD 3-4	(ref.)	(ref.)
CKD 5	9.032 (-7.625, 25.690)	8.281 (-8.896, 25.458)
CKD 5d	**27.875 (11.331, 44.419)**[a]	**30.077 (12.937, 47.217)**[b]
P for trend	**<0.001**	**<0.001**
Age (years)		-0.365 (-0.890, 0.160)
BMI (kg/m^2)		1.897 (-0.439, 4.232)
Sex		
Male		(ref.)
Female		-1.546 (-14.430, 11.339)

Data are presented as R2* in s^{-1} (95% CI). The adjusted model was adjusted for age, sex, and BMI.
Bold *P*-values consider statistical significance. [a] $P < 0.05$; [b] $P < 0.01$.

TABLE 5 Association of R2* (s^{-1}) with CKD groups and iPTH in the adjusted model.

Independent variable	Adjusted + iPTH
CKD groups	
CKD 3-4	(ref.)
CKD 5	5.522 (-11.421, 22.465)
CKD 5d	**19.660 (0.205, 39.114)**[a]
P for trend	0.042
iPTH (pg/mL)	**0.033 (0.001, 0.064)**[a]

Data are presented as R2* in s^{-1} (95% CI), adjusted for age, sex, and BMI.
Bold *P*-values consider statistical significance. [a] $P < 0.05$.

compared with overweight and healthy subjects measured with bone biopsy. Similar results were found in older and young men, as well as post- and pre-menopausal women (38–41). This reminds us that when studying the changes in BMF caused by metabolic diseases, we need to strictly control the effects of age and BMI to avoid getting wrong conclusions. In the few two imaging studies on lumbar BMF in patients with CKD (22, 23), a small sample study found that vertebral BMF in CKD stages 3b-4 (n=8) was 13.8% higher than healthy controls (n=8); another study found that vertebral BMF in eGFR < 45 mL/min/1.73m^2 (n=58) was 3.7% higher than eGFR > 60 mL/min/1.73m^2 (n=297). Both studies suggest that patients with CKD tended to have increased BMF compared to healthy controls. However, among the CKD patients in our study, BMF did not increase significantly when CKD severity increased. Probably because they compared CKD patients with healthy people, whereas our study subjects were all CKD patients, the cohort structure was different. Therefore, in patients with severe CKD, BMF may have reached a plateau and will not increase significantly with disease progression.

In this study, we found that bone marrow R2* value was higher in more severe CKD, and adjustment of iPTH attenuated the original association between CKD groups and R2*. This means that changes in R2* are associated with both CKD and iPTH. This may be related to end-stage CKD trabecular sclerosis. Trabecular sclerosis has long been regarded as a feature of MBD, and is more pronounced in patients with uremia. Although this increase does not imply an increase in bone strength, as irregular TB may lose its appropriate connectivity and 3D structure (42, 43). Meanwhile, there is strong indirect evidence that secondary hyperparathyroidism is a major cause, as this condition always occurs with CKD progression (8, 9). This may be related to the anabolic action of PTH on TB (8). The best explanation for PTH to induce bone anabolism in TB is that it promotes osteoblast survival and/or osteoblastogenesis (44). In the CKD, bone is regarded as one of the classical targets of PTH because PTH1R (PTH 1 receptor) is expressed in osteoclasts, osteocytes, and osteoblasts (45). PTH excess usually has an anabolic action on TB and a catabolic action on cortical bone. The reasons for this differential effect of PTH on trabecular and cortical bone are not

fully understood (9, 44). However, since adjusting iPTH only attenuated the association but did not make it disappear, suggesting that there were other factors in CKD that impair bone health. Previous studies have shown that abnormalities such as chronic metabolic acidosis and chronic inflammation caused by CKD can also impair bone health (46).

There was no significant difference in aBMD among the three groups and no significant correlation between aBMD and R2*. We consider the main reason is that the aBMD is the projection of a 3D structure on a 2D plane, so it can't distinguish between cortical and trabecular bone (47). MBD is strongly influenced by PTH. As PTH increases, trabecular and cortical bone behave differently (increases and decreases, respectively) (9, 10). In short, the increased trabecular BMD can mask the reduced cortical BMD, thus giving an inconsistent result with the actual bone disease. Therefore, the lack of correlation between the aBMD and R2* values of the lumbar spine may reflect the technical limitations of DXA, not a lack of correlation between the true trabecular BMD and R2* values.

Besides, 25-(OH)-VitD did not tend to decrease with more severe CKD stages. The possible reason for this is that most patients were supplemented with vitamin D. Studies reveal that exogenous vitamin D supplementation can increase 25-(OH)-VitD (24). Therefore, it is limited for 25-(OH)-VitD to evaluate bone metabolism in CKD.

The advantages of this study include: (1) IDEAL-IQ is a sequence that has already been used in clinical applications and provides convenient quantification of bone marrow components; (2) This study included more comprehensive bone metabolism markers at one time; (3) The exclusion criteria were strictly established in this study to exclude patients related to diseases or drugs that may affect bone metabolism, making results more reliable. However, this study also has some limitations: (1) This study is exploratory cross-sectional and cannot determine a causal association between CKD severity and bone marrow, therefore more prospective studies are required; (2) We didn't include many other factors that affect bone, such as chronic inflammation, chronic metabolic acidosis, and premature hypogonadism.

In conclusion, the bone marrow R2* value measured by IDEAL-IQ sequence is associated with CKD severity and iPTH. The R2* of IDEAL-IQ has the potential to reflect lumbar bone changes in patients with CKD.

Data availability statement

The raw data supporting the conclusions of this article will be made available by the authors, without undue reservation.

Ethics statement

The studies involving human participants were reviewed and approved by Medical Ethics Committee of Tongji Hospital, Tongji Medical College, Huazhong University of Science and Technology. The patients/participants provided their written informed consent to participate in this study.

Author contributions

FH and XL concept and design. YX and TH designed the study, evaluated the data, and wrote the manuscript. DW devised the outline of the manuscript. YW, SH, and YZ collected the information and analyzed the data. PZ created the figures for the manuscript. WL and XL critically revised the manuscript. All authors contributed to the article and approved the submitted version.

Funding

This study was supported by the National Natural Science Foundation of China (NSFC) (No. 81930045 and 31630025).

Conflict of interest

WL was employed by GE Healthcare.

The remaining authors declare that the research was conducted in the absence of any commercial or financial relationships that could be construed as a potential conflict of interest.

Publisher's note

Supplementary material

The Supplementary Material for this article can be found online at: https://www.frontiersin.org/articles/10.3389/fendo.2022.980576/full#supplementary-material

References

1. Purcell CA, Abebe M, Adebayo OM, Afarideh M, Agarwal SK, Agudelo-Botero M, et al. Global, regional, and national burden of chronic kidney disease, 1990–2017: A systematic analysis for the global burden of disease study 2017. *Lancet* (2020) 395(10225):709–33. doi: 10.1016/S0140-6736(20)30045-3.

2. Chen TK, Knicely DH, Grams ME. Chronic kidney disease diagnosis and management: A review. *JAMA* (2019) 322(13):1294–304. doi: 10.1001/jama.2019.14745

3. Kidney Disease: Improving Global Outcomes (KDIGO) CKD-MBD Update Work Group. KDIGO 2017 clinical practice guideline update for the diagnosis, evaluation, prevention, and treatment of chronic kidney disease-mineral and bone disorder (CKD-MBD). *Kidney Int Suppl* (2017) 7(1):1–59. doi: 10.1016/j.kisu.2017.04.001

4. Sharma AK, Toussaint ND, Masterson R, Holt SG, Rajapakse CS, Ebeling PR, et al. Deterioration of cortical bone microarchitecture: Critical component of renal osteodystrophy evaluation. *Am J Nephrol* (2018) 47(6):376–84. doi: 10.1159/000489671

5. Moe S, Drüeke T, Cunningham J, Goodman W, Martin K, Olgaard K, et al. Definition, evaluation, and classification of renal osteodystrophy: A position statement from kidney disease: Improving global outcomes (KDIGO). *Kidney Int* (2006) 69(11):1945–53. doi: 10.1038/sj.ki.5000414

6. Kidney Disease: Improving Global Outcomes (KDIGO) CKD-MBD Work Group. KDIGO clinical practice guideline for the diagnosis, evaluation, prevention, and treatment of chronic kidney disease-mineral and bone disorder (CKD-MBD). *Kidney Int Suppl* (2009) 113):S1–S130. doi: 10.1038/ki.2009.188

7. Sprague SM, Bellorin-Font E, Jorgetti V, Carvalho AB, Malluche HH, Ferreira A, et al. Diagnostic accuracy of bone turnover markers and bone histology in patients with CKD treated by dialysis. *Am J Kidney Dis* (2016) 67(4):559–66. doi: 10.1053/j.ajkd.2015.06.023

8. Levin A, Bakris GL, Molitch M, Smulders M, Tian J, Williams LA, et al. Prevalence of abnormal serum vitamin d, PTH, calcium, and phosphorus in patients with chronic kidney disease: Results of the study to evaluate early kidney disease. *Kidney Int* (2007) 71(1):31–8. doi: 10.1038/sj.ki.5002009

9. Parfitt AM. A structural approach to renal bone disease. *J Bone Mineral Res* (1998) 13(8):1213–20. doi: 10.1359/jbmr.1998.13.8.1213

10. Calvi LM, Sims NA, Hunzelman JL, Knight MC, Giovannetti A, Saxton JM, et al. Activated parathyroid hormone/parathyroid hormone-related protein receptor in osteoblastic cells differentially affects cortical and trabecular bone. *J Clin Invest* (2001) 107(3):277–86. doi: 10.1172/JCI11296

11. Xiong Y, He T, Wang Y, Liu WV, Hu S, Zhang Y, et al. CKD stages, bone metabolism markers, and cortical porosity index: Associations and mediation effects analysis. *Front Endocrinol* (2021) 12. doi: 10.3389/fendo.2021.775066

12. Iseri K, Dai L, Chen Z, Qureshi AR, Brismar TB, Stenvinkel P, et al. Bone mineral density and mortality in end-stage renal disease patients. *Clin Kidney J* (2020) 13(3):307–21. doi: 10.1093/ckj/sfaa089

13. Sebag GH, Moore SG. Effect of trabecular bone on the appearance of marrow in gradient-echo imaging of the appendicular skeleton. *Radiology* (1990) 174(3 Pt 1):855–9. doi: 10.1148/radiology.174.3.2305069

14. Wehrli FW, Song HK, Saha PK, Wright AC. Quantitative MRI for the assessment of bone structure and function. *Nmr Biomed* (2006) 19(7):731–64. doi: 10.1002/nbm.1066

15. Majumdar S, Newitt D, Jergas M, Gies A, Chiu E, Osman D, et al. Evaluation of technical factors affecting the quantification of trabecular bone structure using magnetic resonance imaging. *Bone (New York NY)* (1995) 17(4):417–30. doi: 10.1016/S8756-3282(95)00263-4

16. Majumdar S, Genant HK. *In vivo* relationship between marrow T2* and trabecular bone density determined with a chemical shift-selective asymmetric spin-echo sequence. *J Magnetic Resonance Imaging* (1992) 2(2):209–19. doi: 10.1002/jmri.1880020215

17. Majumdar S, Thomasson D, Shimakawa A, Genant HK. Quantitation of the susceptibility difference between trabecular bone and bone marrow: Experimental studies. *Magnetic Resonance Med* (1991) 22(1):111–27. doi: 10.1002/mrm.1910220112

18. Davis CA, Genant H, Dunham J. The effects of bone on proton NMR relaxation times of surrounding liquids. *Invest Radiol* (1986) 21(6):472–7. doi: 10.1097/00004424-198606000-00005

19. Veldhuis-Vlug AG, Rosen CJ. Clinical implications of bone marrow adiposity. *J Internal Med* (2018) 283(2):121–39. doi: 10.1111/joim.12718

20. Griffith JF, Yeung DK, Antonio GE, Lee FK, Hong AW, Wong SY, et al. Vertebral bone mineral density, marrow perfusion, and fat content in healthy men and men with osteoporosis: Dynamic contrast-enhanced MR imaging and MR spectroscopy. *Radiology* (2005) 236(3):945–51. doi: 10.1148/radiol.2363041425

21. Griffith JF, Yeung DK, Antonio GE, Wong SY, Kwok TC, Woo J, et al. Vertebral marrow fat content and diffusion and perfusion indexes in women with varying bone density: MR evaluation. *Radiology* (2006) 241(3):831–8. doi: 10.1148/radiol.2413051858

22. Moorthi RN, Fadel W, Eckert GJ, Ponsler-Sipes K, Moe SM, Lin C, et al. Bone marrow fat is increased in chronic kidney disease by magnetic resonance spectroscopy. *Osteoporosis Int* (2015) 26(6):1801–7. doi: 10.1007/s00198-015-3064-7

23. Woods GN, Ewing SK, Sigurdsson S, Kado DM, Ix JH, Hue TF, et al. Chronic kidney disease is associated with greater bone marrow adiposity. *J Bone Mineral Res* (2018) 33(12):2158–64. doi: 10.1002/jbmr.3562

24. Pimentel A, Ureña-Torres P, Zillikens M. Fractures in patients with CKD-diagnosis, treatment, and prevention: A review by members of the European calcified tissue society and the European renal association of nephrology dialysis and transplantation. *Kidney Int* (2017) 92(6):1343–55. doi: 10.1016/j.kint.2017.07.021

25. Ge M, Zhang J, Wu B, Liu Z, Song H, Meng X, et al. Effect of gadolinium on hepatic fat quantification using multi-echo reconstruction technique with T2* correction and estimation. *Eur Radiol* (2016) 26(6):1913–20. doi: 10.1007/s00330-015-3981-z

26. Aoki T, Yamaguchi S, Kinoshita S, Hayashida Y, Korogi Y. Quantification of bone marrow fat content using iterative decomposition of water and fat with echo asymmetry and least-squares estimation (IDEAL): Reproducibility, site variation and correlation with age and menopause. *Br J Radiol* (2016) 89(1065):20150538. doi: 10.1259/bjr.20150538

27. Serai SD, Dillman JR, Trout AT. Proton density fat fraction measurements at 1.5- and 3-T hepatic MR imaging: Same-day agreement among readers and across two imager manufacturers. *Radiology* (2017) 284(1):244–54. doi: 10.1148/radiol.2017161786

28. Zeng Z, Ma X, Guo Y, Ye B, Xu M, Wang W. Quantifying bone marrow fat fraction and iron by MRI for distinguishing aplastic anemia from myelodysplastic syndromes. *J Magnetic Resonance Imaging* (2021) 54(6):1754–60. doi: 10.1002/jmri.27237

29. Carmona R, Pritz J, Bydder M, Gulaya S, Zhu H, Williamson CW, et al. Fat composition changes in bone marrow during chemotherapy and radiation therapy. *Int J Radiat OncologyBiologyPhys* (2014) 90(1):155–63. doi: 10.1016/j.ijrobp.2014.05.041

30. Eskreis-Winkler S, Corrias G, Monti S, Zheng J, Capanu M, Krebs S, et al. IDEAL-IQ in an oncologic population: Meeting the challenge of concomitant liver fat and liver iron. *Cancer Imaging* (2018) 18(1):51. doi: 10.1186/s40644-018-0167-3

31. Chen R, Bai Y, Liu T, Zhang G, Han Y, Chen L, et al. Evaluation of glypican-3 expression in hepatocellular carcinoma by using IDEAL IQ magnetic resonance imaging. *Acad Radiol* (2021) 28(8):e227–34. doi: 10.1016/j.acra.2020.05.015

32. Nickolas TL, Cremers S, Zhang A, Thomas V, Stein E, Cohen A, et al. Discriminants of prevalent fractures in chronic kidney disease. *J Am Soc Nephrol* (2011) 22(8):1560–72. doi: 10.1681/ASN.2010121275

33. Nickolas TL, Leonard MB, Shane E. Chronic kidney disease and bone fracture: A growing concern. *Kidney Int* (2008) 74(6):721–31. doi: 10.1038/ki.2008.264

34. Ketteler M, Block GA, Evenepoel P, Fukagawa M, Herzog CA, McCann L, et al. Executive summary of the 2017 KDIGO chronic kidney disease-mineral and bone disorder (CKD-MBD) guideline update: What's changed and why it matters. *Kidney Int* (2017) 92(1):26–36. doi: 10.1016/j.kint.2017.04.006

35. Malluche HH, Davenport DL, Cantor T, Monier-Faugere MC. Bone mineral density and serum biochemical predictors of bone loss in patients with CKD on dialysis. *Clin J Am Soc Nephrol* (2014) 9(7):1254–62. doi: 10.2215/CJN.09470913

36. Levey AS, Stevens LA, Schmid CH, Zhang YL, Castro AR, Feldman HI, et al. A new equation to estimate glomerular filtration rate. *Ann Internal Med* (2009) 150(9):604–12. doi: 10.7326/0003-4819-150-9-200905050-00006

37. Cohen A, Dempster DW, Recker RR, Lappe JM, Zhou H, Zwahlen A, et al. Abdominal fat is associated with lower bone formation and inferior bone quality in healthy premenopausal women: A transiliac bone biopsy study. *J Clin Endocrinol Metab* (2013) 98(6):2562–72. doi: 10.1210/jc.2013-1047

38. Bredella MA, Gerweck AV, Barber LA, Breggia A, Rosen CJ, Torriani M, et al. Effects of growth hormone administration for 6 months on bone turnover and bone marrow fat in obese premenopausal women. *Bone* (2014) 62:29–35. doi: 10.1016/j.bone.2014.01.022

39. Bredella MA, Lin E, Gerweck AV, Landa MG, Thomas BJ, Torriani M, et al. Determinants of bone microarchitecture and mechanical properties in obese men. *J Clin Endocrinol Metab* (2012) 97(11):4115–22. doi: 10.1210/jc.2012-2246

40. Bredella MA, Torriani M, Ghomi RH, Thomas BJ, Brick DJ, Gerweck AV, et al. Vertebral bone marrow fat is positively associated with visceral fat and inversely associated with IGF-1 in obese women. *Obes (Silver Spring)* (2011) 19 (1):49–53. doi: 10.1038/oby.2010.106

41. Bredella MA, Gill CM, Gerweck AV, Landa MG, Kumar V, Daley SM, et al. Ectopic and serum lipid levels are positively associated with bone marrow fat in obesity. *Radiology* (2013) 269(2):534–41. doi: 10.1148/radiol.13130375

42. Leonard MB. A structural approach to the assessment of fracture risk in children and adolescents with chronic kidney disease. *Pediatr Nephrol* (2007) 22 (11):1815–24. doi: 10.1007/s00467-007-0490-6

43. Amling M, Grote HJ, Vogel M, Hahn M, Delling G. Three-dimensional analysis of the spine in autopsy cases with renal osteodystrophy. *Kidney Int* (1994) 46(3):733–43. doi: 10.1038/ki.1994.328

44. Silva BC, Costa AG, Cusano NE, Kousteni S, Bilezikian JP, et al. Catabolic and anabolic actions of parathyroid hormone on the skeleton. *J Endocrinol Invest* (2011) 34(10):801–10. doi: 10.3275/7925

45. Langub MC, Monier-Faugere MC, Qi Q, Geng Z, Koszewski NJ, Malluche HH, et al. Parathyroid hormone/parathyroid hormone-related peptide type 1 receptor in human bone. *J Bone Mineral Res* (2001) 16(3):448–56. doi: 10.1359/jbmr.2001.16.3.448

46. Mcnerny E, Nickolas TL. Bone quality in chronic kidney disease: Definitions and diagnostics. *Curr Osteoporosis Rep* (2017) 15(3):207–13. doi: 10.1007/s11914-017-0366-z

47. Leonard MB. A structural approach to skeletal fragility in chronic kidney disease. *Semin Nephrol* (2009) 29(2):133–43. doi: 10.1016/j.semnephrol.2009.01.006

frontiers | Frontiers in Endocrinology

TYPE Original Research
PUBLISHED 27 September 2022
DOI 10.3389/fendo.2022.990487

OPEN ACCESS

EDITED BY
Ling Wang,
Beijing Jishuitan Hospital, China

REVIEWED BY
David L Waning,
Penn State College of Medicine, United States
Lu Yin,
Chinese Academy of Medical Sciences and Peking Union Medical College, China

*CORRESPONDENCE
Ming Wang
wm15930115215@163.com
Jian Zhao
zhaojiansohu@126.com

†These authors have contributed equally to this work and share first authorship

SPECIALTY SECTION
This article was submitted to Bone Research, a section of the journal Frontiers in Endocrinology

RECEIVED 10 July 2022
ACCEPTED 09 September 2022
PUBLISHED 27 September 2022

CITATION
Li J, Wang Y, Zhang X, Zhang P, Su Y, Bai L, Wang Y, Wang M and Zhao J (2022) Associations of muscle size and fatty infiltration with bone mineral density of the proximal femur bone. *Front. Endocrinol.* 13:990487. doi: 10.3389/fendo.2022.990487

Associations of muscle size and fatty infiltration with bone mineral density of the proximal femur bone

Junfei Li[1†], Yijing Wang[2†], Xuesong Zhang[1], Ping Zhang[1], Yunshan Su[3], Lin Bai[1], Yali Wang[1], Ming Wang[1*] and Jian Zhao[1*]

[1]Department of Radiology, The Third Hospital of Hebei Medical University, Shijiazhuang, China, [2]Department of Radiology, Hebei General Hospital, Shijiazhuang, China, [3]Department of Pediatric Orthopedics, The Third Hospital of Hebei Medical University, Shijiazhuang, China

Purpose: To investigate the relationship of muscle atrophy and fat infiltration around the hip joint with areal bone mineral density (aBMD) in each subregion of the proximal femur.

Materials and methods: In total, 144 participants (66 women and 78 men) were examined by quantitative computed tomography (QCT), and areal bone mineral density (aBMD) of the femoral neck (FN), trochanter (TR), and intertrochanter (IT) of the proximal femur were obtained. The cross-sectional area (CSA) and proton density fat fraction (PDFF) of the gluteus maximus (G.MaxM), gluteus medius (G.MedM), gluteus minimus (G.MinM), and iliopsoas (IliopM) were obtained *via* magnetic resonance imaging (MRI) using the mDIXON-Quant sequence. A multivariate generalized linear model was used to evaluate the correlation of the CSA and PDFF of muscles with aBMD in all subregions of the proximal femur.

Results: The FN integral (Int) aBMD was significantly associated with the G.MaxM CSA (men: $P = 0.002$; women: $P = 0.008$) and PDFF (men: $P < 0.001$; women: $P = 0.047$). Some muscle indexes were related to the FN aBMD in males or females, including the CSA of G.MedM, G.MinM, and IliopM as well as the PDFF of IliopM and G.MinM. Associations of hip muscle parameters with the TR Int aBMD in both males and females were observed, including G.MaxM CSA (men: $P < 0.001$; women: $P = 0.028$) and G.MaxM PDFF (men: $P = 0.031$; women: $P = 0.038$). Other muscle indexes, including G.MedM and IliopM, were related to the TR aBMD, mainly affecting the aBMD of TR cortical (Cort) and TR Int. The IT Int aBMD and IT Cort aBMD showed significant correlation with the muscle indexes of G. MaxM, IliopM, and G.MedM, including the PDFF and CSA in males and females. Further, more indicators of the G.MedM and IliopM correlated with the TR and IT aBMD compared to the FN aBMD.

Conclusions: The CSA of gluteus muscles and iliopsoas had a positive association with the aBMD in the proximal femur, and the PDFF of gluteus muscles and iliopsoas had a negative correlation with the aBMD in the proximal femur. In addition, there was an interaction of the proximal femur aBMD with the muscle size and fatty infiltration of hip muscles.

KEYWORDS

muscle cross-sectional area, water/fat imaging, quantitative computed tomography (QCT), proximal femur, bone mineral density (BMD)

Introduction

Osteoporosis is characterized by the absence of trabeculae and cortical bone, which can be diagnosed on the basis of low bone mineral density (BMD). Bone and muscle are closely related in embryogenesis, growth, and aging, and the interaction between bone and muscle is not only based on the mechanical loads and physical forces generated by muscle contraction but also on endocrine factors (1, 2). With the increase of age, osteoporosis is often accompanied by sarcopenia, which has been shown to be associated with low BMD (3, 4). Many studies have demonstrated that changes in bone mass are closely associated with changes in muscle mass. A positive correlation exists between bone and muscle, with a higher lean body mass associated with increased BMD and vice versa (5–7). Fatty infiltration of muscle and bone is known to contribute to sarcopenia and osteoporosis, most likely related to the negative impact of the secretion of inflammatory cytokines by both bone marrow and body fat in a process known as lipotoxicity (8, 9). Osteoporosis is the most important risk factor for fragility fractures, and osteoporotic fragility fracture of the hip is one of the most common fracture types. Reduced muscle mass and function leads to falls and a higher rate of hip fractures. Osteoporosis and reduced skeletal muscle mass are important risk factors for brittle hip fractures in the elderly (10, 11). Most previous studies have independently assessed muscle and fatty infiltration based on dual energy X-ray absorptiometer (DXA), while the direct relationship of muscle size and intramuscular adipose tissue with the proximal femur BMD has not been elucidated.

The modern Dixon technique uses water/fat separation magnetic resonance imaging (MRI) based on chemical shift, which quantifies intramuscular adipose tissue and shows good consistency with magnetic resonance spectroscopy (MRS) (12). However, MRI not only visualizes the anatomical structure but also quantifies the proton density fat fraction (PDFF) with good spatial resolution, short acquisition time, and accurate fat quantification (13, 14). Computed tomography X-ray absorptiometry (CTXA) is a QCTPro (Mindways Inc., Austin, TX) scanning analysis module, which generates two-dimensional (2D) images from three-dimensional (3D) images of the proximal femur region of interest (ROI) and evaluates the areal BMD (aBMD) of integral (Int), trabecular (Trab), and cortical (Cort) bone by region (femoral neck, FN; trochanter, TR; intertrochanter, IT) (15). In contrast to DXA, quantitative computed tomography (QCT) distinguishes cortical bone from trabecular bone. For the measurement of aBMD in the proximal femur, QCT aBMD has good consistency with DXA (16, 17).

To investigate the relationship between muscle atrophy and fatty infiltration around the hip joint and aBMD in the proximal femur, we used a six-echo chemical shift encoded water-fat MRI (mDIXON-Quant, Philips Healthcare) to assess the muscle PDFF representing the proportion of adipose tissue in muscle and the cross-sectional area (CSA) representing muscle volume around the hip joint. QCT was used to calculate the aBMD of the proximal femur. In this prospective cross-sectional study, we examined the correlation of PDFF and CSA of the gluteus maximus (G.MaxM), gluteus medius (G.MedM), gluteus minimus (G.MinM), and iliopsoas muscle (IliopM) with the QCT assessment of the aBMD of FN, TR, and IT, respectively, in middle-aged and elderly subjects.

Materials and methods

Study participants

Participants who were subjected to examination of the proximal femur aBMD were recruited from the physical examination center of our hospital. The study was approved by the Ethics Committee of The Third Hospital of Hebei Medical University. Informed consent was obtained for each participant. The inclusion criteria were as follows: 1) at least 30 years old and in good health; and 2) no MRI contraindications, such as cardiac pacemaker and claustrophobia. The exclusion criteria were as follows: 1) hip tumor; 2) a history of trauma and stunting; 3) previous hip surgery; 4) previous or current use of steroid hormones, calcitonin, estrogen, and other drugs affecting

bone metabolism; and 5) diseases that limit activity and function (Figure 1).

MRI examination

All hip MRI examinations were performed on the same 3.0T MR scanner (Ingenia CX, Phillips, Amsterdam, Netherlands) using a 32-channel torso coil. The MRI sequence parameters of water/fat based on chemical shift coding (mDIXON Quant, Philips Healthcare) were as follows: axial = fast field echo (FFE); repetition time (TR) = 8 ms; echo time (TE) 1 = 1.15 ms; echo spacing = shortest; field of view = 400 × 267 × 325 mm; matrix size = 376 × 299; voxel = 2.5 × 1.5 × 3.0 mm; slice thickness = 5 mm; flip angle = 3°; number of signal averaged (NSA) = 1; and acquisition time = 48 s. Six echoes were used for the quantification of PDFF. All MR images were reviewed and analyzed by a radiologist (XSZ).

All muscle measurements were performed by the same investigator (XSZ) with more than 2 years of experience who was unaware of the aBMD results. The MR images of water/fat based on chemical shift coding were transferred to the post-processing workstation (InterlliSpace^{TM} Portal, ISP, Philips), and PDFF maps were automatically generated. Seven fat peaks were modeled and T2* corrected. The CSA and PDFF of muscles were measured at the maximum CSA level on the axial fat fraction maps. The G.MaxM at the level of the lower margin of the fourth sacral vertebra and the G.MedM at the level of the first sacral vertebra were analyzed. The G.MinM and IliopM at the level of 0.5 - 1.5 cm at the upper acetabulum margin were analyzed. Free-hand drawn ROIs were separately placed in the axial view of the right sides of the G.MaxM, G.MedM, G.MinM, and IliopM on the fat fraction maps. Each ROI was drawn along the margin of the muscle and outlined muscle contours (Figure 2). The PDFF and CSA of G.MaxM, G.MedM, G.MinM, and IliopM were obtained directly. After completing ROI delineation, the PDFF and CSA of G.MaxM, G.MedM, G.MinM, and IliopM were directly obtained from the fat fraction map. Approximately 3 min were required to draw all the ROIs of hip muscles for each subject.

In addition, 20 subjects' images were randomly selected from the entire data set to evaluate the intra- and inter-reader reliability by a second radiologist (JFL) with more than 2 years of experience. For evaluating the consistency and reliability of different observers, intraclass correlation coefficient (ICC) was determined as follows: ICC < 0.4, poor consistency; 0.4 < ICC < 0.75, moderate consistency; and ICC > 0.75, good consistency. For the bilateral test, a test level of $\alpha = 0.05$ was used. Good intra-observer (intra-class correlation coefficients, ICC 0.889–0.978, $P < 0.001$) and moderate inter-observer (ICC 0.693–0.971, $P < 0.001$) agreements of the muscle measures were found.

QCT examination

CT scans of subjects' hip joints were performed on a 64-row Siemens Somatom Definition CT scanner (Siemens, Erlangen, Germany) with a Mindways calibrated body model (Mindways Software Inc., Austin, Texas, USA). The acquisition parameters were as follows: 120 kV; 217 mAs; pitch of 1.2; reconstruction slice thickness of 1 mm; reconstruction field of view 50 cm; and medium reconstruction kernel (B40f). The scanning range was 1 cm above the femoral head to 3 cm below the lesser trochanter. The subjects' knees were flat, and their feet were rotated inwards to reduce overlap between the

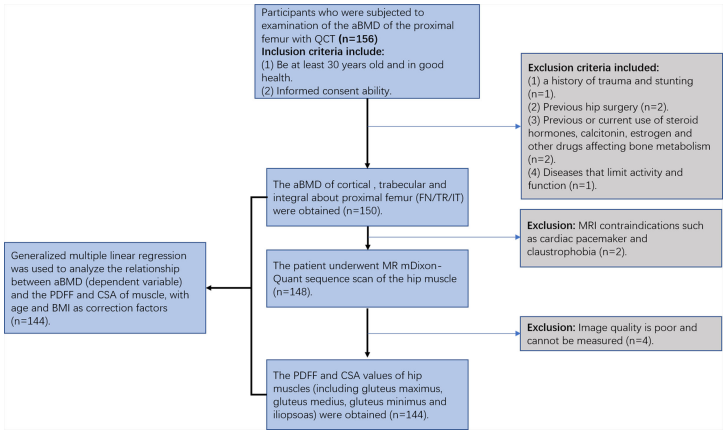

FIGURE 1
Flow chart of the patient population included in the present study.

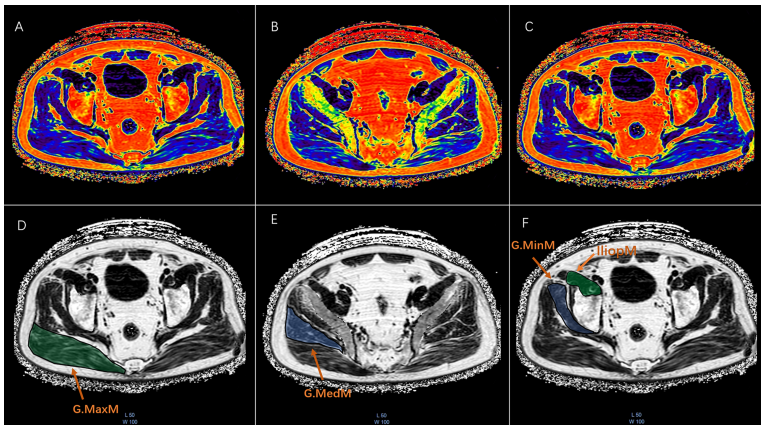

FIGURE 2
The ROI drawn freehand was placed at the maximum CSA of the fat fraction plot on the axial map of the right gluteus maximus (G.MaxM), gluteus medius (G.MedM), gluteus minimus (G.MinM), and iliopsoas muscle (IliopM). Each ROI was plotted along the edge of the muscle to obtain the PDFF and CSA as shown in the pseudocolor and FF maps of G.MaxM **(A, D)**, G.MedM **(B, E)**, G.MinM, and IliopM **(C, F)**.

proximal femur and the acetabulum on the 2D projected image. This study analyzed hip CT scans using the commercial QCTPro (Mindways Inc., Austin, Texas, USA) CTXA module. Three standard DXA hip ROIs were generated, namely, FN, TR, and IT, and DXA equivalent aBMD results of each ROI were obtained. The FN ROI was a narrow frame 10 or 15 mm wide to avoid the overlap between the acetabulum and FN in 2D projection images (Figure 3). In the present study, the World Health Organization (WHO) BMD criteria for osteoporosis were used as follows: osteoporosis was defined by a BMD T-score of -2.5 or less at the FN or total hip; osteopenia was defined by a BMD T-score between -1.0 and -2.5 at the FN or total hip; and normal was defined by a BMD T-score of -1 or more at the FN or total hip.

Statistical analyses

Statistical analyses were performed using SPSS Statistics (IBM, version 26) with a significance level of 0.05. For data with normal distribution, the two independent samples *t*-test was used for comparison between men and women. For data with non-normal distribution, the two-sample Mann-Whitney U test was used to analyze the differences between men and women. The analysis was stratified by sex due to differences in underlying pathological mechanisms of changes in aBMD, muscle CSA, and PDFF between men and women. Generalized multiple linear regression was used to analyze the relationship of the aBMD (dependent variable) of the FN, TR, and IT with the PDFF and CSA of the G.MaxM, G.MedM, G.MinM, and IliopM.

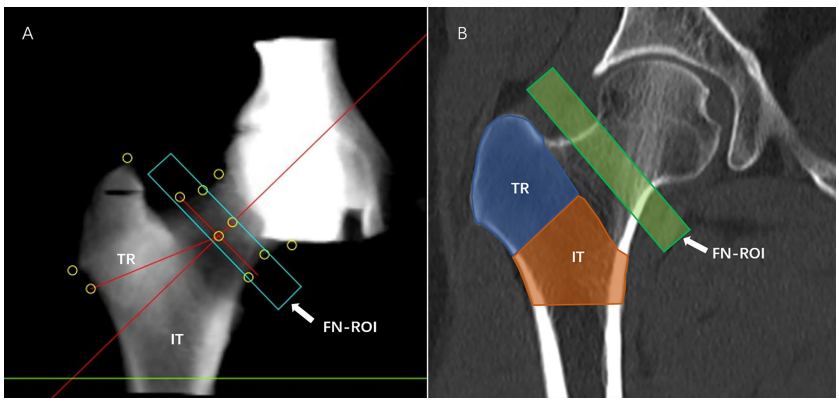

FIGURE 3
aBMD measurement. QCTPro CTXA was used to analyze the aBMD of the proximal femur, including the FN, TR, and IT **(A, B)**.

To improve various muscle indexes were measured and transferred using sex-specific SD, respectively. Age and BMI were used as correction factors.

Results

Study sample characteristics

In total, 144 healthy subjects were included for analysis as shown in Table 1. There were 78 males, including 33 subjects with normal BMD, 33 subjects with osteopenia, and 12 subjects with osteoporosis, and there were 66 females, including 20 subjects with normal BMD, 22 subjects with osteopenia, and 24 subjects with osteoporosis. Men had higher a CSA in the G.MaxM (4372.21 vs. 3463.33 mm^2), G.MedM (2997.23 vs. 2269.58 mm^2), G.MinM (1149.31 vs. 811.15 mm^2), and IliopM (1697.37 vs. 1020.38 mm^2) than women ($P < 0.05$). The PDFF of the G.MaxM (17.86 vs. 21.53%) and IliopM (8.69 vs. 11.15%) in men was lower than that in women ($P < 0.05$). Women also had a higher PDFF in the G.MedM (14.65 vs. 13.92%) and G.MinM (11.67 vs. 10.41%) in men, but there was no statistical difference ($P > 0.05$). Women had a lower aBMD at some sites, including the FN Trab (0.20 vs. 0.23 g/cm^2), FN Int (0.62 vs. 0.67 g/cm^2), TR Cort (0.32 vs. 0.36 g/cm^2), TR Trab (0.16 vs. 0.31 g/cm^2), TR Int (0.47 vs. 0.67 g/cm^2), IT Cort (0.52 vs. 0.78 g/cm^2), IT Trab (0.25 vs. 0.29 g/cm^2), and IT Int (0.78 vs. 1.05 g/cm^2) compared to men ($P < 0.05$), but there was no statistical difference for the FN Cort (0.42 vs. 0.45 g/cm^2, $P > 0.05$).

FN aBMD

The adjusted beta coefficients and 95% confidence interval (CI) of the FN aBMD sites (FN Int, FN Trab, and FN Cort aBMD) with continuous muscle indexes per sex-specific standard deviation (SD) increase are shown in Table 2 and Table 3. The FN Int aBMD was significantly associated with the G.MaxM CSA (men: $P = 0.002$; women: $P = 0.008$) and PDFF (men: $P < 0.001$; women: $P = 0.047$). There were associations between the FN Cort aBMD and the CSA of G.MaxM (men: $P = 0.002$; women: $P = 0.002$) and G.MaxM PDFF (men: $P < 0.049$; women: $P = 0.003$). In men, 0.194 and -0.196 g/cm^2 of FN Int aBMD increased with one SD increase of G.MedM area (95% CI, 0.018, 0.370; $P = 0.031$) and

TABLE 1 Clinical characteristics of the subjects[b].

Characteristics (Mean ± SD)		Males ($N = 78$)	Females ($N = 66$)	P-Value
Age (years)		57.81 ± 12.07	61.88 ± 10.93	**0.032**
Height (cm)		171.74 ± 0.50	160.18 ± 0.69	**<0.001**
Weight (kg)		76.56 ± 11.24	65.41 ± 10.24	**<0.001**
BMI (kg/m^2)		25.93 ± 0.40	25.44 ± 0.41	0.388
CSA(mm^2)				
G.MaxM		4372.21 ± 1066.84	3463.33 ± 754.64	**<0.001**
G.MedM		2997.23 ± 701.84	2269.58 ± 591.70	**<0.001**
G.MinM		1149.31 ± 264.22	811.15 ± 195.66	**<0.001**
IliopM		1697.37 ± 257.08	1020.38 ± 328.68	**<0.001**
PDFF (%)				
G.MaxM		17.86 ± 6.17	21.53 ± 6.49	**0.001**
G.MedM		13.92 ± 4.77	14.65 ± 4.75	0.412
G.MinM		10.41 ± 5.33	11.67 ± 6.13	0.343
IliopM		8.69 ± 3.33	11.15 ± 3.83	**<0.001**
FN aBMD(g/cm^2)	Cort	0.445 ± 0.434	0.423 ± 0.126	0.184
	Trab	0.228 ± 0.057	0.197 ± 0.525	**0.001**
	Int	0.667 ± 0.105	0.616 ± 0.148	**0.009**
TR aBMD(g/cm^2)	Cort	0.361 ± 0.072	0.321 ± 0.093	**0.023**
	Trab	0.313 ± 0.059	0.157 ± 0.063	**<0.001**
	Int	0.673 ± 0.111	0.467 ± 0.117	**<0.001**
IT aBMD(g/cm^2)	Cort	0.776 ± 0.131	0.524 ± 0.129	**<0.001**
	Trab	0.285 ± 0.048	0.247 ± 0.058	**<0.001**
	Int	1.054 ± 0.154	0.774 ± 0.153	**<0.001**

The independent-samples **t** test was used. Most of the remaining data were non-normally distributed, and Mann-Whitney U test was used. (SD, standard deviance; BMI, body mass index; PDFF, proton density fat fraction; CSA, cross-sectional area; G.MaxM, gluteus maximus muscle; G.MedM, gluteus medius muscle; G.MinM, gluteus minimus muscle; IliopM, iliopsoas muscle; aBMD, areal bone mineral density; FN, femoral neck; TR, trochanter; IT, intertrochanter; Int, integral; Trab, trabecular; Cort, cortical). [b]The bold type indicates statistical difference ($P < 0.05$).

TABLE 2 Generalized multiple linear standardized regression coefficients and 95% CIs between the aBMD of the FN and various muscle indexes[a,b,c] in males.

Males

Variables	FN Int aBMD (g/cm^2)		FN Cort aBMD (g/cm^2)		FN Trab aBMD (g/cm^2)	
CSA (mm^2)	β (95% CI)	P	β (95% CI)*10^{-3}	P	β (95% CI)*10^{-3}	P
G.MaxM	0.308(0.109, 0.507)	**0.002**	0.413(0.147, 0.679)	**0.002**	0.246(-0.057, 0.549)	0.112
G.MedM	0.194(0.018, 0.370)	**0.031**	0.086(-0.149, 0.321)	0.472	0.091(-0.176, 0.358)	0.505
G.MinM	0.061(-0.105, 0.227)	0.470	-0.149(-0.370, 0.072)	0.187	0.198(-0.054, 0.450)	0.124
IliopM	-0.080(-0.225, 0.065)	0.279	-0.078(-0.272, 0.115)	0.427	0.037(-0.184, 0.257)	0.744
PDFF(%)						
G.MaxM	-0.362(-0.541, -0.182)	**<0.001**	-0.238(-0.477, 0.001)	**0.049**	-0.103(-0.375, 0.170)	0.460
G.MedM	-0.176(-0.383, 0.030)	0.094	-0.170(-0.446, 0.106)	0.226	-0.013(-0.327, 0.301)	0.936
G.MinM	0.065(-0.086, 0.215)	0.398	0.143(-0.058, 0.343)	0.164	0.107(-0.122, 0.336)	0.361
IliopM	-0.196(-0.348, -0.045)	**0.011**	-0.240(-0.442, -0.037)	**0.020**	-0.203(-0.433, 0.028)	0.085

PDFF, proton density fat fraction; CSA, cross-sectional area; G.MaxM, gluteus maximus muscle; G.MedM, gluteus medius muscle; G.MinM, gluteus minimus muscle; IliopM, iliopsoas muscle; aBMD, areal bone mineral density; FN, femoral neck; Int, integral; Trab, trabecular; Cort, cortical. [a]Adjusted for age and body mass index (BMI). [b] The bold type indicates statistical difference (P < 0.05). [c]β for standard deviance increase of continuous muscle variables.

PDFF of IliopM (95% CI, -0.348, -0.045; P = 0.011), but this significance was not observed in women. The FN Cort aBMD negatively correlated with the IliopM PDFF in men (β, -0.240; 95%CI, -0.442, 0.037; P = 0.020) and G.MinM PDFF in women (β, -0.329; 95%CI, -0.599, -0.058; P = 0.017). Associations between the FN Trab aBMD and the CSA of G.MinM (P = 0.018) and IliopM (P = 0.008) were found only in women.

TR aBMD

The results of generalized linear models for the associations between the TR aBMD and muscle indexes are presented in Table 4 and Table 5. Some muscle indexes were related to the TR Int aBMD in both men and women, including the G.MaxM CSA (men: P < 0.001; women: P = 0.028) and G.MaxM PDFF (men: P = 0.031; women: P = 0.038). In addition to the above correlation with the TR Int aBMD, associations with the G.MaxM CSA were found for the TR Cort aBMD (P = 0.002) and TR Trab aBMD (P = 0.001) in men but not in women. Moreover, the G.MedM CSA was also correlated with the TR Int aBMD (P < 0.001), TR Cort aBMD (P = 0.047), and TR Trab aBMD (P = 0.017) in men. In women, 0.404 and -0.199 g/cm^2 of the TR Int aBMD increased with one SD increase of IliopM CSA (95% CI, 0.204, 0.603; P < 0.001) and IliopM PDFF (95% CI, -0.382, -0.016; P = 0.033), but this significance was not found in

TABLE 3 Generalized multiple linear standardized regression coefficients and 95% CIs between the aBMD of the FN and various muscle indexes[a,b,c] in females.

Females

Variables	FN Int aBMD (g/cm^2)		FN Cort aBMD (g/cm^2)		FN Trab aBMD (g/cm^2)	
CSA (mm^2)	β (95% CI)	P	β (95% CI)	P	β (95% CI)	P
G.MaxM	0.435(0.116, 0.754)	**0.008**	0.551(0.196, 0.905)	**0.002**	0.079(-0.279, 0.437)	0.664
G.MedM	-0.033(-0.321, 0.255)	0.823	-0.217(-0.538, 0.103)	0.183	0.175(-0.148, 0.498)	0.287
G.MinM	0.164(-0.057, 0.385)	0.147	0.015(-0.231, 0.260)	0.908	0.299(0.051, 0.547)	**0.018**
IliopM	0.049(-0.201, 0.299)	0.702	-0.079(-0.357, 0.199)	0.578	0.378(0.098, 0.658)	**0.008**
PDFF(%)						
G.MaxM	-0.290(-0.577, -0.004)	**0.047**	-0.477(-0.795, -0.159)	**0.003**	0.002(-0.319, 0.322)	0.992
G.MedM	0.075(-0.294, 0.444)	0.689	0.261(-0.149, 0.671)	0.211	0.129(-0.284, 0.542)	0.541
G.MinM	-0.232(-0.476, 0.011)	0.061	-0.329(-0.599, -0.058)	**0.017**	-0.211(-0.484, 0.062)	0.130
IliopM	-0.024(-0.253, 0.205)	0.836	-0.044(-0.299, 0.211)	0.735	0.235(-0.022, 0.492)	0.073

PDFF, proton density fat fraction; CSA, cross-sectional area; G.MaxM, gluteus maximus muscle; G.MedM, gluteus medius muscle; G.MinM, gluteus minimus muscle; IliopM, iliopsoas muscle; aBMD, areal bone mineral density; FN, femoral neck; Int, integral; Trab, trabecular; Cort, cortical. [a]Adjusted for age and body mass index (BMI). [b]The bold type indicates statistical difference (P < 0.05). [c]β for standard deviance increase of continuous muscle variables.

TABLE 4 Generalized multiple linear standardized regression coefficients and 95% CIs between the aBMD of the TR and various muscle indexes[a,b,c] in males.

Males

Variables	TR Int aBMD (g/cm^2)		TR Cort aBMD (g/cm^2)		TR Trab aBMD (g/cm^2)	
CSA (mm^2)	β (95% CI)	P	β (95% CI)	P	β (95% CI)	P
G.MaxM	0.473(0.275, 0.672)	**<0.001**	0.422(0.149, 0.695)	**0.002**	0.441(0.183, 0.700)	**0.001**
G.MedM	0.047(-0.128, 0.222)	0.600	0.090(-0.150, 0.331)	0.462	-0.028(-0.256, 0.200)	0.812
G.MinM	-0.168(-0.333, -0.003)	**0.046**	-0.147(-0.373, 0.080)	0.205	-0.017(-0.232, 0.198)	0.876
IliopM	-0.028(-0.173, 0.116)	0.702	0.032(-0.167, 0.230)	0.756	-0.027(-0.215, 0.161)	0.780
PDFF(%)						
G.MaxM	-0.197(-0.375, 0.018)	**0.031**	-0.139(-0.384, 0.107)	0.268	-0.217(-0.450, 0.015)	0.066
G.MedM	-0.444(-0.650, -0.238)	**<0.001**	-0.274(-0.557, 0.009)	**0.047**	-0.328(-0.596, -0.060)	**0.017**
G.MinM	0.132(-0.017, 0.282)	0.083	0.032(-0.174, 0.238)	0.761	0.176(-0.019, 0.371)	0.078
IliopM	-0.034(-0.185, 0.116)	0.654	-0.055(-0.262, 0.153)	0.606	-0.020(-0.217, 0.176)	0.841

PDFF, proton density fat fraction; CSA, cross-sectional area; G.MaxM, gluteus maximus muscle; G.MedM, gluteus medius muscle; G.MinM, gluteus minimus muscle; IliopM, iliopsoas muscle; aBMD, areal bone mineral density; TR, trochanter; Int, integral; Trab, trabecular; Cort, cortical. [a]Adjusted for age and body mass index (BMI). [b]The bold type indicates statistical difference (P < 0.05). [c]β for standard deviance increase of continuous muscle variables.

men. Other muscle indexes were related to the TR aBMD in women, including the IliopM CSA (P = 0.004) to TR Cort aBMD, the G.MaxM PDFF (P = 0.014) to TR Cort aBMD, and the IliopM PDFF (P = 0.001) to TR Trab aBMD.

IT aBMD

Table 6 and Table 7 show the results from the multivariate generalized linear models, assessing the associations of the IT aBMD with eight muscle indexes, including the CSA and PDFF of the G. MaxM, G.MedM, G.MinM, and IliopM. The IT Int aBMD showed a significant association with the G. MaxM CSA (men: P = 0.005; women: P < 0.001), G. MaxM PDFF (only women, P = 0.041), IliopM CSA (only men, P = 0.007), IliopM PDFF (men: P = 0.001; women: P = 0.003), G.MedM CSA (only women, P < 0.001), and G.MedM PDFF (only women, P = 0.038). Associations with the IT Cort aBMD were found for the G.MaxM CSA in men (P = 0.014), G.MedM CSA in women (P = 0.022), IliopM CSA in men (P = 0.039), G.MedM PDFF in women (P = 0.010), and IliopM PDFF in women (P = 0.001). No significance was found for the IT Trab aBMD (all P > 0.05).

Discussion

The innovation of this study lies in the independent analysis of the relationship of the PDFF and CSA of the muscles around

TABLE 5 Generalized multiple linear standardized regression coefficients and 95% CIs between the aBMD of the TR and various muscle indexes[a,b,c] in females.

Females

Variables	TR Int aBMD (g/cm^2)		TR Cort aBMD (g/cm^2)		TR Trab aBMD (g/cm^2)	
CSA(mm^2)	β(95% CI)	P	β(95% CI)	P	β(95% CI)	P
G.MaxM	0.286(0.031, 0.541)	**0.028**	0.192(-0.102, 0.487)	0.201	-0.256(-0.672, 0.160)	0.227
G.MedM	0.033(-0.197, 0.263)	0.779	0.036(-0.231, 0.302)	0.794	0.348(-0.027, 0.724)	0.069
G.MinM	-0.075(-0.252, 0.101)	0.403	-0.177(-0.381, 0.027)	0.090	-0.094(-0.382, 0.194)	0.173
IliopM	0.404(0.204, 0.603)	**<0.001**	0.340(0.109, 0.571)	**0.004**	-0.206(-0.119, 0.532)	0.214
PDFF(%)						
G.MaxM	-0.241(-0.470, 0.013)	**0.038**	-0.331(-0.595, -0.067)	**0.014**	0.267(-0.106, 0.639)	0.161
G.MedM	0.066(-0.229, 0.360)	0.662	0.310(-0.030, 0.651)	0.074	0.074(-0.406, 0.554)	0.763
G.MinM	-0.050(-0.244, 0.144)	0.615	-0.121(-0.346, 0.104)	0.291	-0.221(-0.538, 0.096)	0.173
IliopM	-0.199(-0.382, -0.016)	**0.033**	-0.139(-0.350, 0.073)	0.199	-0.493(-0.791, -0.194)	**0.001**

PDFF, proton density fat fraction; CSA, cross-sectional area; G.MaxM, gluteus maximus muscle; G.MedM, gluteus medius muscle; G.MinM, gluteus minimus muscle; IliopM, iliopsoas muscle; aBMD, areal bone mineral density; TR, trochanter; Int, integral; Trab, trabecular; Cort, cortical. [a]Adjusted for age and body mass index (BMI). [b]The bold type indicates statistical difference (P < 0.05). [c]β for standard deviance increase of continuous muscle variables.

TABLE 6 Generalized multiple linear standardized regression coefficients and 95% CIs between the aBMD of the IT and various muscle indexes[a,b,c] in males.

Males

Variables	IT Int aBMD (g/cm^2)		IT Cort aBMD (g/cm^2)		IT Trab aBMD (g/cm^2)	
CSA (mm^2)	β (95% CI)	P	β (95% CI)	P	β (95% CI)	P
G.MaxM	0.319(0.096, 0.542)	**0.005**	0.317(0.065, 0.568)	**0.014**	0.008(-0.328, 0.344)	0.964
G.MedM	0.142(-0.055, 0.339)	0.158	0.192(-0.030, 0.414)	0.091	-0.041(-0.337, 0.256)	0.787
G.MinM	-0.077(-0.262, 0.109)	0.417	-0.177(-0.386, 0.032)	0.097	0.168(-0.112, 0.447)	0.240
IliopM	0.224(0.061, 0.386)	**0.007**	0.193(0.009 0.376)	**0.039**	0.096(-0.149, 0.340)	0.443
PDFF(%)						
G.MaxM	-0.091(-0.291, 0.110)	0.375	-0.036(-0.262, 0.190)	0.755	-0.071(-0.373, 0.231)	0.645
G.MedM	-0.102(-0.333, 0.130)	0.389	-0.062(-0.323, 0.199)	0.643	-0.244(-0.593, 0.104)	0.169
G.MinM	0.107(-0.061, 0.276)	0.212	0.060(-0.130, 0.250)	0.537	0.117(-0.136, 0.371)	0.364
IliopM	-0.296(-0.466, -0.127)	**0.001**	-0.315(-0.506, -0.123)	**0.001**	-0.105(-0.360, 0.151)	0.422

PDFF, proton density fat fraction; CSA, cross-sectional area; G.MaxM, gluteus maximus muscle; G.MedM, gluteus medius muscle; G.MinM, gluteus minimus muscle; IliopM, iliopsoas muscle; aBMD, areal bone mineral density; IT, intertrochanter; Int, integral; Trab, trabecular; Cort, cortical. [a]Adjusted for age and body mass index (BMI). [b]The bold type indicates statistical difference ($P < 0.05$). [c]β for standard deviance increase of continuous muscle variables.

the hip joint with proximal femur aBMD. The present study is the first to demonstrate that both the CSA and PDFF in the muscles around the hip joint are associated with proximal femur aBMD, suggesting that muscle size and fat infiltration in this area influence the proximal femur aBMD. We applied MR-Dixon technology to quantify muscle adipose content, which quantifies muscle adipose tissue, including intramuscular and intermuscular adipose tissue, with high resolution.

The cellular origins of fatty accumulation in muscle arise through several different pathways. One direct route is *via* the accumulation of lipid within myofibers themselves, which is known as intramuscular fat. Another pathway is an accumulation of adipocytes within skeletal muscle, which is known as intermuscular fat (18). Conventional T1-weighted MRI only assesses visible adipose tissue in T1-weighted images, but it is unable to assess small lipid concentrations in localized muscular regions (19). Chemical shift-based water/fat separation methods, including Dixon techniques and the iterative decomposition of water and fat with echo asymmetry and least-squares estimation (IDEAL), overcome the limitations of conventional T1-weighted imaging by allowing high spatial resolution for quantification of adipose tissue in localized regions, including intramuscular and intermuscular lipids. In addition, to obtain true proximal femur aBMD, we used QCT, which has been demonstrated to have good consistency with DXA.

TABLE 7 Generalized multiple linear standardized regression coefficients and 95% CIs between the aBMD of the IT and various muscle indexes[a,b,c] in females.

Females

Variables	IT Int aBMD (g/cm^2)		IT Cort aBMD (g/cm^2)		IT Trab aBMD (g/cm^2)	
CSA (mm^2)	β (95% CI)	P	β (95% CI)	P	β (95% CI)	P
G.MaxM	0.363(0.160, 0.567)	**<0.001**	0.177(-0.117, 0.471)	0.238	0.069(-0.296, 0.435)	0.711
G.MedM	0.338(0.155, 0.522)	**<0.001**	0.309(0.044, 0.574)	**0.022**	0.135(-0.195, 0.465)	0.424
G.MinM	0.092(-0.049, 0.233)	0.200	0.161(-0.043, 0.364)	0.122	0.176(-0.077, 0.430)	0.173
IliopM	0.086(-0.074, 0.245)	0.292	-0.030(-0.260, 0.200)	0.797	0.175(-0.112, 0.461)	0.232
PDFF(%)						
G.MaxM	-0.190(-0.372, -0.008)	**0.041**	-0.016(-0.279, 0.248)	0.907	-0.288(-0.616, 0.040)	0.085
G.MedM	-0.249(-0.484, -0.014)	**0.038**	-0.445(-0.784, -0.105)	**0.010**	-0.060(-0.483, 0.362)	0.780
G.MinM	0.120(-0.035, 0.275)	0.129	0.194(-0.030, 0.418)	0.090	0.008(-0.271, 0.287)	0.955
IliopM	-0.220(-0.366, -0.074)	**0.003**	-0.342(-0.553, -0.131)	**0.001**	0.048(-0.214, 0.311)	0.719

PDFF, proton density fat fraction; CSA, cross-sectional area; G.MaxM, gluteus maximus muscle; G.MedM, gluteus medius muscle; G.MinM, gluteus minimus muscle; IliopM, iliopsoas muscle; aBMD, areal bone mineral density; IT, intertrochanter; Int, integral; Trab, trabecular; Cort, cortical. [a]Adjusted for age and body mass index (BMI). [b]The bold type indicates statistical difference ($P < 0.05$). [c]β for standard deviance increase of continuous muscle variables.

Muscle CSA or muscle thickness, as a simple and practical muscle volume estimation method, has been widely used as an indirect indicator of muscle strength (20, 21). As for the selection of muscle level, the CSA around the muscle abdomen decreases to the greatest extent due to disuse, while the CSA around the muscle end does not significantly change (22, 23). Therefore, to better evaluate the changes of CSA in the muscles around the hip joint, we selected the maximum CSA of the muscle (similar to the muscle abdomen) as the evaluation level. The present study showed that the CSA of the G.MaxM was positively correlated with the aBMD of all subregions of the proximal femur and that it mainly affects the Int aBMD and Cort aBMD of the FN, TR, and IT. The present study also found that the CSA of the IliopM and G.MedM was positively associated with the Int aBMD and Cort aBMD of the TR and IT. Moreover, the cortical shell of long bones is crucial for fracture prevention because it is the main compressive and flexural resistant structure of bone (24, 25). Therefore, the present results suggested that the CSA of the G.MaxM, IliopM, and G.MedM is a protective factor against proximal femoral fractures by influencing proximal femoral aBMD, especially cortical aBMD. The increase in soft tissue thickness mainly dependent on the CSA of muscles in the proximal femur reduces the risk of fracture by reducing the force applied to the femur during lateral falls (26–28), supporting our view from another aspect.

The interaction between bone and muscle is mainly realized by mechanical stimulation and secreted bioactive factors. Mechanical tension caused by muscle initiates osteogenic activity, and both osteoblasts and osteocytes respond to mechanical stimulation. Mechanical transduction also induces cascades of biochemical signals, including the production of hormones and growth factors, which affect the coupling process of bone formation and bone resorption (29). As an indicator of muscle strength, muscle CSA partly reflects the mechanical tension between muscle and bone, suggesting that mechanical stimulation between muscle and bone may be one of the mechanisms by which the CSA of muscle affects the aBMD in the proximal femur. The G.MaxM is the main and strongest muscle of the hip joint, providing the greatest power for the movement of the hip joint and also affecting the aBMD of most regions in the proximal femur. It is possible that the CSA of the IliopM and G.MedM mainly affects the BMD of the TR and IT through mechanical stimulation of muscle attachment.

Fatty infiltration of skeletal muscle is an important manifestation of skeletal muscle aging, which reflects the decrease of skeletal muscle function and muscle strength (30, 31). Previous studies have found that BMD loss is correlated with decreased muscle mass, strength, and function, which is mainly manifested as lean muscle loss and fat infiltration (3, 13). The present results showed that the PDFFs of several muscles were negatively associated with the aBMD of subregions of the proximal femur as follows: the G.MaxM was negatively associated with the aBMD of the FN, TR, and IT; the G.MedM was negatively associated with the aBMD of the TR and IT; and the IliopM was negatively associated with the aBMD of the FN, TR, and IT. Lu (32) found that the lipid infiltration of the G.MaxM and mid-thigh muscle is associated with the aBMD of the proximal femur, which agreed with the present study. Intramuscular fat infiltration impairs the ability of the skeletal muscle to produce normal protein, resulting in decreased insulin sensitivity. Impaired normal protein synthesis leads to reduced muscle strength and muscle atrophy (18, 33). Therefore, muscle fat infiltration in the buttocks reduces the mechanical stimulation to the bone at this site, resulting in a decrease in the BMD of the proximal femur, suggesting that fatty infiltration of muscle negatively affects aBMD at the proximal femur. Moreover, increased fat content of the gluteal muscles contributes to reduced lower extremity performance, conferring increased risk of loss of mobility, falls, and skeletal fractures (34), which is consistent with a previous study showing that reducing muscle fat infiltration and improving muscle strength significantly reduces fracture risk (35, 36).

The present study showed that more indicators of the G.MedM and IliopM correlated with the aBMD of the TR and IT than the aBMD of the FN. Decreased BMD in different areas of the proximal femur may lead to different types of osteoporotic fractures, such as FN fractures or intertrochanteric fractures. It has been reported that the BMD of the TR and IT in the IT fracture group is lower than that in the FN fracture group (37, 38). Wang et al. (36) found that intertrochanteric aBMD is a better predictor of hip fracture than the FN and total hip aBMD, indicating that intertrochanteric aBMD has a better correlation with hip fractures. Thus, increased CSA and decreased PDFF in the G.MedM and IliopM may be protective factors for intertrochanteric fractures. Physical activity and regular exercise reduce muscle fat content, increase muscle CSA, and enhance bone strength, which reduces the risk of hip fractures (18, 39).

The present study found that the PDFF in the hip muscle was negatively correlated with the aBMD in the proximal femur and that the CSA was positively correlated with the aBMD. Skeletal muscle fat infiltration and muscle atrophy coexist with age, which may be due to the different forms of dysfunction in skeletal muscle fibers and the distribution of muscle fiber types in different functional muscle tissues (40, 41). The accumulation of intramuscular lipid with aging is not homogenous across different fiber types. Type I fibers are oxidative slow-twitch fibers that contain high intramuscular lipid content and many mitochondria. In contrast, type II fibers are glycolytic fast-twitch fibers that have low intramuscular lipid content and

low aerobic capacity. Type I fibers tend to accumulate more intramuscular lipids with age in human subjects than fast-twitch oxidative fibers (42). The number and degree of atrophy of type II muscle fibers in skeletal muscle of patients with osteoporosis are greater than that of type I muscle fibers, and a significant correlation between the degree of type II myofiber atrophy and proximal femoral BMD has been reported in previous studies (43). The downregulation of IGF-1/PI3K/Akt activity that occurs in osteoporosis may lead to muscle atrophy. Moreover, because IGF-1/PI3K/Akt activity controls glucose uptake in skeletal muscle, the downregulation of this activity may affect mainly glycolytic fibers (type II) due to their capacity of utilizing glucose to produce energy (43, 44). With age, muscles rich in type II fiber atrophy more and accumulate less lipids than muscles rich in type I fiber.

There were several limitations to this study. First, because this study was a cross-sectional study, we were unable to explore the longitudinal relationship between muscle and the proximal femur aBMD. Second, the study population consisted of middle-aged and elderly non-hip disease individuals from one center, which may limit the generalization of the results to other ethnic groups and other age groups. Third, due to the small number of participants in this study, the differences between male and female indicators were not further discussed. Studies with larger samples are needed to further compare the differences between men and women as well as to obtain additional evidence for the relationship between the muscles around the hip joint and the BMD of the proximal femur. Finally, the lack of data on physical activity and muscle strength may reduce the interpretation of the findings.

In conclusion, the CSA of the gluteus muscle and iliopsoas muscle has a positive association with the proximal femur aBMD, and the PDFF of the gluteus muscle and iliopsoas muscle has a negative correlation with the proximal femur aBMD. A better understanding of the relationship of the PDFF and CSA of the muscle with the proximal femur BMD will help provide a better understanding of the prevention of osteoporosis and related complications. Therefore, the CSA and PDFF of the gluteus muscle and iliopsoas muscle may be important factors and clinically significant targets for the treatment of osteoporosis.

Data availability statement

The original contributions presented in the study are included in the article/supplementary material. Further inquiries can be directed to the corresponding author.

Ethics statement

The studies involving human participants were reviewed and approved by Ethics Committee of the Third Hospital of Hebei Medical University. The patients/participants provided their written informed consent to participate in this study.

Author contributions

JL and YiW participated in manuscript drafting, study design, and statistical analyses. XZ and JL participated in MRI data acquisition. YS and PZ participated in writing (review and editing). LB and YaW participated in QCT measurements. MW and JZ participated in study design and manuscript revisions. All authors contributed to the article and approved the submitted version.

Conflict of interest

The authors declare that the research was conducted in the absence of any commercial or financial relationships that could be construed as a potential conflict of interest.

Publisher's note

References

1. Lang TF. The bone-muscle relationship in men and women. *J Osteoporos* (2011) 2011:702735. doi: 10.4061/2011/702735

2. Herrmann M, Engelke K, Ebert R, Müller-Deubert S, Rudert M, Ziouti F, et al. Interactions between muscle and bone-where physics meets biology. *Biomolecules* (2020) 10:432. doi: 10.3390/biom10030432

3. He H, Liu Y, Tian Q, Papasian CJ, Hu T, Deng HW. Relationship of sarcopenia and body composition with osteoporosis. *Osteoporos Int* (2016) 27:473–82. doi: 10.1007/s00198-015-3241-8

4. Verschueren S, Gielen E, O'Neill TW, Pye SR, Adams JE, Ward KA, et al. Sarcopenia and its relationship with bone mineral density in middle-aged and elderly European men. *Osteoporos Int* (2013) 24:87–98. doi: 10.1007/s00198-012-2057-z

5. Demontiero O, Boersma D, Suriyaarachchi P, Duque G. Clinical outcomes of impaired muscle and bone interactions. *Clin Rev Bone Miner Metab* (2014) 12:86–92. doi: 10.1007/s12018-014-9164-7

6. Burr DB. Muscle strength, bone mass, and age-related bone loss. *J Bone Miner Res* (1997) 12:1547–51. doi: 10.1359/jbmr.1997.12.10.1547

7. Sjoblom S, Suuronen J, Rikkonen T, Honkanen R, Kroger H, Sirola J. Relationship between postmenopausal osteoporosis and the components of clinical sarcopenia. *Maturitas* (2013) 75:175–80. doi: 10.1016/j.maturitas.2013.03.016

8. Maugeri D, Russo MS, Franzé C, Motta V, Motta M, Destro G, et al. Correlations between c-reactive protein, interleukin-6, tumor necrosis factor-alpha and body mass index during senile osteoporosis. *Arch Gerontol Geriatr* (1998) 27:159–63. doi: 10.1016/s0167-4943(98)00110-1

9. Ng A, Duque G. Osteoporosis as a lipotoxic disease. *Bonekey Osteovision* (2010) 7:108–23. doi: 10.1138/20100435

10. Burge R, Dawson-Hughes B, Solomon DH, Wong JB, King A, Tosteson A. Incidence and economic burden of osteoporosis-related fractures in the united states, 2005-2025. *J Bone Miner Res* (2007) 22:465–75. doi: 10.1359/jbmr.061113

11. Becker DJ, Kilgore ML, Morrisey MA. The societal burden of osteoporosis. *Curr Rheumatol Rep* (2010) 12:186–91. doi: 10.1007/s11926-010-0097-y

12. Kumar D, Link TM, Jafarzadeh SR, LaValley MP, Majumdar S, Souza RB. Association of quadriceps adiposity with an increase in knee cartilage, meniscus, or bone marrow lesions over three years. *Arthritis Care Res (Hoboken)* (2021) 73:1134–9. doi: 10.1002/acr.24232

13. Zhao Y, Huang M, Serrano Sosa M, Cattell R, Fan W, Li M, et al. Fatty infiltration of paraspinal muscles is associated with bone mineral density of the lumbar spine. *Arch Osteoporos* (2019) 14:99. doi: 10.1007/s11657-019-0639-5

14. Yoo HJ, Hong SH, Kim DH, Choi JY, Chae HD, Jeong BM, et al. Measurement of fat content in vertebral marrow using a modified dixon sequence to differentiate benign from malignant processes. *J Magn Reson Imaging* (2017) 45:1534–44. doi: 10.1002/jmri.25496

15. Liu Y, Wang L, Su Y, Brown K, Yang R, Zhang Y, et al. CTXA hip: the effect of partial volume correction on volumetric bone mineral density data for cortical and trabecular bone. *Arch Osteoporos* (2020) 15:50. doi: 10.1007/s11657-020-00721-8

16. Cheng X, Wang L, Wang Q, Ma Y, Su Y, Li K. Validation of quantitative computed tomography-derived areal bone mineral density with dual energy X-ray absorptiometry in an elderly Chinese population. *Chin Med J (Engl)* (2014) 127:1445–9.

17. Khoo BCC, Brown K, Cann C, Zhu K, Henzell S, Low V, et al. Comparison of QCT-derived and DXA-derived areal bone mineral density and T scores. *Osteoporos Int* (2009) 20:1539–45. doi: 10.1007/s00198-008-0820-y

18. Hamrick MW, McGee-Lawrence ME, Frechette DM. Fatty infiltration of skeletal muscle: mechanisms and comparisons with bone marrow adiposity. *Front Endocrinol (Lausanne)* (2016) 7:69. doi: 10.3389/fendo.2016.00069

19. Karampinos DC, Baum T, Nardo L, Alizai H, Yu H, Carballido-Gamio J, et al. Characterization of the regional distribution of skeletal muscle adipose tissue in type 2 diabetes using chemical shift-based water/fat separation. *J Magn Reson Imaging* (2012) 35:899–907. doi: 10.1002/jmri.23512

20. Yamauchi K, Kato C, Kato T. Characteristics of individual thigh muscles including cross-sectional area and adipose tissue content measured by magnetic resonance imaging in knee osteoarthritis: a cross-sectional study. *Rheumatol Int* (2019) 39:679–87. doi: 10.1007/s00296-019-04247-2

21. Cotofana S, Hudelmaier M, Wirth W, Himmer M, Ring-Dimitriou W, Sänger AM, et al. Correlation between single-slice muscle anatomical cross-sectional area and muscle volume in thigh extensors, flexors and adductors of perimenopausal women. *Eur J Appl Physiol* (2010) 110:91–7. doi: 10.1007/s00421-010-1477-8

22. Yamauchi K, Yoshiko A, Suzuki S, Kato C, Akima H, Kato T, et al. Muscle atrophy and recovery of individual thigh muscles as measured by magnetic resonance imaging scan during treatment with cast for ankle or foot fracture. *J Orthop Surg (Hong Kong)* (2017) 25:2309499017739765. doi: 10.1177/2309499017739765

23. Yamauchi K, Suzuki S, Kato C, Kato T. Atrophy of individual thigh muscles measured by MRI in older adults with knee osteoarthritis: A cross-sectional study. *Ann Phys Rehabil Med* (2020) 63:38–45. doi: 10.1016/j.rehab.2019.06.018

24. Carpenter RD, Sigurdsson S, Zhao S, Lu Y, Eiriksdottir G, Sigurdsson G, et al. Effects of age and sex on the strength and cortical thickness of the femoral neck. *Bone* (2011) 48:741–7. doi: 10.1016/j.bone.2010.12.004

25. Engelke K. Quantitative computed tomography-current status and new developments. *J Clin Densitom* (2017) 20:309–21. doi: 10.1016/j.jocd.2017.06.017

26. Bouxsein ML, Szulc P, Munoz F, Thrall E, Sornay-Rendu E, Delmas PD. Contribution of trochanteric soft tissues to fall force estimates, the factor of risk, and prediction of hip fracture risk. *J Bone Miner Res* (2007) 22:825–31. doi: 10.1359/jbmr.070309

27. Nielson CM, Bouxsein ML, Freitas SS, Ensrud KE, Orwoll ES. Trochanteric soft tissue thickness and hip fracture in older men. *J Clin Endocrinol Metab* (2009) 94:491–6. doi: 10.1210/jc.2008-1640

28. Dufour AB, Roberts B, Broe KE, Kiel DP, Bouxsein ML, Hannan MT. The factor-of-risk biomechanical approach predicts hip fracture in men and women: the framingham study. *Osteoporos Int* (2012) 23:513–20. doi: 10.1007/s00198-011-1569-2

29. Hoyan L, Yi-Xian Q. The effects of frequency-dependent dynamic muscle stimulation on inhibition of trabecular bone loss in a disuse model. *Bone* (2008) 43:1093–100. doi: 10.1016/j.bone.2008.07.253

30. Wang L, Yin L, Zhao Y, Su Y, Sun W, Chen S, et al. Muscle density, but not size, correlates well with muscle strength and physical performance. *J Am Med Dir Assoc* (2021) 22:751–9. doi: 10.1016/j.jamda.2020.06.052

31. Kumar D, Karampinos DC, MacLeod TD, Lin W, Nardo L, Li X, et al. Quadriceps intramuscular fat fraction rather than muscle size is associated with knee osteoarthritis. *Osteoarthritis Cartilage* (2014) 22(2):226–34. doi: 10.1016/j.joca.2013.12.005

32. Yin L, Xu Z, Wang L, Li W, Zhao Y, Su Y, et al. Associations of muscle size and density with proximal femur bone in a community dwelling older population. *Front Endocrinol (Lausanne)* (2020) 11:503. doi: 10.3389/fendo.2020.00503

33. Rivas DA, McDonald DJ, Rice NP, Haran PH, Dolnikowski GG, Fielding RA. Diminished anabolic signaling response to insulin induced by intramuscular lipid accumulation is associated with inflammation in aging but not obesity. *Am J Physiol Regul Integr Comp Physiol* (2016) 310:R561–9. doi: 10.1152/ajpregu.00198.2015

34. Goodpaster BH, Park SW, Harris TB, Kritchevsky SB, Nevitt M, Schwartz AV, et al. The loss of skeletal muscle strength, mass, and quality in older adults: the health, aging and body composition study. *J Gerontol A Biol Sci Med Sci* (2006) 61:1059–64. doi: 10.1093/gerona/61.10.1059

35. Wang L, Yin L, Zhao Y, Su Y, Sun W, Liu Y, et al. Muscle density discriminates hip fracture better than CTXA hip areal bone mineral density. *J Cachexia Sarcopenia Muscle* (2020) 11:1799–812. doi: 10.1002/jcsm.12616

36. Wang L, Yin L, Yang M, Ge Y, Liu Y, Su Y, et al. Muscle density is an independent risk factor of second hip fracture: a prospective cohort study. *J Cachexia Sarcopenia Muscle* (2022) 13:1927–37. doi: 10.1002/jcsm.12996

37. Cho Y, Lee I, Ha SH, Park JH, Park JH. Comparison of hip subregion bone mineral density to the type of proximal femur fracture. *Arch Osteoporos* (2020) 15(1):122. doi: 10.1007/s11657-020-00789-2

38. Wu CC, Wang CJ, Shyu YI. Variations in bone mineral density of proximal femora of elderly people with hip fractures: a case-control analysis. *J Trauma* (2011) 71:1720–5. doi: 10.1097/TA.0b013e3182185aeb

39. Leenders M, Verdijk LB, van der Hoeven L, van Kranenburg J, Nilwik R, van Loon LJ. Elderly men and women benefit equally from prolonged resistance-type exercise training. *J Gerontol A Biol Sci Med Sci* (2013) 68:769–79. doi: 10.1093/gerona/gls241

40. Hirschfeld HP, Kinsella R, Duque G. Osteosarcopenia: where bone, muscle, and fat collide. *Osteoporos Int* (2017) 28:2781–90. doi: 10.1007/s00198-017-4151-8

41. Johnson MA, Polgar J, Weightman D, Appleton D. Data on the distribution of fibre types in thirty-six human muscles an autopsy study. *J Neurol Sci* (1973) 18:111–29. doi: 10.1016/0022-510x(73)90023-3

42. Gueugneau M, Coudy-Gandilhon C, Théron L, Meunier B, Barboiron C, Combaret L, et al. Skeletal muscle lipid content and oxidative activity in relation to muscle fiber type in aging and metabolic syndrome. *J Gerontol A Biol Sci Med Sci* (2015) 70:566–76. doi: 10.1093/gerona/glu086

43. Terracciano C, Celi M, Lecce D, Baldi J, Rastelli E, Lena E, et al. Differential features of muscle fiber atrophy in osteoporosis and osteoarthritis. *Osteoporos Int* (2013) 24:1095–100. doi: 10.1007/s00198-012-1990-1

44. Perrini S, Laviola L, Carreira MC, Cignarelli A, Natalicchio A, Giorgino F. The GH/IGF1 axis and signaling pathways in the muscle and bone: mechanisms underlying age-related skeletal muscle wasting and osteoporosis. *J Endocrinol* (2010) 205:201–10. doi: 10.1677/JOE-09-0431

frontiers | Frontiers in Endocrinology

TYPE Study Protocol
PUBLISHED 14 November 2022
DOI 10.3389/fendo.2022.1010102

OPEN ACCESS

EDITED BY
Antonino Catalano,
University of Messina, Italy

REVIEWED BY
Luca Soraci,
IRCCS INRCA, Italy
Jakub Antoni Kortas,
Gdansk University of Physical Education and Sport, Poland

*CORRESPONDENCE
Gang Wang
wgnet158@163.com
Ling Wang
doctorwl@bjmu.edu.cn
Liang Lyu
lyuliang0720@hotmail.com

†These authors have contributed equally to this work

SPECIALTY SECTION
This article was submitted to Bone Research, a section of the journal Frontiers in Endocrinology

RECEIVED 02 August 2022
ACCEPTED 24 October 2022
PUBLISHED 14 November 2022

CITATION
Liu X, Ma C, Wang S, Liang Z, Yang J, Zhou J, Shu Y, He Z, Zong J, Wu L, Peng P, Su Y, Gao M, Shen K, Zhao H, Ruan J, Ji S, Yang Y, Tang T, Yang Z, Luo G, Zeng M, Zhang W, He B, Cheng X, Wang G, Wang L and Lyu L (2022) Screening of osteoporosis and sarcopenia in individuals aged 50 years and older at different altitudes in Yunnan province: Protocol of a longitudinal cohort study. *Front. Endocrinol.* 13:1010102. doi: 10.3389/fendo.2022.1010102

Screening of osteoporosis and sarcopenia in individuals aged 50 years and older at different altitudes in Yunnan province: Protocol of a longitudinal cohort study

Xingli Liu[1,2,3,4], Cunwen Ma[5], Shiping Wang[6], Zhengrong Liang[7], Juntao Yang[8], Jun Zhou[9], Yi Shu[10], Zhengying He[11], Jilong Zong[12], Lizhi Wu[13], Peiqian Peng[14], Yi Su[15], Meng Gao[3,4], Kaiming Shen[5], Hong Zhao[6], Jilu Ruan[7], Shaoxuan Ji[8], Yunhui Yang[9], Taisong Tang[10], Zongfa Yang[11], Guangyin Luo[12], Meng Zeng[13], Weiwan Zhang[14], Bo He[16], Xiaoguang Cheng[17], Gang Wang[3,4*†], Ling Wang[17*†] and Liang Lyu[1,2,3,4*†]

[1]Faculty of Life science and Technology, Kunming University of Science and Technology, Kunming, China, [2]Medical School, Kunming University of Science and Technology, Kunming, China, [3]Department of Radiology, The First People's Hospital of Yunnan Province, Kunming, Yunnan, China, [4]Department of Radiology, The Affiliated Hospital of Kunming University of Science and Technology, Kunming, China, [5]Department of Radiology, The People's Hospital of Wenshan Prefecture, Wenshan, China, [6]Department of Radiology, Anning First people's Hospital, Kunming University of Science and Technology, Anning, China, [7]Department of Radiology, Qujing Second People's Hospital of Yunnan Province, Qujing, China, [8]Department of Radiology, Dali Bai Autonomous Prefecture People's Hospital, Dali, China, [9]Department of Radiology, Xishuangbanna Dai Autonomous Prefecture People's Hospital, Jinghong, China, [10]Department of Radiology, Southern Central Hospital of Yunnan Province, Honghe, China, [11]Department of Radiology, Diqing Tibetan Autonomous Prefecture People's Hospital, Xianggelila, China, [12]Department of Radiology, The First People's Hospital of Zhaotong, Zhaotong, China, [13]Department of Radiology, Hekou People's Hospital, Honghe, China, [14]Department of Radiology, Nujiang People's Hospital, Nujiang, China, [15]Key Laboratory of Molecular Epidemiology of Hunan Province, School of Medicine, Hunan Normal University, Changsha, China, [16]Department of Radiology, The First Affiliated Hospital of Kunming Medical University, Kunming, China, [17]Department of Radiology, Beijing Jishuitan Hospital, Beijing, China

Introduction: Musculoskeletal system gradually degenerates with aging, and a hypoxia environment at a high altitude may accelerate this process. However, the comprehensive effects of high-altitude environments on bones and muscles remain unclear. This study aims to compare the differences in bones and muscles at different altitudes, and to explore the mechanism and influencing factors of the high-altitude environment on the skeletal muscle system.

Methods: This is a prospective, multicenter, cohort study, which will recruit a total of 4000 participants over 50 years from 12 research centers with different

altitudes (50m~3500m). The study will consist of a baseline assessment and a 5-year follow-up. Participants will undergo assessments of demographic information, anthropomorphic measures, self-reported questionnaires, handgrip muscle strength assessment (HGS), short physical performance battery (SPPB), blood sample analysis, and imaging assessments (QCT and/or DXA, US) within a time frame of 3 days after inclusion. A 5-year follow-up will be conducted to evaluate the changes in muscle size, density, and fat infiltration in different muscles; the muscle function impairment; the decrease in BMD; and the osteoporotic fracture incidence. Statistical analyses will be used to compare the research results between different altitudes. Multiple linear, logistic regression and classification tree analyses will be conducted to calculate the effects of various factors (e.g., altitude, age, and physical activity) on the skeletal muscle system in a high-altitude environment. Finally, a provisional cut-off point for the diagnosis of sarcopenia in adults at different altitudes will be calculated.

Ethics and dissemination: The study has been approved by the institutional research ethics committee of each study center (main center number: KHLL2021-KY056). Results will be disseminated through scientific conferences and peer-reviewed publications, as well as meetings with stakeholders.

Clinical Trial registration number: http://www.chictr.org.cn/index.aspx, identifier ChiCTR2100052153.

KEYWORDS

osteoporosis, sarcopenia, elderly, altitudes, protocol

Introduction

Osteoporosis has become a public health concern with the rate of aging in the global population increasing (1). Identifying the risk factors for osteoporosis could help prevent the condition's development. Environmental factors (such as altitude, sunlight, and temperature) have been proposed to influence bone mineral density (2). Basu M et al. found proximal phalanx bone impairment in healthy males who migrated from an altitude of 3542m to an extreme altitude (5400–6700m) in India where they stayed for 4 months (3). A Chinese study reported that people living in Tibet have lower spine bone mass compared with people who live at low altitudes (4). An animal experiment also showed that bone mass was significantly and negatively affected by exposure to a high-altitude environment. With the increase in altitude (1850~5450m), negative changes in the morphometric and geometric properties of the femur were observed (5). The loss of bone mass and/or decrease in bone density is the main manifestation of osteoporosis. As expected, several studies based on large sample sizes have found that highlanders have a higher risk of osteoporosis (6) and are more likely to suffer hip fractures (7–9). The above research results may be related to the mechanism that high altitude-induced hypoxia may stimulate the secretion of many hormones that have affected bone mineral metabolisms (3, 10). For example, activities of bone-specific alkaline phosphatase and 25(OH) vitamin D were both found to decrease significantly in the high-altitude area (3). Notably, the relationship between high altitude and bone status is still insufficient. Existing studies are also limited by their designs for certain people and/or small sample sizes. In particular, some studies only included narrow-altitude ranges (about 100~200 m), which restricts effective comparisons between distinct altitudes. This can sometimes lead to conflicting results (9, 11). A reasonable and wider range of elevation comparison design can contribute to explore the effect of hypoxia on bone and reveal the potential effective threshold. So far, no studies have been conducted in China on the prevalence of osteoporosis in the general population in high-altitude areas. More studies, especially longitudinal cohort studies, are essential to investigate the prevalence of osteoporosis and the potential risk factors for bone mass loss in the plateau area.

Hypoxia causes complex angio-adaptive and endocrine adaptations in skeletal muscle, resulting in the growth,

stabilization, or regression of muscle capillaries as well as changes in blood biochemical markers (e.g., significant reductions in plasma leptin and homocysteine, insulin, and C-reactive protein) (12, 13). High-altitude hypoxic environments have been demonstrated to influence a person's body composition (e.g., reductions in body weight, fat-free mass, fat mass, muscle mass, and/or body water) (14–17). Studies have been conducted on the relationship between altitude and muscle or body function, particularly in sports training. Altitude hypoxia training has become a popular means to increase endurance athletes' performance for decades (18–22). What's more, current research indicates that chronic intermittent hypoxic–hyperoxic periods exposure at rest is beneficial for older patients with cardiovascular and metabolic diseases or cognitive impairment to improve physical and cognitive performance and reduce cardiometabolic risk factors (23). Despite much research in this area to date, the results are highly controversial as intraindividual and interindividual variabilities (24, 25). More studies are needed to confirm and extend the evidence.

The loss of muscle mass, strength, and/or physical function is often referred to as sarcopenia, which is closely related to adverse clinical outcomes (15–17). Sarcopenia will have a major impact on the Asian aging population (26). The diagnosis of sarcopenia is also highly variable due to race, measurement methods, and living environments (27, 28). High-altitude hypoxia is considered to be able to facilitate sarcopenia and fat distribution (26, 29, 30). Chinese studies indicated that the incidences of sarcopenia in the high-altitude population (altitude>3500m and altitude at 2260m) were significantly higher than those in the plain population (26, 31). Specific cutoff values established according to altitudes for sarcopenia in the plateau populations seem more reasonable. However, very limited relevant studies are available. The assessment of muscle mass is a crucial element in diagnosing sarcopenia. Bioelectrical impedance analysis (BIA) or dual X-ray absorptiometry (DXA) were the most commonly used methods in the past. Nevertheless, the correlation of muscle mass with muscle strength, and more generically, with muscle function is low, and this discrepancy may be partially related to the presence of fatty infiltration (32, 33). The recent European Working Group on Sarcopenia in Older People recently replaced "low muscle mass" with "low muscle strength" as a primary determinant of sarcopenia (34) implying that muscle mass based on DXA and BIA may not be sufficient in the detection of sarcopenia and that methods with higher sensitivity in sarcopenia screening are warranted. Skeletal muscle area based on segmentation technology and muscle density measured by quantitative computed tomography (QCT) were considered to be more promising in the assessment of sarcopenia (35–37). However, the sarcopenia definition based on CT assessments of muscle size and density is lacking.

The musculoskeletal system operates as a finely coordinated unit, interconnected not only by mechanical aspects but also by humoral factors. Muscle seems to possess the "upper hand" in its relationship with bone (38). Muscle loading induces a range of biomechanical signals necessary for bone growth and remodeling. Also, osteoporosis or fractures will lead to muscle atrophy and muscle mass reduction (38). Indeed, several muscles and bone-derived hormones (e.g., leptin, insulin, GH/IGF-1, myostatin, FGF2, and sexual steroids) are under active investigation to better explain the complex cross-talk and discrete hormonal influences between muscle and bone (38). Therefore, simultaneous assessment of bone and muscle may help gain a more complete picture of disease prevention and treatment in a certain area.

High altitude is generally defined as an altitude higher than 1500m above sea level, which is further classified into three grades: high altitude (1500-3500m); ultra-high altitude (3500-5500m); and very high altitude (>5500 meters) (39). The main environmental stressor associated with high altitude is decreasing atmospheric oxygen pressure. Other environmental stressors include low temperatures, humidity, and increased ultraviolet radiation (40). The impact of altitude on the musculoskeletal system is diverse and contingent upon the altitude in question. Existing studies are limited by their designs for comparison between two altitudes (26, 41). As a result, studies at different altitudes cannot be directly compared. Multi-altitude control studies can comprehensively depict the changes in the musculoskeletal system at different altitudes.

As a province with an altitude fluctuation ranging from less than 100 meters to more than 3,000 meters, Yunnan province has a particular advantage in the study of the effects of altitude on osteoporosis and sarcopenia. This study is a multi-center cohort study in 12 regions where the altitude fluctuations range from 50 to 3500 meters. The primary aims of this study are listed as follows: Firstly, to compare the baseline prevalence of osteoporosis and sarcopenia in the over-50-year-old population at different altitudes and establish a provisional cut-off point based on QCT for the diagnosis of sarcopenia in adults according to altitude. Secondly, the bone and muscle characteristics of people at different altitudes are compared, such as bone density, muscle mass, muscle density, and biological indicators. Thirdly, follow up for 5 years and compare the incidence of adverse events (fall, osteoporosis fracture, death, etc) at different altitudes. The secondary study aims to explore the effect and mechanism of a high-altitude environment on the skeletal muscle system.

Methods and analysis

This longitudinal cohort study aims to investigate the prevalence of osteoporosis and sarcopenia in Yunnan

Province. Multicenter control at different altitudes can give insight into how altitude affects bone and muscle.

Study design

The sarcopenia and osteoporosis study in Yunnan province (SOY study, Trial registration number: ChiCTR2100052153) is a multicenter, prospective, cohort study. The study protocol consists of three main steps: recruitment, a baseline visit, and five years follow-up visit (Figure1).

Recruitment strategy

The enrolment of potential subjects is assessed by investigators at each clinical center according to the inclusion and exclusion criteria. Each subject will sign an informed consent form before officially entering the study. The subjects of the SOY study are enrolled in 12 centers at different altitudes (Figure 2). The inclusion criteria are that participants should be aged over 50 years old and living at the research site for more than 10 years. Exclusion criteria were as follows: a. Inability to stand or walk independently; b. Deformity of the lumbar spine and hip joint; c. Tumors treated with radiotherapy or chemotherapy; d. Patients with metallic implants *in vivo*; e. Other serious or life-threatening diseases (e.g. severe stroke). Recruitment will start in August 2022 except for the main study center the First People's Hospital of Yunnan Province in which recruitment started in April 2021. Baseline visits and follow-up details are shown in Table 1.

Ethical approval for the cohort study is obtained from the ethics committee of each study center [Main study center-The First People's Hospital of Yunnan Province No. KHLL2021-KY056]. The study is conducted by ethical principles according to the Declaration of Helsinki. Radiation safety and protection measures are strictly implemented throughout the study. Informed consent is obtained from each participant at the nearest participating imaging center.

The estimation of sample size

The sample size necessary for this study is set at 4000. The overall prevalence of osteoporosis at the femoral neck in adults aged above 50 years was reported to be 16%, or even up to 30% in postmenopausal women (29, 42). The overall prevalence of sarcopenia was reported to range from 5.5% to 25.7% (30). Thus, the number of 4000 is set to get the estimated overall prevalence of osteoporosis to be within 5% of the prevalence in the real world and considering the attrition rate of about 10%. This number is also needed to detect a significant difference (at least 5%) in prevalence proportions between the highest level of altitude and the lowest one. This number is also needed to detect significant results from the prospective cohort (survival analysis) with a two-tailed level of significance of 5% and statistical power of 80% when a risk factor for osteoporotic fracture is assumed to exist in 20% of participants at baseline and to increase a background fracture risk of 6% by 50% during the 5-year follow-up period. The SPSS 26.0 software (IBM, Armonk,

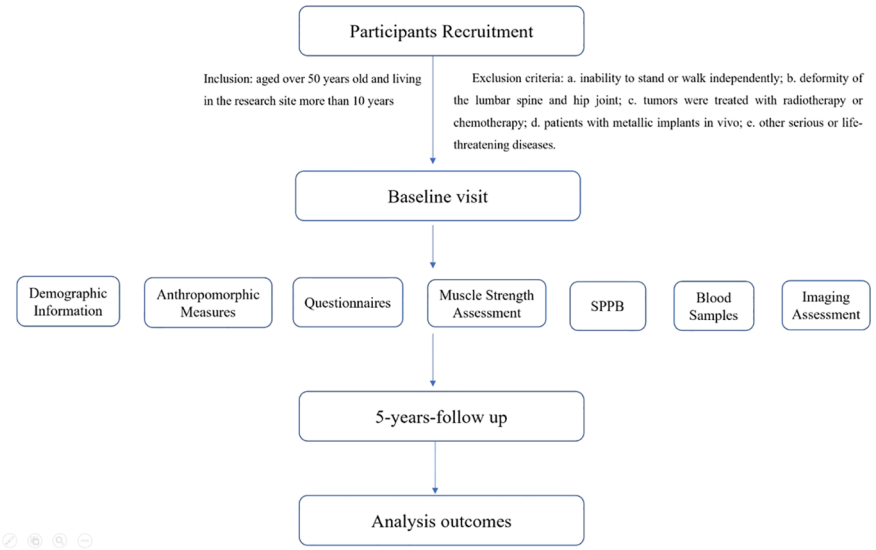

FIGURE 1
Flow chart of study design and procedures. SPPB, short physical performance battery. The analysis outcomes included: the changes in muscle size, density, and fat infiltration in different muscles, the decrease in BMD, the muscle function impairment, and the osteoporotic fracture incidence during a five-year follow-up period.

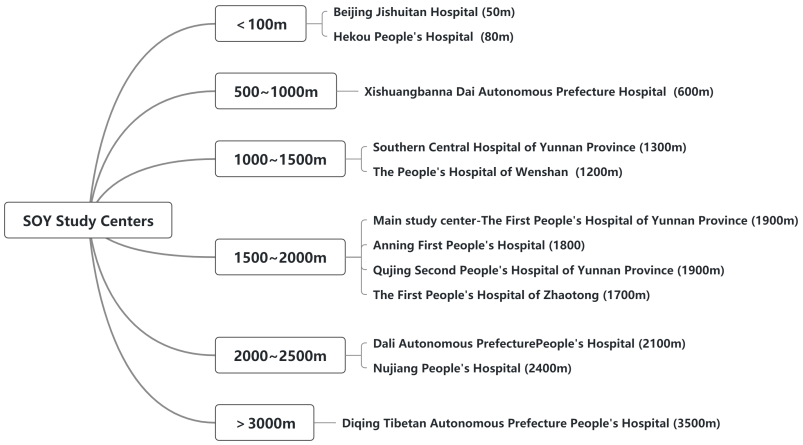

FIGURE 2
Recruitment centers and specific altitude.

TABLE 1 Items and procedures of the study at baseline and each follow-up.

	Baseline	1 year ± 30 days	2 years ± 30 days	3 years ± 30 days	4 years ± 30 days	5 years ± 30 days
Informed consent	X	–	–	–	–	–
Questionnaire survey	X	X	X	X	X	X
Muscle strength assessment (HGS)	X	X	X	X	X	X
Short physical performance battery (SPPB)	X	X	X	X	X	X
QCT scan	X	X	X	X	X	X
DXA scan	X*	X*	X*	X*	–	X*
Ultrasonic	X*	X*	X*	X*	–	X*
Blood collection	X*	X*	X*	X*	X*	X*

X, an item that will be collected.
X*, item that will be selectively carried out in viable centers.
-, item that will not be collected.

NY, United States) will be chosen. The level of significance desired for this study is α=0.05, with a power level of β=0.2.

Baseline visit

The demographic information, anthropomorphic measures, questionnaires, muscle strength assessment, short physical performance battery (SPPB), collection of blood samples, and imaging assessments (QCT and/or DXA, US) are scheduled to be conducted on each participant.

Detailed demographic measures include age, biological age calculated based on somatic variables (43), gender, ethnicity, residence, education, occupational status, daily physical questionnaire (IPAQ), eating habits (e.g. tea intake, vegans, red meat/white meat intake/both), fall risk screening, fracture history (time/frequency/fracture site), alcohol intake, smoking history, medical history (calcium/vitamin D/hormone), menopausal age, fall history (time, frequency, location), disease history (rheumatoid arthritis/secondary osteoporosis).

Anthropomorphic measures consist of height, weight, waist, and maximum calf circumference. The SARC-F questionnaire will be used to predict potential persons with sarcopenia at risk for poor functional outcomes (described below Table 2).

Muscle strength assessment with HGS. HGS of the dominant hand will be measured using a Jamar dynamometer (Jamar, Los Angeles, CA), two attempts with a 30-second interval between them were recorded in kilograms, and the maximum value will be chosen for further analysis.

A short physical performance battery (SPPB) includes a 4m gait speed (GS), a five-times repeated chair sit-to-stand (STS) and a balance test (semi-tandem, full-tandem, and single-leg stand time) will be recorded.

TABLE 2 SARC-F questionnaire.

Component	Question	Score
Strength	How much difficulty do you have in lifting and carrying 10 pounds?	one = 0 Some = 1 A lot or unable = 2
Assistance in walking	How much difficulty do you have walking across a room?	None = 0 Some = 1 A lot, use aids, or unable = 2
Rise from a chair	How much difficulty do you have transferring from a chair or bed?	None = 0 Some = 1 A lot or unable without help = 2
Climb stairs	How much difficulty do you have climbing a flight of 10 stairs?	None = 0 Some = 1 A lot or unable = 2
Falls	How many times have you fallen in the past year?	None = 0 1-3 falls = 1 4 or more falls = 2

Blood sample collection is mainly for laboratory examination, such as hepatic and renal function, 25(OH)D, BGP, PTH, Calcium, biochemical markers of bone turnover, biochemical markers of bone metabolism, leptin, insulin, GH/IGF-1, myostatin, FGF2, and sex steroids.

Imaging assessments include abdomen quantitative computed tomography (QCT), dual-energy X-ray absorptiometry (DXA), and appendicular limb ultrasound. Evaluation indicators include muscle density, muscle size, intermuscular fat size, BMD (measured by QCT and/or DXA), and whole-body composition analysis. The trunk muscle, gluteus muscle, and appendicular limb muscle are the object muscles being evaluated. The BMD values (mg/cm^3) of the L1 and L2 vertebral bodies are measured according to the QCT protocol (44) (Figure 3). The spinal vBMD was represented by the average vBMD value of L1–L2. In each subject, abdominal CT scans with a Mindways calibrated QCT acquisition phantom (Mindways Software Inc, Austin, TX, USA). For cross-calibration, a single European Spine Phantom (ESP-122) will be scanned at all centers before scanning the subjects.

Notably, QCT is a required item for all research centers.

Follow-up visit

A 5-year follow-up will be conducted to evaluate the changes in muscle size, density, and fat infiltration in different muscles, the decrease of BMD, muscle function impairment, and osteoporotic fracture incidence. Details of the assessments of the follow-up visits are shown in Table 1.

The diagnosis criteria of osteoporosis

The diagnostic criteria of osteoporosis for QCT, recommended by the International Society for Clinical Densitometry in 2007 (45) and the American College of Radiology in 2008 (46), are used to classify the subjects as normal if average vBMD >120 mg/cm^3, osteopenia if vBMD between 120 and 80 mg/cm^3, and osteoporosis if vBMD <80 mg/cm^3.

The diagnosis criteria of sarcopenia

According to the 2019 consensus update on sarcopenia diagnosis and treatment of the Asian working group for sarcopenia (AWGS 2019), the new diagnosis of sarcopenia was low muscle mass accompanied by low muscle strength or low physical performance. AWGS 2019 also defines persons with low muscle mass, low muscle strength, and low physical performance as having "severe sarcopenia" (30).

The specified cutoffs for each diagnostic component were as followed: low muscle strength was defined as handgrip strength < 28 kg for men and <18 kg for women; criteria for low physical performance were 6-m walk<1.0 m/s, short physical performance battery(SPPB) score ≤ 9, or 5-time chair stand test ≤ 12 seconds. Muscle mass assessment was retained the original cutoffs for height-adjusted: dual-energy X-ray absorptiometry<7.0 kg/m^2 in men and <5.4 kg/m^2 in women; and bioimpedance<7.0 kg/m^2 in men and <5.7 kg/m^2 in women.

Data management

All data will be transferred to the First People's Hospital of Yunnan Province for analysis and quality control. The study data will be collected and managed in a database created using Epidata 3.1. Through this database, all questionnaire contents can be digitized to prepare for further classification, comparison, and statistical analysis, such as activity, diet habits, medication history, etc. All muscle function evaluations, imaging scans, and

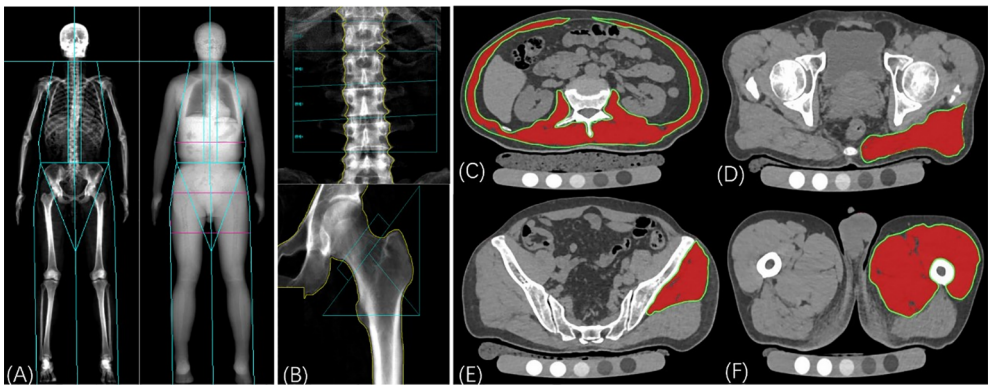

FIGURE 3
Dual-energy X-ray absorptiometry (DXA) and computed tomography (CT) assessments. **(A)**: the whole body DXA scan for body composition analysis, mainly for the evaluation of muscle and fat mass. **(B)**: Areal BMD was calculated by the DXA scan of the lumbar spine and left hip. **(C)**~**(F)**: Muscle assessments with QCT including muscle density, muscle area, and intermuscular fat area. **(C)**: Measurement of trunk muscle at mid-L2 level; **(D)**: Measurement of cross-sectional area and mean computed tomography values of the gluteus maximus muscle at the level of the greater trochanter of the femur; **(E)**: Measurement of the gluteus medius and minimus muscle at the third sacral level; **(F)**: Measurement of the middle thigh muscle level. The muscle region is represented by the area highlighted in red. The area of intramuscular fat infiltration is obtained by subtracting the area of red ROI from the area of green ROI with the threshold segmentation method.

measurements were performed according to the unified standards of the study. All investigators taking care of data collection will be trained before the project begins.

Statistical analysis

Baseline cross-sectional analysis between sarcopenia/osteoporosis and altitude will be conducted, including the prevalence, imaging parameters, SPPB, and blood sample indexes of skeletal muscle. The 5-year follow-up data will focus on comparing the rate of skeletal muscle degradation at different altitudes and the incidence of adverse events such as falls and fractures during the follow-up period. One-way ANOVA will be used to compare the research results between different altitudes. Multiple linear and logistic regression analyses were conducted to calculate the effects of various factors (e.g., altitude, age, and physical activity) on the skeletal muscle system in a high-altitude environment. Cox proportional hazards models were used to calculate the strength of BMD, muscle density, and muscle mass to predict the risk of major osteoporotic fractures. Provisional cutoff points based on QCT were defined for the variables used to screen for sarcopenia or osteoporosis using the 20th percentile of their population distributions.

Discussion

Osteoporosis and sarcopenia are highly prevalent in older adults. Studies have shown that osteoporosis and hip fractures are more common in high-altitude areas. However, the extent to which altitude affects bones, or how, is not yet clear. There are few studies on muscle at high altitudes, and the results are inconsistent at different study altitudes. So, it is necessary to make a systematic comparison at multiple altitudes. What's more, the current diagnostic criteria for osteoporosis are relatively well-established, but there are still many uncertainties about the diagnostic criteria for sarcopenia. Many researchers are trying to propose more suitable diagnostic criteria for sarcopenia (47, 48). But so far, there is no specific diagnostic cut-off value for sarcopenia for residents at high altitudes.

To the best of our knowledge, this is the first multicenter cohort study with multiple altitude levels. The 5-year follow-up study design enables us to compare the changes of bone and muscle not only horizontally in time, but also longitudinally at different altitudes. This makes it possible to better describe the relationship between the skeletal muscle system and altitude environment, then put forward a more objective and reasonable explanation for the situation in which existing research results are inconsistent or even opposite due to different study altitudes (26, 41).

As far as we know, this is also the first study to assess bone and muscle at multiple altitudes simultaneously. Analysis of musculoskeletal interactions can provide valuable information about how the altitude environment affects the body.

In conclusion, this study will make an important contribution to the understanding of the health status of bone and muscle at different altitudes in Yunnan. The relationship between the musculoskeletal system and altitude can be more comprehensively discussed because of the availability of multiple altitude data sets. The study will provide essential data for developing individualized diagnostic criteria for sarcopenia in

Yunnan and help to establish altitude-specific intervention and treatment strategies.

Strengths and limitations of this study

The strengths of this study were listed as follows: Firstly, this is the first multicenter cohort study about bone and muscle characteristics of adults at different altitudes and would provide valuable reference data for adults aged over 50 years in plateau areas.

Secondly, the 5-year follow-up design provides longitudinal comparative data. Detailed changes and potential relationships in bone mass and muscle characteristics of older adults in high-altitude hypoxia environments can be dynamically recorded for further analysis. QCT and/or DXA measurements can provide more accurate assessment means of osteoporosis and sarcopenia diagnosis.

By the way, the limitations of this study are deserving of attention. Firstly, there is potential for high dropout rates of older adult participants due to physical decline or death. Secondly, external validation is lacking in this study.

Ethics statement

The studies involving human participants were reviewed and approved by The First People's Hospital of Yunnan Province KHLL2021-KY056. The patients/participants provided their written informed consent to participate in this study.

Author contributions

GW, LW, LL: Conceptualization; Project administration; Funding acquisition; Supervision, Writing - Review & Editing. XL: Data Curation; Data analysis; Writing - Original Draft; Supervision, investigators training. CM, SW, ZL, JY, JuZ, YSh, ZH, JiZ, LZW, PP, MG, KS, HZ, JR, SJ, YY, TT, ZY, GL, MZ, WZ, XC, BH: Subject recruitment; Research data collection and recording. YS: Sample size calculation, statistical analysis. All authors contributed to the article and approved the submitted version.

Funding

This work was supported by the national natural science foundation of China [grant number:81901718, 81771831]; Beijing hospitals authority youth program [grant number: qml20200402]; The Beijing hospitals authority clinical medicine development of special funding support [grant number: zylx202107]; Yunnan "ten thousand people plan" famous doctor special project [grant number: ynwr-my-2019-011] and The Clinical Medical Center Open Project of the first people's hospital of Yunnan province [grant number:2022YJZX-LN10, 2022LCZXKF-HX06].

Conflict of interest

The authors declare that the research was conducted in the absence of any commercial or financial relationships that could be construed as a potential conflict of interest.

Publisher's note

References

1. Grewe JM, Knapstein PR, Donat A, Jiang S, Smit DJ, Xie W, et al. The role of sphingosine-1-phosphate in bone remodeling and osteoporosis. *Bone Res* (2022) 10:34. doi: 10.1038/s41413-022-00205-0

2. Camacho-Cardenosa M, Camacho-Cardenosa A, Timón R, Olcina G, Tomas-Carus P, Brazo-Sayavera J. Can hypoxic conditioning improve bone metabolism? A systematic review. *Int J Environ Res Public Health* (2019) 16:1799–819 doi: 10.3390/ijerph16101799

3. Basu M, Malhotra AS, Pal K, Chatterjee T, Ghosh D, Haldar K, et al. Determination of bone mass using multisite quantitative ultrasound and biochemical markers of bone turnover during residency at extreme altitude: A longitudinal study. *High Alt Med Biol* (2013) 14:150–4. doi: 10.1089/ham.2012.1042

4. Zhou L, Song J, Yang S, Meng S, Lv X, Yue J, et al. Bone mass loss is associated with systolic blood pressure in postmenopausal women with type 2 diabetes in Tibet: A retrospective cross-sectional study. *Osteopor Int* (2017) 28:1693–8. doi: 10.1007/s00198-017-3930-6

5. Bozzini C, Champin GM, Alippi RM, Bozzini CE. Static biomechanics in bone from growing rats exposed chronically to simulated high altitudes. *High alt Med Biol* (2013) 14:367–74. doi: 10.1089/ham.2013.1038

6. Ranhotra HS, Sharma R. Moderately high altitude habitation modulates lipid profile and alkaline phosphatase activity in aged khasis of meghalaya. *Indian J Clin Biochem* (2010) 25:51–6. doi: 10.1007/s12291-010-0011-4

7. Nilson F, Moniruzzaman S, Andersson R. A comparison of hip fracture incidence rates among older adults in Sweden by latitude and sunlight exposure. *Scand J Public Health* (2014) 42:201–6. doi: 10.1177/1403494813510794

8. Gong XF, Li XP, Zhang LX, Center JR, Bliuc D, Shi Y, et al. Current status and distribution of hip fractures among older adults in China. *Osteopor Int* (2021) 32:1785–93. doi: 10.1007/s00198-021-05849-y

9. Dahl C, Madsen C, Omsland TK, Søgaard AJ, Tell GS, Holvik K, et al. Contribution of elevation and residential proximity to the coast in explaining geographic variations in hip fracture incidence. A Norwegian epidemiologic

osteoporosis studies (NOREPOS) study. *Osteopor Int* (2021) 32:1001–6. doi: 10.1007/s00198-020-05736-y

10. Muzylak M, Price JS, Horton MA. Hypoxia induces giant osteoclast formation and extensive bone resorption in the cat. *Calcif Tissue Int* (2006) 79:301–9. doi: 10.1007/s00223-006-0082-7

11. Takeda M, Hamano T, Kohno K, Yano S, Shiwaku K, Nabiki T. Association between geographic elevation, bone status, and exercise habits: The shimane CoHRE study. *Int J Environ Res Public Health* (2015) 12:7392–9. doi: 10.3390/ijerph120707392

12. Bosco G, Paoli A, Rizzato A, Marcolin G, Guagnano MT, Doria C, et al. Body composition and endocrine adaptations to high-altitude trekking in the Himalayas. *Adv Exp Med Biol* (2019) 1211:61–8. doi: 10.1007/5584_2019_414

13. Lemieux P, Birot O. Altitude, exercise, and skeletal muscle angio-adaptive responses to hypoxia: A complex story. *Front Physiol* (2021) 12:735557. doi: 10.3389/fphys.2021.735557

14. Wen X, An P, Chen WC, Lv Y, Fu Q. Comparisons of sarcopenia prevalence based on different diagnostic criteria in Chinese older adults. *J Nutr Health Aging* (2015) 19:342–7. doi: 10.1007/s12603-014-0561-x

15. Chen LK, Liu LK, Woo J, Assantachai P, Auyeung TW, Bahyah KS, et al. Sarcopenia in Asia: Consensus report of the Asian working group for sarcopenia. *J Am Med Dir Assoc* (2014) 15:95–101. doi: 10.1016/j.jamda.2013.11.025

16. Buckinx F, Landi F, Cesari M, Fielding RA, Visser M, Engelke K, et al. Pitfalls in the measurement of muscle mass: A need for a reference standard. *J Cachexia Sarcopenia Muscle* (2018) 9:269–78. doi: 10.1002/jcsm.12268

17. Hamad N, Travis SP. Weight loss at high altitude: pathophysiology and practical implications. *Eur J Gastroenterol Hepatol* (2006) 18:5–10. doi: 10.1097/00042737-200601000-00002

18. Strzała M, Ostrowski A, Szyguła Z. Altitude training and its influence on physical endurance in swimmers. *J Hum kinet* (2011) 28:91–105. doi: 10.2478/v10078-011-0026-9

19. Sanchez AMJ, Borrani F. Effects of intermittent hypoxic training performed at high hypoxia level on exercise performance in highly trained runners. *J Sports Sci* (2018) 36:2045–52. doi: 10.1080/02640414.2018.1434747

20. Sharma AP, Saunders PU, Garvican-Lewis LA, Clark B, Welvaert M, Gore CJ, et al. Improved performance in national-level runners with increased training load at 1600 and 1800 m. *Int J sport Physiol* (2019) 14:286–95. doi: 10.1123/ijspp.2018-0104

21. Malgoyre A, Prola A, Meunier A, Chapot R, Serrurier B, Koulmann N, et al. Endurance is improved in female rats after living high-training high despite alterations in skeletal muscle. *Front Sports Act Living* (2021) 3:663857. doi: 10.3389/fspor.2021.663857

22. Flaherty G, O'Connor R, Johnston N. Altitude training for elite endurance athletes: A review for the travel medicine practitioner. *Travel Med Infect Dis* (2016) 14:200–11. doi: 10.1016/j.tmaid.2016.03.015

23. Behrendt T, Bielitzki R, Behrens M, Herold F, Schega L. Effects of intermittent hypoxia-hyperoxia on performance- and health-related outcomes in humans: A systematic review. *Sports Med Open* (2022) 8:70. doi: 10.1186/s40798-022-00450-x

24. Millet GP, Brocherie F. Hypoxic training is beneficial in elite athletes. *Med Sci Sport exer* (2020) 52:515–8. doi: 10.1249/MSS.0000000000002142

25. Siebenmann C, Dempsey JA. Hypoxic training is not beneficial in elite athletes. *Med Sci sport exer* (2020) 52:519–22. doi: 10.1249/MSS.0000000000002141

26. Ye L, Wen Y, Chen Y, Yao J, Li X, Liu Y, et al. Diagnostic reference values for sarcopenia in tibetans in China. *Sci Rep* (2020) 10:3067. doi: 10.1038/s41598-020-60027-0

27. Seo Y, Kim M, Shin H, Won C. Perceived neighborhood environment associated with sarcopenia in urban-dwelling older adults: The kor ean frailty and aging cohort study (KFACS). *Int J Environ Res Public Health* (2021) 18:6292–307. doi: 10.3390/ijerph18126292

28. Mazocco L, Gonzalez MC, Barbosa-Silva TG, Chagas P. Sarcopenia in Brazilian rural and urban older adults women: Is there any difference? *Nutrition* (2019) 58:120–4. doi: 10.1016/j.nut.2018.06.017

29. Kanis JA, McCloskey EV, Johansson H, Oden A, Melton LJ, Khaltaev N. A reference standard for the description of osteoporosis. *Bone* (2008) 42:467–75. doi: 10.1016/j.bone.2007.11.001

30. Chen LK, Woo J, Assantachai P, Auyeung TW, Chou MY, Iijima K, et al. Asian Working group for sarcopenia: 2019 consensus update on sarcopenia diagnosis and treatment. *J Am Med Dir Assoc* (2020) 21:300–7.e2. doi: 10.1016/j.jamda.2019.12.012

31. Pan SQ, Li YM, Li XF, Xiong R. Sarcopenia in geriatric patients from the plateau region of qinghai-Tibet: A cross-sectional study. *World J Clin cases* (2021) 9:5092–101. doi: 10.12998/wjcc.v9.i19.5092

32. Goodpaster BH, Park SW, Harris TB, Kritchevsky SB, Nevitt M, Schwartz AV, et al. The loss of skeletal muscle strength, mass, and quality in older adults: The health, aging, and body composition study. *J Gerontol A Biol Sci Med Sci* (2006) 61:1059–64. doi: 10.1093/gerona/61.10.1059

33. Hughes VA, Frontera WR, Wood M, Evans WJ, Dallal GE, Roubenoff R, et al. Longitudinal muscle strength changes in older adults: Influence of muscle mass, physical activity, and health. *J Gerontol A Biol Sci Med Sci* (2001) 56:B209–17. doi: 10.1093/gerona/56.5.b209

34. Cruz-Jentoft AJ, Bahat G, Bauer J, Boirie Y, Bruyere O, Cederholm T, et al. Sarcopenia: revised European consensus on definition and diagnosis. *Age Ageing* (2019) 48:601. doi: 10.1093/ageing/afy169

35. Engelke K, Museyko O, Wang L, Laredo JD. Quantitative analysis of skeletal muscle by computed tomography imaging-state of the art. *J Orthop Translat* (2018) 15:91–103. doi: 10.1016/j.jot.2018.10.004

36. Wang L, Yin L, Zhao Y, Su Y, Sun W, Chen S, et al. Muscle density, but not size, correlates well with muscle strength and physical performance. *J Am Med Dir Assoc* (2021) 22:751–9.e2. doi: 10.1016/j.jamda.2020.06.052

37. Wang L, Yin L, Yang M, Ge Y, Liu Y, Su Y, et al. Muscle density is an independent risk factor of second hip fracture: A prospective cohort study. *J Cachexia Sarcopenia Muscle* (2022) 13(3):1927–37. doi: 10.1002/jcsm.12996

38. Girgis CM. Integrated therapies for osteoporosis and sarcopenia: from signaling pathways to clinical trials. *Calcified Tissue Int* (2015) 96:243–55. doi: 10.1007/s00223-015-9956-x

39. Baniya S, Holden C, Basnyat B. Reentry high altitude pulmonary edema in the Himalayas. *High Alt Med Biol* (2017) 18:425–7. doi: 10.1089/ham.2017.0088

40. Savioli G, Ceresa IF, Gori G, Fumoso F, Gri N, Floris V, et al. Pathophysiology and therapy of high-altitude sickness: Practical approach in emergency and critical care. *J Clin Med* (2022) 11. doi: 10.3390/jcm11143937

41. Liu X, Wang L, Gao M, Wang G, Tang K, Yang J, et al. Comparison of muscle density in middle-aged and older Chinese adults between a high-altitude area (Kunming) and a low-altitude area (Beijing). *Front Endocrinol* (2021) 12:811770. doi: 10.3389/fendo.2021.811770

42. Kanis JA. Assessment of fracture risk and its application to screening for postmenopausal osteoporosis: synopsis of a WHO report. *WHO Study Group Osteopor Int* (1994) 4:368–81. doi: 10.1007/BF01622200

43. Yoo J, Kim Y, Cho ER, Jee SH. Biological age as a useful index to predict seventeen-year survival and mortality in koreans. *BMC Geriatr* (2017) 17:7. doi: 10.1186/s12877-016-0407-y

44. Wang L, Su Y, Wang Q, Duanmu Y, Yang M, Yi C, et al. Validation of asynchronous quantitative bone densitometry of the spine: Accuracy, short-term reproducibility, and a comparison with conventional quantitative computed tomography. *Sci Rep* (2017) 7:6284. doi: 10.1038/s41598-017-06608-y

45. Engelke K, Adams JE, Armbrecht G, Augat P, Bogado CE, Bouxsein ML, et al. Clinical use of quantitative computed tomography and peripheral quantitative computed tomography in the management of osteoporosis in adults: the 2007 ISCD official positions. *J Clin Densitom* (2008) 11:123–62. doi: 10.1016/j.jocd.2007.12.010

46. Cheng X, Wang L, Zeng Q, et al. he China guideline for the diagnosis criteria of osteoporosis with quantitative computed tomography(QCT) (2018). *Chinese J Osteoporosis* (2019) 25(6):733–7. doi: 10.3969/j.issn.1006-7108.2019.06.001

47. Abdalla PP, Dos Santos Carvalho A, Dos Santos AP, Venturini ACR, Alves TC, Mota J, et al. Cut-off points of knee extension strength allometrically adjusted to identify sarcopenia risk in older adults: A cross-sectional study. *Arch Gerontol Geriat* (2020) 89:104100. doi: 10.1016/j.archger.2020.104100

48. Choe YR, Joh JY, Kim YP. Clinically relevant cut-off points for the diagnosis of sarcopenia in older Korean people. *J Gerontol A-biol* (2017) 72(12):1724–31. doi: 10.1093/gerona/glx052

frontiers | Frontiers in Endocrinology

TYPE Original Research
PUBLISHED 15 December 2022
DOI 10.3389/fendo.2022.1087110

OPEN ACCESS

EDITED BY
Ling Wang,
Beijing Jishuitan Hospital, China

REVIEWED BY
Yimin Ma,
Beijing Jishuitan Hospital, China
Xia Du,
Affiliated Hospital of Guizhou Medical University, China

*CORRESPONDENCE
Xianjing Peng
pengxianjing@csu.edu.cn

†These authors have contributed equally to this work

SPECIALTY SECTION
This article was submitted to Bone Research, a section of the journal Frontiers in Endocrinology

RECEIVED 02 November 2022
ACCEPTED 28 November 2022
PUBLISHED 15 December 2022

CITATION
Wang Y, Li S, Zhang Z, Sun S, Feng J, Chen J, Pei Y and Peng X (2022) Accelerated loss of trunk muscle density and size at L1 vertebral level in male patients with COPD. *Front. Endocrinol.* 13:1087110. doi: 10.3389/fendo.2022.1087110

Accelerated loss of trunk muscle density and size at L1 vertebral level in male patients with COPD

Ying Wang[1,2†], Sidong Li[3†], Zhenyi Zhang[1,4†], Shiqi Sun[1], Juntao Feng[2,5], Jinbiao Chen[6], Yigang Pei[1,2] and Xianjing Peng[1,2*]

[1]Department of Radiology, Xiangya Hospital, Central South University, Changsha, China, [2]National Clinical Research Center for Geriatric Disorders, Xiangya Hospital, Changsha, China, [3]Division of Life Sciences and Medicine, University of Science and Technology of China, Hefei, China, [4]Department of Radiology, Taojiang County People's Hospital, Yiyang, China, [5]Department of Respiratory Medicine, Xiangya Hospital, Central South University, Changsha, China, [6]Department of Medical Records & Information, Central South University, Changsha, China

Background and purpose: Weight loss and muscle mass loss are common in patients with chronic obstructive pulmonary disease (COPD). Muscle density and fat infiltration based on CT images may be more sensitive than muscle mass by DXA in the assessment of sarcopenia for COPD patients. However, the age-related changes of cross-sectional trunk muscle compositions based on lung CT scans are still unknown. Thus, we aimed to investigate over time the change in muscle density, size, and fat deposition of L1-level trunk muscles in patients with COPD.

Materials and methods: 129 male COPD patients with a second chest CT scan (from 2013-2019 to 2014-2020) were enrolled. The CT images at first and second CT scans are analyzed by OsiriX software. Trunk muscles at the level of the 1st lumbar vertebrae were selected for analysis. Attenuation of lumbar vertebrae 1 was also measured from chest CT images. The pulmonary function values were calculated based on forced expiratory volume in 1 second (FEV1) and forced vital capacity (FVC).

Results: The mean age of the 129 patients with COPD was 69.7 years. The durations of COPD of this cohort were from 8-17 years. The mean area and density of L1 trunk muscles were 85.5 cm^2 and 36.4 HU. At baseline, muscle area and density and vertebral density were negatively associated with age ($p<0.0001$), while the intermuscular fat area and the fat infiltration ratio were not significantly associated with age ($p>0.05$). The per-year loss of trunk muscle area was 2.83 cm^2 ($p<0.0001$) which accounts for 3.3% decrease per year, and the per-year decrease of trunk muscle density was 2.41 HU ($p<0.0001$) which accounts for 6.6% decrease per year. The per-year increase of intermuscular fat in trunk muscles was 0.57 cm^2 ($p=0.006$) which accounts for 11.1% increase per year. The bone density loss was 5.63 HU/per year ($p<0.0001$).

10.3389/fendo.2022.1087110

Conclusion: Men with COPD had accelerated muscle loss as well as increased fat infiltration. Compared to muscle quantity loss, the decline in muscle quality is much larger, indicating the importance of relevant interventions focusing on improving muscle quality.

KEYWORDS

chronic obstructive pulmonary disease, L1-trunk muscle, muscle size, muscle density, change

Introduction

Chronic obstructive pulmonary disease (COPD) is the fourth leading cause of death worldwide and is often characterized by chronic inflammation and extrapulmonary changes that impair quality of life and physical activity (1). Thus, weight loss and muscle mass loss are common in patients with COPD (2), and the risk of developing sarcopenia in COPD patients is increasing, with a prevalence ranging from 15% to 55% (3). Furthermore, sarcopenia appears to negatively affect clinical outcomes related to function and health in patients with COPD (4). Therefore, early detection of sarcopenia might be critical to better designing therapeutic interventions like pulmonary rehabilitation.

Skeletal muscle mass is usually measured by dual energy X-ray absorptiometry (DXA) and bioelectrical impedance analysis (BIA). Unlike DXA/BIA, which only measures muscle quantity, CT measures both muscle quantity (e.g., muscle cross-sectional area [CSA] or muscle index) and muscle quality (e.g, muscle attenuation or fat infiltration) (5). CT-based muscle metrics show promise in predicting the risk of osteoporotic fracture (6–8) and hip refracture (9), as well as the mortality (10–12). Muscle density and fat infiltration may be more sensitive than muscle mass by DXA in the assessment of sarcopenia for COPD patients.

In clinical practice, routine lung CT is often performed in COPD patients to help characterize COPD phenotypes and screen for lung cancer (13). Therefore, compared with DXA, the use of lung CT might offer the opportunity to routinely assess the sarcopenia in COPD patients. However, the age-related changes of cross-sectional trunk muscle compositions based on lung CT scans are still unknown, which impedes the understanding of the relationships between muscle metrics and COPD.

In this retrospective follow-up cohort study, by using state-of-the-art imaging, we aimed to investigate over time the change in muscle density, size, and fat deposition of L1-level trunk muscles in patients with COPD. We also aimed to explore the relations among muscle measurements, duration of COPD, and pulmonary function.

Materials and methods

Participants

The retrospective study was approved by the Institutional Review Board of Xiangya Hospital, and the informed consent from the patients was waived. We searched both the medical record and the PACS for all patients who met the following inclusion criteria: a male aged 50 years or older with a diagnosis of COPD according to the Global Initiative for Chronic Obstructive Lung Disease (GOLD) criteria (14) between Jan 1, 2013, and Dec 31, 2019; two diagnostic chest CT scans with an interval time of at least 3 months. This yielded 129 male patients with a second chest CT scan (from 2013-2019 to 2014-2020).

Patients with other conditions that cause sarcopenia including chronic liver disease, end stage renal disease, and active cancer were excluded. Bronchial asthma, interstitial pneumonia, or bronchiectasis, thoracic or upper lumbar vertebrae degenerative disease or history of operation on the vertebrae, without a second chest CT scan were also excluded.

CT scans

CT imaging was performed with two CT scanners (Aquilion one 320, Toshiba, Tokyo, Japan; SOMATOM Definition, Siemens, Erlangen, Germany). All patients were scanned in the supine position during deep inspiration without intravenous contrast. The two scans of most COPD patients were performed on a same scanner to avoid the inter-scanner differences. Scan parameters were 120kVp, auto current setting based on BMI, 1mm slice thickness, 50 cm field of view, and 512×512 matrix in spiral and standard reconstructions.

Muscle and bone measurements

The DICOM images of COPD patients at first and second CT scans are analyzed by OsiriX software (Lite version 10.0.2,

Pixmeo, Geneva, Switzerland) which was downloaded from http://www.osirix-viewer.com/, and was previously assessed as a user-friendly image analysis software package for the Apple Mac OS. All muscle measurements were acquired by one of the investigators who, in preparation for the measurements, received training in chest CT imaging assessments focusing on trunk muscle morphology. For practice purposes, a sample of about 20 images was analyzed with the OsiriX software application prior to the beginning of the measurement study. Trunk muscles at the level of the 1st lumbar vertebrae were selected for analysis. Using the 'pencil' tool to outline the muscles as ROIs. Then open the 'growing' window, -29 to 150 HU as the threshold to segment muscle tissue from fat (Figures 1A, B). The area and mean CT values were displayed in the Segmentation preview box. The pre-segmentation ROI was defined as "Muscle Fat", and the area of pre-segmentation ROI minus the area of segmented muscle was the fat area (intermuscular fat).

Attenuation of lumbar vertebrae 1 (L1) was also measured by the same investigator with the OsiriX software application from chest CT images. A circular region of interest (ROI) was drawn at the mid-vertebral body, avoiding the cortical bone and the posterior internal vertebral venous plexus.

Pulmonary function testing and other covariates

The pulmonary function values were calculated based on forced expiratory volume in 1 second (FEV1) and forced vital capacity (FVC) by using standardized equipment (MasterScreen, JAEGER/Carefusion, Hoechberg, Germany).

Demographic and anthropometric covariates included age, height, weight, duration of COPD. Health-related covariates included hemoglobin, mean hemoglobin concentration, mean corpuscular hemoglobin, white blood cell count, red blood cell count, platelet distribution width, mean platelet volume.

Statistical analysis

Baseline characteristics were described with mean ± standard deviation for continuous variables and frequency and percent for categorical variables. Generalized linear models were used to study the association of muscle indexes with age, duration of disease, and pulmonary function. Moreover, we assessed the impact of COPD duration, age, and pulmonary function on muscle indexes by categorizing participants with COPD using 10 years, age using 70 years, and FEV1% using 40 as the cut-off value. Comparisons were made by two-sample t-test or Wilcoxon Signed Rank tests for continuous variables.

A two-sided P value less than 0.05 was considered statistically significant. All analyses were performed using SAS 9.4.

Results

Baseline parameters

The demographic data and baseline measurements were shown in Table 1. The mean age of the 129 patients with COPD was 69.7 years. The durations of COPD of this cohort were from 8-17 years. The mean area and density of L1 trunk muscles were 85.5 cm^2 and 36.4 HU, and the mean bone attenuation of L1 was 113.8 HU. This COPD cohort had a mean FEV1 of 40.3%. The blood routine examinations of this cohort were normal.

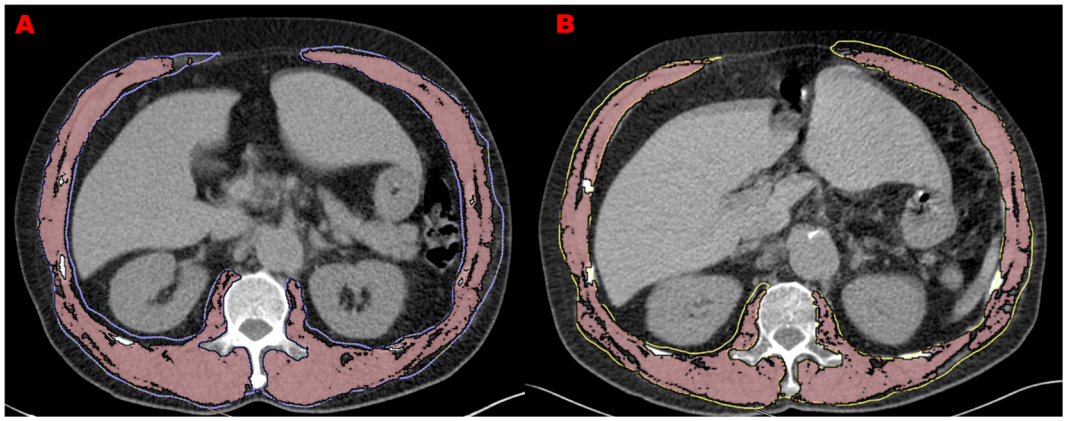

FIGURE 1
Muscle measurements at two screening chest CTs in 66-year-old man with COPD. **(A)** refers to L1 level CT image of 1st CT scan with the measurement of trunk muscle density (31.9 HU) and size (140.7 cm^2). **(B)** refers to L1 level CT image of 2nd CT scan performed 3 years after the initial one with the measurement of trunk muscle density (26.1 HU) and size (114.8 cm^2).

10.3389/fendo.2022.1087110

Associations of muscle and bone indexes with age, duration of COPD and pulmonary function

At baseline, Figure 2A shows that muscle area and density and vertebral density were negatively associated with age ($p<0.0001$), while the intermuscular fat area and the fat infiltration ratio were not significantly associated with age ($p>0.05$). The duration of COPD was only negatively associated with muscle area ($p=0.0011$), but was not associated with muscle and vertebral density (Figure 2B). Figure 2C shows that FEV1, % was not significantly associated with any measurement.

The per-year changes in muscle and bone indexes were not significantly associated with age, duration of COPD and FEV1, % (Figures 3A–C).

Per-year changes of muscle metrics

Table 2 shows the absolute changes and per year changes in muscle and bone indexes between the two CT scans for the male COPD patients. The per-year loss of trunk muscle area was 2.83 cm^2 ($p<0.0001$) which accounts for 3.3% decrease per year, and the per-year decrease of trunk muscle density was 2.41 HU ($p<0.0001$) which accounts for 6.6% decrease per year. The per-year increase of intermuscular fat area in trunk muscles was 0.57 cm^2 ($p=0.006$) which accounts for 11.1% increase per year. For male COPD patients, the bone density loss was 5.63 HU/per year ($p<0.0001$). For the subgroup analysis, the group aged under 70 years had a higher intermuscular fat area (0.98 cm^2) increase per year compared to that of the group aged over 70 years (0.09 cm^2). However, the difference of muscle fat infiltration per year between two age groups was border significant ($p=0.04$). The COPD duration and the pulmonary function had no effect on the per-year change of all muscle indexes (Table 3).

TABLE 1 Characteristics of study participants at baseline (N=129).

	Mean ± SD
Age, yrs	69.7 ± 10.0
Height, cm	164.2 ± 6.8
Weight, kg	56.1 ± 9.8
Duration of disease, yrs	10 (8-17)
Muscle and bone indexes	
Muscle Fat Area, cm^2	93.9 ± 20.8
Muscle area, cm^2	85.5 ± 18.0
Fat area, cm^2	8.8 ± 5.4
Fat infiltration, %	0.09 ± 0.04
Muscle density, HU	36.4 ± 6.9
Vertebrae density, HU	113.8 ± 43.9
Blood routine examination	
Hemoglobin, g/L	128.9 ± 21.2
Mean hemoglobin concentration, g/L	325.7 ± 11.3
Mean corpuscular hemoglobin, pg	30.4 ± 2.1
White blood cell count, 10^9/L	7.3 ± 2.7
Red blood cell count, 10^12/L	4.3 ± 0.6
Platelet distribution width, %	13.8 ± 3.2
Mean platelet volume, fL	9.6 ± 1.2
Pulmonary function*	
FEV1, L	0.98 (0.61-1.30)
FEV1, %	40.3 (24.5-60.2)
FVC, L	2.4 (2.0-2.8)
FVC, %	77.0 (65.9-96.9)
FEV1/FVC	0.37 (0.28-0.51)

*Pulmonary function was available for 84 patients.
FEV1, forced expiratory volume in the first second; FVC, forced vital capacity.

Discussion

To the best of our knowledge, our findings first demonstrated the rate of decline in muscle size and density in older COPD patients, and we discovered that older male COPD patients had accelerated loss of muscle size and density, as well as increased intermuscular fat deposits. Our results also indicate that compared to muscle quantity decreased, the rate of muscle quality loss is doubled, implying that the interventions for sarcopenia of COPD patients should be focused on muscle quality.

In the last decade, there has been a rapid increase in the use of CT measured muscle CSA and density in the evaluation of sarcopenia, especially for opportunistic applications. A recent review showed that the total abdominal wall muscles are mostly favored for muscle CSA and density measurements, and measuring trunk muscle in an axial slice is the best standard for CT-based calculation of total body muscle mass (15). Further, a recent opportunistic use of CT study demonstrated that the L1 trunk muscle measurement allows sarcopenia assessment using both chest and abdominal CT scans (11), which indicates our outcomes could generate the potential yield of opportunistic CT screening of sarcopenia for COPD patients.

The decline rate of muscle mass in older adults was reported as approximately 0.51%, which is much lower than that of muscle strength, which was 2.5 to 4% in a year (16). The cross-sectional results showed that muscle mass decreased less than 0.5% per year in both genders when compared the young adults (18 to 45 years old) and the elderly (65 years old or over) (16). However, our results indicated that the muscle size loss in older male patients with COPD was 3.3% in a year, which is much higher than older adults without COPD.

Inflammation is the main feature of chronic obstructive pulmonary disease. Usually, the inflammatory response of COPD patients is not limited to the lungs but is also accompanied by systemic chronic inflammation (1). Systemic

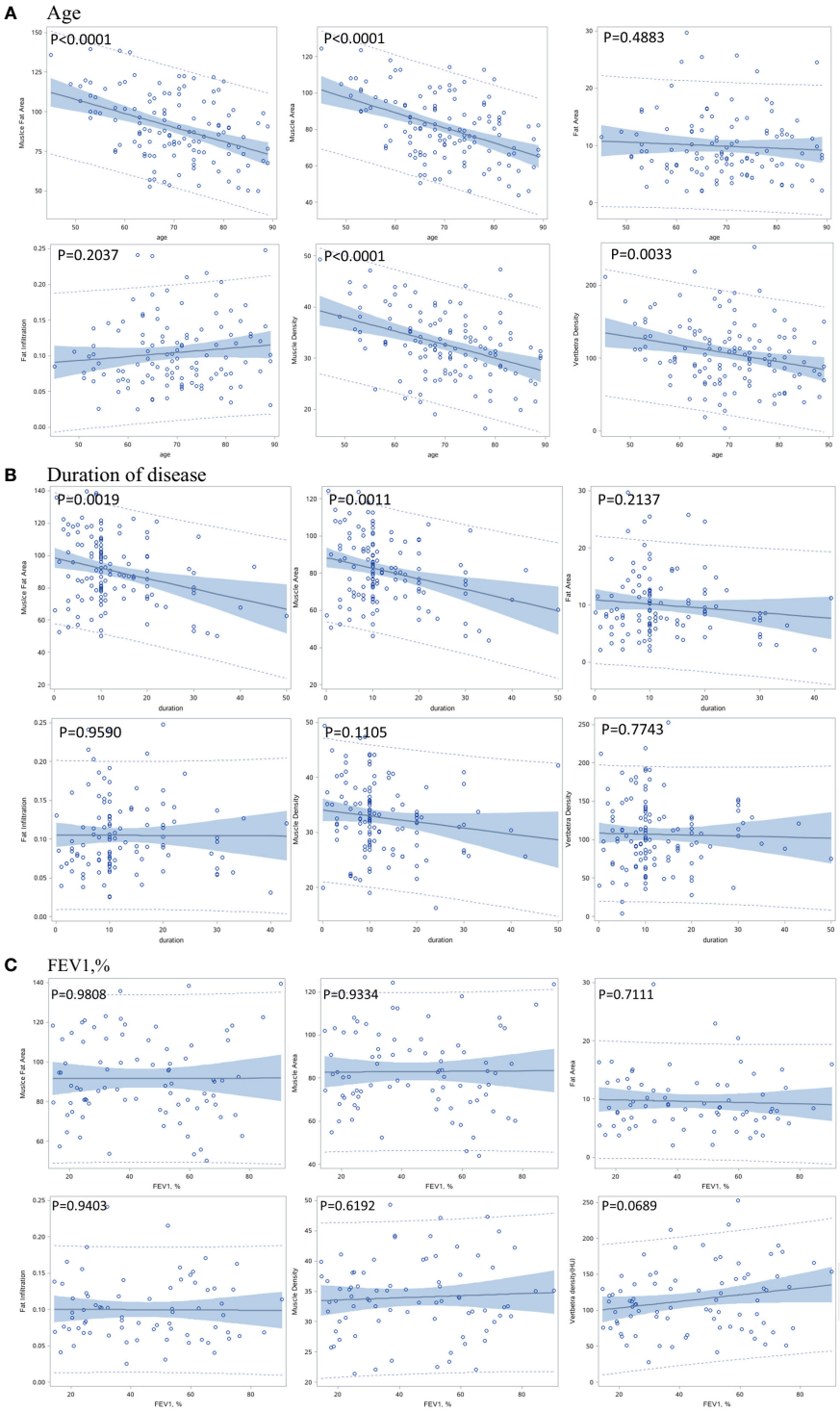

FIGURE 2
Correlation between baseline muscle and bone indexes with age **(A)**, duration of disease **(B)**, and pulmonary function **(C)**.

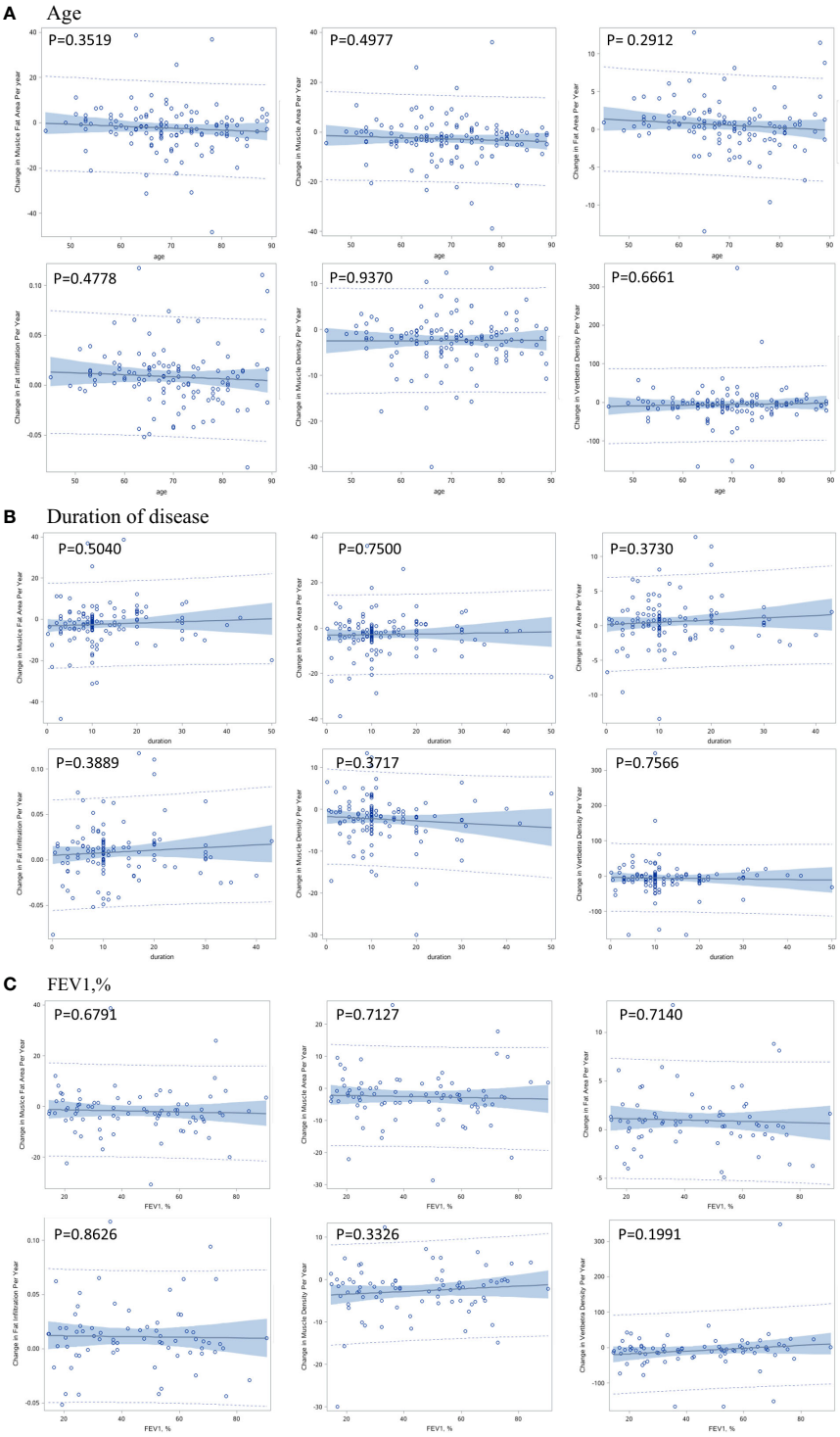

FIGURE 3
Correlation between per-year change in muscle and bone indexes with age **(A)**, duration of disease **(B)**, and pulmonary function **(C)**.

TABLE 2 Per-year Change in muscle and bone indexes in COPD patients.

	First measurement	Second measurement	Change	Per year change (n%)	P value
Muslce Fat Area, cm^2	93.95 ± 20.94	90.28 ± 20.91	-3.67 ± 8.75	-2.36 ± 10.29(-2.5%)	<0.0001
Muscle area, cm^2	85.54 ± 18.07	81.1 ± 17.86	-4.44 ± 7.67	-2.83 ± 8.73(-3.3%)	<0.0001
Fat area, cm^2	9.04 ± 5.42	9.9 ± 5.59	0.85 ± 3.26	0.57 ± 3.37(6.3%)	0.006
Fat infiltration, %	0.09 ± 0.04	0.1 ± 0.05	0.01 ± 0.03	0.01 ± 0.03(11.1%)	<0.0001
Muscle density, HU	36.53 ± 6.97	32.73 ± 6.55	-3.8 ± 5.59	-2.41 ± 5.64(6.6%)	<0.0001
Vertbetra density, HU	114.14 ± 43.93	106.6 ± 44.06	-7.55 ± 29.96	-5.63 ± 47.8(4.9%)	<0.0001

Analysis was conducted among patients with complete information on muscle and bone indexes in two measurements. Comparisons between two measurements were conducted using paired t tests and signed rank tests according to the normality of distribution.

chronic inflammatory responses can lead to sarcopenia in COPD patients (1). On the other hand, sarcopenia was found to be associated with increased levels of systemic inflammation in COPD patients (17). In addition to the inflammation effect, physical inactivity caused by COPD is also a critical trigger for muscle loss as inactivity results in disuse-atrophy (3). Thus, in our study, the muscle loss of COPD patients was much larger than the numbers in the reports with normal elderly men without COPD.

The observations of larger declines of muscles, especially the muscle density, are meaningful because previous reports have demonstrated reduced attenuation in the range of 3–6 HU among people with strength deconditioning and low back pain (18, 19). Furthermore, the 2.41 HU decrease in COPD men per year is parallel to a 15% decrease over four decades in a previous report (20). Notably, the mean value (36.9HU) of muscle density in our study was adjacent to the myosteatosis diagnostic cut points (from ≤22.0 HU to ≤44.4 HU) for muscle attenuation in cancer patients (12). L1 trunk muscle density may be a potential risk factor for mortality in patients with COPD as other reports (14, 21).

Insight of the muscle size and density decreases and increased fat infiltration observed among male COPD patients in this study is also important to recognize the potential for intervention strategies that could be implemented to mitigate these detriments to muscle health. A study ever showed that muscle quality is more impaired in COPD patients with sarcopenia (22). Our results might indicate the importance of a rapid increase in muscle quality favoring a combination of resistance and aerobic exercises as commonly applied in pulmonary rehabilitation. Exercise training programs are of high importance, and it is a limitation of our study that we did not assess routine physical activity and exercises in this cohort.

Limitations

Our study has several limitations. First, not all participants were stable COPD patients. Some of them came to our hospital for the second CT scan because of the aggravating COPD for in-hospital treatments. Second, we did not perform a detailed assessment of physical function, which may have added to a better understanding of the causes of accelerated loss of muscle in COPD patients. Third, we did not collect information about smoking history, which is known to affect muscle loss (23). Forth, the inflammation related information is not available in this study. One cause of the COPD related muscle loss is the inflammation status of the COPD patients.

In conclusion, COPD men had accelerated muscle loss and increased muscle fat infiltration. Compared to muscle size loss, the decline in muscle density was much larger, indicating the

TABLE 3 Per-year change in muscle indexes in subgroups.

	Disease duration			Age			FEV1%		
	<=10 yrs (n=75)	>10 yrs (n=50)	P value	<=70 yrs (n=67)	>70 yrs (n=59)	P value	<40 (n=39)	>=40 (n=42)	P value
Muslce Fat Area, cm^2	-3.19 ± 10.71	-1.13 ± 9.71	0.14	-1.61 ± 9.32	-3.21 ± 11.31	0.29	-0.96 ± 9.51	-2.61 ± 8.57	0.33
Muscle area, cm^2	-3.25 ± 9.18	-2.22 ± 8.15	0.21	-2.41 ± 7.67	-3.3 ± 9.84	0.86	-1.82 ± 7.81	-3.32 ± 7.69	0.36
Fat area, cm^2	0.32 ± 3.24	0.98 ± 3.59	0.99	0.98 ± 3.27	0.09 ± 3.45	0.01	1.19 ± 3.19	0.73 ± 2.87	0.65
Fat infiltration, %	0.01 ± 0.03	0.01 ± 0.04	1.00	0.01 ± 0.03	0.01 ± 0.03	0.04	0.01 ± 0.03	0.01 ± 0.03	0.70
Muscle density, HU	-1.73 ± 5.21	-3.36 ± 6.18	0.21	-2.59 ± 6.16	-2.2 ± 5.03	0.86	-3.05 ± 6.58	-2.34 ± 5.05	0.84

Analysis was conducted among patients with complete information on muscle indexes in two measurements. Comparisons between two groups were conducted using Wilcoxon two-Sample tests.

importance of relevant interventions focusing on improving muscle quality.

Data availability statement

The raw data supporting the conclusions of this article will be made available by the authors, without undue reservation.

Ethics statement

The studies involving human participants were reviewed and approved by Medical Ethics Committee of Xiangya Hospital of Central South University. Written informed consent for participation was not required for this study in accordance with the national legislation and the institutional requirements.

Author contributions

All authors contributed to this study. YW: Designing the study and preparing the initial draft. ZZ: Data collect and analysis. SL: Data analysis and interpretation. JF and JC: Data acquisition, data analysis. YP: Critically revising the final manuscript. XP: Designing the study, conceptualization and critical revision for intellectual content. All authors contributed to the article and approved the submitted version.

Conflict of interest

The authors declare that the research was conducted in the absence of any commercial or financial relationships that could be construed as a potential conflict of interest.

Publisher's note

All claims expressed in this article are solely those of the authors and do not necessarily represent those of their affiliated organizations, or those of the publisher, the editors and the reviewers. Any product that may be evaluated in this article, or claim that may be made by its manufacturer, is not guaranteed or endorsed by the publisher.

References

1. Sepulveda-Loyola W, Osadnik C, Phu S, Morita AA, Duque G, Probst VS. Diagnosis, prevalence, and clinical impact of sarcopenia in COPD: a systematic review and meta-analysis. *J cachexia sarcopenia muscle* (2020) 11(5):1164–76. doi: 10.1002/jcsm.12600

2. Kwan HY, Maddocks M, Nolan CM, Jones SE, Patel S, Barker RE, et al. The prognostic significance of weight loss in chronic obstructive pulmonary disease-related cachexia: a prospective cohort study. *J cachexia sarcopenia muscle* (2019) 10 (6):1330–8. doi: 10.1002/jcsm.12463

3. van Bakel SIJ, Gosker HR, Langen RC, Schols A. Towards personalized management of sarcopenia in COPD. *Int J Chron Obstruct Pulmon Dis* (2021) 16:25–40. doi: 10.2147/COPD.S280540

4. Benz E, Trajanoska K, Lahousse L, Schoufour JD, Terzikhan N, De Roos Eetal/> Sarcopenia in COPD: a systematic review and meta-analysis. *Eur Respir Rev* (2019) 28 (154):190049. doi: 10.1183/16000617.0049-201910.1183/16000617.0049-2019

5. Wang L, Yin L, Zhao Y, Su Y, Sun W, Chen S, et al. Muscle density, but not size, correlates well with muscle strength and physical performance. *J Am Med Directors Assoc* (2021) 22(4):751–9 e2. doi: 10.1016/j.jamda.2020.06.052

6. Wang L, Yin L, Zhao Y, Su Y, Sun W, Liu Y, et al. Muscle density discriminates hip fracture better than computed tomography X-ray absorptiometry hip areal bone mineral density. *J cachexia sarcopenia Muscle* (2020) 11(6):1799–812. doi: 10.1002/jcsm.12616

7. Wang L, Li S, Liu Y, Li K, Yin L, Su Y, et al. Greater bone marrow fat and myosteatosis are associated with lower vBMD but not asymptomatic vertebral fracture. *Eur Radiol* (2022). doi: 10.1007/s00330-022-08979-x

8. Lang T, Cauley JA, Tylavsky F, Bauer D, Cummings S, Harris TB. Computed tomographic measurements of thigh muscle cross-sectional area and attenuation coefficient predict hip fracture: The health, aging, and body composition study. *J Bone Mineral Res* (2010) 25(3):513–9. doi: 10.1359/jbmr.090807

9. Wang L, Yin L, Yang M, Ge Y, Liu Y, Su Y, et al. Muscle density is an independent risk factor of second hip fracture: a prospective cohort study. *J cachexia sarcopenia muscle* (2022) 13(3):1927–37. doi: 10.1002/jcsm.12996

10. Wang L, Yin L, Yang M, Cheng X. Muscle composition and the imminent mortality risk after hip fracture. *J cachexia sarcopenia Muscle* (2022). doi: 10.1002/jcsm.13090

11. Lenchik L, Lenoir KM, Tan J, Boutin RD, Callahan KE, Kritchevsky SB, et al. Opportunistic measurement of skeletal muscle size and muscle attenuation on computed tomography predicts 1-year mortality in Medicare patients. *journals gerontology Ser A Biol Sci Med Sci* (2019) 74(7):1063–9. doi: 10.1093/gerona/gly183

12. McGovern J, Dolan RD, Horgan PG, Laird BJ, McMillan DC. Computed tomography-defined low skeletal muscle index and density in cancer patients: observations from a systematic review. *J cachexia sarcopenia muscle* (2021) 12 (6):1408–17. doi: 10.1002/jcsm.12831

13. Mazzone P, Powell CA, Arenberg D, Bach P, Detterbeck F, Gould MK, et al. Components necessary for high-quality lung cancer screening: American college of chest physicians and American thoracic society policy statement. *Chest* (2015) 147 (2):295–303. doi: 10.1378/chest.14-2500

14. Tanimura K, Sato S, Fuseya Y, Hasegawa K, Uemasu K, Sato A, et al. Quantitative assessment of erector spinae muscles in patients with chronic obstructive pulmonary disease. novel chest computed tomography-derived index for prognosis. *Ann Am Thorac Soc* (2016) 13(3):334–41. doi: 10.1513/AnnalsATS.201507-446OC

15. Amini B, Boyle SP, Boutin RD, Lenchik L. Approaches to assessment of muscle mass and myosteatosis on computed tomography: A systematic review. *journals gerontology Ser A Biol Sci Med Sci* (2019) 74(10):1671–8. doi: 10.1093/gerona/glz034

16. Mitchell WK, Williams J, Atherton P, Larvin M, Lund J, Narici M. Sarcopenia, dynapenia, and the impact of advancing age on human skeletal muscle size and strength; a quantitative review. *Front Physiol* (2012) 3:260. doi: 10.3389/fphys.2012.00260

17. Byun MK, Cho EN, Chang J, Ahn CM, Kim HJ. Sarcopenia correlates with systemic inflammation in COPD. *Int J Chron Obstruct Pulmon Dis* (2017) 12:669–75. doi: 10.2147/COPD.S130790

18. Hicks GE, Simonsick EM, Harris TB, Newman AB, Weiner DK, Nevitt MA, et al. Trunk muscle composition as a predictor of reduced functional capacity in the health, aging and body composition study: the moderating role of back pain. *journals gerontology Ser A Biol Sci Med Sci* (2005) 60(11):1420–4. doi: 10.1093/gerona/60.11.1420

19. Aubrey J, Esfandiari N, Baracos VE, Buteau FA, Frenette J, Putman CT, et al. Measurement of skeletal muscle radiation attenuation and basis of its biological variation. *Acta Physiol (Oxf)* (2014) 210(3):489–97. doi: 10.1111/apha.12224

20. Anderson DE, D'Agostino JM, Bruno AG, Demissie S, Kiel DP, Bouxsein ML. Variations of CT-based trunk muscle attenuation by age, sex, and specific muscle. *journals gerontology Ser A Biol Sci Med Sci* (2013) 68(3):317–23. doi: 10.1093/gerona/gls168

21. Tanimura K, Sato S, Sato A, Tanabe N, Hasegawa K, Uemasu K, et al. Accelerated loss of antigravity muscles is associated with mortality in patients with COPD. *Respiration* (2020) 99(4):298–306. doi: 10.1159/000506520

22. van de Bool C, Gosker HR, van den Borst B, Op den Kamp CM, Slot IG, Schols AM. Muscle quality is more impaired in sarcopenic patients with chronic obstructive pulmonary disease. *J Am Med Directors Assoc* (2016) 17(5):415–20. doi: 10.1016/j.jamda.2015.12.094

23. Attaway AH, Welch N, Yadav R, Bellar A, Hatipoglu U, Meli Y, et al. Quantitative computed tomography assessment of pectoralis and erector spinae muscle area and disease severity in chronic obstructive pulmonary disease referred for lung volume reduction. *COPD* (2021) 18(2):191–200. doi: 10.1080/15412555.2021.1897560

frontiers | Frontiers in Endocrinology

TYPE Original Research
PUBLISHED 12 January 2023
DOI 10.3389/fendo.2022.1099919

OPEN ACCESS

EDITED BY
Ling Wang,
Beijing Jishuitan Hospital, China

REVIEWED BY
Yuanyuan Qin,
Huazhong University of Science and Technology, China
Siqi Wang,
Nanjing Medical University, China

*CORRESPONDENCE
Qing-Ling Li
liqingl3@mail.sysu.edu.cn
Hui-Jun Hu
huhuijun@mail.sysu.edu.cn
Ruo-Mi Guo
guoruomi86@mail.sysu.edu.cn

†These authors have contributed equally to this work

SPECIALTY SECTION
This article was submitted to Bone Research, a section of the journal Frontiers in Endocrinology

RECEIVED 16 November 2022
ACCEPTED 27 December 2022
PUBLISHED 12 January 2023

CITATION
Zheng C-S, Wen H-Q, Lin W-S, Luo X-W, Shen L-S, Zhou X, Zou F-Y, Li Q-L, Hu H-J and Guo R-M (2023) Quantification of lumbar vertebral fat deposition: Correlation with menopausal status, non-alcoholic fatty liver disease and subcutaneous adipose tissue.
Front. Endocrinol. 13:1099919.
doi: 10.3389/fendo.2022.1099919

Quantification of lumbar vertebral fat deposition: Correlation with menopausal status, non-alcoholic fatty liver disease and subcutaneous adipose tissue

Chu-Shan Zheng[1,2†], Hui-Quan Wen[1†], Wu-Sheng Lin[1†], Xiao-Wen Luo[1], Li-Shan Shen[1], Xiang Zhou[1], Feng-Yun Zou[1], Qing-Ling Li[1,3*], Hui-Jun Hu[1,2*] and Ruo-Mi Guo[1*]

[1]Department of Radiology, Third Affiliated Hospital of Sun Yat-sen University, Guangzhou, China, [2]Department of Radiology, Sun Yat-Sen Memorial Hospital, Sun Yat-sen University, Guangzhou, Guangdong, China, [3]Department of VIP Medical Center, Third Affiliated Hospital of Sun Yat-sen University, Guangzhou, Guangdong, China

Purpose: To assess abdominal fat deposition and lumbar vertebra with iterative decomposition of water and fat with echo asymmetry and least-squares estimation (IDEAL-IQ) and investigate their correlation with menopausal status.

Materials and Methods: Two hundred forty women who underwent routine abdominal MRI and IDEAL-IQ between January 2016 and April 2021 were divided into two cohorts (first cohort: 120 pre- or postmenopausal women with severe fatty livers or without fatty livers; second cohort: 120 pre- or postmenopausal women who were obese or normal weight). The fat fraction (FF) values of the liver (FF_{liver}) and lumbar vertebra (FF_{lumbar}) in the first group and the FF values of subcutaneous adipose tissue (SAT) (FF_{SAT}) and FF_{lumbar} in the second group were measured and compared using IDEAL-IQ.

Results: Two hundred forty women were evaluated. FF_{lumbar} was significantly higher in both pre- and postmenopausal women with severe fatty liver than in patients without fatty livers (premenopausal women: $p < 0.001$, postmenopausal women: $p < 0.001$). No significant difference in the FF_{lumbar} was observed between obese patients and normal-weight patients among pre- and postmenopausal women (premenopausal women: $p = 0.113$, postmenopausal women: $p = 0.092$). Significantly greater lumbar fat deposition was observed in postmenopausal women than in premenopausal women with or without fatty liver and obesity ($p < 0.001$ for each group). A high correlation was detected between FF_{liver} and FF_{lumbar} in women with severe fatty liver (premenopausal women: r=0.76, p<0.01; postmenopausal women: r=0.82, p<0.01).

10.3389/fendo.2022.1099919

Conclusion: Fat deposition in the vertebral marrow was significantly associated with liver fat deposition in postmenopausal women.

KEYWORDS

magnetic resonance imaging, subcutaneous fat, severe fatty liver, postmenopausal women, fat fraction

Introduction

Osteoporosis is characterized by reduced bone density, increased bone fragility, and susceptibility to fracture. The reduced bone density occurring in individuals with osteoporosis is associated with an increase in vertebral bone marrow fat deposition (1, 2). Age is associated with changes in the musculoskeletal system. Substantial decreases in skeletal muscle function and bone density occur with aging (3, 4).The yellow bone marrow gradually replaces the red bone marrow in the vertebral body with increasing age (3, 5). Estrogen is another important factor affects bone composition. A reduction in estrogen levels promotes bone loss and the development of osteoporosis (6). Thus, osteoporosis is common in elderly individuals, especially in postmenopausal women (7). Furthermore, accumulating evidence has shown that postmenopausal women have increased abdominal adiposity, including subcutaneous adipose tissue (SAT) and visceral adipose tissue (VAT), compared to premenopausal women (8, 9). According to recent studies, abdominal adiposity is associated with osteopenia and osteoporosis (10, 11). Proinflammatory cytokines, such as tumor necrosis factor-α and interleukin-6, secreted by VAT are known to promote bone metabolism and resorption (12). Non-alcoholic fatty liver disease (NAFLD) is a multiple-system disease that is strongly associated with abdominal obesity (13), and VAT may cause NAFLD (14). Preliminary evidence also suggests that NAFLD may be associated with a decrease in bone mineral density (15). However, the relationship between vertebral bone marrow fat and abdominal adiposity, especially SAT and liver fat, remains unknown. And the possible contribution of abdominal adiposity to osteoporosis in postmenopausal women has not been well characterized.

MRI methods are the most accurate noninvasive techniques for quantifying body fat and bone marrow fat. MR spectroscopy is the most commonly used method to examine quantitative fat measurements (16). However, it has drawbacks, such as a long scan time, small imaging range, and substantial postprocessing, which may be impractical in some clinical settings (17, 18). Iterative decomposition of water and fat with echo asymmetry and least-squares estimation (IDEAL-IQ) imaging is a new method that steadily separates fat and water using three asymmetric echo times and the three-point Dixon method. In IDEAL-IQ, an iterative least-squares decomposition algorithm is employed to solve for a fat fraction map, a water fraction map, and an R2* map simultaneously (17, 18). By incorporating an R2* map into the algorithm, IDEAL-IQ accounts for T2* effects/field inhomogeneity and yields a proton density fat fraction that is not confounded by iron overload (19–21). IDEAL-IQ has been reported to accurately quantify hepatic fat deposition with good correlations observed between hepatic MR spectroscopy and liver biopsy (22–24). It was also used to measure the fat content in other organs and tissues, such as the pancreas, kidney, and bone marrow, in individuals with NAFLD (25, 26). IDEAL-IQ has been considered a valuable tool for providing information on fat content in clinical settings.

Therefore, using IDEAL-IQ as the noninvasive imaging methodology, we aimed to investigate the correlation between SAT, NAFLD, and vertebral bone marrow fat in a population of middle-aged females and investigate the correlations between fat deposits and menopausal status.

Materials and methods

Subjects

A total of 2360 middle-aged females (age range, 45 - 55 years old) who had received an abdominal MRI from January 2016 to April 2021 presented for a medical examination. The final data were acquired retrospectively from 240 middle-aged female subjects (age range, 45 – 55 years old; mean age, 48.50 ± 3.54 years old). Our institutional research ethics committee approved this study (02-005-01), and written informed consent was obtained from all study participants.

Our study consisted of two cohorts of patients, and each cohort included four groups. Propensity score matching was used to choose patients at a 1:1 ratio for the two cohorts' patients, followed by subgrouping. The patient selection flowchart is shown in Figure 1. Women were categorized as postmenopausal if they had no menstrual cycle in the previous 12 months, whether owing to natural cessation or hysterectomy

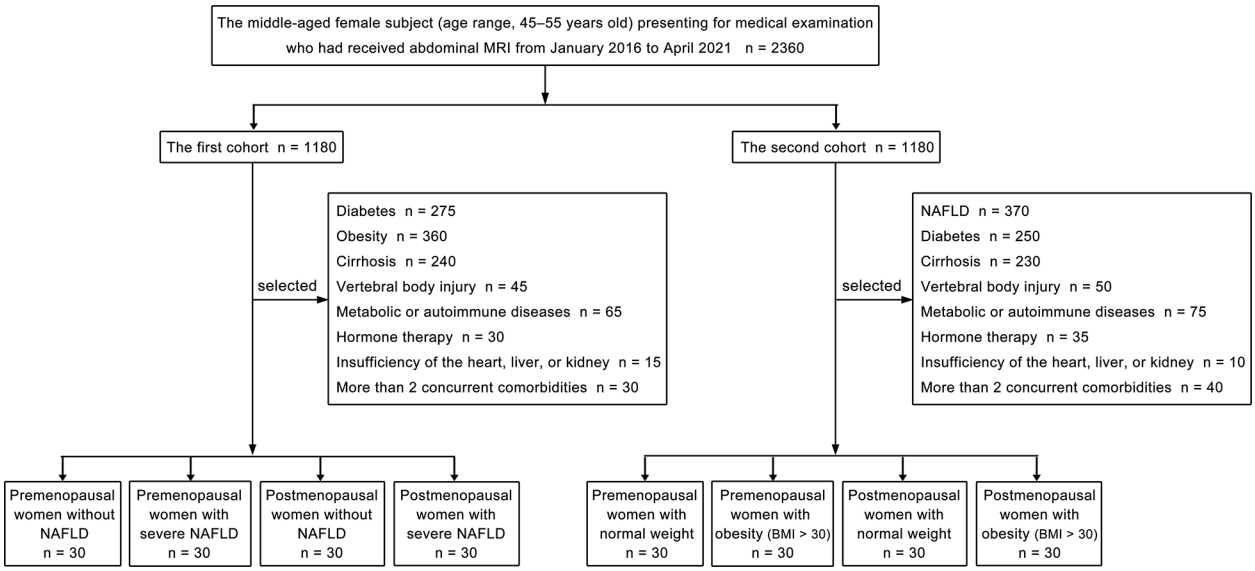

FIGURE 1
Flowchart of the patient selection process.

and/or oophorectomy (27). The first part of our study included the following four groups: premenopausal women without NAFLD (liver fat content is less than 5%) (28), premenopausal women with severe NAFLD (liver fat content is greater than 28%) (28), postmenopausal women without NAFLD, and postmenopausal women with severe NAFLD. Thirty patients were included in each group, and we quantitatively measured the fat deposition in the lumbar vertebra and liver of patients from each group. Patients with diabetes; obesity; cirrhosis; vertebral body injury; metabolic or autoimmune diseases; hormone therapy; insufficiency of the heart, liver, or kidney; or more than 2 concurrent comorbidities were excluded from the first cohort. The second cohort of patients in our study included the following four groups: premenopausal women with normal weight (body mass index, [BMI] 18- < 25 kg/m^2) (29), premenopausal women with obesity (BMI > 30 kg/m^2) (29), postmenopausal women with normal weight, and postmenopausal women with obesity (BMI > 30 kg/m^2). Thirty patients were included in each group, and the fat deposition in the lumbar vertebra and subcutaneous fat were measured quantitatively. Patients with NAFLD; diabetes; cirrhosis; vertebral body injury; metabolic or autoimmune diseases; hormone therapy; insufficiency of the heart, liver, or kidney; or more than 2 concurrent comorbidities were excluded from the second cohort.

Of the 1180 consecutive patients in the first cohort, 1060 were excluded due to diabetes (n = 275), obesity (n = 360), cirrhosis (n = 240), vertebral body injury (n = 45), metabolic or autoimmune diseases (n = 65), hormone therapy (n = 30), insufficiency of the heart, liver or kidney (n = 15), or the presence of more than 2 concurrent comorbidities (n = 30). Accordingly, 120 women (mean age ± standard deviation, 49.50 ± 4.95 years old; range, 45 - 55 years old) were finally included in the first cohort. Of the 1180 consecutive patients in the second cohort, 1060 were excluded due to NAFLD (n = 370), diabetes (n = 250), cirrhosis (n = 230), vertebral body injury (n = 50), metabolic or autoimmune diseases (n = 75), hormone therapy (n = 35), insufficiency of the heart, liver or kidney (n = 10), or the presence of more than 2 concurrent comorbidities (n = 40). Accordingly, 120 women (mean age ± standard deviation, 49.00 ± 2.83 years old; range, 45 - 55 years old) were finally included in the second cohort. Significant differences in the mean age were not observed among the four groups (30 patients in each group) in the first or second cohorts of our study (Tables 1, 2).

Magnetic resonance imaging

This study was performed using a 3.0 T MRI scanner (Discovery 750 and Signa Architect, GE Healthcare, Milwaukee, Wisconsin, USA) equipped with a 32-channel, phased-array torso coil by two radiologists. Before scanning, patients were trained to hold their breath for > 20 s at the end of expiration. Prior to IDEAL, the routine sequences, liver acquisition with volume acceleration and fast spin–echo T2-weighted images (T2WI) with fat saturation of the abdomen were recorded. The detailed acquisition parameters are shown in Supplementary Material and listed in Supplementary Table 1.

The IDEAL-IQ sequence was used on the abdomen in the axis plane. The following six groups of images were obtained

TABLE 1 Clinicopathologic characteristics of 120 patients in the first cohort.

Characteristics	Severe NAFLD-pre	Without NAFLD-pre	Severe NAFLD-post	Without NAFLD-post	P values			
					Severe NAFLD-pre vs. Without NAFLD-pre	Severe NAFLD-post vs. Without NAFLD-post	Severe NAFLD-pre vs. Severe NAFLD-post	Without NAFLD-pre vs. Without NAFLD-post
No. of patients	30	30	30	30	–	–	–	–
Mean Age (years old)	49.37	49.30	49.13	49.77	0.93	0.37	0.75	0.53
Mean body weight (kg)	52.07	51.35	52.10	51.20	0.48	0.35	0.97	0.88
Mean height(m)	1.61	1.58	1.62	1.59	0.76	0.71	0.79	0.72
Mean BMI(kg/m^2)	23.54	22.67	21.85	22.68	0.39	0.45	0.36	0.41

BMI, body mass index; NAFLD, non-alcoholic fatty liver disease; Severe NAFLD-pre, Premenopausal with severe NAFLD; Without NAFLD-pre, Premenopausal without NAFLD; Severe NAFLD-post, Postmenopausal with severe NAFLD; Without NAFLD-post, Postmenopausal without NAFLD.

once the IDEAL sequence was scanned: in-phase image, out-of-phase image, pure water image, pure fat image, fat fraction (FF) map, and R2* relaxation rate image. The adipose contents of the fat infiltration regions were directly measured using the FF map, and the measurements represent the percentage of fat content in the local bone mass, SAT, and liver.

Image analysis

The IDEAL datasets were transferred to the workstation and processed using Functool 6.3.1 software (GE Healthcare, Milwaukee, Wisconsin, USA). Two radiologists independently evaluated the MRI studies. For the quantitative analysis of the FF values of the liver (FF_{liver}), the radiologists independently placed three circulars (20 mm diameter) regions of interest (ROIs) in the liver on a plane passing through the main portal vein division: (1) in the right lobe of the liver (segment 6), (2) in segment 4 of the liver and (3) in the left lobe of the liver (segment 2/3). All ROIs were placed in the liver, avoiding major vessels, ligaments, and bile ducts, ensuring that each ROI was surrounded by liver parenchyma. Subcutaneous fat was defined as adipose tissue measured from the abdominal muscle wall to the skin. For the quantitative analysis of the FF values of SAT (FF_{SAT}), box-shaped ROIs were placed on the left, middle, and right levels of the anterior abdominal subcutaneous fat in the upper abdomen. The ROIs were approximately 20 mm^3. For the quantitation of FF values of the lumbar vertebra (FF_{lumbar}), box-shaped ROIs were placed on each lumbar vertebra at the upper, middle, and lower levels (L1–L4) on the axial FF map, which avoids tumor diseases, bone island, Schmorl's node, etc. in the vertebral body. The ROIs were approximately 20 mm^3. Each

TABLE 2 Clinicopathologic characteristics of 120 patients in the second cohort.

Characteristics	Obese-pre	Normal weight-pre	Obese-post	Normal weight-post	P values			
					Obese-pre vs. Normal weight-pre	Obese-post vs. Normal weight-post	Obese-pre vs. Obese-post	Normal weight-pre vs. Normal weight-post
No. of patients	30	30	30	30	–	–	–	–
Mean Age (years old)	49.70	49.10	49.07	49.90	0.41	0.25	0.38	0.27
Mean body weight (kg)	82.27	51.52	82.40	51.37	< 0.001	< 0.001	0.72	0.88
Mean height(m)	1.62	1.59	1.61	1.58	0.77	0.72	0.78	0.71
Mean BMI(kg/m^2)	33.86	23.24	34.15	22.95	< 0.001	< 0.001	0.41	0.47

BMI, body mass index; Obese-pre, Premenopausal with obese; Normal weight-pre, Premenopausal with normal weight; Obese-post, Postmenopausal with obese; Normal weight-post, Postmenopausal with normal weight.

area was measured 3 times, and the mean value was calculated. The liver fat content is less than 5% in the normal population and greater than 28% in patients with severe NAFLD (29).

Statistical analysis

All the data are presented as the means ± standard deviations, and a *P value* of less than 0.05 was considered significant. Differences in FF_{liver}, FF_{SAT}, and FF_{lumbar} were analyzed using t tests with Bonferroni's correction or the Mann–Whitney U test. The correlation coefficients were calculated by Spearman rank between the FF_{liver}, FF_{SAT}, and FF_{lumbar}. The interobserver consistency of the FF values (independently determined by two radiologists) was evaluated using the Bland–Altman analysis and the intraclass correlation coefficient (ICC). One author analyzed all data using GraphPad Prism 9 software (GraphPad Software Inc., San Diego, CA, USA).

Results

The images of all patients were clear and usable. The interobserver consistency of the FF_{lumbar} in the first cohort of patients was analyzed by constructing a Bland–Altman plot (Figure 2), and the 95% limits of agreement were -0.11 to 0.11, -0.06 to 0.06, -0.06 to 0.07, and -0.04 to 0.05, respectively. For the quantitative measurement of FF_{lumbar} in premenopausal without NAFLD group and premenopausal with severe NAFLD group, interobserver agreement was high (ICC = 0.91, 0.93; 95% confidence interval (CI) 0.90–0.93, 0.91–0.95), and intraobserver agreement was also high (ICC = 0.92, 0.92; 95% CI 0.91–0.94, 0.90–0.94). The Bland–Altman analysis and ICC showed that the two radiologists had good consistency in the measured values.

Examples of fat deposition in patients without NAFLD and severe NAFLD before or after menopause in the first part are shown in Figure 3. The mean FF_{lumbar} and the FF_{liver} were measured separately in the four groups and are summarized in Table 3. In premenopausal women and postmenopausal

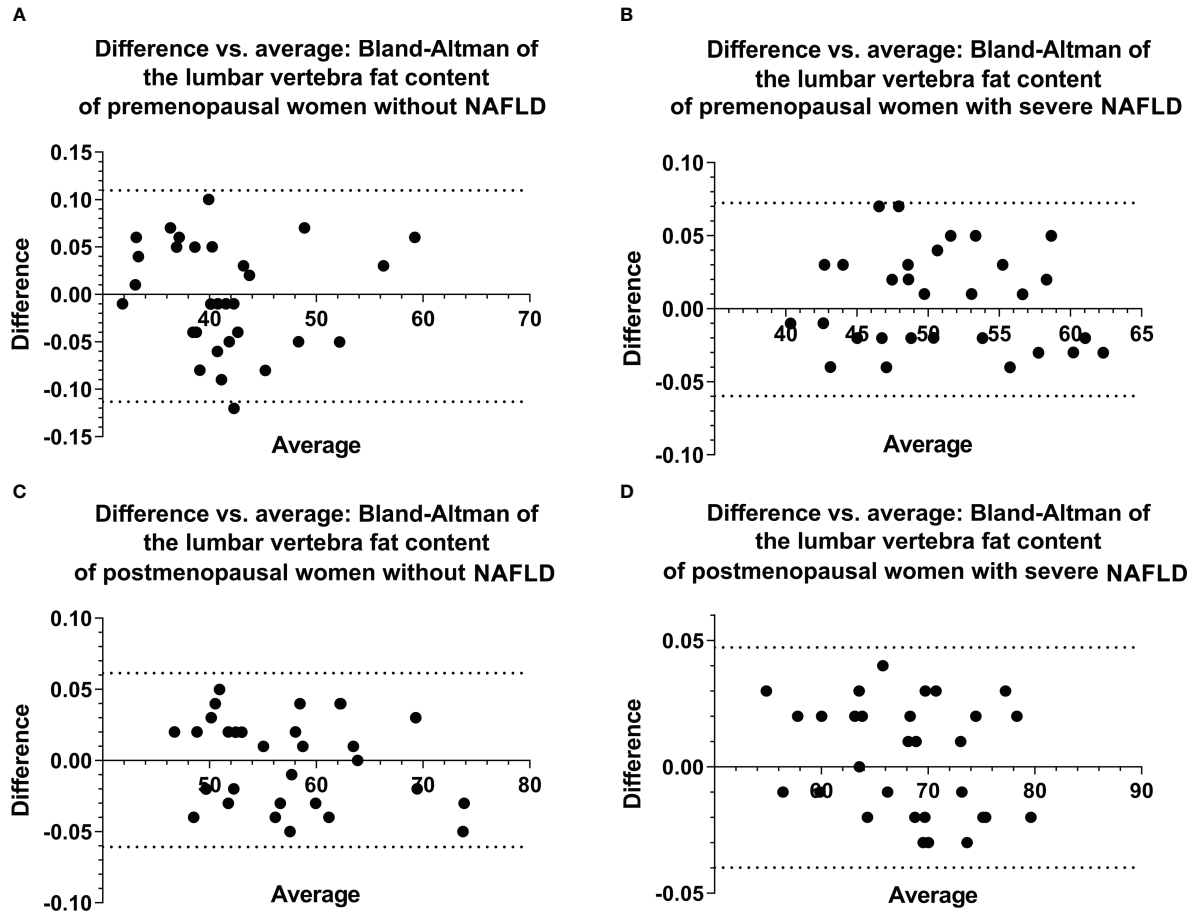

FIGURE 2
Bland–Altman plots of ROI-based FF values for the lumbar vertebra were obtained from two observations of the first cohort **(A–D)**, showing excellent correlations, a negligible bias, and 95% limits of agreement of approximately ± 0.113 or less. ROI, region of interest, FF, fat fraction.

10.3389/fendo.2022.1099919

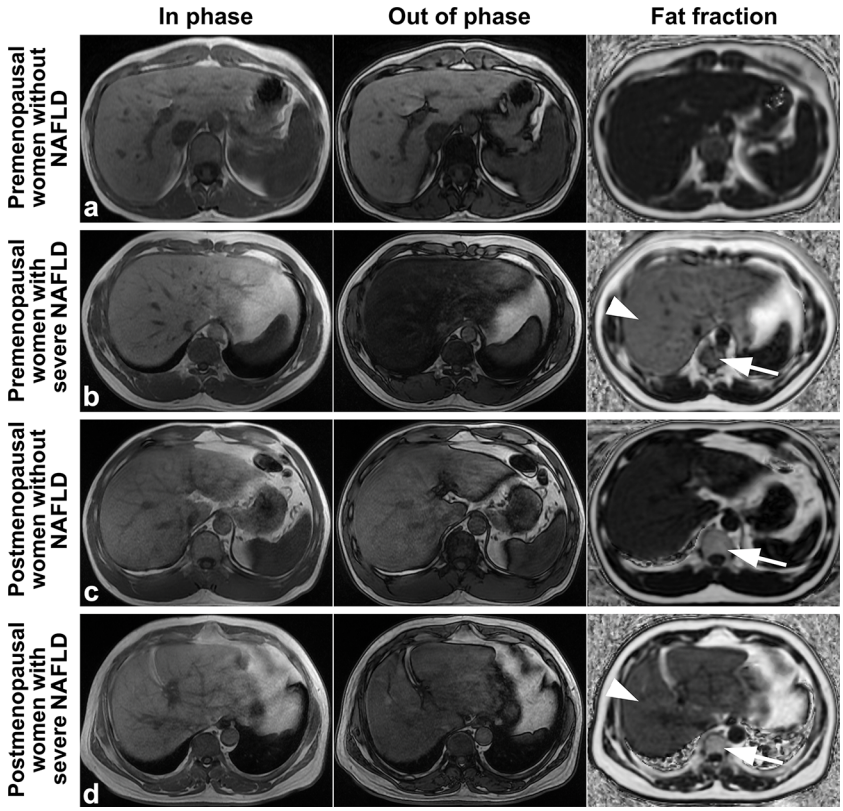

FIGURE 3
Images of premenopausal and postmenopausal women without NAFLD or with severe NAFLD **(A)** a 47 years old premenopausal woman without NAFLD; **(B)** a 45 years old premenopausal woman with severe NAFLD; **(C)** a 55 years old postmenopausal woman without NAFLD; and **(D)** a 57 years old postmenopausal woman with severe NAFLD). The fat deposition was visible by the decrease in the signal in the axial conventional T1-in phase and out-of-phase images of the mDIXON-Quant sequence and was measured in the fraction map of the IDEAL-IQ sequence. The example showed that fat deposition in a lumbar vertebra (arrows) increased after menopause in patients without NAFLD or with severe NAFLD (arrowheads). IDEAL-IQ, iterative decomposition of water and fat with echo asymmetry and least-squares estimation.

women, the FF_{lumbar} were higher in patients with severe NAFLD than in patients without NAFLD (premenopausal women: 50.95 ± 6.03 vs. 41.58 ± 6.37, $p < 0.001$, t = 5.85; postmenopausal women: 68.11 ± 6.49 vs. 57.48 ± 7.38, $p < 0.001$, t = 5.92). Additionally, in patients with severe NAFLD or without NAFLD, the FF_{lumbar} were higher in postmenopausal women than in premenopausal women (severe NAFLD: 68.11 ± 6.49 vs. 50.94 ± 6.03, $p < 0.001$, t = 10.62; without NAFLD: 57.48 ± 7.38 vs. 41.58 ± 6.37, $p < 0.001$, t = 8.93). Significant differences in the FF_{lumbar} were observed between patients without NAFLD and with severe NAFLD in both premenopausal and postmenopausal women (Figures 4A, B).

TABLE 3 The fat fraction values of the lumbar vertebra and liver in the first cohort.

Characteristics	Severe NAFLD-pre	Without NAFLD-pre	Severe NAFLD-post	Without NAFLD-post	P values			
					Severe NAFLD-pre vs. Without NAFLD-pre	Severe NAFLD-post vs. Without NAFLD-post	Severe NAFLD-pre vs. Severe NAFLD-post	Without NAFLD-pre vs. Without NAFLD-post
FF_{lumbar} (mean ± SD)	50.95 ± 6.03	41.58 ± 6.37	68.11 ± 6.49	57.48 ± 7.38	= 0.001	= 0.001	= 0.001	= 0.001
FF_{liver} (mean ± SD)	34.10 ± 4.79	2.85 ± 0.94	34.17 ± 4.60	3.13 ± 0.91	= 0.001	= 0.001	0.95	0.24

SD, standard deviation; FF_{liver}, fat fraction values of the liver; FF_{lumbar}, fat fraction values of lumbar; NAFLD, non-alcoholic fatty liver disease; Severe NAFLD-pre, Premenopausal with severe NAFLD; Without NAFLD-pre, Premenopausal without NAFLD; Severe NAFLD-post, Postmenopausal with severe NAFLD; Without NAFLD-post, Postmenopausal without NAFLD.

A high correlation was detected between FF_{lumbar} and the FF_{liver} in women with severe NAFLD (premenopausal women: r = 0.76, $p < 0.01$; postmenopausal women: r = 0.82, $p < 0.01$) (Table 4; Figures 4C–F). The correlation between FF_{lumbar} and the FF_{liver} was better in postmenopausal women with severe NAFLD than in premenopausal women with severe NAFLD.

Examples of fat deposition in obese patients and normal-weight patients in the second cohort before or after menopause

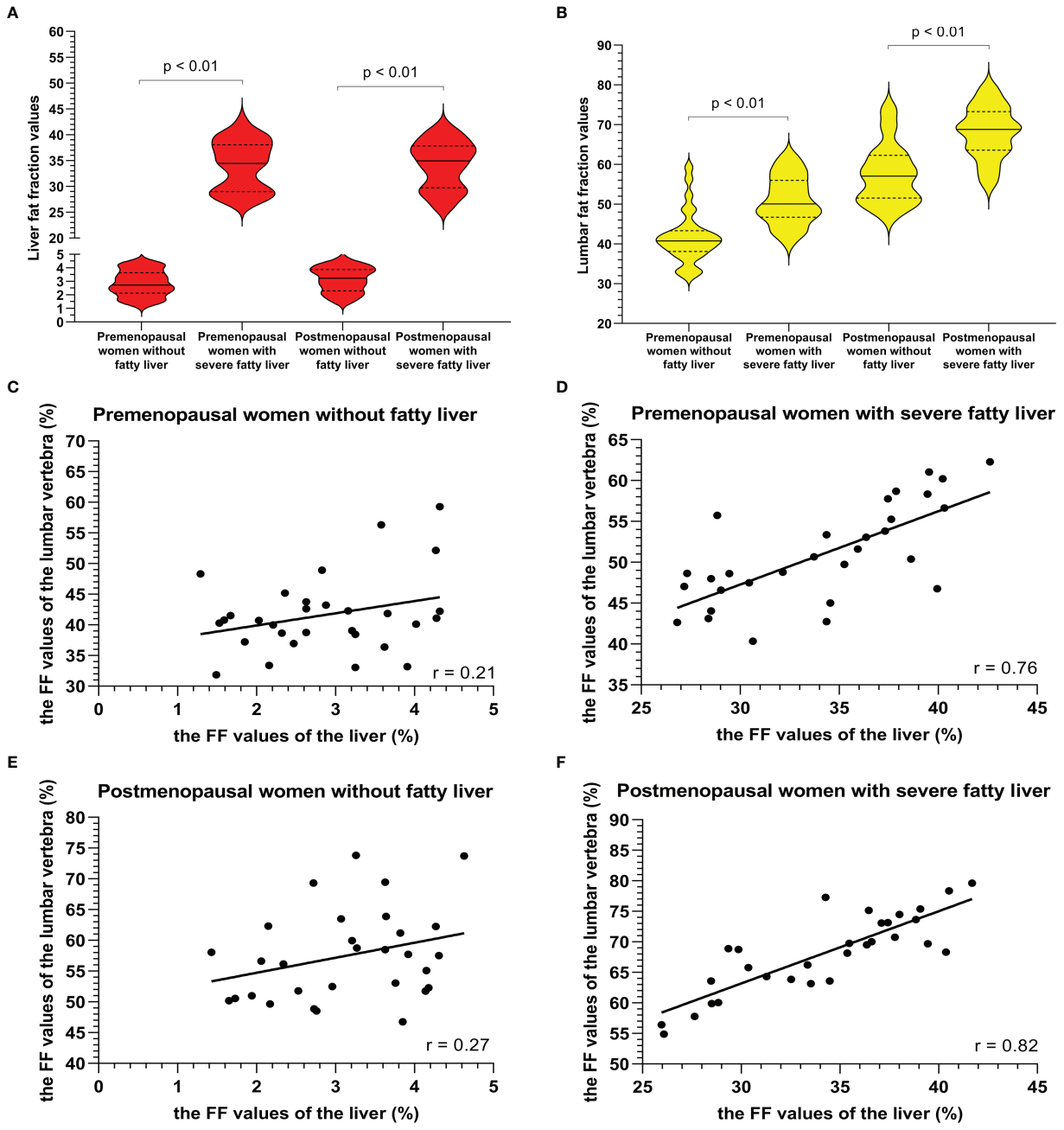

FIGURE 4
The violin plot analyzing the fat fraction values for the liver fat content **(A)** and lumbar fat content **(B)** in four groups (premenopausal women without NAFLD, premenopausal women with severe NAFLD, postmenopausal women without NAFLD, and postmenopausal women with severe NAFLD; 30 subjects in each group) confirmed that the lumbar fat content of patients with severe NAFLD more than that without NAFLD before menopause ($p < 0.01$) and after menopause ($p < 0.01$). The correlation plots for the correlations between FF_{lumbar} and the FF_{liver} **(C–F)** The correlation between FF_{lumbar} and the FF_{liver} in premenopausal **(C)** or postmenopausal **(E)** women without NAFLD was no different. A high correlation was detected between FF_{lumbar} and the FF_{liver} in women with severe NAFLD (premenopausal women: $r = 0.76$, $p < 0.01$; postmenopausal women: $r = 0.82$, $p < 0.01$) **(D, F)**.

10.3389/fendo.2022.1099919

TABLE 4 The correlation coefficients between the FF_{liver}, FF_{SAT}, and FF_{lumbar}.

	Group	r	95% confidence interval	p value
FF_{liver} vs. FF_{lumbar}	Premenopausal women without NAFLD	0.21	-0.10 to 0.53	0.13
	Premenopausal women with severe NAFLD	0.76	0.51 to 0.89	< 0.01
	Postmenopausal women without NAFLD	0.27	-0.11 to 0.58	0.15
	Postmenopausal women with severe NAFLD	0.82	0.65 to 0.91	< 0.01
FF_{SAT} vs. FF_{lumbar}	Premenopausal women with normal weight	0.21	-0.12 to 0.51	0.28
	Premenopausal women with obesity	0.35	0.07 to 0.63	0.19
	Postmenopausal women with normal weight	0.23	-0.15 to 0.56	0.22
	Postmenopausal women with obesity	0.39	0.12 to 0.69	0.17

FF_{liver}, fat fraction values of the liver; FF_{SAT}, fat fraction values of subcutaneous adipose tissue; FF_{lumbar}, fat fraction values of lumbar; NAFLD, non-alcoholic fatty liver disease.

are shown in Figure 5. The mean FF_{lumbar} and the FF_{SAT} were measured separately in the four groups and are summarized in Table 5. Both in premenopausal women and postmenopausal women, no significant difference in the FF_{lumbar} was observed obese patients and in normal-weight patients (premenopausal women: 44.15 ± 4.73 vs. 41.17 ± 5.49, p = 0.113, t = 5.18; postmenopausal women: 61.39 ± 6.75 vs. 57.15 ± 6.83, p = 0.092, t = 6.42). Postmenopausal women had higher FF_{lumbar} than premenopausal women, regardless of the presence of obesity (obese: 61.39 ± 6.75 vs. 42.98 ± 4.73, p < 0.001, t = 12.23; normal weight: 57.15 ± 6.83 vs. 41.17 ± 5.49, p < 0.001, t = 9.99). Significant differences in the FF values of lumbar vertebra were observed between premenopausal women and postmenopausal women, but not between patients with obesity or without obesity (Figures 6A, B). No statistically significant correlation was found between the FF_{lumbar} and the FF_{SAT} in this cohort (Table 4; Figures 6C-F).

Discussion

Our study focused on the association between abdominal adipose tissue and vertebral marrow fat in middle-aged women using the IDEAL-IQ methodology. Our analyses indicated that the vertebral marrow fat content was increased in postmenopausal women and that liver fat deposition potentially aggravated this situation. However, no statistically significant correlation was observed between vertebral marrow fat and subcutaneous fat deposition.

Traditionally, adipose tissue was postulated to exert a protective effect on bone. Researchers have speculated that this protective effect may be due to the stimulation of bone formation by the high mechanical load associated with overweight and obesity (11). However, a recent study showed that different local fat compartments are responsible for different metabolic effects and different effects on bone (30, 31). Wang et al. indicated that SAT has no relation to bone mineral density (BMD) in Chinese women < 55 years old (32). In contrast, Melissa et al. revealed that VAT and SAT had inverse associations with BMD in obese adolescent girls, with SAT exhibiting positive associations and VAT showing negative associations (33). In our study, SAT had no correction with vertebral marrow fat in postmenopausal women. Our results are consistent with a study of older Chinese women (32). However, the results are different from studies of obese adolescent girls (30, 33). This difference is probably because the population age in our study was much older than that in the studies of young girls, and

TABLE 5 The fat fraction values of lumbar vertebra and subcutaneous fat in the second cohort.

Characteristics	Obese-pre	Normal weight-pre	Obese-post	Normal weight-post	P values			
					Obese-pre vs. Normal weight-pre	Obese-post vs. Normal weight-post	Obese-pre vs. Obese-post	Normal weight-pre vs. Normal weight-post
FF_{lumbar} (mean ± SD)	44.15 ± 4.73	41.17 ± 5.49	61.39 ± 6.75	57.15 ± 6.83	0.11	0.09	= 0.001	= 0.001
FF_{SAT} (mean ± SD)	92.57 ± 0.92	81.15 ± 2.90	95.74 ± 0.87	80.88 ± 2.92	= 0.001	= 0.001	0.41	0.73

SD, standard deviation; SAT, subcutaneous adipose tissue; FF_{SAT}, fat fraction values of subcutaneous adipose tissue; FF_{lumbar}, fat fraction values of lumbar; Obese-pre, Premenopausal with obese; Normal weight-pre, Premenopausal with normal weight; Obese-post, Postmenopausal with obese; Normal weight-post, Postmenopausal with normal weight.

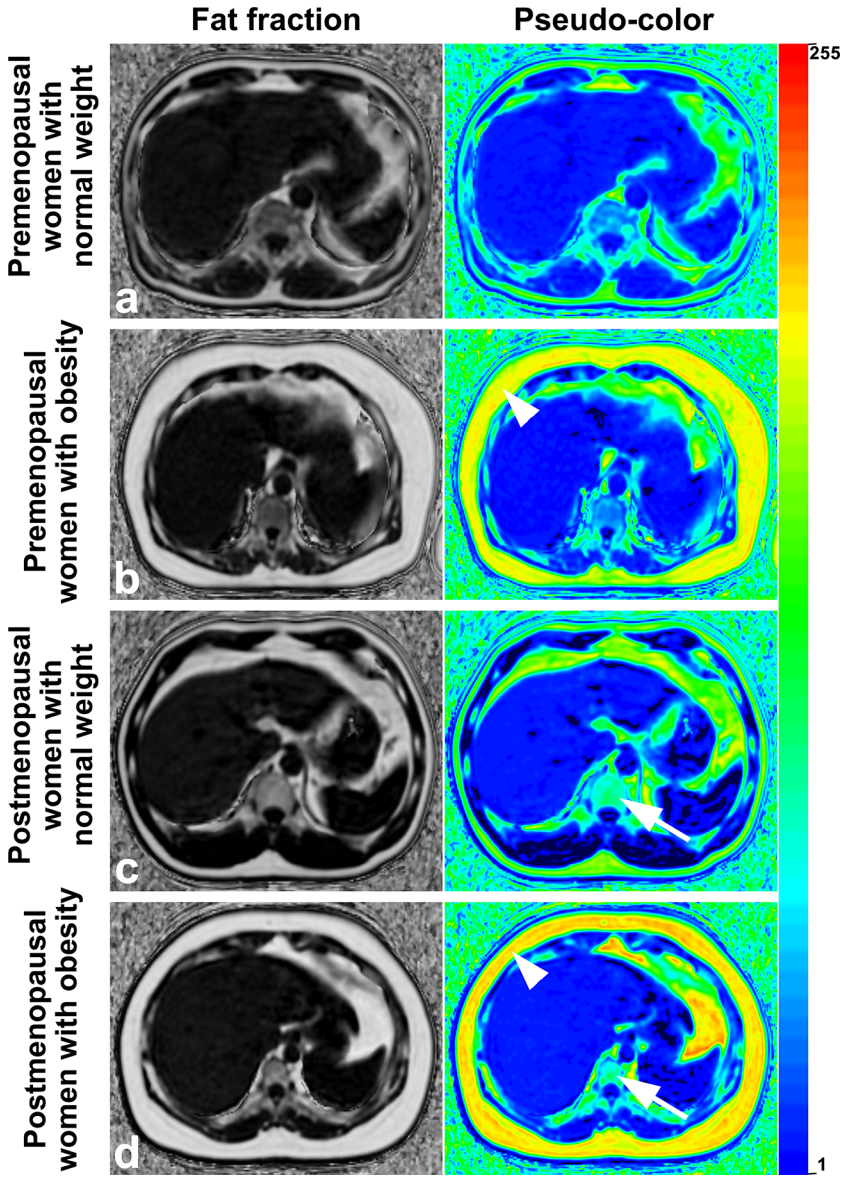

FIGURE 5
Images of premenopausal and postmenopausal women with obesity or normal weight patients **(A)** a 46 years old premenopausal woman with normal weight; **(B)** a 44 years old premenopausal woman with obesity; **(C)** a 53 years old postmenopausal woman with normal weight; and **(D)** a 56 years old postmenopausal woman with obesity). Fat deposition in subcutaneous sites (arrowheads) and lumbar vertebrae (arrows) was visible and was measured in the fraction map and pseudocolor images of the IDEAL-IQ sequence. Examples showed that fat deposition in the lumbar vertebra increased after menopause in both obese patients and normal-weight patients. IDEAL-IQ, iterative decomposition of water and fat with echo asymmetry and least-squares estimation.

the estrogen level of the population in our study was much lower than that in young girls.

NAFLD is strongly associated with abdominal obesity and metabolic disturbances (13). Preliminary data also suggest that NAFLD may be associated with other common and chronic debilitating conditions, particularly low BMD (14, 34). Our study found that liver fat deposition potentially aggravated vertebral marrow fat content in postmenopausal women. Adipose-modulated biochemical signals may explain some associations between fat mass and bone metabolism. Adipose tissue secretes various inflammatory cytokines and hormones, such as tumor necrosis factor-α and interleukin-6. These inflammatory cytokines promote osteoclast differentiation and activation and inhibit osteoclast apoptosis (34, 35). NAFLD may participate in bone metabolism *via* the systemic release of multiple proinflammatory, procoagulant, pro-oxidant and profibrogenic mediators and/or *via*

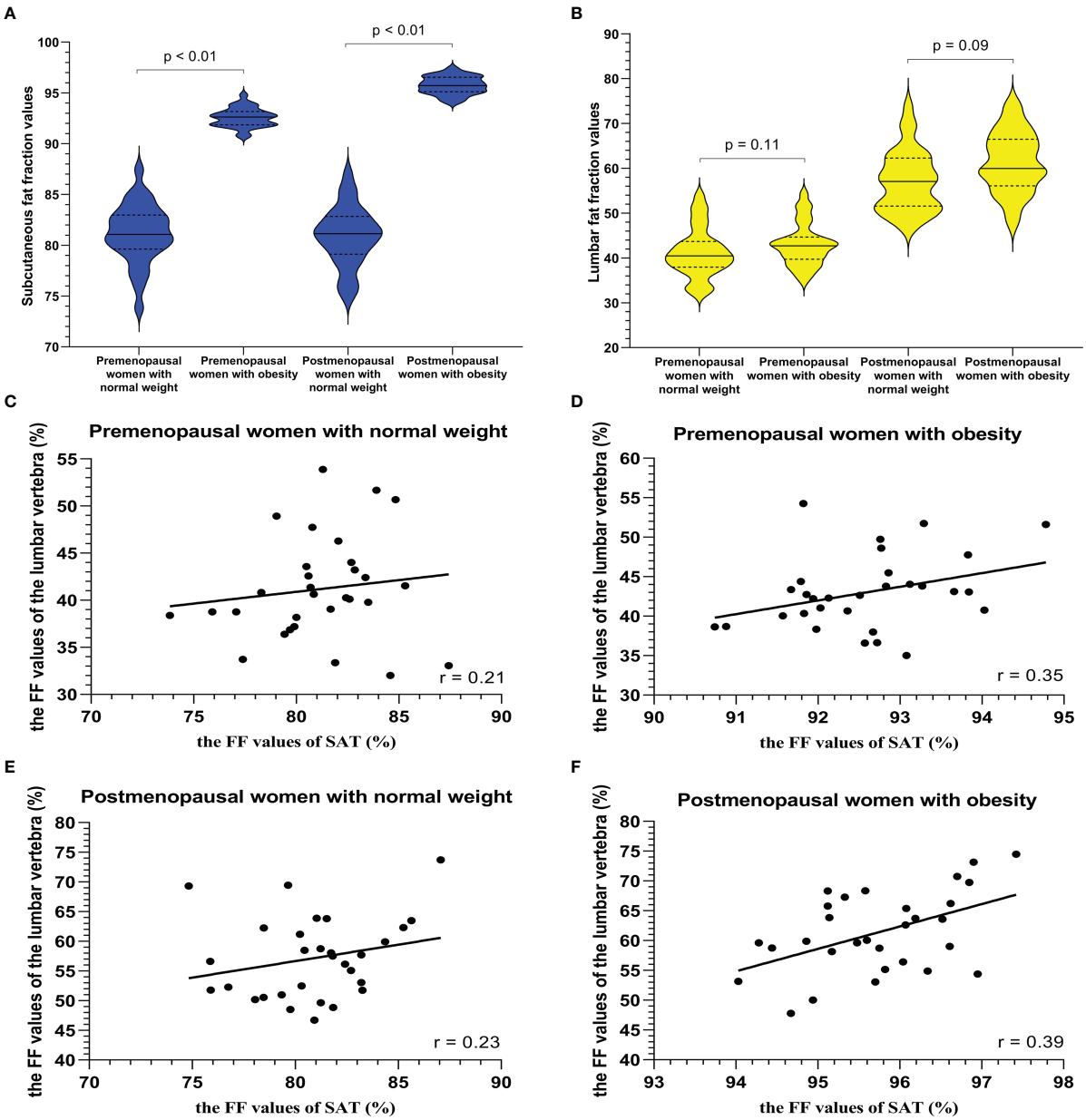

FIGURE 6
The violin plot analyzing fat fraction values for a subcutaneous site **(A)** and lumbar vertebra **(B)** in four groups (premenopausal women with normal weight, premenopausal women with obesity (BMI > 30 kg/m2), postmenopausal women with normal weight, and postmenopausal women with obesity (BMI > 30 kg/m2); 30 subjects in each group) confirmed that there is no statistical difference between the lumbar fat content of obese patients and that of normal-weight patients before menopause (p = 0.11) and after menopause (p = 0.09), and the subcutaneous fat content in the obese patients more than that in normal weight subjects (p < 0.01). BMI = body mass index. The correlation plots for the correlations between FF_{lumbar} and the FF_{SAT} **(C–F)** The correlation between FF_{lumbar} and the FF_{SAT} in premenopausal or postmenopausal women without or with obesity was no different **(C–F)**.

the direct effect on hepatic and systemic insulin resistance (35, 36). The previousstudy also reported a positive correlation between hepatic fat content and bone marrow fat content in children with known or suspected NAFLD (37). However, the correlation in our study was much higher than that in this previous study. This difference is probably due to the subjects enrolled were not the same. In our study, subjects were over 45 years old which was much older than that in the previous. Besides, the patients with severe NAFLD were enrolled in our study. Estrogen level and varying degrees of NAFLD severity may be the reason for the above results.

Osteoporosis is characterized by a low BMD and progressive deterioration of the bone microarchitecture. The fat content in bone marrow is negatively correlated with BMD because the lost bone mass in the vertebral space is infilled with fatty bone marrow (38, 39). Therefore, the increase in vertebral marrow fat may reflect the progression of osteoporosis. Our findings are consistent with previous studies revealing that the menopause transition is associated with increased central adiposity (6, 36, 40) and confirmed a higher incidence of osteoporosis in postmenopausal women than in premenopausal women.

Our study has several limitations. First, our study was a retrospective cross-sectional study. As a cross-sectional study, we are unable to establish a causal relationship between liver fat and vertebral marrow fat. A further longitudinal prospective study with a large sample size is warranted to validate the current findings. Second, we were unable to control for the potential factors affecting bone loss and vertebral marrow fat deposition, such as dietary calcium intake or vitamin D supplementation. Third, this study did not focus on the thickness or volume of subcutaneous fat but on the percentage of fat in subcutaneous fat (mainly composed of fat and water). Finally, our study population included only middle-aged women, and our findings cannot be extrapolated to young women or the male skeleton. This approach limits the generalizability of the results but should not affect the internal validity.

Conclusions

This study describes a precise and noninvasive IDEAL-IQ technology to measure the fat content of vertebral marrow, SAT, and liver in pre- or postmenopausal women. FF_{lumbar} was significantly higher in postmenopausal women than in premenopausal women. FF_{lumbar} was higher in patients with severe NAFLD than in patients without NAFLD, but FF_{lumbar} was not significantly different between obese patients with subcutaneous fat deposition and normal-weight patients, indicating that fat deposition in the vertebral marrow was significantly associated with liver fat deposition in postmenopausal women with severe NAFLD. Furthermore, our findings support the hypothesis that liver fat deposition is relative to vertebral fat deposition (which may cause osteoporosis) in postmenopausal women.

Data availability statement

The original contributions presented in the study are included in the article/Supplementary Material. Further inquiries can be directed to the corresponding authors.

Ethics statement

The studies involving human participants were reviewed and approved by the Institutional Research Ethics Committee of the Third Affiliated Hospital of Sun Yat-Sen University (02-005-01). The patients/participants provided their written informed consent to participate in this study.

Author contributions

C-SZ, R-MG: Data collection, Data analysis, Manuscript writing. H-QW, W-SL, X-WL, F-YZ, and XZ: Data collection. H-JH, Q-LL, L-SS, and R-MG: Data analysis, Manuscript editing. R-MG: Project development, Data analysis, Manuscript editing. All authors contributed to the article and approved the submitted version.

Funding

This study was supported by grants from the National Natural Science Foundation of China (No. 81801757), Guangdong Basic and Applied Basic Research Foundation (No. 2022A1515010369, 2019A1515012051), and Guangzhou Science and Technology Plan (No. 202201020421).

Conflict of interest

The authors declare that the research was conducted in the absence of any commercial or financial relationships that could be construed as a potential conflict of interest.

Publisher's note

All claims expressed in this article are solely those of the authors and do not necessarily represent those of their affiliated organizations, or those of the publisher, the editors and the reviewers. Any product that may be evaluated in this article, or claim that may be made by its manufacturer, is not guaranteed or endorsed by the publisher.

Supplementary material

The Supplementary Material for this article can be found online at: https://www.frontiersin.org/articles/10.3389/fendo.2022.1099919/full#supplementary-material

References

1. Zhang LY, Li SL, Hao S, Yuan Z. Quantification of fat deposition in bone marrow in the lumbar vertebra by proton MRS and in-phase and out-of-phase MRI for the diagnosis of osteoporosis. *J X-Ray Sci Technol* (2016) 24(2):257–66. doi: 10.3233/XST-160549

2. Devlin MJ, Rosen CJ. The bone-fat interface: basic and clinical implications of marrow adiposity. *Lancet Diabetes Endo* (2015) 3(2):141–7. doi: 10.1016/S2213-8587(14)70007-5

3. Kugel H, Jung C, Schulte O, Heindel W. Age- and sex-specific differences in the h-1-spectrum of vertebral bone marrow. *J Magn Reson Imaging* (2001) 13 (2):263–8. doi: 10.1002/1522-2586(200102)13:2<263::aid-jmri1038>3.0.co;2-m

4. Wang L, Yin L, Zhao Y, Su Y, Sun W, Liu Y, et al. Muscle density discriminates hip fracture better than computed tomography X-ray absorptiometry hip areal bone mineral density. *J Cachexia Sarcopenia Muscle.* (2020) 11(6):1799–812. doi: 10.1002/jcsm.12616

5. Justesen J, Stenderup K, Ebbesen EN, Mosekilde L, Steiniche T, Kassem M. Adipocyte tissue volume in bone marrow is increased with aging and in patients with osteoporosis. *Biogerontology* (2001) 2(3):165–71. doi: 10.1023/a:1011513223894

6. Khosla S, Monroe DG. Regulation of bone metabolism by sex steroids. *Cold Spring Harb Perspect Med* (2018) 8(1):a031211. doi: 10.1101/cshperspect.a031211

7. Khosla S, Oursler MJ, Monroe DG. Estrogen and the skeleton. *Trends Endocrinol Metab* (2012) 23(11):576–81. doi: 10.1016/j.tem.2012.03.008

8. van der Leeuw J, Wassink AM, van der Graaf Y, Westerveld HE, Visseren FL. Second manifestations of ARTerial disease (SMART) study group. age-related differences in abdominal fat distribution in premenopausal and postmenopausal women with cardiovascular disease. *Menopause* (2013) 20(4):409–17. doi: 10.1097/gme.0b013e31827212a5

9. Lv Y, Wang F, Sheng Y, Xia F, Jin Y, Ding G, et al. Estrogen supplementation deteriorates visceral adipose function in aged postmenopausal subjects *via* Gas5 targeting IGF2BP1. *Exp Gerontol.* (2022) 163:111796. doi: 10.1016/j.exger.2022.111796

10. Gkastaris K, Goulis DG, Potoupnis M, Anastasilakis AD, Kapetanos G. Obesity, osteoporosis and bone metabolism. *J Musculoskelet Neuronal Interact* (2020) 20(3):372–81.

11. Yang SM, Nguyen ND, Center JR, Eisman JA, Nguyen TV. Association between abdominal obesity and fracture risk: a prospective study. *J Clin Endocr Metab* (2013) 98(6):2478–83. doi: 10.1210/jc.2012-2958

12. Yoo HJ, Park MS, Yang SJ, Kim TN, Lim K, Kang HJ, et al. The differential relationship between fat mass and bone mineral density by gender and menopausal status. *J Bone Miner Metab* (2012) 30(1):47–53. doi: 10.1007/s00774-011-0283-7

13. Andronescu CI, Purcarea MR, Babes PA. Nonalcoholic fatty liver disease: epidemiology, pathogenesis and therapeutic implications. *J Med Life* (2018) 11(1):20–3.

14. Zubáňová V, Červinková Z, Kučera O, Palička V. The connection between MicroRNAs from visceral adipose tissue and non-alcoholic fatty liver disease. *Acta Med* (2021) 64(1):1–7. doi: 10.14712/18059694.2021.1

15. Targher G, Lonardo A, Rossini M. Nonalcoholic fatty liver disease and decreased bone mineral density: is there a link? *J Endocrinol Invest* (2015) 38 (8):817–25. doi: 10.1007/s40618-015-0315-6

16. Schellinger D, Lin CS, Fertikh D, Lee JS, Lauerman WC, Henderson F, et al. Normal lumbar vertebrae: anatomic, age, and sex variance in subjects at proton MR spectroscopy - initial experience. *Radiology* (2000) 215(3):910–6. doi: 10.1148/radiology.215.3.r00jn42910

17. Kim H, Taksali SE, Dufour S, Befroy D, Goodman TR, Petersen KF, et al. Comparative MR study of hepatic fat quantification using single-voxel proton spectroscopy, two-point dixon and three-point IDEAL. *Magn Reson Med* (2008) 59 (3):521–7. doi: 10.1002/mrm.21561

18. Aoki T, Yamaguchi S, Kinoshita S, Hayashida Y, Korogi Y. Quantification of bone marrow fat content using iterative decomposition of water and fat with echo asymmetry and least-squares estimation (IDEAL): reproducibility, site variation and correlation with age and menopause. *Br J Radiol* (2016) 89(1065):20150538. doi: 10.1259/bjr.20150538

19. Kang GH, Cruite I, Shiehmorteza M, Wolfson T, Gamst AC, Hamilton G, et al. Reproducibility of MRI-determined proton density fat fraction across two different MR scanner platforms. *J Magn Reson Imaging* (2011) 34(4):928–34. doi: 10.1002/jmri.22701

20. Johnson BL, Schroeder ME, Wolfson T, Gamst AC, Hamilton G, Shiehmorteza M, et al. Effect of flip angle on the accuracy and repeatability of hepatic proton density fat fraction estimation by complex data-based, T1-independent, T2*-corrected, spectrum-modeled MRI. *J Magn Reson Imaging* (2014) 39(2):440–7. doi: 10.1002/jmri.24153

21. Tang A, Desai A, Hamilton G, Wolfson T, Gamst A, Lam J, et al. Accuracy of MR imaging-estimated proton density fat fraction for classification of dichotomized histologic steatosis grades in nonalcoholic fatty liver disease. *Radiology* (2015) 274(2):416–25. doi: 10.1148/radiol.14140754

22. Idilman IS, Aniktar H, Idilman R, Kabacam G, Savas B, Elhan A, et al. Hepatic steatosis: quantification by proton density fat fraction with MR imaging versus liver biopsy. *Radiology* (2013) 267(3):767–75. doi: 10.1148/radiol.13121360

23. Permutt Z, Le TA, Peterson MR, Seki E, Brenner DA, Sirlin C, et al. Correlation between liver histology and novel magnetic resonance imaging in adult patients with nonalcoholic fatty liver disease - MRI accurately quantifies hepatic steatosis in NAFLD. *Aliment Pharm Ther* (2012) 36(1):22–9. doi: 10.1111/j.1365-2036.2012.05121.x

24. Guo YH, Chen YJ, Zhang XT, Mei YJ, Yi PW, Wang Y, et al. Magnetic susceptibility and fat content in the lumbar spine of postmenopausal women with varying bone mineral density. *J Magn Reson Imaging* (2019) 49(4):1020–8. doi: 10.1002/jmri.26279

25. Idilman IS, Tuzun A, Savas B, Elhan AH, Celik A, Idilman R, et al. Quantification of liver, pancreas, kidney, and vertebral body MRI-PDFF in nonalcoholic fatty liver disease. *Abdom Imaging* (2015) 40(6):1512–9. doi: 10.1007/s00261-015-0385-0

26. Shen N, Li XY, Zheng S, Zhang L, Fu Y, Liu XM, et al. Automated and accurate quantification of subcutaneous and visceral adipose tissue from magnetic resonance imaging based on machine learning. *Magn Reson Imaging* (2019) 64:28–36. doi: 10.1016/j.mri.2019.04.007

27. Gibson CJ, Huang AJ, McCaw B, Subak LL, Thom DH, Van Den Eeden SK. Associations of intimate partner violence, sexual assault, and posttraumatic stress disorder with menopause symptoms among midlife and older women. *JAMA Intern Med* (2019) 179(1):80–7. doi: 10.1001/jamainternmed.2018.5233

28. Guo Z, Blake GM, Li K, Liang W, Zhang W, Zhang Y, et al. Liver fat content measurement with quantitative CT validated against MRI proton density fat fraction: a prospective study of 400 healthy volunteers. *Radiology* (2020) 294 (1):89–97. doi: 10.1148/radiol.2019190467

29. Dikaiou P, Björck L, Adiels M, Lundberg CE, Mandalenakis Z, Manhem K, et al. Obesity, overweight and risk for cardiovascular disease and mortality in young women. *Eur J Prev Cardiol* (2021) 28(12):1351–9. doi: 10.1177/2047487320908983

30. Crivelli M, Chain A, da Silva ITF, Waked AM, Bezerra FF. Association of visceral and subcutaneous fat mass with bone density and vertebral fractures in women with severe obesity. *J Clin Densitom.* (2021) 24(3):397–405. doi: 10.1016/j.jocd.2020.10.005

31. Yamaguchi T, Kanazawa I, Yamamoto M, Kurioka S, Yamauchi M, Yano S, et al. Associations between components of the metabolic syndrome versus bone mineral density and vertebral fractures in patients with type 2 diabetes. *Bone* (2009) 45(2):174–9. doi: 10.1016/j.bone.2009.05.003

32. Wang L, Wang W, Xu L, Cheng XG, Ma YM, Liu D, et al. Relation of visceral and subcutaneous adipose tissue to bone mineral density in Chinese women. *Int J Endocrinol* (2013) 2013:378632. doi: 10.1155/2013/378632

33. Russell M, Mendes N, Miller KK, Rosen CJ, Lee H, Klibanski A, et al. Visceral fat is a negative predictor of bone density measures in obese adolescent girls. *J Clin Endocrinol Metab* (2010) 95(3):1247–55. doi: 10.1210/jc.2009-1475

34. Zhu X, Yan H, Chang X, Xia M, Zhang L, Wang L, et al. Association between non-alcoholic fatty liver dis-ease-associated hepatic fibrosis and bone mineral density in postmenopausal women with type 2 diabetes or impaired glucose regulation. *BMJ Open Diabetes Res Care* (2020) 8(1):e000999. doi: 10.1136/bmjdrc-2019-000999

35. Cao JJ. Effects of obesity on bone metabolism. *J Orthop Surg Res* (2011) 6:30. doi: 10.1186/1749-799X-6-30

36. Yu AH, Duan-Mu YY, Zhang Y, Wang L, Guo Z, Yu YQ, et al. Correlation between non-alcoholic fatty liver disease and visceral adipose tissue in non-obese Chinese adults: A CT evaluation. *Korean J Radiol* (2018) 19(5):923–9. doi: 10.3348/kjr.2018.19.5.923

37. Yu NY, Wolfson T, Middleton MS, Hamilton G, Gamst A, Angeles JE, et al. Bone marrow fat content is correlated with hepatic fat content in paediatric non-alcoholic fatty liver disease. *Clin Radiol* (2017) 72(5):425.e9–425.e14. doi: 10.1016/j.crad.2016.11.017

38. Di Iorgi N, Rosol M, Mittelman SD, Gilsanz V. Reciprocal relation between marrow adiposity and the amount of bone in the axial and appendicular skeleton of young adults. *J Clin Endocr Metab* (2008) 93 (6):2281–6. doi: 10.1210/jc.2007-2691

39. Schwartz AV, Sigurdsson S, Hue TF, Lang TF, Harris TB, Rosen CJ, et al. Vertebral bone marrow fat associated with lower trabecular BMD and prevalent vertebral fracture in older adults. *J Clin Endocr Metab* (2013) 98(6):2294–300. doi: 10.1210/jc.2012-3949

40. Igarashi Y, Tanaka M, Okada H, Hashimoto Y, Kumagai M, Yamaoka M, et al. Visceral adipose tissue quality was associated with nonalcoholic fatty liver disease, independent of its quantity. *Nutr Metab Cardiovasc Dis* (2022) 32 (4):973–80. doi: 10.1016/j.numecd.2022.01.009

frontiers | Frontiers in Endocrinology

TYPE Original Research
PUBLISHED 23 March 2023
DOI 10.3389/fendo.2023.1117438

OPEN ACCESS

EDITED BY
Jiang Du,
University of California, San Diego,
United States

REVIEWED BY
Dina Moazamian,
University of California, San Diego,
United States
Meiling Jin,
Beijing Chaoyang Hospital, Capital Medical University, China
Bhavsimran Malhi,
University of California, San Diego,
United States

*CORRESPONDENCE
Xiaoguang Cheng
xiao65@263.net
Dongliang Zhang
zhangdongliang@Jst-hosp.com.cn

†These authors have contributed equally to this work and share first authorship

‡These authors have contributed equally to this work

SPECIALTY SECTION
This article was submitted to Bone Research, a section of the journal Frontiers in Endocrinology

RECEIVED 06 December 2022
ACCEPTED 09 March 2023
PUBLISHED 23 March 2023

CITATION
Fu C, Yan D, Wang L, Duan F, Gu D, Yao N, Sun M, Wang D, Lin X, Wu Y, Wang X, Cheng X and Zhang D (2023) High prevalence of sarcopenia and myosteatosis in patients undergoing hemodialysis. *Front. Endocrinol.* 14:1117438. doi: 10.3389/fendo.2023.1117438

High prevalence of sarcopenia and myosteatosis in patients undergoing hemodialysis

Chen Fu[1†], Dong Yan[2†], Ling Wang[2], Fangfang Duan[3], Dalong Gu[2], Ning Yao[2], Mingke Sun[2], Di Wang[1], Xuya Lin[1], Yanglei Wu[4], Xiaofei Wang[1], Xiaoguang Cheng[2*‡] and Dongliang Zhang[1*‡]

[1]Department of Nephrology, Beijing Jishuitan Hospital, Beijing, China, [2]Department of Radiology, Beijing Jishuitan Hospital, Beijing, China, [3]Clinical Epidemiology Research Center, Beijing Jishuitan Hospital, Beijing, China, [4]MR Collaboration, Siemens Healthineers Ltd., Beijing, China

Background and purpose: Sarcopenia is highly prevalent (28.5–40.3%) in patients undergoing hemodialysis and leads to poor clinical outcomes. However, the association between muscle quality and sarcopenia in patients receiving hemodialysis remains unclear. Therefore, we aimed to explore the association between muscle cross-sectional area (CSA) and proton-density fat-fraction (PDFF) in patients with sarcopenia undergoing hemodialysis.

Methods: Seventy-six patients undergoing hemodialysis for > 3 months were enrolled. Their handgrip strength (HGS), short physical performance battery (SPPB) performance, and appendicular skeletal muscle mass index (ASMI) were measured. Sarcopenia was defined using the Asian Working Group for Sarcopenia 2019 consensus update. All patients underwent quantitative magnetic resonance imaging. CSA and PDFF were measured for the thigh, trunk, and gluteus muscles.

Results: The prevalence of probable, confirmed, and severe sarcopenia in this study was 73.7%, 51.3%, and 22.4%, respectively. Older age (OR: 1.061, $P < 0.003$); lower body mass index (BMI) (OR: 0.837, $P = 0.008$), albumin (OR: 0.765, $P = 0.004$), prealbumin (OR: 0.987, $P = 0.001$), predialysis blood urea nitrogen (BUN) (OR: 0.842, $P < 0.001$), predialysis creatinine (OR: 0.993, $P < 0.001$), phosphorus (OR: 0.396, $P = 0.047$); lower CSA of the thigh (OR: 0.58, $P = 0.035$), third lumbar (L3) trunk (OR: 0.37, $P = 0.004$), gluteus minimus and medius (OR: 0.28, $P = 0.001$), and gluteus maximus (OR: 0.28, $P= 0.001$); and higher PDFF of the thigh (OR: 1.89, $P = 0.036$) and L3 trunk (OR: 1.71, $P = 0.040$) were identified as sarcopenia risk factors. The gluteus minimus and medius CSA was lower in patients with sarcopenia than in those without after adjusting for age and BMI (OR: 0.37, $P = 0.017$). Higher thigh ($P = 0.031$) and L3 trunk ($P = 0.006$) muscle PDFF were significantly associated with lower HGS. Furthermore, higher thigh ($P = 0.011$) and L3 trunk ($P = 0.010$) muscle PDFF were also inversely correlated with lower ASMI.

Conclusion: Our findings demonstrate the high prevalence of sarcopenia and myosteatosis in patients undergoing hemodialysis and might trigger a paradigm shift in intervention strategies for patients receiving hemodialysis.

KEYWORDS

hand-grip strength, hemodialysis, muscle cross-sectional area, proton-density fat-fraction, sarcopenia, myosteatosis, quantitative MRI

1 Introduction

Sarcopenia is characterized by a gradual decline in physical performance, strength, and skeletal muscle mass (1, 2). It has a prevalence of between 28.5% and 40.3% in patients receiving hemodialysis (3–7) and results in poor clinical outcomes (7–9). The complex pathophysiology of sarcopenia may be exacerbated by metabolic acidosis, oxidative stress, accumulated uremic toxins, inflammation, insulin resistance, malnutrition, protein restriction, decreased appetite, myostatin overexpression, ubiquitination, and physical inactivity (10). Therefore, sarcopenia is a major problem in patients undergoing hemodialysis.

Skeletal muscle mass is the largest component of human free adipose tissue (11). Muscle quality refers to both micro- and macroscopic changes in muscle architecture and composition, and to the amount of function delivered per unit mass of muscle (12). The loss of skeletal muscle mass is one criterion for sarcopenia (1). Moreover, despite the minimal loss in skeletal muscle mass, skeletal muscle function can be drastically reduced with aging (13). This discrepancy may be partially caused by fatty infiltration, which is an aspect of muscle quality. Most studies on sarcopenia in patients undergoing hemodialysis have measured muscle mass using bioelectrical impedance analysis (BIA) (5, 8). However, while BIA is an easy and inexpensive method, it cannot distinguish fat in muscle individually and can therefore not be used to measure muscle fat infiltration (14), usually known as muscle quality. Therefore, whether muscle fat infiltration, namely myosteatosis, exists in patients undergoing hemodialysis remains unclear. Computerized tomography (CT) is an imaging modality that evaluates fat indirectly based on X-ray attenuation (15, 16). However, as CT attenuation values are affected by a variety of factors, including iron, copper, glycogen, fibrosis, and edema, fat quantification is bound to be inaccurate (15). CT scanners manufactured by different vendors demonstrate inherent variations in attenuation values (17). This variability can lead to a platform dependent measurement of fat content, and is thus an important limitation of CT. What is more, participants are exposed to radiation during measurements.

Previous studies (18, 19) suggest that assessing muscle quantity is more important than quantifying muscle mass in the general population. Muscle quantity can be assessed by measuring proton-density fat-fraction (PDFF) using the multi-echo Dixon technique. Recently, assessing fat and water contents has become possible in various body parts through an advanced chemical shift encoding-based water-fat separate magnetic resonance imaging (MRI) approach without invasive quantitative methods (20–22). As a reliable method for quantifying muscle fat infiltration, this method is similar to MR spectroscopy (the "gold" standard) (23, 24); furthermore, the reproducibility of findings produced with this method is high (25).This indicates that PDFFs calculated using the multi-echo Dixon technique accurately reflect fat content.

Typical anatomical locations for skeletal muscle measurements based on computed tomography (CT) are the thigh, hip, and trunk. Additionally, the size and density of the abdominal and thigh muscle bundles are well-established parameters used in cancer studies (26). However, no studies are available on how these muscles contribute to strength and physical performance in patients receiving hemodialysis. Furthermore, no literature has been published on sarcopenia associated with intramuscular adipose tissue in patients undergoing hemodialysis.

Therefore, this study aimed to identify the prevalence of sarcopenia and myosteatosis in patients undergoing hemodialysis and to explore associations among muscle CSA, myosteatosis, and muscle function. We also aimed to identify the clinical and imaging risk factors for sarcopenia in patients undergoing hemodialysis.

2 Materials and methods

2.1 Study participants

This study was conducted from February 2022 to September 2022. Seventy-six patients undergoing hemodialysis at Beijing Jishuitan Hospital were included. Patients were eligible for inclusion if they were > 18 years of age, had undergone hemodialysis for at least 3 months, three times weekly, on Mondays, Wednesdays, and Fridays, or Tuesdays, Thursdays, and Saturdays, with each session lasting for 3.5–4 h. Exclusion criteria included cognitive or physical disabilities that prevented full participation (e.g., mental retardation, blindness, use of a wheelchair, hand disability, amputated limbs); comorbid medical conditions (e.g., malignant tumors, active inflammatory diseases, pregnancy) or muscular, neuromuscular, or neurologic

disorders (e.g., Alzheimer's or Parkinson's disease); or antipsychotic medication and corticosteroids use.

This study was conducted in accordance with the principles of the Declaration of Helsinki. The study protocol was reviewed and approved by the Beijing Jishuitan Hospital Ethics Committee (approval number: 202112-11-01). All participants or their legal representatives provided written informed consent. The analyses presented here were based on baseline data taken from a larger, registered trial that can be assessed here: ClinicalTrialsRegistry.gov (NCT05242055).

2.2 Clinical and biological parameters

The following clinical variables were recorded: age, sex, cause of renal disease, and dialysis vintage. Anthropometric variables recorded were height, post-dialysis weight, and BMI (dry weight (kg)/height $(m)^2$). The following biological variables were recorded: hemoglobin, serum albumin (bromocresol green method), prealbumin, predialysis blood urea nitrogen (BUN), predialysis creatinine, serum phosphorus, serum bicarbonate, highly sensitive C-reactive protein (hs-CRP; by nephelometry), and dialysis efficacy (Kt/V urea; serum urea was assessed before and after dialysis sessions to calculate urea Kt/V according to the formula of Daugirdas (27)). Laboratory measurements were performed immediately before initiating the Monday or Tuesday hemodialysis session, which was scheduled exactly 68 h after the previous session (i.e., Friday or Saturday). Blood samples were obtained from the central venous catheter, arteriovenous fistula, or graft.

2.3 Diagnosis of sarcopenia

2.3.1 Muscle mass

Muscle mass was measured using dual-energy X-ray absorptiometry (DXA) (28). Each patient underwent whole-body DXA scanning (GE Lunar Corp, Madison, WI, USA; software version enCORE-17) at 20–24 h after completing the dialysis session (4). Appendicular skeletal mass (ASM) was calculated as the sum of lean soft tissue from the arms and legs (29). ASM/$height^2$ (kg/m^2) was calculated as the relative ASMI. The Asian Working Group for Sarcopenia (AGWS) 2019 criteria for low muscle mass (low ASMI) in sarcopenia diagnosis are as follows: < 7.0 kg/m^2 and < 5.4 kg/m^2 in men and women, respectively (1).

2.3.2 Muscle strength

Muscle strength was assessed based on handgrip strength (HGS) using a Jamar J00105 hydraulic handheld dynamometer. More precisely, HGS was measured in each hand alternately before and after hemodialysis. First, the patient's arms were placed on armrests while they sat upright in a chair. Next, the elbow of the arm holding the dynamometer was bent at 90° against the patient's side.

Subsequently, patients were instructed to squeeze the dynamometer's handle as hard as possible for approximately 3 seconds (30). The highest values of the four trials were recorded. Reduced muscle strength was defined as an HGS measurement of < 28 kg in men and < 18 kg in women (1).

2.3.3 Muscle function

Muscle function was assessed using five-times chair stand time and the SPPB (short physical performance battery), while physical performance was measured the day before the start of the dialysis session. The SPPB assesses lower-body function, including strength, balance, and mobility (31). The SPPB comprises three subtests: five-times repeated chair sit-to-stand [STS time], gait speed [GS], and balance. The balance subtest consisted of three parts, with increasing difficulty levels: unaided feet-together stand, semi-tandem stand, and full-tandem stand. The patients were timed until they moved for 10 seconds. GS was assessed while patients walked 4 meters at their usual pace, with a stationary start. The average time of the two trials was recorded. Patients were asked to fold their arms across their chest and perform five chair stands as quickly as possible to assess their STS time. There were three subtests, each with a score between 0 and 4, and a total score ranging from 0 to 12. Higher SPPB scores indicate better physical function (7). The AWGS 2019 recommends an SPPB total score ≤9 or a five-time STS ≥ 12 seconds as the cut-off for low physical performance (1).

2.3.4 Definition of sarcopenia status

AWGS 19 criteria were adopted for diagnosing sarcopenia (1). First, possible sarcopenia is defined as reduced muscle strength or poor muscle function. Confirmed sarcopenia is defined as reduced low muscle mass and poor muscle function (low STS or SPPB) or low muscle strength. Lastly, severe sarcopenia is characterized by low muscle mass, low strength, and poor muscle function. Supplementary File S1 shows the details of this classification.

2.4 Magnetic resonance data acquisition

On the same day as the DXA examination, the participants underwent a multi-echo 3D spoiled gradient-echo sequence (q-Dixon) for fat fraction quantification using a 3.0-T MRI system (MAGNETOM VIDA, Siemens Healthcare GmbH, Erlangen, Germany). The MRI scanning protocol for participants included axial 2-pt and 6-point (q-Dixon) Dixon scanning of the lumbar spine and thigh. Two-point Dixon scanning was used to obtain a high-resolution anatomical structure, while the q-Dixon scan generated a water image, fat image, T2* map, and PDFF. The total scan time for each patient was 116 seconds. Supplementary File S2 summarizes the MRI protocols.

2.5 Image analyses

The CSA and fat content of the thigh muscles, trunk muscle at the L3 level, gluteus minimus/medius muscle (G. Med/MinM), and gluteus maximus muscle (G. MaxM) were measured. Muscle edges

can be visually identified by clear cavities of fat in the muscle. Position criteria for the measurement section are as follows: A) left thigh muscles: 3 cm below the lesser trochanter; B) trunk muscle at the level of the L3 vertebral transverse process; C) left G. Med/MinM muscles at the S3 level; and D) left G.MaxM at the level of the greater trochanter of the femur (Figure 1, Supplementary File S3 show the names of all evaluated muscles).

ITK-SNAP software (Lite version 3.8.0) (32) was used for manual segmentation of the muscle to obtain the muscle area described above. The segmentation was created by a research staff member blinded to participant outcomes. First, DICOM images of the patients were imported into the ITK-SNAP software. Second, muscle labels were measured by manually delineating the region-of-interest (ROI) on the axial T2 images to obtain the CSA value. Once drawn, a radiologist verified the label location and extent to ensure segmentation accuracy. Third, to obtain the PDFF value, the workstation automatically copied the ROI to the fat-fraction map. Finally, the CSA and PDFF of the muscles were automatically calculated using ITK-SNAP software based on measurements taken at the same level in each patient (32).

2.6 Statistical analysis

Analyses were performed using the Statistical Package for Social Sciences software (version 21.0; SPSS Inc., Chicago, IL, USA). Statistical significance was set at $P < 0.05$.

Statistical modelling was restricted to confirmed sarcopenia. Continuous variables are presented as either the mean ± standard deviation (SD) or the median and interquartile range. Normality was assessed using the Shapiro–Wilk normality test. Variables were compared between the sarcopenia and non-sarcopenia groups using two-sample *t*-tests or the Mann–Whitney U test. Categorical variables are expressed as absolute (n) and relative frequency (%). Fisher's exact test was used to analyze categorical variables regarding the primary cause of disease. Other categorical variables were analyzed using chi-square tests. The odds ratios (ORs) and 95% confidence intervals (95% CIs) of non-sarcopenia/sarcopenia were calculated using logistic regression models with and without adjustments for the potential risk factors, with CSA and PDFF levels fitted as continuous variables and results expressed in per-SD increase. Furthermore, the contribution of CSA and PDFF to skeletal muscle mass, strength, and muscle function, with and without adjustments for age, BMI, albumin, predialysis BUN, predialysis creatinine, and phosphorus, was estimated through multivariate linear regression.

3 Results

3.1 Participant characteristics and prevalence of sarcopenia in patients undergoing hemodialysis

Among the 76 patients on maintenance hemodialysis, 56 (73.7%), 39 (51.3%), and 17 (22.4%) had probable, confirmed, and severe sarcopenia, respectively, according to the AWGS definition. Table 1 summarizes the baseline characteristics of the 76 patients undergoing hemodialysis. Mean age was 61.8 ± 14.35 years, and 51 (67.1%) participants were male. The causes of end-stage kidney disease included diabetes mellitus (36.8%), chronic glomerulonephritis (22.4%), hypertension nephrosclerosis (25%),

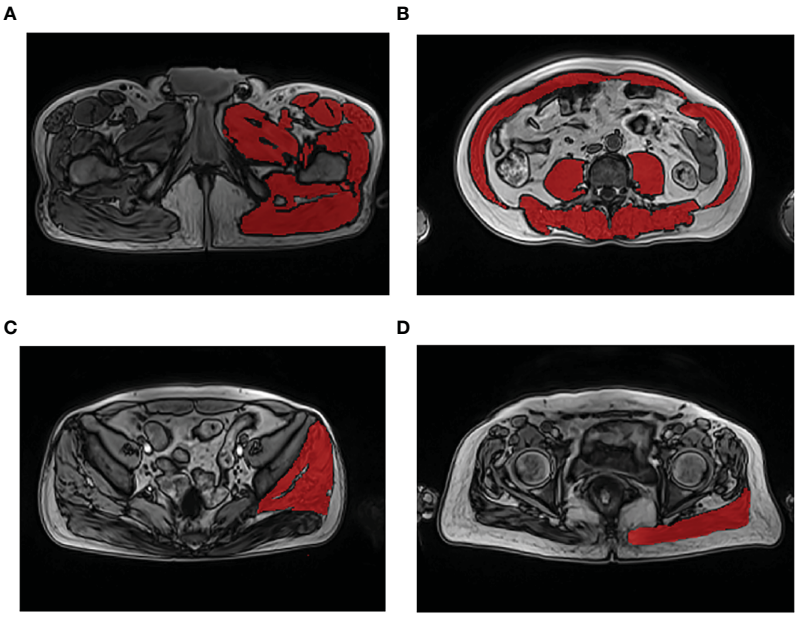

FIGURE 1
Demonstration of muscle segmentation. Measurement of the left thigh muscle group at the level 3 cm below the lesser trochanter **(A)**; measurement of the trunk muscle at the level of the third lumbar vertebra transverse process **(B)**; measurement of the left gluteus medius and minimus muscles at the third sacral (S3) level **(C)**; measurement of the left gluteus maximus muscle at the level of the greater trochanter of the femur gluteus **(D)**.

10.3389/fendo.2023.1117438

TABLE 1 Characteristics of the hemodialysis patients in the sarcopenia and the non-sarcopenia group.

Characteristics	Total (n=76)	Non-sarcopenia n=37	Sarcopenia n=39	*P*
Age, years	61.8 (14.35)	56.46 (13.85)	66.87 (12.12)	**0.001**
Sex (male), n (%)	51 (67.1%)	28 (75.6%)	23 (58.9%)	0.121
Dialysis vintage, Mo	8.00 (4.00-20.5)	10.00 (7.00-48.50)	6.00 (4.00-9.00)	**0.002**
Primary cause of disease				
Diabetic nephropathy, n (%)	28 (36.8%)	9 (24.3%)	19 (48.7%)	**0.014**
Chronic glomerulonephritis, n (%)	17 (22.4%)	12 (32.4%)	5 (12.8%)	**0.037**
Hypertensive nephrosclerosis n (%)	19 (25%)	9 (24.2%)	10 (25.6%)	0.553
Polycystic kidney disease, n (%)	4 (5.3%)	2 (5.4%)	2 (5.1%)	0.672
Interstitial nephritis, n (%)	3 (3.9%)	2 (5.4%)	1 (2.6%)	0.48
Lupus nephritis, n (%)	2 (2.6%)	0 (0%)	2 (5.1%)	0.26
Obstructive nephropathy, n (%)	3 (3.9%)	3 (8.1%)	0 (0%)	0.111
Anthropometry measures				
Weight, kg	63.75 (13.40)	68.96 (12.32)	58.81 (12.61)	**0.001**
Height, cm	165.54 (9.22)	167.68 (8.31)	163.51 (9.68)	**0.048**
BMI, kg/m^2	23.15 (3.96)	24.43 (3.45)	21.94 (4.07)	**0.005**
Skeletal muscle measures				
ASM, kg	18.19 (14.03,21.17)	20.31 (17.30,23.19)	15.14 (11.89,21.32)	**0.004**
ASMI	6.01 (1.09)	6.77 (0.85)	5.30 (0.76)	**<0.001**
Male		7.14 (0.51)	5.51 (0.71)	**<0.001**
Female		5.59 (0.57)	4.99 (0.74)	**0.036**
Handgrip strength, kg	23.86 (11.15)	29.81 (10.99)	18.22 (7.99)	**<0.001**
Male		33.75 (8.98)	21.54 (8.04)	**<0.001**
Female		17.56 (6.97)	13.44 (5.07)	0.102
Slow 5- time chair stand test, n (%)	46 (60.5%)	22 (59.5%)	24 (61.5%)	0.853
Low SPPB score, n (%)	38 (50.0%)	8 (21.6%)	30 (76.9%)	**<0.001**
Laboratory data				
Hemoglobin, g/L	106.16 (18.71)	107.92 (16.23)	104.49 (20.87)	0.425
Albumin, g/L	36.18 (3.56)	37.51 (2.17)	34.92 (2.13)	**0.001**
prealbumin, mg/L	268.33 (80.57)	302.76 (59.25)	235.68 (85.078)	**<0.001**
Predialysis BUN (mmol/L)	22.32 (6.27)	25.13 (5.90)	19.66 (5.45)	**<0.001**
Predialysis Creatinine(μmol/L)	811.09 (302.00)	997.41 (256.00)	634.34 (228.17)	**<0.001**
Phosphorus, mmol/L	1.63 (0.53)	1.75 (0.51)	1.51 (0.54)	
Bicarbonate, mmol/L	21.42 (3.02)	21.07 (0.17)	**21.76 (0.77)**	0.321
hs-CRP, mg/L	2.38 (1.28,5.83)	2.03 (1.20-5.85)	2.72 (1.59-5.81)	0.199
Kt/V	1.41 (0.24)	1.37 (0.26)	1.44 (0.23)	0.208
Muscle measurement by MRI				
Thigh muscle CSA (mm^2)	8559.82 (1656.81)	8985.42 (1650.33)	8156.05 (1579.2)	**0.028**

(Continued)

TABLE 1 Continued

Characteristics	Total (n=76)	Non-sarcopenia n=37	Sarcopenia n=39	*P*
L3 trunk muscle CSA (mm^2)	9493.45 (8299.73,10094.9)	9592.4 (9019.55,11920.6)	9409.13 (8082.2,9649.52)	**0.015**
G.Med/MinM CSA (mm^2)	2979.33 (2584.15,3204.6)	3012.73 (2926.76,3860.15)	2952.08 (2025,2989.15)	**<0.001**
G.MaxM CSA (mm^2)	2799.33 (2514.94,3153.68)	2862.09 (2761.07,3607.03)	2773.42 (2171.34,2827.91)	**<0.001**
Thigh muscle PDFF (%)	10.56 (8.61,11.94)	9.92 (7.65,10.94)	11.29 (10.28,13.76)	**0.001**
L3 trunk muscle PDFF (%)	13.51 (3.05)	10.13 (3.95)	12.13 (35.95)	**0.033**
G.Med/MinM PDFF (%)	14.39 (14.39,15.56)	14.23 (10.92,15.81)	14.47 (14.02,15.47)	0.257
G.MaxM PDFF (%)	15.47(13.65,16.09)	14.68(11.28,15.92)	15.73(15.09,16.59)	**0.015**

Data are expressed as numbers, percentages, mean ± standard deviation, or median (interquartile range).For the comparisons between groups, t-tests were used for normally distributed and the Mann-Whitney U test for skewed variables. Fisher's exact test was used to analyze categorical variables regarding the primary cause of disease. Other categorical variables were analyzed using chi-square tests. Values of P < 0.05 are marked in bold.

BMI, body mass index; ASM, appendicular skeletal muscle mass; ASMI, ASM index (ASM/height2); SPPB, short physical performance battery; BUN, blood urea nitrogen; hs-CRP, high-sensitive C-reactive protein; Kt/V, dialysis efficacy; L3 trunk, third lumbar trunk; G.Med/MinM, gluteus medius and minimus muscles; G.MaxM, gluteus maximus muscle; CSA, muscle cross-sectional area; PDFF, proton-density fat-fraction.

and other nephropathies (15.7%). A low ASMI, low HSG, slow five-time STS, and low SPPB scores were observed in 64.5%, 48.7%, 50%, and 60.5% of all patients, respectively.

3.2 Risk factors for sarcopenia in patients undergoing hemodialysis

Table 1 shows differences in hemodialysis status between the patients with sarcopenia and those without. Patients with sarcopenia were older ($P < 0.001$); had a lower BMI ($P = 0.005$), weight ($P = 0.001$), height ($P = 0.048$), ASM ($P < 0.001$), ASMI ($P < 0.001$), HGS ($P < 0.001$), SPPB score ($P < 0.001$), albumin ($P = 0.001$), prealbumin ($P = 0.001$), predialysis BUN ($P < 0.001$), predialysis creatinine ($P < 0.001$), phosphorus ($P = 0.042$), thigh muscle CSA ($P = 0.028$), L3 trunk muscle CSA ($P = 0.015$), G. Med/MinM CSA ($P < 0.001$), and G. MaxM CSA ($P < 0.001$); they also exhibited a higher dialysis vintage in Supplementary File S5 ($P = 0.002$), and a higher PDFF of the thigh muscle ($P = 0.001$), L3 trunk muscle ($P = 0.033$) and G. MaxM ($P = 0.015$).

Supplementary File S4 shows the risk factors for sarcopenia in patients receiving hemodialysis. Older age (OR: 1.061, $P < 0.003$); lower BMI (OR: 0.837, $P = 0.008$), albumin (OR: 0.765, $P = 0.004$), prealbumin (OR: 0.987, $P = 0.001$), BUN (OR 0.842, $P < 0.001$), predialysis creatinine (OR: 0.993, $P < 0.001$), and phosphorus (OR: 0.396, $P = 0.047$); and a higher PDFF of the thigh muscle (OR: 1.89, $P = 0.036$) and the L3 trunk muscle (OR: 1.71, $P = 0.040$) were identified as sarcopenia risk factors.

3.3 Associations of the CSA and PDFF with sarcopenia in patients undergoing hemodialysis

Logistic regression showed that muscle CSA and PDFF were significant predictors of sarcopenia among patients undergoing hemodialysis in this study, as shown in Supplementary File S5 and Figure 2. Except for the PDFF of G.MaxM and G. Med/MinM, the CSA and PDFF of the other muscles correlated with sarcopenia. For a per-SD increase in the CSA of G. Med/MinM, the OR for sarcopenia was 0.371 (95% CI: 0.164–0.839) in a multivariable model adjusted for age and BMI.

3.4 Association of the CSA and PDFF with muscle function measures

Tables 2–4 present the simple and multiple linear regression analyses of CSA and PDFF concerning HGS, SPPB score, and ASMI, respectively. In the unadjusted model (model 1), the

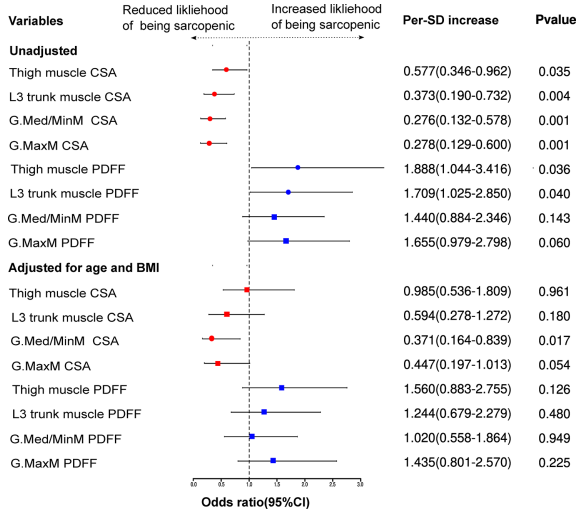

FIGURE 2
Association of muscle measurements with sarcopenia in hemodialysis patients. P < 0.05 was considered statistically significant. CI, confidence interval; L3 trunk, third lumbar trunk; G.Med/MinM, gluteus medius and minimus muscles; G.MaxM, gluteus maximus muscle; PDFF, proton-density fat-fraction. circle = significant; square = non-significant.

TABLE 2 Independency of muscle measurements and handgrip strength.

Measurement	HGS (kg)									
	model 1		model 2		model 3		model 4		model 5	
	β	*P*	β	*P*	β	*P*	β	*P*	β	
Thigh muscle CSA (mm^2)	0.503	**<0.001**	0.483	**<0.001**	0.433	**<0.001**	0.382	**0.001**	0.267	**0.018**
L3 trunk muscle CSA (mm^2)	0.518	**<0.001**	0.504	**<0.001**	0.448	**<0.001**	0.402	**0.001**	0.227	0.062
G.Med/MinM CSA (mm^2)	0.552	**<0.001**	0.543	**<0.001**	0.490	**<0.001**	0.454	**<0.001**	0.280	**0.020**
G.MaxM CSA (mm^2)	0.383	**0.001**	0.349	**0.005**	0.304	**0.007**	0.221	0.079	0.079	0.500
Thigh muscle PDFF (%)	-0.381	**0.001**	-0.372	**0.001**	-0.317	**0.004**	-0.300	**0.005**	-0.209	**0.031**
L3 trunk muscle PDFF (%)	-0.443	**<0.001**	-0.447	**<0.001**	-0.353	**0.003**	-0.344	**0.003**	-0.287	**0.006**
G.Med/MinM PDFF (%)	-0.325	**0.004**	-0.337	**0.002**	-0.202	0.100	-0.203	0.086	-0.187	0.073
G.MaxM PDFF (%)	-0.351	**0.002**	-0.378	**0.001**	-0.259	**0.024**	-0.281	**0.011**	-0.194	0.053

β is the regression coefficient. Values of P < 0.05 are marked in bold.
L3 trunk, third lumbar trunk; G.Med/MinM, gluteus minimus and medius muscle; G.MaxM, gluteus maximus muscle; CSA, muscle cross-sectional area; PDFF, proton-density fat-fraction. model 1, unadjusted; model 2, adjusted for BMI; model 3, adjusted for age; model 4, adjusted for age and BMI; model 5, adjusted for age, BMI, albumin, predialysis BUN, predialysis creatinine, and phosphorus.

muscle CSA and PDFF were significantly associated with HGS. Except for the L3 trunk muscle CSA, the CSA and PDFF of the other muscles were significantly associated with the SPPB score. Additionally, the CSA and PDFF of the other muscles were significantly associated with ASMI, excluding the G. Med/MinM PDFF and G. MaxM PDFF. After adjustments for age, BMI, albumin, predialysis BUN, predialysis creatinine, and phosphorus (model 5), a lower HGS was associated with lower thigh muscle CSA (ß = 0.267, $P = 0.018$) and G. Med/MinM CSA (ß = 0.280, $P < 0.020$), and a higher PDFF of the thigh muscle (ß = -0.209, $P = 0.031$) and L3 trunk muscle (ß =-0.287, $P = 0.006$). However, the muscle CSA and PDFF were not associated with the SPPB score after adjustments for age, BMI, albumin, predialysis BUN, predialysis creatinine, and phosphorus (model 5). Contrary to the SPPB results, in model 5, a lower ASMI was associated with a lower CSA of the thigh muscle (ß = 0.364, $P = 0.001$), L3 trunk muscle (ß = 0.428, $P < 0.001$), G. Med/MinM (ß = 0.342, $P = 0.003$), and G. MaxM (ß = 0.315, $P = 0.004$). Moreover, a lower ASMI was also associated with a higher PDFF of the thigh muscle (ß = -0.236, $P = 0.011$) and L3 trunk muscle (ß = -0.259, $P = 0.010$).

4 Discussion

In this study, we identified probable, confirmed, and severe sarcopenia in 73.7%, 51.3%, and 22.4% of patients undergoing hemodialysis, respectively. Older age; lower BMI, albumin, prealbumin, predialysis BUN, predialysis creatinine, and

TABLE 3 Independency of muscle measurements and SPPB score.

Measurement	SPPB score									
	model 1		model 2		model 3		model 4		model 5	
	β	*P*	β	*P*	β	*P*	β	*P*	β	
Thigh muscle CSA (mm^2)	0.165	0.161	0.150	0.236	0.015	0.888	-0.064	0.593	-0.128	0.279
L3 trunk muscle CSA (mm^2)	0.194	0.097	0.185	0.146	0.036	0.744	-0.045	0.712	-0.170	0.171
G.Med/MinM CSA (mm^2)	0.365	**0.001**	0.388	**0.002**	0.242	**0.024**	0.213	0.076	0.087	0.488
G.MaxM CSA (mm^2)	0.250	**0.032**	0.258	**0.048**	0.116	0.286	0.047	0.706	-0.064	0.595
Thigh muscle PDFF (%)	-0.254	**0.029**	-0.251	**0.032**	-0.154	0.145	-0.144	0.172	-0.074	0.460
L3 trunk muscle PDFF (%)	-0.284	**0.014**	-0.286	**0.014**	-0.078	0.502	-0.072	0.536	-0.068	0.535
G.Med/MinM PDFF (%)	-0.321	**0.005**	-0.331	**0.004**	-0.126	0.280	-0.131	0.257	-0.121	0.258
G.MaxM PDFF (%)	-0.318	**0.006**	-0.331	**0.004**	-0.172	0.117	-0.183	0.093	-0.161	0.116

β is the regression coefficient; The values of P < 0.05 were marked in bold.
L3 trunk, third lumbar trunk; G.Med/MinM,gluteus minimus and medius muscle; G.MaxM, gluteus maximus muscle; CSA, muscle cross-sectional area; PDFF, proton-density fat-fraction. model 1, Unadjusted. model 2, Adjusted for BMI. model 3, Adjusted for age. model 4, Adjusted for age and BMI. model 5, Adjusted for age, BMI, albumin, predialysis BUN, predialysis creatinine, and phosphorus.

TABLE 4 Independency of muscle measurements and ASMI.

Measurement	ASMI (kg/m^2)									
	model 1		model 2		model 3		model 4		model 5	
	β	*P*	β	*P*	β	*P*	β	*P*	β	*P*
Thigh muscle CSA (mm^2)	0.550	**<0.001**	0.414	**<0.001**	0.573	**<0.001**	0.407	**<0.001**	0.364	**0.001**
L3 trunk muscle CSA (mm^2)	0.635	**<0.001**	0.509	**<0.001**	0.674	**<0.001**	0.525	**<0.001**	0.428	**<0.001**
G.Med/MinM CSA (mm^2)	0.602	**<0.001**	0.471	**<0.001**	0.622	**<0.001**	0.468	**<0.001**	0.342	**0.003**
G.MaxM CSA (mm^2)	0.569	**<0.001**	0.420	**<0.001**	0.587	**<0.001**	0.411	**<0.001**	0.315	**0.004**
Thigh muscle PDFF (%)	-0.363	**0.001**	-0.341	**<0.001**	-0.356	**0.002**	-0.321	**0.001**	-0236	**0.011**
L3 trunk muscle PDFF (%)	-0.305	**0.007**	-0.313	**0.001**	-0.323	**0.012**	-0.303	**0.005**	-0.259	**0.010**
G.Med/MinM PDFF (%)	-0.221	0.056	-0.246	**0.012**	-0.216	0.098	-0.218	**0.048**	-0.193	0.055
G.MaxM PDFF (%)	-0.193	0.095	-0.248	**0.012**	-0.176	0.154	-0.218	**0.036**	-0.156	0.109

β is the regression coefficient. Values of P < 0.05 are marked in bold.
L3 trunk, third lumbar trunk; G.Med/MinM, gluteus minimus and medius muscle; G.MaxM, gluteus maximus muscle; CSA, muscle cross-sectional area; PDFF, proton-density fat-fraction. model 1, unadjusted. model 2, adjusted for BMI. model 3, adjusted for age. model 4, adjusted for age and BMI. model 5, adjusted for age, BMI, albumin, predialysis BUN, predialysis creatinine, and phosphorus.

phosphorus levels; lower CSA of the thigh muscle, L3 trunk muscle, G. Med/MinM, and G. MaxM; and a higher PDFF of the thigh and L3 trunk muscle were identified as sarcopenia risk factors. G. Med/MinM CSA was higher in those without sarcopenia after adjusting for age and BMI. The lower thigh and G. Min/Med muscle CSA, as well as the higher thigh and L3 trunk muscle PDFF, were associated with lower HGS after adjustments for known risk factors. Moreover, a higher thigh and L3 trunk muscle PDFF inversely correlated with a lower ASMI.

In a recent meta-analysis including studies with 692 056 participants, the prevalence of sarcopenia in the general population was approximately 10.0%–27.0% (33). Because of the co-existence of factors such as uremic toxins, insulin resistance, or oxidative stress in patients with renal failure (34), they are more likely to develop sarcopenia. Shu et al. (7) recently published a meta-analysis showing that the sarcopenia prevalence was 28.5% (95% CI: 22.9–34.1%) and varied from 25.9% (I^2 = 94.9%, 95% CI: 20.4–31.3%; combined criteria) to 34.6% (I^2 = 98.1%, 95% CI: 20.9–48.2%; low muscle mass alone) in patients receiving hemodialysis almost two times the prevalence observed in patients without chronic kidney disease (CKD). Interestingly, we found similar results. The prevalence of confirmed sarcopenia in our study was 51.3%, based on the AWGS (2019) definition, and the prevalence of sarcopenia in our patients receiving hemodialysis was higher than that in patients undergoing hemodialysis in previous studies (7). This difference may be due to the following reasons: First, the populations selected differed (hospitalized and outpatients). Second, different instruments were used to assess muscle mass (DXA, bioelectrical impedance analysis, magnetic resonance imaging, and body composition monitors). DXA is the "gold" standard, and other detection methods may overestimate muscle mass due to overhydration in patients undergoing hemodialysis (35). Third, the difference may be due to the large variability in diagnostic criteria, such as those propsed by the European Working Group on Sarcopenia in Older People, the AWGS, the Foundation for the National Institutes of Health Sarcopenia Project, and the International Working Group on Sarcopenia.

The pathogenesis of sarcopenia remains unclear, and only a few reports have discussed the pathogenesis of sarcopenia in patients receiving hemodialysis. To identify the risk factors of sarcopenia in such patients, we categorized our sample into two groups, one with sarcopenia and one without. Our analyses show that older age was a risk factor for sarcopenia in our patients undergoing hemodialysis, which is consistent with previous results in the general population as well as in patients receiving hemodialysis (4, 6), and may be related to alpha motor neuron loss caused by aging (36). Furthermore, we found that a higher BMI and predialysis BUN and higher serum albumin, prealbumin, and phosphate levels were sarcopenia-protective factors in our patients receiving hemodialysis. These results are in agreement with previous findings reported in the literature (4, 5, 9). The reduction in the abovementioned indicators is reflective of poor oral intake, malnutrition, and poor nutritional status (37), which may result in reduced protein synthesis and muscle weakness (38). Therefore, it is appropriate to implement precise nutritional measures for patients undergoing hemodialysis.

A low predialysis creatinine level was found as a risk factor for sarcopenia in patients undergoing hemodialysis in our study. This marker is influenced by muscle mass (6, 9). We identified that the primary cause of the disease was diabetic nephropathy, which was significantly associated with sarcopenia in our patients receiving hemodialysis, in agreement with the literature (38, 39).

Some studies have found no statistically significant association between dialysis vintage and sarcopenia (5, 6, 9). However, a lower dialysis vintage was associated with sarcopenia in our study. We considered the following reason as the cause for this finding: most of our patients had a low dialysis vintage (in 71% of cases, the dialysis vintage was < 12 months); therefore, the dialysis-related indicators may not have had time to develop. Previous studies have reported that sarcopenia in patients receiving hemodialysis is

mainly associated with hs-CRP (39), hemoglobin (6), and Kt/V (38). No correlations were found between these indicators and sarcopenia, which may be due to the limited sample as well as to the fact that patients with good control of the above indicators were under dialysis care and receiving a pharmacological intervention.

An individual's muscle quality can be measured by both micro- and macro-scale changes in muscle architecture and composition, as well as by muscle function per unit of muscle mass (12).. Various imaging techniques, including CT and MRI, have been used to assess muscle quality in study settings, including the measurement of fat infiltration and muscle attenuation (40, 41). There is a strong association between fatty infiltration in the muscles and reduced muscle function (18). Several pathways contribute to the accumulation of fatty acids in muscles, and the accumulation of lipids within myofibers, also known as intramuscular fat, is one direct route. Adipocytes, which accumulate within the skeletal muscle as intermuscular fat, represent another pathway (42). Here, we used MR Dixon technology to quantify the amount of muscle adipose tissue, including intramuscular and intermuscular adipose tissue.

In addition to assessing the traditional risk factors for sarcopenia in patients undergoing hemodialysis, we evaluated new muscle measurements, such as CSA and PDFF. To our knowledge, no previous study has compared CSA and PDFF findings between patients with and without sarcopenia using quantitative MRI scans in those receiving hemodialysis. Using quantitative MRI, our study showed that muscle CSA reduction (thigh muscle, L3 trunk muscle, G.MaxM, and G. Med/MinM) and PDFF increase (thigh muscle, L3 trunk muscle, and G.MaxM) were influencing factors of sarcopenia in patients undergoing hemodialysis. Further analysis using binary logistic regression showed that the muscle CSA reduction (thigh muscle, L3 trunk muscle, G.MaxM, and G.Med/MinM) and PDFF increase (thigh muscle, L3 trunk muscle, and G.MaxM) were risk factors for developing sarcopenia. Our analyses demonstrate that the CSA reduction of G.MaxM and G.Med/MinM independently predicted sarcopenia, even after adjusting for age and BMI. Studies conducted as part of the Health ABC project have also shown age-related decreases in thigh muscle density or increased fatty infiltration in the thigh muscle (43), which may explain why some indicators were not statistically significant after age adjustments. After adjustments for age, BMI, albumin, predialysis BUN, predialysis creatinine, and phosphorus, muscle CSA and PDFF were not significantly associated with sarcopenia, which may partially be explained by low power due to the limited sample size, or by direct effects of chronic kidney disease on muscle function.

The assessment of muscle quality is expected to guide treatment decisions. Therefore, we assessed muscle measurements (CSA and PDFF) and muscle characteristics (muscle mass, strength, and function). We found that low muscle CSA and high PDFF were risk factors for lower muscle strength. After full adjustments for age, BMI, and other laboratory risk factors, CSA reduction (thigh muscle, L3 trunk muscle, and G.MaxM) and PDFF increase (thigh muscle, L3 trunk muscle, and G.Med/MinM) were also identified as risk factors for lower muscle strength. Some previous studies have reached similar conclusions, and muscle strength can be indirectly measured using muscle volume (26, 44, 45). However, Wang et al. (18) found no associations between HGS and midthigh muscle variables (neither muscle area nor density).

Our study suggests that CSA reduction (G. Med/MinM and G.MaxM) and PDFF increase (thigh muscle, L3 trunk muscle, G. Med/MinM, and G.MaxM) are also risk factors for lower muscle function. Particularly, after adjusting for BMI, CSA reduction (G. Med/MinM and G.MaxM) and PDFF increase (thigh muscle, L3 trunk muscle, G. Med/MinM, and G.MaxM) were identified as risk factors for lower muscle function. Our results confirm that muscle CSA and PDFF are important parameters for detecting lower muscle function, which is in line with other studies (16, 46). The fat fraction in the thigh muscle was associated with performance in a timed up-and-go test after adjusting for muscle area in controlled acromegaly (47). Moreover, older adults with low trunk muscle density are more likely to have poor balance and exhibit faster declines in functional capacity (16). Anderson et al. (16) found no association between L2 trunk muscle volume and the SPPB score, as well as between L2 trunk muscle density and the SPPB score, which is inconsistent with our results. Our findings show that only the G. Med/MinM CSA predicted lower muscle function after adjusting for age and BMI. Additionally, we identified low G. Med/MinM CSA as the most sensitive indicator of lower muscle function. Other studies reported similar results: Andrew et al., for example, found that normal gait is largely influenced by the G. Med/Min muscles of the hip (48). The G. Med/MinM, which is known as the "rotator cuff of the hip," inserts into the greater trochanter of the femur. It maintains balance by acting as an abductor and rotator of the hip during normal walking (49). Similarly, a recent study found that stair climbing, sitting up and standing down, and walking are associated with smaller gluteus muscles (50). Therefore, the G. Med/MinM may be a key muscle group to focus on in future studies.

This study has some limitations. First, since this was a single-center study conducted in China, the results may not be generalizable to other patient populations and countries. Second, this study had a cross-sectional design, which prevented us from analyzing causal relationships between sarcopenia and muscle measurements (CSA and PDFF) in hemodialysis patients. Third, a limited patient sample was enrolled in this study, and some indicators were not found to influence sarcopenia, which may have been due to the resulting low power. Fourth, as image registration was not applied in this study, the absolute values of the cross-sectional area could have been affected by slight changes in image orientation. Fifth, some potentially relevant information was not collected, such as details on peripheral vascular disease, physical activity, nutritional status, and some muscle-affecting medicines (e.g., those belonging to the statin family). Therefore, a multicenter study with a larger sample size would be beneficial in evaluating this issue in the future.

In conclusion, our findings demonstrate the value of fat content assessments within skeletal muscles in patients with sarcopenia undergoing hemodialysis and might trigger a paradigm shift in intervention strategies for sarcopenia. In the future, assessments of

muscle fat infiltration and muscle CSA may help guide treatment choices (i.e., precise nutritional exercise interventions) and monitor treatment responses.

Data availability statement

The raw data supporting the conclusions of this article will be made available by the authors, without undue reservation.

Ethics statement

The studies involving human participants were reviewed and approved by the Beijing Jishuitan Hospital Ethics Committee (ethics committee approval number: 202112-11-01). The patients/participants provided their written informed consent to participate in this study.

Author contributions

XC, DZ, CF, and LW designed the study. CF and DY prepared the first draft of the paper. NY, LW, MS, DW, XL, and XW contributed to the data collection, such as information collection, scanning, and data input. DY and YW edited the draft. FD and CF were responsible for the statistical analysis of the data. CF, DZ, and LW supervised the study and paper organization. All authors contributed to the article and approved the submitted version.

Funding

This project was supported by Beijing JST Research Funding (code: ZR-202210, ZR-202214), the National Natural Science Foundation of China (grant no. 81901718), the Beijing Hospitals Authority Youth Programme (code: QML20200402), Beijing Hospitals Authority Clinical Medicine Development of Special Funding Support (code: ZYLX202107), and the Beijing Talents Fund (grant no. 2015000021467G177).

Acknowledgments

The authors would like to thank Mingjie Wang, Lingran Yuan, and Yunqing Xia; they greatly contributed to the image processing of this paper. We also would like to thank Editage (www.editage.cn) for English language editing. We thank the study participants for contributing their time and effort.

Conflict of interest

Author YW was employed by Siemens Healthineers Ltd.

The remaining authors declare that the research was conducted in the absence of any commercial or financial relationships that could be construed as a potential conflict of interest.

Publisher's note

Supplementary material

The Supplementary Material for this article can be found online at: https://www.frontiersin.org/articles/10.3389/fendo.2023.1117438/full#supplementary-material

References

1. Chen L, Woo J, Assantachai P, Auyeung T, Chou M, Iijima K, et al. Asian Working group for sarcopenia: 2019 consensus update on sarcopenia diagnosis and treatment. *J Am Med Dir Assoc* (2020) 21:300–07. doi: 10.1016/j.jamda.2019.12.012

2. Cruz-Jentoft AJ, Bahat G, Bauer J, Boirie Y, Bruyère O, Cederholm T, et al. Sarcopenia: revised European consensus on definition and diagnosis. *Age Ageing* (2019) 48:601. doi: 10.1093/ageing/afz046

3. Ren H, Gong D, Jia F, Xu B, Liu Z. Sarcopenia in patients undergoing maintenance hemodialysis: incidence rate, risk factors and its effect on survival risk. *Ren Fail* (2016) 38:364–71. doi: 10.3109/0886022X.2015.1132173

4. Mori K, Nishide K, Okuno S, Shoji T, Emoto M, Tsuda A, et al. Impact of diabetes on sarcopenia and mortality in patients undergoing hemodialysis. *BMC Nephrol* (2019) 20:105. doi: 10.1186/s12882-019-1271-8

5. Umakanthan M, Li JW, Sud K, Duque G, Guilfoyle D, Cho K, et al. Prevalence and factors associated with sarcopenia in patients on maintenance dialysis in Australia–a single centre, cross-sectional study. *Nutrients* (2021) 13:3284. doi: 10.3390/nu13093284

6. Ding Y, Chang L, Zhang H, Wang S. Predictive value of phase angle in sarcopenia in patients on maintenance hemodialysis. *Nutrition* (2022) 94:111527. doi: 10.1016/j.nut.2021.111527

7. Shu X, Lin T, Wang H, Zhao Y, Jiang T, Peng X, et al. Diagnosis, prevalence, and mortality of sarcopenia in dialysis patients: A systematic review and meta-analysis. *J Cachexia Sarcopenia Muscle* (2022) 13:145–58. doi: 10.1002/jcsm.12890

8. Sánchez-Tocino ML, Miranda-Serrano B, López-González A, Villoria-González S, Pereira-García M, Gracia-Iguacel C, et al. Sarcopenia and mortality in older hemodialysis patients. *Nutrients* (2022) 14:2354. doi: 10.3390/nu14112354

9. Kittiskulnam P, Chertow GM, Carrero JJ, Delgado C, Kaysen GA, Johansen KL. Sarcopenia and its individual criteria are associated, in part, with mortality among patients on hemodialysis. *Kidney Int* (2017) 92:238–47. doi: 10.1016/j.kint.2017.01.024

10. Wang XH, Mitch WE, Price SR. Pathophysiological mechanisms leading to muscle loss in chronic kidney disease. *Nat Rev Nephrol* (2022) 18:138–52. doi: 10.1038/s41581-021-00498-0

11. Janssen I, Heymsfield SB, Wang ZM, Ross R. Skeletal muscle mass and distribution in 468 men and women aged 18-88 yr. *J Appl Physiol (1985)* (2000) 89:81–8. doi: 10.1152/jappl.2000.89.1.81

12. McGregor RA, Cameron-Smith D, Poppitt SD. It is not just muscle mass: a review of muscle quality, composition and metabolism during ageing as determinants of muscle function and mobility in later life. *Longevity Healthspan* (2014) 3:9. doi: 10.1186/2046-2395-3-9

13. Goodpaster BH, Park SW, Harris TB, Kritchevsky SB, Nevitt M, Schwartz AV, et al. The loss of skeletal muscle strength, mass, and quality in older adults: the health, aging and body composition study. *J Gerontol Biol Sci Med Sci* (2006) 61:1059–64. doi: 10.1093/gerona/61.10.1059

14. KYLE U. Bioelectrical impedance analysis?part I: review of principles and methods. *Clin Nutr* (2004) 23:1226–43. doi: 10.1016/j.clnu.2004.06.004

15. Limanond P, Raman SS, Lassman C, Sayre J, Ghobrial RM, Busuttil RW, et al. Macrovesicular hepatic steatosis in living related liver donors: correlation between CT and histologic findings. *Radiology* (2004) 230:276–80. doi: 10.1148/radiol.2301021176

16. Anderson DE, Quinn E, Parker E, Allaire BT, Muir JW, Rubin CT, et al. Associations of computed tomography-based trunk muscle size and density with balance and falls in older adults. *Journals Gerontology Ser A: Biol Sci Med Sci* (2016) 71:811–16. doi: 10.1093/gerona/glv185

17. Birnbaum BA, Hindman N, Lee J, Babb JS. Multi-detector row CT attenuation measurements: assessment of intra- and interscanner variability with an anthropomorphic body CT phantom. *Radiology* (2007) 242:109–19. doi: 10.1148/radiol.2421052066

18. Wang L, Yin L, Zhao Y, Su Y, Sun W, Chen S, et al. Muscle density, but not size, correlates well with muscle strength and physical performance. *J Am Med Dir Assoc* (2021) 22:751–59. doi: 10.1016/j.jamda.2020.06.052

19. Delmonico MJ, Harris TB, Visser M, Park SW, Conroy MB, Velasquez-Mieyer P, et al. Longitudinal study of muscle strength, quality, and adipose tissue infiltration. *Am J Clin Nutr* (2009) 90:1579–85. doi: 10.3945/ajcn.2009.28047

20. Grimm A, Meyer H, Nickel MD, Nittka M, Raithel E, Chaudry O, et al. Evaluation of 2-point, 3-point, and 6-point Dixon magnetic resonance imaging with flexible echo timing for muscle fat quantification. *Eur J Radiol* (2018) 103:57–64. doi: 10.1016/j.ejrad.2018.04.011

21. Naarding KJ, van der Holst M, van Zwet EW, van de Velde NM, de Groot I, Verschuuren J, et al. Association of elbow flexor MRI fat fraction with loss of hand-to-Mouth movement in patients with duchenne muscular dystrophy. *Neurology* (2021) 97:e1737–42. doi: 10.1212/WNL.0000000000012724

22. Koch G. Editorial for "Bone marrow fat measured by a chemical shift-encoded sequence (IDEAL-IQ) in patients with and without metabolic syndrome". *J Magn Reson Imaging* (2021) 54:154. doi: 10.1002/jmri.27645

23. Marty B, Reyngoudt H, Boisserie JM, Le Louer J, AAE C, Fromes Y, et al. Water-fat separation in MR fingerprinting for quantitative monitoring of the skeletal muscle in neuromuscular disorders. *Radiology* (2021) 300:652–60. doi: 10.1148/radiol.2021204028

24. Schweitzer L, Geisler C, Pourhassan M, Braun W, Glüer C, Bosy-Westphal A, et al. What is the best reference site for a single MRI slice to assess whole-body skeletal muscle and adipose tissue volumes in healthy adults? *Am J Clin Nutr* (2015) 102:58–65. doi: 10.3945/ajcn.115.111203

25. Grimm A, Meyer H, Nickel MD, Nittka M, Raithel E, Chaudry O, et al. Repeatability of Dixon magnetic resonance imaging and magnetic resonance spectroscopy for quantitative muscle fat assessments in the thigh. *J cachexia sarcopenia Muscle* (2018) 9:1093–100. doi: 10.1002/jcsm.12343

26. Linder N, Schaudinn A, Langenhan K, Krenzien F, Hau HM, Benzing C, et al. Power of computed-tomography-defined sarcopenia for prediction of morbidity after pancreaticoduodenectomy. *BMC Med Imaging* (2019) 19:32. doi: 10.1186/s12880-019-0332-6

27. Daugirdas JT. Second generation logarithmic estimates of single-pool variable volume Kt/V: an analysis of error. *J Am Soc Nephrol JASN* (1993) 4:1205–13. doi: 10.1681/ASN.V451205

28. Scafoglieri A, Clarys JP. Dual energy X-ray absorptiometry: gold standard for muscle mass? *J Cachexia Sarcopenia Muscle* (2018) 9:786–87. doi: 10.1002/jcsm.12308

29. Heymsfield SB, Smith R, Aulet M, Bensen B, Lichtman S, Wang J, et al. Appendicular skeletal muscle mass: measurement by dual-photon absorptiometry. *Am J Clin Nutr* (1990) 52:214–18. doi: 10.1093/ajcn/52.2.214

30. Esteban-Cornejo I, Ho FK, Petermann-Rocha F, Lyall DM, Martinez-Gomez D, Cabanas-Sánchez V, et al. Handgrip strength and all-cause dementia incidence and mortality: findings from the UK biobank prospective cohort study. *J Cachexia sarcopenia Muscle* (2022) 13:1514–25. doi: 10.1002/jcsm.12857

31. Guralnik JM, Simonsick EM, Ferrucci L, Glynn RJ, Berkman LF, Blazer DG, et al. A short physical performance battery assessing lower extremity function: association with self-reported disability and prediction of mortality and nursing home admission. *J Gerontol (Kirkwood)* (1994) 49:M85. doi: 10.1093/geronj/49.2.M85

32. Yushkevich PA, Gao Y, Gerig G. ITK-SNAP: An interactive tool for semi-automatic segmentation of multi-modality biomedical images. *Annu Int Conf IEEE Eng Med Biol Society. IEEE Eng Med Biol Society. Annu Int Conf* (2016) 2016:3342–45. doi: 10.1109/EMBC.2016.7591443

33. Petermann Rocha F, Balntzi V, Gray SR, Lara J, Ho FK, Pell JP, et al. Global prevalence of sarcopenia and severe sarcopenia: a systematic review and meta-analysis. *J Cachexia Sarcopenia Muscle* (2022) 13:86–99. doi: 10.1002/jcsm.12783

34. Noor H, Reid J, Slee A. Resistance exercise and nutritional interventions for augmenting sarcopenia outcomes in chronic kidney disease: A narrative review. *J Cachexia Sarcopenia Muscle* (2021) 12:1621–40. doi: 10.1002/jcsm.12791

35. Hoppe K, Schwermer K, Klysz P, Radziszewska D, Sawatiuk P, Baum E, et al. Cardiac troponin T and hydration status as prognostic markers in hemodialysis patients. *Blood Purif* (2015) 40:139–45. doi: 10.1159/000376603

36. Valenzuela PL, Cobo F, Diez-Vega I, Sanchez-Hernandez R, Pedrero-Chamizo R, Verde-Rello Z, et al. Physical performance, plasma s-klotho, and all-cause mortality in elderly dialysis patients: A prospective cohort study. *Exp Gerontol* (2019) 122:123–28. doi: 10.1016/j.exger.2019.05.003

37. Akchurin OM, Kaskel F. Update on inflammation in chronic kidney disease. *Blood Purif* (2015) 39:84–92. doi: 10.1159/000368940

38. Uemura K, Doi T, Lee S, Shimada H. Sarcopenia and low serum albumin level synergistically increase the risk of incident disability in older adults. *J Am Med Dir Assoc* (2019) 20:90–3. doi: 10.1016/j.jamda.2018.06.011

39. Wilkinson TJ, Miksza J, Yates T, Lightfoot CJ, Baker LA, Watson EL, et al. Association of sarcopenia with mortality and end-stage renal disease in those with chronic kidney disease: A UK biobank study. *J Cachexia Sarcopenia Muscle* (2021) 12:586–98. doi: 10.1002/jcsm.12705

40. Ruan XY, Gallagher D, Harris T, Albu J, Heymsfield S, Kuznia P, et al. Estimating whole body intermuscular adipose tissue from single cross-sectional magnetic resonance images. *J Appl Physiol (1985)* (2007) 102:748–54. doi: 10.1152/japplphysiol.00304.2006

41. Larsen BA, Wassel CL, Kritchevsky SB, Strotmeyer ES, Criqui MH, Kanaya AM, et al. Association of muscle mass, area, and strength with incident diabetes in older adults: The health ABC study. *J Clin Endocrinol Metab* (2016) 101:1847–55. doi: 10.1210/jc.2015-3643

42. Wang L, Yin L, Yang M, Ge Y, Liu Y, Su Y, et al. Muscle density is an independent risk factor of second hip fracture: A prospective cohort study. *J Cachexia Sarcopenia Muscle* (2022) 13:1927–37. doi: 10.1002/jcsm.12996

43. Cao L, Chen S, Zou C, Ding X, Gao L, Liao Z, et al. A pilot study of the SARC-f scale on screening sarcopenia and physical disability in the Chinese older people. *J Nutr Health Aging* (2014) 18:277–83. doi: 10.1007/s12603-013-0410-3

44. Hayashida I, Tanimoto Y, Takahashi Y, Kusabiraki T, Tamaki J. Correlation between muscle strength and muscle mass, and their association with walking speed, in community-dwelling elderly Japanese individuals. *PloS One* (2014) 9:e111810. doi: 10.1371/journal.pone.0111810

45. Engelke K, Museyko O, Wang L, Laredo J. Quantitative analysis of skeletal muscle by computed tomography imaging–state of the art. *J Orthop Translat* (2018) 15:91–103. doi: 10.1016/j.jot.2018.10.004

46. Wang L, Yin L, Zhao Y, Su Y, Sun W, Liu Y, et al. Muscle density discriminates hip fracture better than computed tomography X-ray absorptiometry hip areal bone mineral density. *J Cachexia Sarcopenia Muscle* (2020) 11:1799–812. doi: 10.1002/jcsm.12616

47. Martel-Duguech L, Alonso-Pérez J, Bascuñana H, Díaz-Manera J, Llauger J, et al. Intramuscular fatty infiltration and physical function in controlled acromegaly. *Eur J Endocrinol* (2021) 185:167–77. doi: 10.1530/EJE-21-0209

48. Chi AS, Long SS, Zoga AC, Parker L, Morrison WB. Association of gluteus medius and minimus muscle atrophy and fall-related hip fracture in older individuals using computed tomography. *J Comput Assist Tomogr* (2016) 40:238–42. doi: 10.1097/RCT.0000000000000341

49. Addison O, Inacio M, Bair WN, Beamer BA, Ryan AS, Rogers MW. Role of hip abductor muscle composition and torque in protective stepping for lateral balance recovery in older adults. *Arch Phys Med Rehabil* (2017) 98:1223–28. doi: 10.1016/j.apmr.2016.10.009

50. Damm P, Brackertz S, Streitparth F, Perka C, Bergmann G, Duda GN, et al. ESB clinical biomechanics award 2018: Muscle atrophy-related increased joint loading after total hip arthroplasty and their postoperative change from 3 to 50months. *Clin Biomech (Bristol Avon)* (2019) 65:105–09. doi: 10.1016/j.clinbiomech.2019.04.008

frontiers | Frontiers in Endocrinology

TYPE Systematic Review
PUBLISHED 26 April 2023
DOI 10.3389/fendo.2023.1044039

OPEN ACCESS

EDITED BY
Ling Wang,
Beijing Jishuitan Hospital, China

REVIEWED BY
Neha Dole,
University of Arkansas for Medical Sciences, United States
Adana A. M. Llanos,
Columbia University, United States

*CORRESPONDENCE
Yun Hak Kim
yunhak10510@pusan.ac.kr
Tae Sik Goh
taesikgoh@pusan.ac.kr

†These authors have contributed equally to this work and share first authorship

‡These authors have contributed equally to this work and share last authorship

SPECIALTY SECTION
This article was submitted to Bone Research, a section of the journal Frontiers in Endocrinology

RECEIVED 14 September 2022
ACCEPTED 29 March 2023
PUBLISHED 26 April 2023

CITATION
Lee S, Kim JH, Jeon YK, Lee JS, Kim K, Hwang S-K, Kim JH, Goh TS and Kim YH (2023) Effect of adipokine and ghrelin levels on BMD and fracture risk: an updated systematic review and meta-analysis.
Front. Endocrinol. 14:1044039.
doi: 10.3389/fendo.2023.1044039

Effect of adipokine and ghrelin levels on BMD and fracture risk: an updated systematic review and meta-analysis

Seoyul Lee[1†], Jeong Hun Kim[2,3†], Yun Kyung Jeon[2,4], Jung Sub Lee[2,5], Keunyoung Kim[2,6], Sun-Kyung Hwang[3], Jae Ho Kim[1,7], Tae Sik Goh[2,5*‡] and Yun Hak Kim[7,8,9*‡]

[1]Department of Physiology, School of Medicine, Pusan National University, Yangsan, Republic of Korea, [2]Biomedical Research Institute, Pusan National University Hospital, Busan, Republic of Korea, [3]College of Nursing, Pusan National University, Yangsan, Republic of Korea, [4]Department of Internal Medicine, School of Medicine, Pusan National University, Yangsan, Republic of Korea, [5]Department of Orthopaedic Surgery, School of Medicine, Pusan National University, Yangsan, Republic of Korea, [6]Department of Nuclear Medicine, School of Medicine, Pusan National University, Yangsan, Republic of Korea, [7]Research Institute for Convergence of Biomedical Science and Technology, Pusan National University Yangsan Hospital, Yangsan, Republic of Korea, [8]Department of Anatomy, School of Medicine, Pusan National University, Yangsan, Republic of Korea, [9]Department of Biomedical Informatics, School of Medicine, Pusan National University, Yangsan, Republic of Korea

Context: Circulating adipokines and ghrelin affect bone remodeling by regulating the activation and differentiation of osteoblasts and osteoclasts. Although the correlation between adipokines, ghrelin, and bone mineral density (BMD) has been studied over the decades, its correlations are still controversial. Accordingly, an updated meta-analysis with new findings is needed.

Objective: This study aimed to explore the impact of serum adipokine and ghrelin levels on BMD and osteoporotic fractures through a meta-analysis.

Data sources: Studies published till October 2020 in Medline, Embase, and the Cochrane Library were reviewed.

Study selection: We included studies that measured at least one serum adipokine level and BMD or fracture risk in healthy individuals. We excluded studies with one or more of the following: patients less than 18 years old, patients with comorbidities, who had undergone metabolic treatment, obese patients, patients with high physical activities, and a study that did not distinguish sex or menopausal status.

Data extraction: We extracted the data that include the correlation coefficient between adipokines (leptin, adiponectin, and resistin) and ghrelin and BMD, fracture risk by osteoporotic status from eligible studies.

Data synthesis: A meta-analysis of the pooled correlations between adipokines and BMD was performed, demonstrating that the correlation between leptin and BMD was prominent in postmenopausal women. In most cases, adiponectin

levels were inversely correlated with BMD. A meta-analysis was conducted by pooling the mean differences in adipokine levels according to the osteoporotic status. In postmenopausal women, significantly lower leptin (SMD = -0.88) and higher adiponectin (SMD = 0.94) levels were seen in the osteoporosis group than in the control group. By predicting fracture risk, higher leptin levels were associated with lower fracture risk (HR = 0.68), whereas higher adiponectin levels were associated with an increased fracture risk in men (HR = 1.94) and incident vertebral fracture in postmenopausal women (HR = 1.18).

Conclusions: Serum adipokines levels can utilize to predict osteoporotic status and fracture risk of patients.

Systematic review registration: https://www.crd.york.ac.uk/prospero/display_record.php?ID=CRD42021224855, identifier CRD42021224855.

KEYWORDS

adipokines, ghrelin, bone mineral density, fracture risk, meta-analysis

Introduction

Bones, the support system our body and protectors of internal organs, and adipose tissue, the largest endocrine tissue in the body, are closely related to nutrient metabolism and energy storage. Obesity plays a protective role in bone mineral density (BMD) (1, 2). However, a low body weight is a major risk factor for osteoporotic low-energy fractures (3, 4). Therefore, body mass index (BMI) obtained by diving body weight (in kilograms) by height (in meters) squared is included as a variable in the Fracture Risk Assessment Tool to calculate the fracture risk over 10 years (5). In contrast to previous reports, a high prevalence of obesity has been found in postmenopausal women with osteoporotic fractures (6).

Mesenchymal stem cells (MSCs) are pluripotent progenitor cells that mainly differentiate into adipocytes, osteoblasts, and chondroblasts (7). These three cell lineages differentiate from MSCs by common regulatory factors, such as hormones and cytokines, which determine their proliferation as well. Increased adiposity in the bone marrow of osteoporotic patients supports a link between bone and fat (8). Additionally, adipokines that include leptin, adiponectin, resistin, and visfatin are secreted from adipose tissue and affect bone metabolism, supporting the link between fat and bone (9, 10). Although not produced from adipose tissue, ghrelin, a type of growth hormone secretagogue, also affects lipid metabolism and regulates bone homeostasis (11, 12).

A meta-analysis was previously conducted on the correlation between blood concentrations of adipokines and ghrelin and BMD. The meta-analysis revealed that adiponectin had the inverse correlation with BMD (r = -0.14 to -0.4), independent of fat mass, BMI, and menopausal status. And leptin had the correlation with BMD (r = 0.1 to 0.33) (13). The relationship between the blood concentration of adipokines, bone density, and osteoporotic fractures has been studied extensively in the past 10 years. In particular, several studies have been conducted on the correlation between resistin and BMD measured at various sites, indicating that it has recently been in the spotlight as a biomarker for BMD (14–17). In addition, studies on the association between BMD and leptin or adiponectin have been conducted. Hence, we performed an updated meta-analysis on the impact of serum adipokines on BMD and osteoporotic fractures. According to our analysis, BMD was correlated with serum leptin level and was inversely correlated with serum adiponectin level in postmenopausal women. Furthermore, the fracture risk was predicted to be higher with a lower serum leptin level and higher serum adiponectin level. Serum adipokines levels can utilize to predict osteoporotic status and fracture risk of patients.

Methods

This review was prospectively registered in PROSPERO (CRD42021224855) and followed the guidelines of the preferred reporting items for systematic reviews and meta-analyses.

Search strategy

We searched the literature that was published from April 2010 to October 2020 using Medline, Embase, and the Cochrane Library. To identify studies that assessed the association between adipokines and BMD values, we searched the online databases with the following keywords: (‘adipokine’ OR ‘leptin’ OR ‘adiponectin’ OR ‘resistin’ OR ‘visfatin’ OR ‘ghrelin’) AND (‘bone density’ OR ‘osteoporosis’ OR ‘absorptiometry’ OR ‘fractures’). All searches were restricted to articles on human patients published in English.

Inclusion criteria

Articles that met the following inclusion criteria were evaluated: 1) original studies that performed measurements on humans; 2) articles written in English; 3) studies that included measurement of BMD or fracture risk and at least one of the adipokines or ghrelin levels in serum; 4) studies that included BMD measured using dual-energy X-ray absorptiometry.

Studies with the following criteria were excluded: 1) patients less than 18 years old; 2) patients with comorbidities; 3) obese patients; 4) patients treated with metabolism medications (calcium and vitamin D excluded); 5) patients with high physical activities (such as an athlete); 6) did not distinguish sex or menopausal status in BMD (or fracture risk)-adipokine (or ghrelin) correlation.

Data extraction

Two researchers independently checked the entire search, selection, and extraction processes. To resolve disagreements on matters related to the eligibility of studies or data extraction, a discussion was held between the two researchers or a counsel with a third researcher was included.

We filtered out conference abstracts, reviews, letters, and editorials from the list of studies. We then screened the remaining articles by confirming the title and abstract. After screening the articles, we examined the full text of the selected studies and categorized patients according to sex, menopausal status, assessed BMD site, and measured adipokines or ghrelin.

Finally, we extracted the following data from eligible studies: authors, year of publication, patients' mean age, sex, menopausal status, osteoporotic status, fat mass, BMI, body weight, height, number of patients, method, site, score of BMD evaluation, method and serum level of each adipokines or ghrelin assessment, and correlation and multivariable regression of BMD with adipokines or ghrelin.

Risk of bias in individual studies

We assessed the risk of bias for the individual cohort studies using the Newcastle-Ottawa scale (18). We used the modified version of the Newcastle-Ottawa scale to assess cross-sectional studies (19). The authors (SL, JHK) independently performed the risk of bias assessment in the included studies and confirmed the quality of evidence. The assessment results are presented in Supplementary Tables S1, S2.

Publication bias

We determined whether there was a potential publication bias in the studies using funnel plots. Furthermore, we estimated the asymmetry of funnel plots using Egger's regression test when a group included more than three studies.

Certainty assessment

We assessed the certainty of evidence through the Grading of Recommendations, Assessment, Development, and Evaluations (GRADE) framework. This framework initiates with confirming the study design and then evaluating eight domains: risk of bias, indirectness, inconsistency, imprecision, publication bias, large effect, plausible confounding, and dose-response gradient. After assessing all the noted domains, the quality of evidence is classed as high, moderate, low, or very low (20).

Statistical analyses

A meta-analysis of the pooled correlations between adipokines or ghrelin and BMD was conducted using the inverse of variance method. Furthermore, a random effects model was used in this study. Fisher's z-transformation converted the non-adjusted (simple) correlation coefficients to calculate the pooled correlation coefficients (pooled r), 95% confidence interval (CI), and P value. We quantified statistical heterogeneity among the included studies by calculating the Q and I^2 statistics (21). The pooling correlation meta-analysis and quality assessment of studies were executed using the 'meta' (22) and 'dmetar' (23) packages in R.

We also conducted a meta-analysis by pooling the mean differences in hormone levels according to osteoporotic status using the RevMan 5.0.1.8 software (Nordic Cochrane Center, Copenhagen, Denmark). Results reported in median and interquartile quartile range were converted to estimate the mean and standard deviation according to previously described methods (24). Standardized mean differences (SMD) were calculated for continuous outcome data (method of the inverse of the variance). Publication bias was determined to assess asymmetry using funnel plots.

Results

Selection and characteristics of studies

The search process for the primary studies is shown in the flowchart in Figure 1. In the updated search, 1,126 studies, excluding duplicates, were identified through a database search. A total of 1079 studies were excluded from the assessment based on their title and abstract. The full text of the remaining 57 studies was assessed, and 10 studies were excluded because they did not meet the inclusion criteria; thus, 47 studies were selected for the meta-analysis. Of the 59 studies included in the previous meta-analysis, 57 were included in our study, excluding two abstracts (13). Two abstracts were excluded because they overlapped with the published literature or were inaccessible. Finally, 104 studies were included in this study (14–17, 25–124). The pooled correlation analysis included 11,960 participants (4,790 men, 1,392 premenopausal women, and 5,778 postmenopausal women) across 48 studies. The mean age of participants was 56.6 years for men, 36.3 years

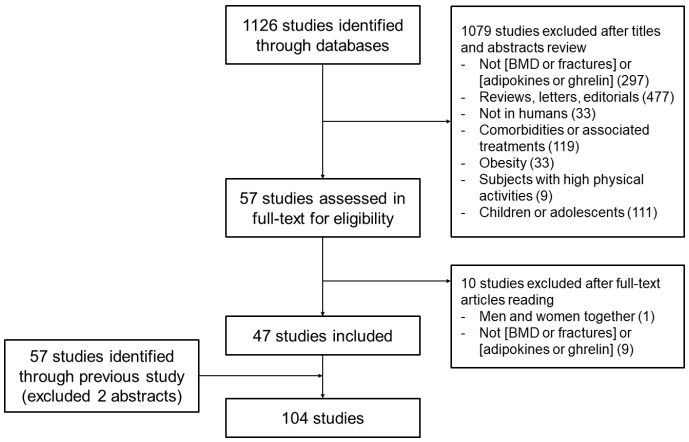

FIGURE 1
Flow chart depicting the search strategy employed to determine eligible studies.

for premenopausal women, and 62.8 years for postmenopausal women. The mean BMI was 25.85 kg/m^2, 21.36 kg/m^2, and 25.12 kg/m^2 for men, premenopausal women, and postmenopausal women, respectively. The mean BMD in lumbar spine site was 1.12 g/cm^2, 1.11 g/cm^2, and 0.92 g/cm^2 for men, premenopausal women, and postmenopausal women, respectively. The mean BMD in femoral neck site was 0.91 g/cm^2, 1.02 g/cm^2, and 0.77 g/cm^2 for men, premenopausal women, and postmenopausal women, respectively. The mean BMD in total body was 1.04 g/cm^2, 1.15 g/cm^2, and 1.00 g/cm^2 for men, premenopausal women, and postmenopausal women, respectively.

Correlations between serum adipokine and ghrelin levels and BMD

We conducted a pooled correlation analysis on the selected studies according to sex, menopausal status, and BMD site (Table 1). The funnel plot for each adipokine, ghrelin, and BMD site is shown in Supplementary Figure S1. To verify the symmetry of each plot, we performed Egger's test (Table 2). A publication bias was found in the correlation between total hip BMD and leptin levels in men; however, no publication bias was detected in other studies. The certainty of the evidence was determined by assessing the eight domains for the outcome of correlations of adipokine levels and BMD. Because all included studies are observational studies, GRADE defaults to low, and some are downgraded to very low due to the risk of bias and inconsistency (Supplementary Table S3).

Over the past decade, many studies have been published on the correlation between adipokine levels and BMD. Several studies have also examined the correlation between leptin and BMD in postmenopausal women, as well as the impact of pre- and post-menopause on adiponectin. A decade ago, only few studies on resistin were conducted; however, since then several new studies for all groups have been performed. Although there are new findings for ghrelin, these could not be used for the meta-analysis because the correlation was not analyzed (Supplementary Figure S2).

In postmenopausal women, leptin level was positively correlated with BMD at the lumbar spine, total hip, femoral neck, and total body (r = 0.18 to 0.29). In addition, the correlation was more robust in postmenopausal women than in other cohorts. In premenopausal women, the correlation was significant at three the sites other than the femoral neck site (r = 0.08 to 0.28). Although the leptin level and BMD correlation at total hip, femoral neck, and total body sites was significant in men (r = 0.09 to 0.12), the correlation coefficients were slightly lower than those in the other two groups (14–16, 36, 38, 43, 46–48, 55, 59, 60, 62, 67, 68, 72, 76, 78, 82, 84, 85, 87–89, 91, 92, 94, 98, 100, 106, 111, 113, 114, 118, 120, 123, 124).

In men and postmenopausal women, adiponectin and BMD at all sites showed a significant inverse correlation (men: r = -0.16 to -0.35, postmenopausal women: r = -0.16 to -0.23). In premenopausal women, adiponectin and BMD correlation was only significant at the femoral neck (r = -0.13) and total body (r = -0.25) sites (15, 16, 30, 33, 44, 50, 60, 62, 66, 68, 72, 79, 84, 85, 89, 90, 94, 95, 110, 112, 120, 124).

Based on the above results, correlations between resistin (14–17, 72, 89, 94, 120) or ghrelin levels (50, 62, 77, 89, 116) and BMD were not statistically significant at any sites.

As the correlations between adipokines and BMD adjusted by body weight or BMI were reduced compared to non-adjusted correlations (125), we examined the data of both non-adjusted and adjusted correlations using body weight, BMI, or fat mass (Table 3). The correlations between leptin and BMD were generally weakened or became insignificant after adjustment for anthropometric measures, and these phenomena were distinct in postmenopausal women as well as men. However, even though the inverse correlation between adiponectin and BMD weakened even after adjustment, most studies still revealed that the correlation was significant. Although the correlations were weakened for resistin, they remained significant in postmenopausal women (lumbar spine

TABLE 1 Pooled correlations between adipokines or ghrelin level and BMD according to sex and menopausal status.

Group	Adipokine/ ghrelin	BMD site	No. of patients	Heterogeneity		Random effects model			Studies
				I^2	p	r	95% CI	p	
Men	Leptin	Lumbar spine	2266	78	< 0.001	0.05	-0.06, 0.15	0.38	(14, 43, 46, 72, 76, 89, 94, 111)
		Total hip	916	30	0.22	0.12	0.04, 0.2	0.004	(14, 72, 94, 111, 123)
		Femoral neck	2146	76	< 0.001	0.11	0.01, 0.21	0.03	(14, 43, 46, 72, 76, 89, 91, 123)
		Total body	1958	36	0.16	0.09	0.02, 0.15	0.009	(14, 72, 76, 82, 94, 123)
	Adiponectin	Lumbar spine	1201	0	0.61	-0.19	-0.25, -0.14	< 0.001	(33, 50, 72, 79, 89, 94)
		Total hip	1029	56	0.08	-0.17	-0.27, -0.08	< 0.001	(50, 72, 79, 94)
		Femoral neck	528	31	0.23	-0.16	-0.26, -0.06	0.003	(33, 50, 72, 89)
		Total body	1029	94	< 0.001	-0.35	-0.56, -0.1	0.007	(50, 72, 79, 94)
	Resistin	Lumbar spine	561	31	0.22	-0.1	-0.21, 0.01	0.07	(14, 72, 89, 94)
		Total hip	249	0	0.58	-0.08	-0.21, 0.04	0.2	(14, 72)
		Femoral neck	249	0	0.93	-0.03	-0.16, 0.09	0.59	(14, 72)
		Total body	249	18	0.27	-0.09	-0.26, 0.08	0.28	(14, 72)
	Ghrelin	Lumbar spine	821	0	0.56	-0.05	-0.12, 0.02	0.19	(50, 77, 89, 116)
		Total hip	741	80	0.006	0.05	-0.15, 0.25	0.6	(50, 77, 116)
		Femoral neck	742	85	0.001	0.09	-0.14, 0.31	0.45	(50, 89, 116)
		Total body	216	0	0.34	0.13	-0.01, 0.26	0.06	(50, 77)
Premenopausal women	Leptin	Lumbar spine	853	4	0.4	0.08	0.01, 0.15	0.03	(15, 43, 55, 59, 60, 67, 92, 111)
		Total hip	320	0	0.84	0.28	0.17, 0.37	< 0.001	(15, 67, 111)
		Femoral neck	669	45	0.1	0.09	-0.02, 0.19	0.12	(15, 43, 59, 60, 67, 92)
		Total body	624	0	0.99	0.19	0.11, 0.26	< 0.001	(15, 55, 59, 60, 68, 92)
	Adiponectin	Lumbar spine	336	57	0.1	-0.07	-0.25, 0.11	0.45	(15, 44, 60)
		Total hip	38	NA	NA	-0.13	-0.43, 0.2	0.44	(15)
		Femoral neck	336	0	0.47	-0.13	-0.23, -0.02	0.02	(15, 44, 60)
		Total body	240	22	0.28	-0.25	-0.38, -0.1	< 0.001	(15, 60, 68)

(Continued)

TABLE 1 Continued

Group	Adipokine/ ghrelin	BMD site	No. of patients	Heterogeneity		Random effects model			Studies
				I^2	p	r	95% CI	p	
	Resistin	Lumbar spine	38	NA	NA	-0.05	-0.36, 0.27	0.77	(15)
		Total hip	38	NA	NA	-0.25	-0.53, 0.08	0.13	(15)
		Femoral neck	38	NA	NA	-0.21	-0.5, 0.12	0.21	(15)
		Total body	38	NA	NA	-0.15	-0.45, 0.18	0.37	(15)
Postmenopausal women	Leptin	Lumbar spine	3456	84	< 0.001	0.18	0.09, 0.27	< 0.001	(15, 16, 36, 38, 43, 46, 47, 55, 62, 67, 84, 85, 87, 88, 92, 98, 100, 111, 113, 118, 120)
		Total hip	2159	35	0.13	0.29	0.23, 0.34	< 0.001	(15, 16, 48, 67, 85, 98, 111, 120, 123, 124)
		Femoral neck	1965	42	0.03	0.22	0.17, 0.28	< 0.001	(15, 16, 36, 38, 43, 46, 62, 67, 84, 88, 92, 98, 100, 106, 114, 118, 123, 124)
		Total body	1625	72	< 0.001	0.26	0.16, 0.35	< 0.001	(15, 36, 47, 55, 62, 78, 92, 100, 106, 114, 118, 120, 123, 124)
	Adiponectin	Lumbar spine	2850	9	0.36	-0.16	-0.2, -0.12	< 0.001	(15, 16, 30, 62, 66, 79, 84, 85, 90, 110, 112, 120)
		Total hip	2053	0	0.46	-0.23	-0.27, -0.18	< 0.001	(15, 16, 79, 85, 90, 95, 120, 124)
		Femoral neck	1024	52	0.04	-0.23	-0.32, -0.13	< 0.001	(15, 16, 62, 66, 84, 95, 112, 124)
		Total body	972	46	0.12	-0.17	-0.27, -0.07	0.001	(15, 62, 79, 120, 124)
	Resistin	Lumbar spine	678	88	< 0.001	-0.03	-0.26, 0.2	0.8	(15–17, 120)
		Total hip	518	48	0.15	0.07	-0.07, 0.2	0.33	(15, 16, 120)
		Femoral neck	342	93	< 0.001	-0.02	-0.43, 0.39	0.91	(15–17)
		Total body	391	83	0.01	0.12	-0.23, 0.44	0.52	(15, 120)
	Ghrelin	Lumbar spine	581	39	0.19	-0.07	-0.21, 0.06	0.29	(62, 77, 116)
		Total hip	493	0	0.7	-0.04	-0.12, 0.05	0.44	(77, 116)
		Femoral neck	540	35	0.22	-0.07	-0.2, 0.06	0.28	(62, 116)
		Total body	129	0	0.42	-0.05	-0.04, 0.17	0.55	(62, 77)

NA, not applicable.

and femoral neck) (120). Studies examining the correlation between visfatin and BMD showed a significant correlation with only total hip in men (r = 0.18) and lumbar spine in postmenopausal women (r = 0.113). However, after adjustment for anthropometric measures, all correlations of visfatin and BMD weakened (94, 112, 120).

We further performed subgroup analysis by geographical populations. In men, pooled correlation coefficients (r) of leptin with BMD were higher in Europe (r = 0.12 to 0.27) populations than in other regions (r = -0.12 to 0.11). Correlations of adiponectin with BMD differed by region but did not appear consistently. Correlations of resistin and ghrelin with BMD were slightly stronger in Europe (resistin: r = -0.05 to -0.31; ghrelin: r = 0.04 to 0.25) than in other areas (resistin: r = -0.03 to -0.08; ghrelin: r = -0.08 to 0.12) (Supplementary Table S4). In premenopausal women, the correlation between entire groups did not appear tendency by

TABLE 2 Summarized results of the Egger's test.

Group/Adipokine	BMD site	Bias	p	Studies
Men				
Leptin	Lumbar spine	1.614	0.344	(14, 43, 46, 72, 76, 89, 94, 111)
	Total hip	2.973	0.006	(14, 72, 94, 111, 123)
	Femoral neck	1.125	0.478	(14, 43, 46, 72, 76, 89, 91, 123)
	Total body	0.734	0.555	(14, 72, 76, 82, 94, 123)
Adiponectin	Lumbar spine	0.414	0.767	(33, 50, 72, 79, 89, 94)
	Total hip	0.588	0.905	(50, 72, 79, 94)
	Femoral neck	-0.787	0.846	(33, 50, 72, 89)
	Total body	-12.946	0.236	(50, 72, 79, 94)
Resistin	Lumbar spine	-2.728	0.072	(14, 72, 89, 94)
	Total hip	NA	NA	(14, 72)
	Femoral neck	NA	NA	(14, 72)
	Total body	NA	NA	(14, 72)
Ghrelin	Lumbar spine	1.376	0.215	(50, 77, 89, 116)
	Total hip	3.603	0.444	(50, 77, 116)
	Femoral neck	4.572	0.355	(50, 89, 116)
	Total body	NA	NA	(50, 77)
Premenopausal women				
Leptin	Lumbar spine	-1.436	0.308	(15, 43, 55, 59, 60, 67, 92, 111)
	Total hip	-0.459	0.759	(15, 67, 111)
	Femoral neck	-1.057	0.653	(15, 43, 59, 60, 67, 92)
	Total body	-0.601	0.201	(15, 55, 59, 60, 68, 92)
Adiponectin	Lumbar spine	0.980	0.840	(15, 44, 60)
	Total hip	NA	NA	(15)
	Femoral neck	0.361	0.897	(15, 44, 60)
	Total body	4.052	0.216	(15, 60, 68)
Resistin	Lumbar spine	NA	NA	(15)
	Total hip	NA	NA	(15)
	Femoral neck	NA	NA	(15)
	Total body	NA	NA	(15)
Postmenopausal women				
Leptin	Lumbar spine	0.055	0.960	(15, 16, 36, 38, 43, 46, 47, 55, 62, 67, 84, 85, 87, 88, 92, 98, 100, 111, 113, 118, 120)
	Total hip	-0.208	0.817	(15, 16, 48, 67, 85, 98, 111, 120, 123, 124)
	Femoral neck	-0.296	0.804	(15, 16, 36, 38, 43, 46, 62, 67, 84, 88, 92, 98, 100, 106, 114, 118, 123, 124)
	Total body	1.343	0.284	(15, 36, 47, 55, 62, 78, 92, 100, 106, 114, 118, 120, 123, 124)
Adiponectin	Lumbar spine	-0.233	0.758	(15, 16, 30, 62, 66, 79, 84, 85, 90, 110, 112, 120)
	Total hip	-0.898	0.239	(15, 16, 79, 85, 90, 95, 120, 124)
	Femoral neck	-1.843	0.234	(15, 16, 62, 66, 84, 95, 112, 124)
	Total body	-0.854	0.604	(15, 62, 79, 120, 124)

(Continued)

TABLE 2 Continued

Group/Adipokine	BMD site	Bias	p	Studies
Resistin	Lumbar spine	2.552	0.681	(15–17, 120)
	Total hip	3.208	0.074	(15, 16, 120)
	Femoral neck	9.979	0.523	(15–17)
	Total body	NA	NA	(15, 120)
Ghrelin	Lumbar spine	-1.443	0.552	(62, 77, 116)
	Total hip	NA	NA	(77, 116)
	Femoral neck	NA	NA	(62, 116)
	Total body	NA	NA	(62, 77)

NA, not applicable.

region (Supplementary Table S5). In postmenopausal women, correlations of leptin with BMD were weaker in Asia (r = 0.07 to 0.25) than in other regions (r = 0.14 to 0.44). Correlations of adiponectin with BMD were similar in all areas. Interestingly, correlations of resistin with BMD were positive in Europe (r = 0.15 to 0.31) and were not in Asia (r = -0.02 to -0.40). Correlations of ghrelin with BMD were more robust in Europe (r = -0.10 to -0.22) than in other regions (r = -0.05 to 0.05) (Supplementary Table S6).

Associations between adipokine and ghrelin levels and BMD

Regression analyses between BMD and adipokines or ghrelin levels were performed in 42 studies (Supplementary Tables S7, S8) (15–17, 26, 28, 29, 33, 35–37, 43, 45, 48, 59–62, 64, 66, 68, 70, 72, 76, 77, 79, 82, 89, 92, 94, 99, 107, 110, 112, 114–118, 120, 122–124).

Multiple regression analyses were performed to determine the variable, including adiponectin, which significantly correlated with the BMD value. A significant inverse correlation between BMD and adiponectin levels was found in 10 of the 16 studies (28, 60, 62, 64, 66, 68, 94, 117, 120, 124). One study that included men revealed that there was a inverse association between lumbar spine (β = -0.163), total hip (β = -0.148), and total body (β = -0.178) BMD and adiponectin levels (94). Three studies that included premenopausal women revealed a inverse association between lumbar spine (β = -0.283; -0.01), femoral neck (β = -0.01), and total body (β = -0.152; -0.01; -0.26) and adiponectin levels (60, 64, 68). Six studies that included postmenopausal women, revealed a inverse association between lumbar spine (β = -0.006; -0.103; B = -2.684), femoral neck (β = -0.27; -0.047; -0.445), total hip (β = -0.112; B = -2.247), total forearm (β = -0.125; B = -2.167), and total body (β = -0.105, -0.385, B = -2.54), and adiponectin level (28, 62, 66, 117, 120, 124). However, no such association was found in six studies (16, 33, 70, 72, 110, 112).

The results of studies examining the association between leptin and BMD are heterogeneous. In men, only one study revealed a positive association (total hip: β = 0.097) (99), and all other study results were not significant or demonstrated a inverse association (43, 45, 76, 82, 89, 94, 107, 123). For women, only two studies with premenopausal women (37, 59) and four studies with postmenopausal women (36, 62, 118, 123) revealed a positive association, whereas the others revealed no significance or a inverse association (16, 28, 35, 43, 48, 60, 70, 92, 99, 114, 117, 122, 124). By adjusting leptin levels by body composition-related variables, the association between leptin and BMD was either weakened, disappeared, or even inverted.

Three studies investigated the association between resistin and BMD (15, 17, 28), and only one found an association (total body BMD of postmenopausal women: β = 0.31) (15). Of the three studies (26, 62, 77) that examined the association between ghrelin and BMD, only one found an association (total hip BMD of young women: β = -0.31) (62).

Collectively, the impact of plasma adipokines or ghrelin levels on BMD would be weak and might be confounded by other body composition parameters.

Associations between adipokine and ghrelin levels and BMD changes

The potential of adipokines or ghrelin to predict BMD changes was assessed in five cohort studies (29, 32, 45, 49, 63).

Araneta et al. reported that adiponectin was not associated with bone loss in men and postmenopausal women (29). According to Barbour et al., adiponectin was associated with hip BMD changes in the highest tertile women (Mean annualized % change = -0.67%) compared to in the lowest tertile (Mean annualized % change = -0.43%) after adjusting for age, race, BMI, diabetes, baseline hip aBMD, and weight change. Leptin was not associated with BMD changes in either men or women (32). Crabbe et al. investigated the correlation between leptin and total hip and forearm BMD changes in older men; however, their results were not statistically significant (45). Fuggle et al. investigated the association between lumbar spine and femoral neck BMD changes with leptin and adiponectin, but they found no association (49). Jürimäe et al. investigated the association between BMD changes and adipokine levels in postmenopausal women, and found a positive association between total body (β = 0.001) and femoral neck (β = 0.001)

10.3389/fendo.2023.1044039

TABLE 3 Non-adjusted and adjusted correlations between adipokines or ghrelin levels and BMD according to sex and menopausal status.

Group/Adipokine	BMD site	Studies	No. of patients	Without adjustment		Adjusted for fat-related variables	
				r	p	r	p
Men							
Leptin	Lumbar spine	Thomas, 2001 (111)	343	-0.12	<0.05	-0.09[a]	NS
		Oh, 2005 (89)	80	-0.08	0.489	-0.24[b]	0.039
		Peng, 2008 (94)	232	0.13	NS	0.01[c]	NS
		Dennison, 2004 (46)	219	0.27	<0.001	0.10[d]	NS
	Total hip	Thomas, 2001 (111)	343	0.05	NS	-0.15[a]	<0.01
		Peng, 2008 (94)	232	0.13	NS	0.05[c]	NS
		Zoico, 2003 (123)	92	0.23	<0.05	0.13[a]	0.236
	Femoral neck	Zoico, 2003 (123)	92	0.25	<0.05	0.13[a]	0.21
		Dennison, 2004 (46)	219	0.30	<0.001	0.04[d]	NS
	Total body	Peng, 2008 (94)	232	-0.01	NS	-0.05[c]	NS
		Morberg, 2003 (82)	317	0.17	<0.05	-0.19[g]	<0.01
		Zoico, 2003 (123)	92	0.19	0.064	0.25[a]	<0.05
Adiponectin	Total hip	Peng, 2008 (94)	232	-0.26	<0.05	-0.14[c]	<0.05
	Femoral neck	Basurto, 2009 (33)	92	-0.24	<0.001	-0.09[e]	NS
	Total body	Peng, 2008 (94)	232	-0.21	<0.05	-0.15[c]	<0.05
Resistin	Lumbar spine	Oh, 2005 (89)	80	-0.24	0.05	-0.31[b]	0.011
		Peng, 2008 (94)	232	-0.02	NS	0.01[c]	NS
	Total hip	Peng, 2008 (94)	232	-0.08	NS	-0.04[c]	NS
	Total body	Peng, 2008 (94)	232	-0.05	NS	-0.09[c]	NS
Visfatin	Lumbar spine	Peng, 2008 (94)	232	0.08	NS	0.05[c]	NS
	Total hip	Peng, 2008 (94)	232	0.18	<0.05	0.14[c]	NS
	Total body	Peng, 2008 (94)	232	0.02	NS	0.01[c]	NS
Ghrelin	Femoral neck	Gonnelli, 2008 (50)	137	0.25	<0.01	0.20[f]	<0.05
Premenopausal women							
Leptin	Lumbar spine	Thomas, 2001 (111)	137	0.05	NS	-0.01[a]	NS
	Total hip	Thomas, 2001 (111)	137	0.31	<0.001	-0.04[a]	NS
Postmenopausal women							
Leptin	Lumbar spine	Thomas, 2001 (111)	165	0.25	<0.01	0.08[a]	NS
		Dennison, 2004 (46)	172	0.36	<0.001	0.14[d]	NS
		Zhang, 2010 (120)	336	0.066	NS	-0.03[c]	NS
	Total hip	Zoico, 2003 (123)	171	0.34	<0.001	0.15[a]	<0.05
		Thomas, 2001 (111)	165	0.44	<0.001	-0.01[a]	NS
		Zhang, 2010 (120)	336	0.162	<0.05	0.06[c]	NS
	Femoral neck	Zoico, 2003 (123)	171	0.33	<0.001	0.16[a]	<0.05
		Dennison, 2004 (46)	172	0.35	<0.001	0.10[d]	NS
	Total body	Zoico, 2003 (123)	171	0.33	<0.001	0.30[a]	<0.001
		Zhang, 2010 (120)	336	0.064	NS	0.02[c]	NS

(Continued)

TABLE 3 Continued

Group/Adipokine	BMD site	Studies	No. of patients	Without adjustment		Adjusted for fat-related variables	
				r	p	r	p
Adiponectin	Lumbar spine	Tohidi, 2012 (112)	382	-0.19	0.0001	-0.09[h]	0.097
		Zhang, 2010 (120)	336	-0.208	<0.05	-0.14[c]	NS
	Total hip	Zoico, 2008 (124)	36	-0.46	<0.001	-0.36[a]	<0.05
		Zhang, 2010 (120)	336	-0.228	<0.05	-0.15[c]	<0.05
	Femoral neck	Zoico, 2008 (124)	36	-0.45	<0.001	-0.36[a]	<0.05
		Tohidi, 2012 (112)	382	-0.14	0.008	-0.03[h]	0.56
	Total body	Zoico, 2008 (124)	36	-0.52	<0.001	-0.42[a]	<0.001
		Zhang, 2010 (120)	336	-0.228	<0.05	-0.13[c]	<0.05
Resistin	Lumbar spine	Tariq, 2020 (17)	160	-0.359	<0.001	-0.26[i]	0.001
		Zhang, 2010 (120)	336	-0.043	NS	-0.04[c]	NS
	Total hip	Zhang, 2010 (120)	336	-0.022	NS	-0.02[c]	NS
	Femoral neck	Tariq, 2020 (17)	160	-0.4	<0.001	-0.26[i]	0.001
	Total body	Zhang, 2010 (120)	336	-0.043	NS	-0.03[c]	NS
Visfatin	Lumbar spine	Tohidi, 2012 (112)	382	0.113	0.043	0.07[h]	0.223
		Zhang, 2010 (120)	336	-0.05	NS	-0.05[c]	NS
	Total hip	Zhang, 2010 (120)	336	-0.027	NS	-0.02[c]	NS
	Femoral neck	Tohidi, 2012 (112)	382	0.084	NS	0.03[h]	0.581
	Total body	Zhang, 2010 (120)	336	-0.054	NS	-0.05[c]	NS

NS, not significant.
Adjustment for anthropometric measures:
[a]Fat mass;
[b]age, BMI;
[c]age, fat mass;
[d]age, alcohol, tobacco, activities, calcium intake, osteoarthritis, BMI;
[e]BMI;
[f]age, BMI, calcium intake;
[g]body weight;
[h]age, weight;
[i]age, hip girth, waist girth, waist to hip (W/H) ratio, weight, height, and BMI.

BMD reduction and leptin, and an inverse association between lumbar spine BMD reduction (β = -0.002) and adiponectin (63).

Based on these results, plasma adipokines or ghrelin levels had a weak or no association with the prediction of BMD changes.

Differences in adipokines or ghrelin levels in patients according to osteoporosis status

A total of 12 studies on the level of adipokines or ghrelin according to the diagnosis of osteoporosis were included (Table 4) (16, 38, 41, 50, 66, 69, 84, 87, 95, 108, 109, 119). The meta-analysis results for leptin levels in postmenopausal women are shown in Figure 2A. Nine studies for leptin involving 757 participants, revealed a high heterogeneity ($P < 0.001$, $I^2 = 94\%$). In postmenopausal women, leptin levels were significantly lower in the osteoporosis group than in the normal BMD group (SMD = -0.88, 95% CI = -1.55, -0.21, P = 0.01). There were two studies on leptin levels according to the presence or absence of osteoporosis in men; however, there was no significant difference between the two groups (SMD = -0.10, 95% CI = -0.39, 0.20, P = 0.52; $I^2 = 0\%$, P = 0.72). The five studies on adiponectin involved 527 postmenopausal participants, and revealed a significantly higher adiponectin level in osteoporotic women with high heterogeneity (SMD = 0.94, 95% CI = 0.17, 1.71, P = 0.02; $I^2 = 95\%$, $P < 0.001$) (Figure 2B). As shown in Figure 2C, three studies on resistin involved 314 postmenopausal women. No significant difference in resistin levels was observed between the osteoporotic and control groups in postmenopausal women (SMD = -0.30, 95% CI = -1.06, 0.45, P = 0.43; $I^2 = 90\%$, $P < 0.001$). All adipokine levels in premenopausal women and adiponectin or resistin levels in men were insufficient for meta-analysis. For other adipokines or ghrelin, insufficient data were available for a meta-analysis.

TABLE 4 Differences in adipokines or ghrelin levels according to osteoporosis status.

Studies	Group	Adipokine/ Ghrelin	Osteoporosis		Normal BMD		
			No.	Mean ± SD	No.	Mean ± SD	p
Odabasi, 2000 (87)	Postmenopausal	Leptin (ng/ml)	50	18.7±1.79	30	22.35±2.2	0.103
Yilmazi, 2005 (119)	Postmenopausal	Leptin (ng/ml)	36	17.03±8.4	30	16.55±8.22	0.15
Canhao, 2008 (41)	Women > 50 yr	Leptin (ng/ml)	24	24.76±15.06	40	26.56±14.57	NS
Kocyigit, 2013 (69)	Postmenopausal	Leptin (ng/ml)	42	44.3±21.2	37	48±23.7	NS
Tariq, 2015 (109)	Postmenopausal	Leptin (ng/ml)	41	19.48±1.6	36	18.56±2.31	NS
Breuil, 2011 (38)	Postmenopausal	Leptin (ng/ml)	20	4.4±1.4	16	7.65±2.7	0.002
Mpalaris, 2016 (84)	Postmenopausal	Leptin (ng/ml)	30	22.47±9.4	80	28.8±14.3	< 0.001
Cervellati, 2016 (16)	Postmenopausal	Leptin (ng/ml)	31	16.1±1.5	43	22.6±1.4	<0.05
Tanna, 2017 (108)	Postmenopausal	Leptin (ng/ml)	83	22±20.3	88	29.6±20.2	<0.01
Papadopoulau, 2004 (91)	Men	Leptin (ng/ml)	44	12.7±11.2	319	14.1±12	NS
Canhao, 2008 (41)	Men	Leptin (ng/ml)	10	9.72±7.63	19	9.48±7.13	NS
Cervellati, 2016 (16)	Postmenopausal	Adiponectin (μg/ml)	31	118.2±13.9	43	75.1±12.6	<0.05
Kim, 2012 (66)	Postmenopausal	Adiponectin (μg/ml)	36	7.23±4.05	56	6.68±5.3	NS
Mpalaris, 2016 (84)	Postmenopausal	Adiponectin (μg/ml)	30	14±7.26	80	9.48±4.89	< 0.001
Pluskiewicz, 2012 (95)	Postmenopausal	Adiponectin (μg/ml)	40	31.04±12.64	40	24.81±12.7	<0.05
Tanna, 2017 (108)	Postmenopausal	Adiponectin (μg/ml)	83	20.2±9.2	88	17.5±8.6	<0.05
Gonnelli, 2008 (50)	Men	Adiponectin (μg/ml)	25	10.1±5.3	47	11.3±3.8	NS
Gonnelli, 2008 (50)	Men	Ghrelin (pg/ml)	25	757.5±92.4	47	853.6±136.8	NS
Mpalaris, 2016 (84)	Postmenopausal	Ghrelin (pg/ml)	30	322.5±172.81	80	309.27±140.89	NS
Tariq, 2021 (17)	Postmenopausal	Resistin (ng/ml)	90	2.18±2.44	70	7.92±8.46	<0.001
Cervellati, 2016 (16)	Postmenopausal	Resistin (ng/ml)	31	11.68±5.74	43	12.57±6.7	NS
Pluskiewicz, 2012 (95)	Postmenopausal	Resistin (ng/ml)	40	3.62±1.45	40	3.29±1.37	NS

NS, not significant.

Correlation between adipokines or ghrelin levels and fragile osteoporotic bone fracture

Three studies reported an association between adipokines or ghrelin levels and the prevalence of vertebral fractures. Prevalent vertebral fracture was observed in 15–35% of participants (85, 108, 118). Two studies demonstrated an inconsistent association between leptin or adiponectin levels and prevalence of vertebral fracture, and one of the two studies was included in a previous meta-analysis. No data were available for other adipokines or ghrelin. Leptin level was positively correlated with the percentage of fat mass. Furthermore, only leptin levels predicted the presence of vertebral fractures in the logistic regression model (odds ratio [OR] = 0.642, 95% CI = 0.429, 0.960; p = 0.031) (118). By contrast, serum leptin level was not associated with fracture risk (OR = 1.006, 95% CI = 0.989, 1.023; p = 0.495) adjusted for age, years since menopause, fat-related parameters, and lifestyle variables (108). The pooled OR for leptin was 0.84 (95% CI = 0.55, 1.30; p = 0.43) (108, 118). Serum adiponectin level was associated with the above-adjusted fracture risk but was not statistically significant (OR = 1.034, 95% CI = 0.998, 1.071; p = 0.06) (108).

A total of six prospective cohort studies reported the association between adipokines and incident fractures (29, 31, 58, 79, 85, 102), and three new articles were included. Three studies reported a relationship between leptin and fracture outcomes (31, 85, 102). Two studies showed inconsistent fracture risk in postmenopausal women; one study with men found no association with fracture risk according to serum leptin levels (31, 85). In a cohort study with an average follow up of 6.5 years, higher leptin levels resulted in lower fracture rates based on an unadjusted model in postmenopausal women (high tertile hazard ratio [HR] = 0.68, middle tertile HR = 0.74; p = 0.009); however, in the adjusted model for age, race, and BMI, the association of leptin levels and fracture rates was attenuated (high tertile HR = 0.98, middle tertile HR = 0.86; p = 0.794) (31). Nakamura et al. showed that lower serum leptin levels were a significant risk factor for incident long-bone fractures (HR = 0.70; 95% CI = 0.50, 0.96) adjusted for age, body weight, hip BMD, prevalent fracture, osteoporosis treatment, serum albumin, calcium, and adiponectin (85). In a study that analyzed men and women

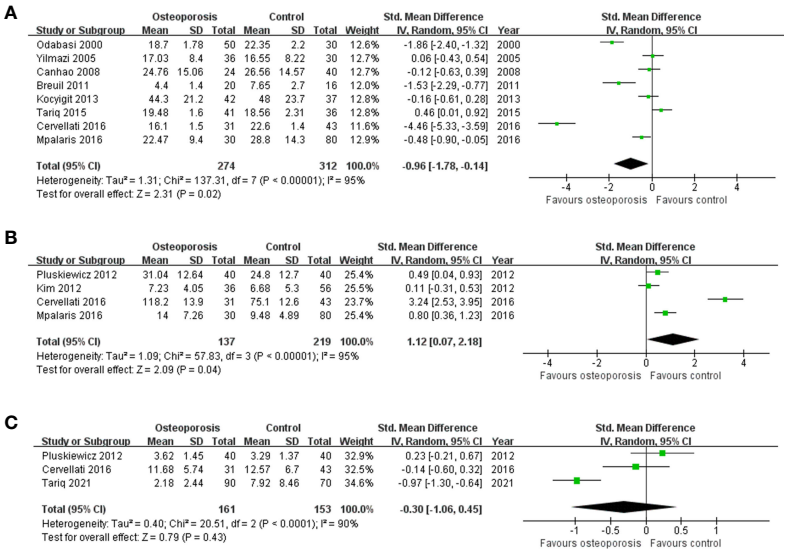

FIGURE 2
Forest plot depicting the differences in adipokine levels according to osteoporosis status in postmenopausal women **(A)** Leptin, **(B)** adiponectin, and **(C)** resistin.

together, the high tertile group with serum leptin levels showed lower fracture risk than the low tertile groups after adjusting for factors (age, sex, menopausal status, body weight, social status, smoking, alcohol consumption, physical activity, diabetes, and creatinine) (102). The HR was 0.25 (95% CI = 0.09, 0.74; p = 0.01 for trend).

For adiponectin, five studies reported a relationship between adiponectin and fracture outcomes (29, 31, 58, 79, 85). Three of the four studies found an association with fracture risk in men (29, 31, 58, 79), and two studies showed inconsistent fracture risk in postmenopausal women according to serum adiponectin levels (31, 85). Michaelsson et al. found that despite the inverse association between adiponectin and BMD, adiponectin did not increase fracture risk in men (adjusted HR = 0.97, 95% CI = 0.86, 1.10; p > 0.05) (79). A community-based longitudinal study followed up fracture data from 277 of 284 men with serial measures, where 21 (7.6%) had at least one vertebral fracture (29). Adiponectin was independently associated with vertebral fractures only in men. The adjusted OR was 1.13 (95% CI: 1.08, 1.23; p = 0.009). Fracture data from 251 of the 261 women with serial measures, revealed that 48 (19.1%) women had a vertebral fracture but no association with adiponectin. Based on a 7.4-years (average, 5.2 years) follow up with the MrOS Sweden cohort of 999 men (58), 150 men (15%) had fractures, with spine fracture being the most common. Adiponectin was associated with a significantly higher incidence of fracture in participants (HR/SD = 1.46; 95% CI = 1.23, 1.72), which was maintained after multivariate adjustment variables for age, time, total hip BMD, general health, and previous fracture (HR = 1.30; 95% CI = 1.09, 1.55). Barbour et al. (31) reported that the fracture rates per 1000 person-years were 27.5 and 14.0 for women and men, respectively, based on a mean follow up of 6.5 years. Adiponectin was significantly associated with fracture risk in men with the highest adiponectin level quartile compared to the lowest quartile (HR = 1.94; 95% CI = 1.20, 3.16) adjusted for age, race, BMI, education, weight change, and total hip BMD. However, no association was found between adiponectin levels and fracture risk in women (HR = 0.98; 95% CI = 0.67, 1.43). Nakamura et al. reported that higher serum adiponectin levels were a significant independent risk factor for incident vertebral fractures in postmenopausal women. The HR of serum adiponectin was 1.18 (95% CI 1.02–1.37, after adjusting for age, body weight, lumbar BMD, prevalent fracture, osteoporosis treatment, serum albumin, calcium, and leptin) (85).

Discussion

We performed an updated meta-analysis on the effects of serum adipokines or ghrelin levels on BMD and fracture risk in healthy adults. Our meta-analysis revealed that postmenopausal women with osteoporosis had significantly lower serum leptin concentrations and higher serum adiponectin concentrations than those in postmenopausal women with normal BMD. Accordingly, the osteoporotic status can be predicted using serum concentrations of leptin and adiponectin in postmenopausal women. In a previous meta-analysis, serum adiponectin levels were not significantly associated with femoral neck BMD in postmenopausal women; however, in this study, BMD values from the lumbar spine, total hip, femoral neck, and total body in postmenopausal women showed a positive correlation with leptin level and a inverse correlation with adiponectin level, which was statistically significant. The correlations between serum leptin or adiponectin concentrations and BMD values from various sites in men and premenopausal women were almost similar to those of the previous

meta-analysis, which demonstrated that femoral neck BMD in men and leptin or adiponectin showed significant correlations, and total body BMD in premenopausal women was significantly correlated with adiponectin level. After adjusting for anthropometric measures, the adiponectin concentrations showed a significant correlation with the BMD value; however, leptin concentrations were not significantly correlated most studies. Although serum resistin concentration did not significantly correlate with the BMD values in the pooled analysis, two studies demonstrated a significant inverse correlation with the lumbar spine BMD values in both postmenopausal women and men, even after adjusting for anthropometric measures (17, 89). Although leptin levels and prevalent vertebral fractures in one study were previously reported to be significant (118), the OR value in the pooled analysis with another study was not significant (108, 118).

Among the 39 pooled analyses listed in Table 1, 13 studies showed high heterogeneity. We attempted to reduce this heterogeneity by reducing the influence of confounders to more accurately determine the effect of adipokines on bone. To rule out the effects of comorbidities or treatments, we only included studies in which healthy participants were enrolled. To diminish this confounding effect, a pooled analysis based on adjusting for anthropometric measures is required. However, due to the lack of individual data, the results could only be compared within each enrolled study; these results are presented in Table 3.

Publication bias, which could have had a most severe impact on the meta-analysis results, was analyzed using the asymmetry of funnel plots and Egger's test. Fortunately, only one publication bias was found when the relationship between total hip BMD and leptin in men was pooled and analyzed. A significant correlation was found between serum leptin and total hip BMD values, analyzed by using pooled correlation. Therefore, the publication bias could be corrected through additional research.

The bone–fat interaction is quite complex, and the precise mechanism has not been elucidated (126). Osteoblasts and adipocytes that make up bone and fat, respectively, originate from the same progenitor called MSCs (7). Therefore, the relationship between bone marrow fat and bone density is inversely proportional to each other (42, 48). The ratio of bone marrow fat increases during menopause, aging, and chronic renal failure, indicating a decrease in bone density and an increase in fracture risk (127). Therefore, it is necessary to study the interaction of ghrelin, which is related to hunger or appetite, or various adipokines mainly produced in adipocytes with osteocytes, osteoblasts, and osteoclasts.

Osteoporosis is a disease in which bone quality deteriorates, and the quantity decreases, which increases the risk of fractures (5). The incidence of osteoporosis is rapidly increasing with the increase in life expectancy. Failure to prevent subsequent fractures in osteoporosis patients leads to an exponential increase in morbidity and mortality (127). Furthermore, osteoporosis has recently emerged as a serious public health concern (128). To prevent, diagnose, treat, and manage osteoporosis, biomarkers are needed. Vitamin D, osteocalcin, and procollagen type 1 N-terminal propeptide are known representative biomarkers (104). Various studies are being conducted to identify additional biomarkers or therapeutic targets, including adipokines and ghrelin (129, 130).

Resistin, a novel adipokine, is expected to serve as a biomarker for osteoporosis diagnosis or a therapeutic target (17, 30, 130). Therefore, many resistin-related studies were included in our meta-analysis. Many studies have been conducted on the effects of adipokines, especially resistin, on bone health over the past 10 years; however, no correlation was found, or insufficient data were available for meta-analysis. Nevertheless, as mentioned above, serum resistin level may have an inverse relationship with the lumbar BMD value in healthy adult men; this notion should be verified in future studies.

Studies on the correlation between visfatin level and BMD have been conducted as studies have shown that visfatin is involved in bone homeostasis and inflammation and regulates glucose metabolism associated with bone metabolism (129). However, the number of studies still needs to be increased, and there is no consistency between studies.

Our study has some limitations. Although age is a confounding factor for our analysis, we could not separate groups by detailed age due to the lack of studies. In the case of women, many studies considered menopause, so it was possible to analyze to some extent according to age roughly by dividing the group into pre and postmenopause. However, in the case of men, only some studies are separated by age. Especially, data on young men were insufficient. Although there were no significant differences in measured adipokine concentrations by adipokine source and assay approaches, their influence could not be completely ruled out. Despite these limitations, this study has several advantages. Our analysis included more studies for leptin, adiponectin, and resistin than the previous analysis. Especially, correlation studies for resistin and BMD in pre and postmenopausal women were newly added current meta-analysis. Moreover, we added data synthesis for adipokine levels in patients according to osteoporotic status. Furthermore, we confirmed publication bias in the entire group and assessed the quality of original studies. Therefore, our analysis reinforced the data quality and reliability of than previous analysis.

In conclusion, our results suggest that leptin is correlated with BMD, and adiponectin is inversely correlated with BMD. In addition, osteoporotic patients had lower leptin levels and higher adiponectin levels than the normal control. Osteoporosis patients are increasing worldwide (128). Using the serum adipokine level as an indicator, a bone density test at an appropriate time can help diagnose osteoporosis. Furthermore, an appropriate diagnosis can help improve the prognosis of many osteoporosis patients by starting treatment at the right time (131).

Data availability statement

The original contributions presented in the study are included in the article/Supplementary Material. Further inquiries can be directed to the corresponding authors.

Author contributions

SL, JeK, TG, and YK contributed to the conception and design of the study. SL and JeK conducted search, selection, and data extraction processes. YJ, JL, TG, and YK discussed the eligibility of the studies. S-KH, JaK, and KK performed the data extraction and statistical analysis. SL and JeK wrote the first draft of the manuscript. YJ, JL, KK, S-KH, JaK, TG, and YK wrote sections of the manuscript. All authors contributed to the article and approved the submitted version.

Funding

The authors disclosed receipt of the following financial support for the research, authorship, and/or publication of this article: This research was supported by the Basic Science Research Program through the National Research Foundation of Korea (NRF), funded by the Ministry of Education [NRF-2021R1F1A1064056, NRF-2018R1A5A2023879, RS-2023-00207946]; the Korean Health Technology R&D project [HI18C2383] through the Korea Health Industry Development Institute (KHIDI), funded by the Ministry of Health & Welfare, Republic of Korea.

Conflict of interest

The authors declare that the research was conducted in the absence of any commercial or financial relationships that could be construed as a potential conflict of interest.

Publisher's note

Supplementary material

The Supplementary Material for this article can be found online at: https://www.frontiersin.org/articles/10.3389/fendo.2023.1044039/full#supplementary-material

References

1. Albala C, Yanez M, Devoto E, Sostin C, Zeballos L, Santos JL. Obesity as a protective factor for postmenopausal osteoporosis. *Int J Obes Relat Metab Disord* (1996) 20(11):1027–32.

2. Greco EA, Fornari R, Rossi F, Santiemma V, Prossomariti G, Annoscia C, et al. Is obesity protective for osteoporosis? evaluation of bone mineral density in individuals with high body mass index. *Int J Clin Pract* (2010) 64(6):817–20. doi: 10.1111/j.1742-1241.2009.02301.x

3. Kuo DP, Chiu YW, Chen PT, Tsai YJ, Hou CH, Chen YL, et al. Associations between body composition and vertebral fracture risk in postmenopausal women. *Osteoporos Int* (2022) 33:589–98. doi: 10.1007/s00198-021-06178-w

4. Topaloglu US, Erol K. Bone mineral density and fracture risk in prediabetes: a controlled cross-sectional study. *Acta Reumatol Port* (2021) 46(1):32–9.

5. Goh TS, Kim E, Jeon YK, Hwangbo L, Kim IJ, Pak K, et al. Spine-hip discordance and frax assessment fracture risk in postmenopausal women with osteopenia from concordant diagnosis between lumbar spine and femoral neck. *J Clin Densitom* (2021) 24(4):548–56. doi: 10.1016/j.jocd.2021.03.008

6. Premaor MO, Pilbrow L, Tonkin C, Parker RA, Compston J. Obesity and fractures in postmenopausal women. *J Bone Miner Res* (2010) 25(2):292–7. doi: 10.1359/jbmr.091004

7. Ko DS, Kim YH, Goh TS, Lee JS. Altered physiology of mesenchymal stem cells in the pathogenesis of adolescent idiopathic scoliosis. *World J Clin cases* (2020) 8 (11):2102–10. doi: 10.12998/wjcc.v8.i11.2102

8. Li J, Lu L, Liu Y, Yu X. Bone marrow adiposity during pathologic bone loss: molecular mechanisms underlying the cellular events. *J Mol Med (Berl)* (2022) 100:167–83. doi: 10.1007/s00109-021-02164-1

9. Aguirre L, Napoli N, Waters D, Qualls C, Villareal DT, Armamento-Villareal R. Increasing adiposity is associated with higher adipokine levels and lower bone mineral density in obese older adults. *J Clin Endocrinol Metab* (2014) 99(9):3290–7. doi: 10.1210/jc.2013-3200

10. Glorie L, D'Haese PC, Verhulst A. Boning up on Dpp4, Dpp4 substrates, and Dpp4-adipokine interactions: logical reasoning and known facts about bone related effects of Dpp4 inhibitors. *Bone* (2016) 92:37–49. doi: 10.1016/j.bone.2016.08.009

11. Delhanty PJ, van der Eerden BC, van Leeuwen JP. Ghrelin and bone. *Biofactors* (2014) 40(1):41–8. doi: 10.1002/biof.1120

12. Lv Y, Liang T, Wang G, Li Z. Ghrelin, a gastrointestinal hormone, regulates energy balance and lipid metabolism. *Biosci Rep* (2018) 38(5):BSR20181061. doi: 10.1042/BSR20181061

13. Biver E, Salliot C, Combescure C, Gossec L, Hardouin P, Legroux-Gerot I, et al. Influence of adipokines and ghrelin on bone mineral density and fracture risk: a systematic review and meta-analysis. *J Clin Endocrinol Metab* (2011) 96(9):2703–13. doi: 10.1210/jc.2011-0047

14. Bilha SC, Branisteanu D, Buzduga C, Constantinescu D, Cianga P, Anisie E, et al. Body composition and circulating estradiol are the main bone density predictors in healthy young and middle-aged men. *J Endocrinol Invest* (2018) 41(8):995–1003. doi: 10.1007/s40618-018-0826-z

15. Bilha SC, Branisteanu D, Buzduga C, Constantinescu D, Cianga P, Anisie E, et al. Modifications in the spectrum of bone mass predictive factors with menopausal status. *Endocr Res* (2018) 43(3):176–85. doi: 10.1080/07435800.2018.1448991

16. Cervellati C, Bonaccorsi G, Bergamini CM, Fila E, Greco P, Valacchi G, et al. Association between circulatory levels of adipokines and bone mineral density in postmenopausal women. *Menopause* (2016) 23(9):984–92. doi: 10.1097/GME.0000000000000655

17. Tariq S, Tariq S, Khaliq S, Lone KP. Serum resistin levels as predictor of low bone mineral density in postmenopausal women. *Health Care Women Int* (2021) 42 (1):82–91. doi: 10.1080/07399332.2020.1798965

18. Wells GA, Shea B, O'Connell D, Peterson J, Welch V, Losos M, et al. The Newcastle-Ottawa scale (Nos) for assessing the quality of nonrandomised studies in meta-analyses. *Oxford* (2000).

19. Herzog R, Alvarez-Pasquin MJ, Diaz C, Del Barrio JL, Estrada JM, Gil A. Are healthcare workers' intentions to vaccinate related to their knowledge, beliefs and attitudes? a systematic review. *BMC Public Health* (2013) 13:154. doi: 10.1186/1471-2458-13-154

20. Mustafa RA, Santesso N, Brozek J, Akl EA, Walter SD, Norman G, et al. The grade approach is reproducible in assessing the quality of evidence of quantitative evidence syntheses. *J Clin Epidemiol* (2013) 66(7):736–42. doi: 10.1016/j.jclinepi.2013.02.004

21. Higgins JP, Thompson SG. Quantifying heterogeneity in a meta-analysis. *Stat Med* (2002) 21(11):1539–58. doi: 10.1002/sim.1186

22. Balduzzi S, Rucker G, Schwarzer G. How to perform a meta-analysis with r: a practical tutorial. *Evid Based Ment Health* (2019) 22(4):153–60. doi: 10.1136/ebmental-2019-300117

23. Harrer M, Cuijpers P, Furukawa TA, Ebert DD. (2021). *Doing Meta-Analysis with R: A Hands-On Guide*. (Boca Raton, FL and London: Chapmann & Hall/CRC Press).

24. Wan X, Wang W, Liu J, Tong T. Estimating the sample mean and standard deviation from the sample size, median, range and/or interquartile range. *BMC Med Res Methodol* (2014) 14:135. doi: 10.1186/1471-2288-14-135

25. Agbaht K, Gurlek A, Karakaya J, Bayraktar M. Circulating adiponectin represents a biomarker of the association between adiposity and bone mineral density. *Endocrine* (2009) 35(3):371–9. doi: 10.1007/s12020-009-9158-2

26. Amini P, Cahill F, Wadden D, Ji Y, Pedram P, Vidyasankar S, et al. Beneficial association of serum ghrelin and peptide yy with bone mineral density in the Newfoundland population. *BMC Endocr Disord* (2013) 13:35. doi: 10.1186/1472-6823-13-35

27. Anastasilakis AD, Polyzos SA, Delaroudis S, Bisbinas I, Sakellariou GT, Gkiomisi A, et al. The role of cytokines and adipocytokines in zoledronate-induced acute phase reaction in postmenopausal women with low bone mass. *Clin Endocrinol (Oxf)* (2012) 77(6):816–22. doi: 10.1111/j.1365-2265.2012.04459.x

28. Ansari MGA, Hussain SD, Wani KA, Yakout SM, Al-Disi D, Alokail MS, et al. Influence of bone mineral density in circulating adipokines among postmenopausal Arab women. *Saudi J Biol Sci* (2020) 27(1):374–9. doi: 10.1016/j.sjbs.2019.10.007

29. Araneta MR, von Muhlen D, Barrett-Connor E. Sex differences in the association between adiponectin and bmd, bone loss, and fractures: the rancho Bernardo study. *J Bone Miner Res* (2009) 24(12):2016–22. doi: 10.1359/jbmr.090519

30. Azizieh FY, Shehab D, Al Jarallah K, Mojiminiyi O, Gupta R, Raghupathy R. Circulatory pattern of cytokines, adipokines and bone markers in postmenopausal women with low bmd. *J Inflammation Res* (2019) 12:99–108. doi: 10.2147/JIR.S203590

31. Barbour KE, Zmuda JM, Boudreau R, Strotmeyer ES, Horwitz MJ, Evans RW, et al. Adipokines and the risk of fracture in older adults. *J Bone Miner Res* (2011) 26 (7):1568–76. doi: 10.1002/jbmr.361

32. Barbour KE, Zmuda JM, Boudreau R, Strotmeyer ES, Horwitz MJ, Evans RW, et al. The effects of adiponectin and leptin on changes in bone mineral density. *Osteoporos Int* (2012) 23(6):1699–710. doi: 10.1007/s00198-011-1768-x

33. Basurto L, Galvan R, Cordova N, Saucedo R, Vargas C, Campos S, et al. Adiponectin is associated with low bone mineral density in elderly men. *Eur J Endocrinol* (2009) 160(2):289–93. doi: 10.1530/EJE-08-0569

34. Bi X, Loo YT, Henry CJ. Relationships between adiponectin and bone: sex difference. *Nutrition* (2020) 70:110489. doi: 10.1016/j.nut.2019.04.004

35. Bilha SC, Bilha A, Ungureanu MC, Matei A, Florescu A, Preda C, et al. Fgf23 beyond the kidney: a new bone mass regulator in the general population. *Horm Metab Res* (2020) 52(5):298–304. doi: 10.1055/a-1151-2342

36. Blain H, Vuillemin A, Guillemin F, Durant R, Hanesse B, de Talance N, et al. Serum leptin level is a predictor of bone mineral density in postmenopausal women. *J Clin Endocrinol Metab* (2002) 87(3):1030–5. doi: 10.1210/jcem.87.3.8313

37. Blum M, Harris SS, Must A, Naumova EN, Phillips SM, Rand WM, et al. Leptin, body composition and bone mineral density in premenopausal women. *Calcif Tissue Int* (2003) 73(1):27–32. doi: 10.1007/s00223-002-1019-4

38. Breuil V, Amri EZ, Panaia-Ferrari P, Testa J, Elabd C, Albert-Sabonnadiere C, et al. Oxytocin and bone remodelling: relationships with neuropituitary hormones, bone status and body composition. *Joint Bone Spine* (2011) 78(6):611–5. doi: 10.1016/j.jbspin.2011.02.002

39. Breuil V, Fontas E, Chapurlat R, Panaia-Ferrari P, Yahia HB, Faure S, et al. Oxytocin and bone status in men: analysis of the Minos cohort. *Osteoporos Int* (2015) 26(12):2877–82. doi: 10.1007/s00198-015-3201-3

40. Breuil V, Panaia-Ferrari P, Fontas E, Roux C, Kolta S, Eastell R, et al. Oxytocin, a new determinant of bone mineral density in post-menopausal women: analysis of the opus cohort. *J Clin Endocrinol Metab* (2014) 99(4):E634–41. doi: 10.1210/jc.2013-4126

41. Canhao H, Fonseca JE, Caetano-Lopes J, Saldanha C, Queiroz MV. Assessment of laboratory measurements and -308 tnfalpha gene promoter polymorphisms in normal bone mineral density. *Clin Rheumatol* (2008) 27(3):301–7. doi: 10.1007/s10067-007-0706-y

42. Chan GMF, Riandini T, Ng SHX, Goh SY, Tan CS, Tai ES, et al. Role of fat and bone biomarkers in the relationship between ethnicity and bone mineral density in older men. *Calcif Tissue Int* (2018) 102(1):64–72. doi: 10.1007/s00223-017-0342-8

43. Chanprasertyothin S, Piaseu N, Chailurkit L, Rajatanavin R, Ongphiphadhanakul B. Association of circulating leptin with bone mineral density in males and females. *J Med Assoc Thai* (2005) 88(5):655–9.

44. Chanprasertyothin S, Saetung S, Payattikul P, Rajatanavin R, Ongphiphadhanakul B. Relationship of body composition and circulatory adiponectin to bone mineral density in young premenopausal women. *J Med Assoc Thai* (2006) 89(10):1579–83.

45. Crabbe P, Goemaere S, Zmierczak H, Van Pottelbergh I, De Bacquer D, Kaufman JM. Are serum leptin and the Gln223arg polymorphism of the leptin receptor determinants of bone homeostasis in elderly men? *Eur J Endocrinol* (2006) 154(5):707–14. doi: 10.1530/eje.1.02130

46. Dennison EM, Syddall HE, Fall CH, Javaid MK, Arden NK, Phillips DI, et al. Plasma leptin concentration and change in bone density among elderly men and women: the Hertfordshire cohort study. *Calcif Tissue Int* (2004) 74(5):401–6. doi: 10.1007/s00223-002-0017-x

47. Di Carlo C, Tommaselli GA, Di Spiezio Sardo A, Sammartino A, Attianese W, Gargano V, et al. Longitudinal evaluation of serum leptin and bone mineral density in early postmenopausal women. *Menopause* (2007) 14(3 Pt 1):450–4. doi: 10.1097/01.gme.0000236936.28454.6a

48. Di Monaco M, Vallero F, Di Monaco R, Mautino F, Cavanna A. Fat body mass, leptin and femur bone mineral density in hip-fractured women. *J Endocrinol Invest* (2003) 26(12):1180–5. doi: 10.1007/BF03349154

49. Fuggle NR, Westbury LD, Syddall HE, Duggal NA, Shaw SC, Maslin K, et al. Relationships between markers of inflammation and bone density: findings from the Hertfordshire cohort study. *Osteoporos Int* (2018) 29(7):1581–9. doi: 10.1007/s00198-018-4503-z

50. Gonnelli S, Caffarelli C, Del Santo K, Cadirni A, Guerriero C, Lucani B, et al. The relationship of ghrelin and adiponectin with bone mineral density and bone turnover markers in elderly men. *Calcif Tissue Int* (2008) 83(1):55–60. doi: 10.1007/s00223-008-9149-y

51. Goulding A, Taylor RW. Plasma leptin values in relation to bone mass and density and to dynamic biochemical markers of bone resorption and formation in postmenopausal women. *Calcif Tissue Int* (1998) 63(6):456–8. doi: 10.1007/s002239900557

52. Gulin T, Kruljac I, Kirigin Bilos LS, Gulin M, Grgurevic M, Borojevic M. The role of adipokines as prognostic factors of one-year mortality in hip fracture patients. *Osteoporos Int* (2017) 28(8):2475–83. doi: 10.1007/s00198-017-4068-2

53. Haam JH, Kim YS, Kim MJ, Koo HS, Kim HY, Kim HJ, et al. A cross-sectional study of the association between adipokine levels and bone mineral density according to obesity and menopausal status in Korean women. *J Bone Miner Metab* (2017) 35 (6):642–8. doi: 10.1007/s00774-016-0801-8

54. Ibrahim SE, ElShishtawy H, Helmy A, A.Galal Z, Salam MHA. Serum leptin concentration, bone mineral density and bone biochemical markers in a sample of Egyptian women: a possible relationship. *Egyptian Rheumatol* (2011) 33(4):171–7. doi: 10.1016/j.ejr.2011.07.001

55. Iwamoto I, Douchi T, Kosha S, Murakami M, Fujino T, Nagata Y. Relationships between serum leptin level and regional bone mineral density, bone metabolic markers in healthy women. *Acta Obstet Gynecol Scand* (2000) 79(12):1060–4. doi: 10.1034/j.1600-0412.2000.0790121060.x

56. Jiang LS, Zhang ZM, Jiang SD, Chen WH, Dai LY. Differential bone metabolism between postmenopausal women with osteoarthritis and osteoporosis. *J Bone Miner Res* (2008) 23(4):475–83. doi: 10.1359/jbmr.071114

57. Johansson H, Oden A, Karlsson MK, McCloskey E, Kanis JA, Ohlsson C, et al. Waning predictive value of serum adiponectin for fracture risk in elderly men: mros Sweden. *Osteoporos Int* (2014) 25(7):1831–6. doi: 10.1007/s00198-014-2654-0

58. Johansson H, Oden A, Lerner UH, Jutberger H, Lorentzon M, Barrett-Connor E, et al. High serum adiponectin predicts incident fractures in elderly men: osteoporotic fractures in men (Mros) Sweden. *J Bone Miner Res* (2012) 27(6):1390–6. doi: 10.1002/jbmr.1591

59. Jurimae J, Jurimae T. Influence of insulin-like growth factor-1 and leptin on bone mineral content in healthy premenopausal women. *Exp Biol Med (Maywood)* (2006) 231(10):1673–7. doi: 10.1177/153537020623101013

60. Jurimae J, Jurimae T. Adiponectin is a predictor of bone mineral density in middle-aged premenopausal women. *Osteoporos Int* (2007) 18(9):1253–9. doi: 10.1007/s00198-007-0365-5

61. Jurimae J, Jurimae T. Plasma adiponectin concentration in healthy pre- and postmenopausal women: relationship with body composition, bone mineral, and metabolic variables. *Am J Physiol Endocrinol Metab* (2007) 293(1):E42–7. doi: 10.1152/ajpendo.00610.2006

62. Jurimae J, Jurimae T, Leppik A, Kums T. The influence of ghrelin, adiponectin, and leptin on bone mineral density in healthy postmenopausal women. *J Bone Miner Metab* (2008) 26(6):618–23. doi: 10.1007/s00774-008-0861-5

63. Jurimae J, Kums T, Jurimae T. Adipocytokine and ghrelin levels in relation to bone mineral density in physically active older women: longitudinal associations. *Eur J Endocrinol* (2009) 160(3):381–5. doi: 10.1530/EJE-08-0673

64. Jurimae J, Rembel K, Jurimae T, Rehand M. Adiponectin is associated with bone mineral density in perimenopausal women. *Horm Metab Res* (2005) 37(5):297–302. doi: 10.1055/s-2005-861483

65. Kim H, Koh H, Ku SY, Kim SH, Kim JH, Kim JG. Association between polymorphisms in period genes and bone density in postmenopausal Korean women. *Climacteric* (2014) 17(5):605–12. doi: 10.3109/13697137.2014.905527

66. Kim JH, Lee DC. Mitochondrial DNA copy number in peripheral blood is associated with femoral neck bone mineral density in postmenopausal women. *J Rheumatol* (2012) 39(7):1465–72. doi: 10.3899/jrheum.111444

67. Kim SM, Kim SH, Lee JR, Jee BC, Ku SY, Suh CS, et al. Association of leptin receptor polymorphisms Lys109arg and Gln223arg with serum leptin profile and bone mineral density in Korean women. *Am J Obstet Gynecol* (2008) 198(4):421 e1–8. doi: 10.1016/j.ajog.2007.10.799

68. King GA, Deemer SE, Thompson DL. Relationship between leptin, adiponectin, bone mineral density, and measures of adiposity among pre-menopausal Hispanic and Caucasian women. *Endocr Res* (2010) 35(3):106–17. doi: 10.3109/07435800.2010.496090

69. Kocyigit H, Bal S, Atay A, Koseoglu M, Gurgan A. Plasma leptin values in postmenopausal women with osteoporosis. *Bosn J Basic Med Sci* (2013) 13(3):192–6. doi: 10.17305/bjbms.2013.2361

70. Kontogianni MD, Dafni UG, Routsias JG, Skopouli FN. Blood leptin and adiponectin as possible mediators of the relation between fat mass and bmd in perimenopausal women. *J Bone Miner Res* (2004) 19(4):546–51. doi: 10.1359/JBMR.040107

71. Lee HJ, Kim H, Ku SY, Choi YM, Kim JH, Kim JG. Association between polymorphisms in leptin, leptin receptor, and beta-adrenergic receptor genes and bone mineral density in postmenopausal Korean women. *Menopause* (2014) 21(1):67–73. doi: 10.1097/GME.0b013e31829366ed

72. Li XP, Zeng S, Wang M, Wu XP, Liao EY. Relationships between serum omentin-1, body fat mass and bone mineral density in healthy Chinese Male adults in changsha area. *J Endocrinol Invest* (2014) 37(10):991–1000. doi: 10.1007/s40618-014-0140-3

73. Liu D, Chen L, Dong S, Yang H, Li L, Liu J, et al. Low bone mass is associated with carotid calcification plaque in Chinese postmenopausal women: the chongqing osteoporosis study. *Climacteric* (2020) 23(3):237–44. doi: 10.1080/13697137.2019.1671818

74. Liu JM, Zhao HY, Ning G, Chen Y, Zhang LZ, Sun LH, et al. Igf-1 as an early marker for low bone mass or osteoporosis in premenopausal and postmenopausal women. *J Bone Miner Metab* (2008) 26(2):159–64. doi: 10.1007/s00774-007-0799-z

75. Liu JM, Zhao HY, Zhao L, Chen Y, Zhang LZ, Tao B, et al. An independent positive relationship between the serum total osteocalcin level and fat-free mass in healthy premenopausal women. *J Clin Endocrinol Metab* (2013) 98(5):2146–52. doi: 10.1210/jc.2013-1112

76. Lorentzon M, Landin K, Mellstrom D, Ohlsson C. Leptin is a negative independent predictor of areal bmd and cortical bone size in young adult Swedish men. *J Bone Miner Res* (2006) 21(12):1871–8. doi: 10.1359/jbmr.060814

77. Makovey J, Naganathan V, Seibel M, Sambrook P. Gender differences in plasma ghrelin and its relations to body composition and bone - an opposite-sex twin study. *Clin Endocrinol (Oxf)* (2007) 66(4):530–7. doi: 10.1111/j.1365-2265.2007.02768.x

78. Martini G, Valenti R, Giovani S, Franci B, Campagna S, Nuti R. Influence of insulin-like growth factor-1 and leptin on bone mass in healthy postmenopausal women. *Bone* (2001) 28(1):113–7. doi: 10.1016/s8756-3282(00)00408-7

79. Michaelsson K, Lind L, Frystyk J, Flyvbjerg A, Gedeborg R, Berne C, et al. Serum adiponectin in elderly men does not correlate with fracture risk. *J Clin Endocrinol Metab* (2008) 93(10):4041–7. doi: 10.1210/jc.2008-0617

80. Mihai G, Gasparik AI, Pascanu IM, Cevei M, Hutanu A, Pop RM. The influence of visfatin, rbp-4 and insulin resistance on bone mineral density in women with treated primary osteoporosis. *Aging Clin Exp Res* (2019) 31(6):889–95. doi: 10.1007/s40520-019-01206-6

81. Mohiti-Ardekani J, Soleymani-Salehabadi H, Owlia MB, Mohiti A. Relationships between serum adipocyte hormones (Adiponectin, leptin, resistin), bone mineral density and bone metabolic markers in osteoporosis patients. *J Bone Miner Metab* (2014) 32(4):400–4. doi: 10.1007/s00774-013-0511-4

82. Morberg CM, Tetens I, Black E, Toubro S, Soerensen TI, Pedersen O, et al. Leptin and bone mineral density: a cross-sectional study in obese and nonobese men. *J Clin Endocrinol Metab* (2003) 88(12):5795–800. doi: 10.1210/jc.2003-030496

83. Morcov C, Vulpoi C, Branisteanu D. Correlation between adiponectin, leptin, insulin growth factor-1 and bone mineral density in pre and postmenopausal women. *Rev Med Chir Soc Med Nat Iasi* (2012) 116(3):785–9.

84. Mpalaris V, Anagnostis P, Anastasilakis AD, Goulis DG, Doumas A, Iakovou I. Serum leptin, adiponectin and ghrelin concentrations in post-menopausal women: is there an association with bone mineral density? *Maturitas* (2016) 88:32–6. doi: 10.1016/j.maturitas.2016.03.004

85. Nakamura Y, Nakano M, Suzuki T, Sato J, Kato H, Takahashi J, et al. Two adipocytokines, leptin and adiponectin, independently predict osteoporotic fracture risk at different bone sites in postmenopausal women. *Bone* (2020) 137:115404. doi: 10.1016/j.bone.2020.115404

86. Nouh O, Abd Elfattah MM, Hassouna AA. Association between ghrelin levels and bmd: a cross sectional trial. *Gynecol Endocrinol* (2012) 28(7):570–2. doi: 10.3109/09513590.2011.593663

87. Odabasi E, Ozata M, Turan M, Bingol N, Yonem A, Cakir B, et al. Plasma leptin concentrations in postmenopausal women with osteoporosis. *Eur J Endocrinol* (2000) 142(2):170–3. doi: 10.1530/eje.0.1420170

88. Oguz S, Tapisiz OL, Aytan H, Gunyeli I, Erdem S, Tuncay G, et al. Is leptin a significant predictor of bone mineral density in postmenopausal Turkish women? *Rheumatol Int* (2009) 29(4):393–6. doi: 10.1007/s00296-008-0711-8

89. Oh KW, Lee WY, Rhee EJ, Baek KH, Yoon KH, Kang MI, et al. The relationship between serum resistin, leptin, adiponectin, ghrelin levels and bone mineral density in middle-aged men. *Clin Endocrinol (Oxf)* (2005) 63(2):131–8. doi: 10.1111/j.1365-2265.2005.02312.x

90. Ozkurt B, Ozkurt ZN, Altay M, Aktekin CN, Caglayan O, Tabak Y. The relationship between serum adiponectin level and anthropometry, bone mass, osteoporotic fracture risk in postmenopausal women. *Eklem Hastalik Cerrahisi* (2009) 20(2):78–84.

91. Papadopoulou F, Krassas GE, Kalothetou C, Koliakos G, Constantinidis TC. Serum leptin values in relation to bone density and growth hormone-insulin like growth factors axis in healthy men. *Arch Androl* (2004) 50(2):97–103. doi: 10.1080/aan.50.2.97.103

92. Pasco JA, Henry MJ, Kotowicz MA, Collier GR, Ball MJ, Ugoni AM, et al. Serum leptin levels are associated with bone mass in nonobese women. *J Clin Endocrinol Metab* (2001) 86(5):1884–7. doi: 10.1210/jcem.86.5.7417

93. Pedone C, Napoli N, Pozzilli P, Lauretani F, Bandinelli S, Ferrucci L, et al. Bone health as a function of adipokines and vitamin d pattern in elderly patients. *Rejuvenation Res* (2013) 16(6):467–74. doi: 10.1089/rej.2013.1436

94. Peng XD, Xie H, Zhao Q, Wu XP, Sun ZQ, Liao EY. Relationships between serum adiponectin, leptin, resistin, visfatin levels and bone mineral density, and bone biochemical markers in Chinese men. *Clin Chim Acta* (2008) 387(1-2):31–5. doi: 10.1016/j.cca.2007.08.012

95. Pluskiewicz W, Adamczyk P, Marek B, Czekajlo A, Drozdzowska B, Kajdaniuk D, et al. Adiponectin and resistin in relationship with skeletal status in women from the rac-Ost-Pol study. *Endokrynol Pol* (2012) 63(6):427–31.

96. Rauch F, Blum WF, Klein K, Allolio B, Schonau E. Does leptin have an effect on bone in adult women? *Calcif Tissue Int* (1998) 63(6):453–5. doi: 10.1007/s002239900556

97. Richards JB, Valdes AM, Burling K, Perks UC, Spector TD. Serum adiponectin and bone mineral density in women. *J Clin Endocrinol Metab* (2007) 92(4):1517–23. doi: 10.1210/jc.2006-2097

98. Roux C, Arabi A, Porcher R, Garnero P. Serum leptin as a determinant of bone resorption in healthy postmenopausal women. *Bone* (2003) 33(5):847–52. doi: 10.1016/j.bone.2003.07.008

99. Ruhl CE, Everhart JE. Relationship of serum leptin concentration with bone mineral density in the united states population. *J Bone Miner Res* (2002) 17(10):1896–903. doi: 10.1359/jbmr.2002.17.10.1896

100. Sahin G, Polat G, Baethis S, Milcan A, Baethdatoethlu O, Erdoethan C, et al. Body composition, bone mineral density, and circulating leptin levels in postmenopausal Turkish women. *Rheumatol Int* (2003) 23(2):87–91. doi: 10.1007/s00296-002-0257-0

101. Scariano JK, Garry PJ, Montoya GD, Chandani AK, Wilson JM, Baumgartner RN. Serum leptin levels, bone mineral density and osteoblast alkaline phosphatase activity in elderly men and women. *Mech Ageing Dev* (2003) 124(3):281–6. doi: 10.1016/s0047-6374(02)00195-1

102. Schett G, Kiechl S, Bonora E, Redlich K, Woloszczuk W, Oberhollenzer F, et al. Serum leptin level and the risk of nontraumatic fracture. *Am J Med* (2004) 117(12):952–6. doi: 10.1016/j.amjmed.2004.07.044

103. Shaarawy M, Abassi AF, Hassan H, Salem ME. Relationship between serum leptin concentrations and bone mineral density as well as biochemical markers of bone turnover in women with postmenopausal osteoporosis. *Fertil Steril* (2003) 79(4):919–24. doi: 10.1016/s0015-0282(02)04915-4

104. Shabat S, Nyska M, Eintacht S, Lis M, Bogomolni A, Berner Y, et al. Serum leptin level in geriatric patients with hip fractures: possible correlation to biochemical parameters of bone remodeling. *Arch Gerontol Geriatr* (2009) 48(2):250–3. doi: 10.1016/j.archger.2008.02.003

105. Shen C, Deng J, Zhou R, Chen J, Fan S, Li Z, et al. Relation between bone mineral density, bone loss and the risk of cardiovascular disease in a Chinese cohort. *Am J Cardiol* (2012) 110(8):1138–42. doi: 10.1016/j.amjcard.2012.05.053

106. Sherk VD, Malone SP, Bemben MG, Knehans AW, Palmer IJ, Bemben DA. Leptin, fat mass, and bone mineral density in healthy pre- and postmenopausal women. *J Clin Densitom* (2011) 14(3):321–5. doi: 10.1016/j.jocd.2011.03.010

107. Sun AJ, Jing T, Heymsfield SB, Phillips GB. Relationship of leptin and sex hormones to bone mineral density in men. *Acta Diabetol* (2003) 40(Suppl 1):S101–5. doi: 10.1007/s00592-003-0039-5

108. Tanna N, Patel K, Moore AE, Dulnoan D, Edwards S, Hampson G. The relationship between circulating adiponectin, leptin and vaspin with bone mineral density (Bmd), arterial calcification and stiffness: a cross-sectional study in post-menopausal women. *J Endocrinol Invest* (2017) 40(12):1345–53. doi: 10.1007/s40618-017-0711-1

109. Tariq S, Tariq S, Alam SS, Baig M. Effect of ibandronate therapy on serum homocysteine and leptin in postmenopausal osteoporotic females. *Osteoporos Int* (2015) 26(3):1187–92. doi: 10.1007/s00198-014-2909-9

110. Tenta R, Kontogianni MD, Yiannakouris N. Association between circulating levels of adiponectin and indices of bone mass and bone metabolism in middle-aged post-menopausal women. *J Endocrinol Invest* (2012) 35(3):306–11. doi: 10.3275/7744

111. Thomas T, Burguera B, Melton LJ3rd, Atkinson EJ, O'Fallon WM, Riggs BL, et al. Role of serum leptin, insulin, and estrogen levels as potential mediators of the relationship between fat mass and bone mineral density in men versus women. *Bone* (2001) 29(2):114–20. doi: 10.1016/s8756-3282(01)00487-2

112. Tohidi M, Akbarzadeh S, Larijani B, Kalantarhormozi M, Ostovar A, Assadi M, et al. Omentin-1, visfatin and adiponectin levels in relation to bone mineral density in Iranian postmenopausal women. *Bone* (2012) 51(5):876–81. doi: 10.1016/j.bone.2012.08.117

113. Ushiroyama T, Ikeda A, Hosotani T, Higashiyama T, Ueki M. Inverse correlation between serum leptin concentration and vertebral bone density in postmenopausal women. *Gynecol Endocrinol* (2003) 17(1):31–6. doi: 10.1080/gye.17.1.31.36

114. Varri M, Niskanen L, Tuomainen T, Honkanen R, Kroger H, Tuppurainen MT. Association of adipokines and estradiol with bone and carotid calcifications in postmenopausal women. *Climacteric* (2016) 19(2):204–11. doi: 10.3109/13697137.2016.1139563

115. Weiss LA, Barrett-Connor E, von Muhlen D, Clark P. Leptin predicts bmd and bone resorption in older women but not older men: the rancho Bernardo study. *J Bone Miner Res* (2006) 21(5):758–64. doi: 10.1359/jbmr.060206

116. Weiss LA, Langenberg C, Barrett-Connor E. Ghrelin and bone: is there an association in older adults?: the rancho Bernardo study. *J Bone Miner Res* (2006) 21(5):752–7. doi: 10.1359/jbmr.060209

117. Wu N, Wang QP, Li H, Wu XP, Sun ZQ, Luo XH. Relationships between serum adiponectin, leptin concentrations and bone mineral density, and bone biochemical markers in Chinese women. *Clin Chim Acta* (2010) 411(9-10):771–5. doi: 10.1016/j.cca.2010.02.064

118. Yamauchi M, Sugimoto T, Yamaguchi T, Nakaoka D, Kanzawa M, Yano S, et al. Plasma leptin concentrations are associated with bone mineral density and the presence of vertebral fractures in postmenopausal women. *Clin Endocrinol (Oxf)* (2001) 55(3):341–7. doi: 10.1046/j.1365-2265.2001.01361.x

119. Yilmazi M, Keles I, Aydin G, Orkun S, Bayram M, Sevinc FC, et al. Plasma leptin concentrations in postmenopausal women with osteoporosis. *Endocr Res* (2005) 31(2):133–8. doi: 10.1080/07435800500229276

120. Zhang H, Xie H, Zhao Q, Xie GQ, Wu XP, Liao EY, et al. Relationships between serum adiponectin, apelin, leptin, resistin, visfatin levels and bone mineral density, and bone biochemical markers in post-menopausal Chinese women. *J Endocrinol Invest* (2010) 33(10):707–11. doi: 10.3275/688610.1007/BF03346674

121. Zhao HY, Bi YF, Ma LY, Zhao L, Wang TG, Zhang LZ, et al. The effects of bisphenol a (Bpa) exposure on fat mass and serum leptin concentrations have no impact on bone mineral densities in non-obese premenopausal women. *Clin Biochem* (2012) 45(18):1602–6. doi: 10.1016/j.clinbiochem.2012.08.024

122. Zhong N, Wu XP, Xu ZR, Wang AH, Luo XH, Cao XZ, et al. Relationship of serum leptin with age, body weight, body mass index, and bone mineral density in healthy mainland Chinese women. *Clin Chim Acta* (2005) 351(1-2):161–8. doi: 10.1016/j.cccn.2004.09.003

123. Zoico E, Zamboni M, Adami S, Vettor R, Mazzali G, Tosoni P, et al. Relationship between leptin levels and bone mineral density in the elderly. *Clin Endocrinol (Oxf)* (2003) 59(1):97–103. doi: 10.1046/j.1365-2265.2003.01808.x

124. Zoico E, Zamboni M, Di Francesco V, Mazzali G, Fantin F, De Pergola G, et al. Relation between adiponectin and bone mineral density in elderly post-menopausal women: role of body composition, leptin, insulin resistance, and dehydroepiandrosterone sulfate. *J Endocrinol Invest* (2008) 31(4):297–302. doi: 10.1007/BF03346361

125. Reid IR, Richards JB. Adipokine effects on bone. *Clinic Rev Bone Miner Metab* (2009) 7:240–8. doi: 10.1007/s12018-009-9048-4

126. Rendina-Ruedy E, Rosen CJ. Bone-fat interaction. *Endocrinol Metab Clin North Am* (2017) 46(1):41–50. doi: 10.1016/j.ecl.2016.09.004

127. Moorthi RN, Fadel W, Eckert GJ, Ponsler-Sipes K, Moe SM, Lin C. Bone marrow fat is increased in chronic kidney disease by magnetic resonance spectroscopy. *Osteoporos Int* (2015) 26(6):1801–7. doi: 10.1007/s00198-015-3064-7

128. Shen Y, Huang X, Wu J, Lin X, Zhou X, Zhu Z, et al. The global burden of osteoporosis, low bone mass, and its related fracture in 204 countries and territories, 1990-2019. *Front Endocrinol (Lausanne)* (2022) 13:882241. doi: 10.3389/fendo.2022.882241

129. Franco-Trepat E, Guillan-Fresco M, Alonso-Perez A, Jorge-Mora A, Francisco V, Gualillo O, et al. Visfatin connection: present and future in osteoarthritis and osteoporosis. *J Clin Med* (2019) 8(8):1178. doi: 10.3390/jcm8081178

130. Kirk B, Feehan J, Lombardi G, Duque G. Muscle, bone, and fat crosstalk: the biological role of myokines, osteokines, and adipokines. *Curr Osteoporos Rep* (2020) 18 (4):388–400. doi: 10.1007/s11914-020-00599-y

131. Tucci JR. Importance of early diagnosis and treatment of osteoporosis to prevent fractures. *Am J Manag Care* (2006) 12(7 Suppl):S181–90.

Frontiers in Endocrinology

Explores the endocrine system to find new therapies for key health issues

The second most-cited endocrinology and metabolism journal, which advances our understanding of the endocrine system. It uncovers new therapies for prevalent health issues such as obesity, diabetes, reproduction, and aging.

Discover the latest Research Topics

See more →

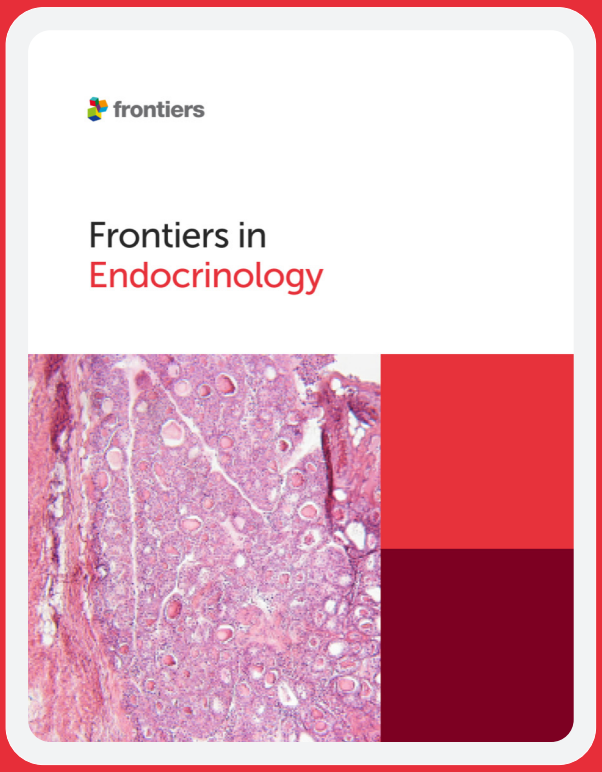

Frontiers

Avenue du Tribunal-Fédéral 34
1005 Lausanne, Switzerland
frontiersin.org

Contact us

+41 (0)21 510 17 00
frontiersin.org/about/contact